CROSS WINDING OF YARN PACKAGES

Submitted in accordance with the requirements for the degree of

Doctor of Philosophy

by

GÜNGÖR DURUR

being an account of work carried out under the supervision of

Dr. M.P.U. Bandara

School of Textile Industries

The University of Leeds

Leeds, LS2 9JT

July 2000

The candidate confirms that the work submitted is his own and that appropriate credit has been given where reference has been made to the work of others.

Dedicated to:

My wife,

My son, Ihsan Umay

and

My daughter, Ceren

ACKNOWLEDGEMENTS

I would like to express my sincere gratitude to my supervisor, Dr. M.P.U. Bandara for his continuous interest, invaluable supervision, thoughtful suggestions and help throughout the course of this work.

I am also thankful to Mr John K. Clarke for his interest, technical assistance and helpful discussion during the work.

Thanks also to Mr. Harbhajan Rait, Mr. John Peckham, and Mr Azim Abadi for their technical assistance.

My sincere gratitude to the Ministry of National Education of The Republic of Turkey for awarding me a scholarship to make this study possible.

My thanks to my friend, Mr Ian Lenton Roberts for his support.

Finally I would like to express my love and heartfelt gratefulness to my family, my wife, Cemile, my son, Ihsan Umay and my daughter, Ceren for their patience, continual encouragement and moral support.

ABSTRACT

Random winding is widely used for the preparation of yarn packages used in a variety of textile processes. Ribboning caused by overwinding of yarn turns at certain places within the package is a basic problem encountered in this process. Standard random winders incorporate some means of ribbon breaking, which strictly speaking have limited effectiveness.

The research reported in thesis was undertaken to realise a random winder capable of detecting the occurrence of ribboning, and taking the ribbon breaking action at these precise times, and thereby achieve 'active' ribbon breaking. Such a winder was realised by the addition of suitable transducers to a standard random winder, which could be controlled by a PC. Winding trials carried out using this equipment established the effectiveness of the concept and also the greater freedom from ribboning the method achieved in comparison with other available methods. Unwinding trials carried out by suitably modifying the winder for measuring yarn unwinding tension were also used to establish the effectiveness of active ribbon breaking.

Preliminary experiments carried out on the above apparatus showed the possibility of constructing a Angle of Double Traverse (ADT) diagram on the VDU of the PC during winding operations, which could serve as a useful aid to follow the progress of the winding operation. It was very useful for showing the occurrence of major and minor ribboning in the wound package, and also for visually indicating the effectiveness of the ribbon breaking procedures.

The diagram was of further use in studying the nature of package driving by the grooved drum. The case of driving a deformable body such as a yarn package on a comparatively non-deformable grooved drum is important for understanding how the package rotates without any obvious slipping. By varying the winding conditions, it was in fact shown that some measurable slip occurs, and these relationships were experimentally established.

Computer simulation is useful to determine the stresses within a wound package, particularly as these cannot be measured using conventional techniques. The results of such a simulation carried out on a random wound package and the comparison of the results with those obtained for a precision wound package are also presented.

CONTENTS

LIST OF FIGURES

LIST OF TABLES

CHAPTER ONE

PART 1

WINDING FUNDAMENTALS

1.1 Introduction

Winding is the process of transferring a yarn from one package to form another package that is more suitable for subsequent processing of the yarn. The most important aspects of winding are the type of package, the method of winding and the type of yarn.

1.2 Types of wound package

There are a vast number of different types of wound packages available to meet the requirements of knitting, weaving, dyeing, texturing and the production of sewing threads, tapes, string, etc.

There are two main types of package: flanged packages and flangeless packages. The advantage of the flangeless type is that it allows over-end withdrawal of yarn during unwinding in the next process. In unwinding a flanged package, the whole package must be rotated. In textile industries, the flangeless package is preferred commonly and is more widely used.

The wound package is also divided into three categories in terms of how the yarn is laid on the package.

- the parallel wound package
- the near-parallel wound package
- the cross-wound package

On the first one of these, a multitude of yarns are laid parallel to one another so that each yarn is wound perpendicular to the package axis. The use of flanges on the bobbin or beam is necessary for the package to be stable. On the second category, one or more yarns are laid nearly parallel to one another owing to the slow traverse used to fill the full length of the flanged bobbin used. The third category, the cross-wound package,

usually consists of a single thread which is laid on the package at an appreciable angle so that layers of yarn cross one another giving stability. The near-parallel wound package and the cross-wound package require a traversing mechanism on the winding machine incorporating a reciprocating action actuated by a guide or cam for each spindle, or a grooved drum.

1.2.1 Types of cross wound package

There are two basic types of cross-wound package: those that have the surface of the package tapered to its axis, and those that have the surface parallel to the axis. The tapered package is called a cone, whereas the package with surface parallel to its axis is a known a tube, or cheese. The size and shape of a cheese is specified when its diameter and traverse length are known, although to specify a cone requires three parameters; the base diameter, the taper, and the traverse length (Fig 1.1).

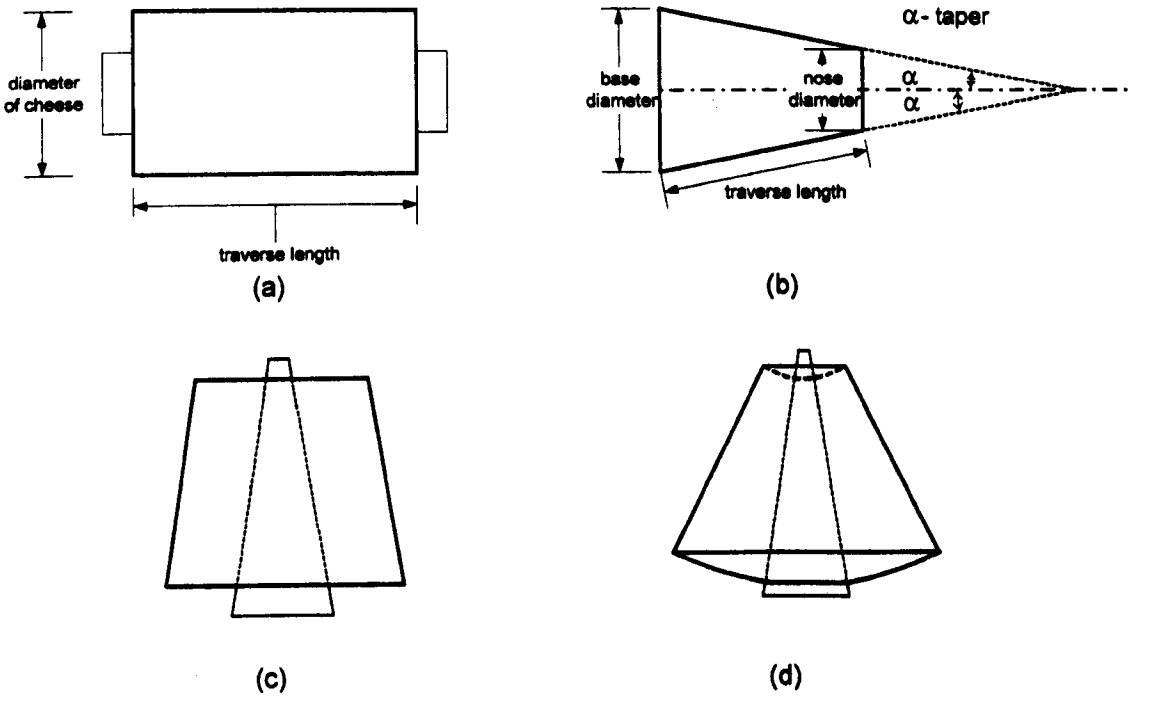

Fig 1.1 (a) Cheese (b) Cone (c) Constant-taper cones (d) Accelerated-taper cones

Yarn can be withdrawn from this kind of package by pulling it over one end of the package. If the yarn is withdrawn at a low speed, yarn will drag on the package surface, and the withdrawal tension is largely influenced by friction, particularly as one coil moves over others which are not yet being unwound. If the yarn withdrawal speed is

sufficiently high, the yarn forms a rotating 'balloon' which rotates about the axis of the package. The unwinding tension is higher due to the centrifugal effect of balloon rotation, and undergoes some fluctuation as the unwinding point moves between the two edges of the package. When the package is a cone, withdrawal is from the nose side of it, and unwinding tension is less fluctuating due to reduced drag of the yarn over the surface of package. Evenness of unwinding tension is so important that cones are in general more popular than cheeses for most applications.

The following tapers are widely used for winding cones: $3^0 30'$, $4^0 20'$, $5^0 57'$, $9^0 15'$. It should be noted here that constant-taper cones are straight-ended but accelerated-taper cones have convex (base) and concave (nose) ends (Fig 1.1).

1.3 Basic cross-winding terminology

Certain standard terms apply to cross winding, which should be defined so as to be able to explain the winding process clearly.

1.3.1 Yarn orientation in cross Winding

There are several angles formed by the lay of yarns in a cross wound package. These are identified in Fig 1.2.

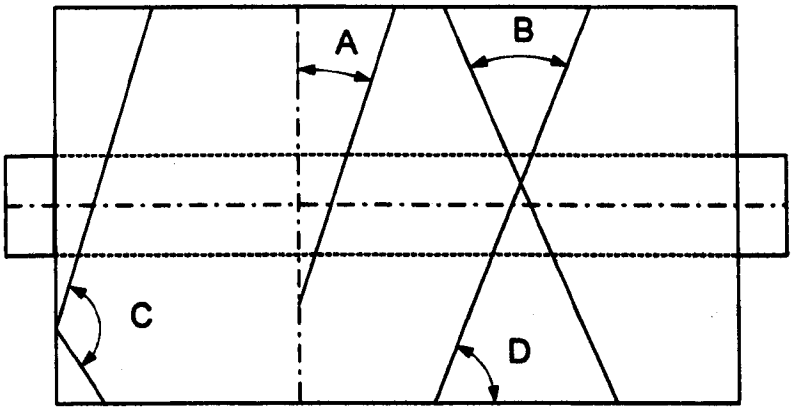

Fig 1.2 Terminology applicable to yarn lay: wind angle (A), crossing angle (B), reversal angle (C) and coil angle (D)

The *wind angle* is defined as the angle (A) between the directions of the yarn lay on the package surface and any plane perpendicular to the package axis. B is called the

crossing angle, and C is called the *angle of reversal.* D is the *coil angle* between the direction of the yarn on the package and the direction of the traverse length [TextInst 95]. In random winding (see section 1.4.2), the wind angle is independent of the diameter because it is produced by surface drive to the package using the grooved drum. On the other hand, the wind angle in precision winding (see section 1.4.1) depends on the package diameter. In this case the wind angle decreases continuously as the package builds up.

1.3.2 Wind ratio and traverse Ratio

The *wind ratio* is the number of revolutions made by the package while the yarn guide makes a single traverse from one end of the package to the other.(i.e. the number of coils laid on the package)

The *traverse ratio* is the number of coils laid on the package during a double traverse of the yarn guide. It is twice the wind ratio. It is also referred to as *Wind per Double Traverse.* This parameter is frequently indicated as *w.*

This is one of the important specifications of a wound package. In random winding, the wind ratio decreases while the package diameter increases whereas it has a constant value in precision winding for all stages of winding.

1.3.3 Traverse length

Traverse length or *traverse* is defined as the distance between extreme positions of a reciprocating thread-guide in one cycle of its movement. In both precision and random winding, traverse length is basically constant. This is true for the majority of cheese and cone packages. A pineapple package uses a traverse which gradually reduces as the package is built up.

1.3.4 Gain

Gain is the angular displacement of the yarn at the beginning of a double traverse, with respect to the corresponding position for the previous double traverse. It is important for the yarn to be displaced at the end of a pattern repeat, so that the next turn will not cause

over winding. The new yarn coil should fall slightly to one side or the other of the first coil. The gain to be used is a minimum gain if the coils are to be laid side by side so as to increase winding density. The minimum gain is dependent on the diameter of the yarn and the diameter of the bobbin used.

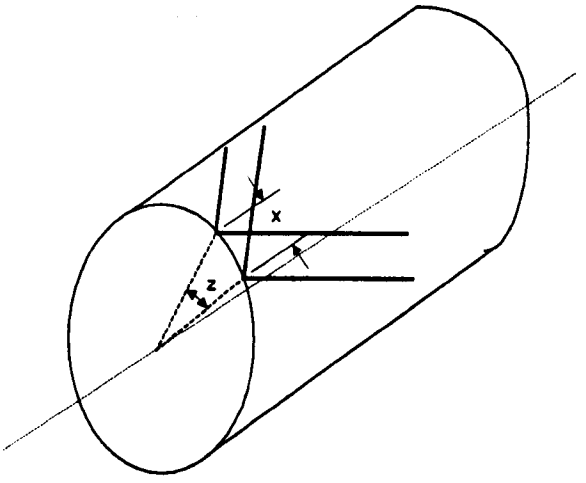

Fig 1.3 Successive coils of yarn

Fig 1.3 shows the package surface with two coils of yarn lying side by side at the end of the package. The displacement of two successive coils is x, and this gives rise the definition of *gain* as the angle z at the centre of the cross-section of the package. The use of the term is mainly confined to precision winding, as discussed later.

1.3.5 Ribboning (Patterning)

If yarn is repeatedly laid on top of or along the same path as the previously wound yarn, this duplication of yarn path on the package creates a defect known as *ribboning* or *patterning*. This condition occurs when the traverse ratio becomes an integer value. It is evident that some ribboning also takes place for values of traverse ratios that differ from an integer by 0.5, 0.25 etc.

In practice it is observed that ribboning is most persistent at small values of wind per double traverse such as 3, 2 or 1. At these values, as the package is relatively large, the rate of change of package diameter is relatively small, and hence ribboning persists for longer. Such ribboning action is normally referred to as *major ribboning*. Stages of ribboning that persist over a relatively small number of package rotations may be termed *minor ribboning* or occasionally *patterning*.

1.3.6 Yarn speed

A basic winding machine rotates the yarn package about a horizontal axis. Yarn being added is supplied in a direction that is perpendicular to the package axis. Some form of a yarn guide is used, which guides the yarn to form helical coils on the package surface. The yarn winding speed V_w results from the vector-sum of the surface speed V_S and the traverse speed V_T. D is the coil angle as in Fig. 1.4.

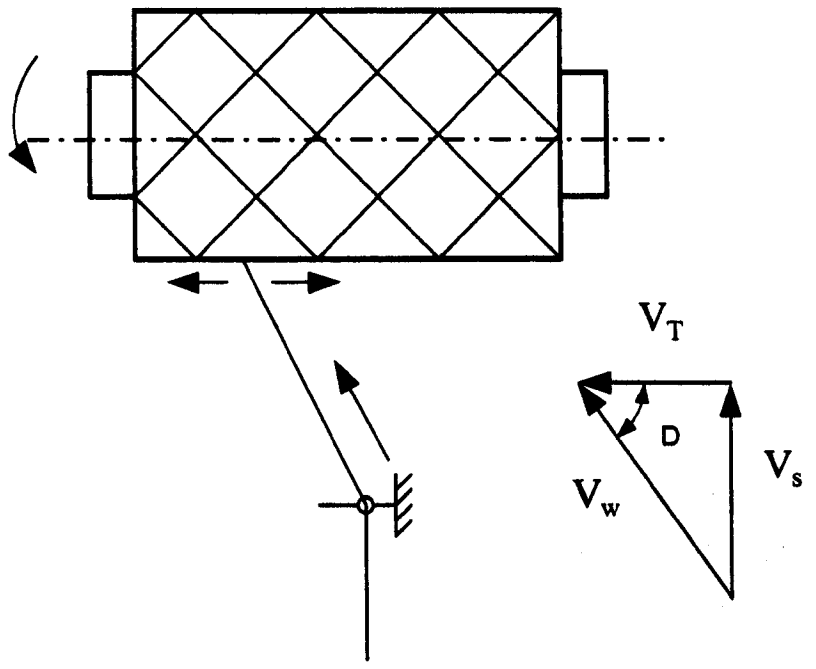

Fig 1.4 Speed relations in winding

- **Winding Speed (V_w)**

Winding speed can be calculated by the following equation.

$$V_w = \sqrt{V_T^2 + V_S^2} \tag{1.1}$$

- **Surface Speed (V_S)**

Surface speed of the yarn package can be given by

$$V_S = \pi * D_P * N_P \tag{1.2}$$

Where

D_P- Package diameter

N_P- Package rotational speed (rpm)

- **Traverse Speed (V_T)**

Traverse speed can be calculated by the equation

$$V_T=2.L.N_d/k \quad (1.3)$$

Where

L – Traverse length

N_d-Rotational speed of the driving roller or cam drum (rpm)

k-driving roller revolutions per double traverse

Note: N_d/k – double traverses per minute

1.3.7 Yarn tension

Tension is applied to a yarn during winding for removing weak places on the yarn and building a stable package of the required density. Yarn tension is introduced by means of a disc tensioner or a gate tensioner [Oxtoby 87]. As a rule of thumb, winding tension should be about 10 - 15 % of the yarn mean-breaking load. With natural fibres this means that weak places will be removed during winding, but for strong synthetics and blends this does not necessarily follow.

1.3.8 Pressure

In precision winding, pressure is applied at the winding point using a smooth roller, which is either driven or which is free to rotate with the package. The level of such pressure applied is a significant factor affecting the density of the package wound. A satisfactory package can be wound over a range of pressure settings depending on the required density of the package. For instance, a soft package suitable for dyeing requires a lower pressure than for a hard packages which is to contain more yarn in a given volume. In random winding the grooved drum serves this function.

1.3.9 Common faults in packages

There are certain types of common faults in wound packages. A major fault applicable to random winding is ribboning or patterning, but this definition of fault has already been given in the previous section. The other possible the faults are the following.

1.3.9.1 Hard edges

More yarn is found to be laid at the reversal points of yarn at the edges of a cross wound package than is theoretically desirable. This occurs due to the slowing down and eventual reversal of the yarn at each end of the package. This leads to some unavoidable differences in package density along the traverse length.

1.3.9.2 Cob-webbing (cross-threading)

Yarn coils may slip at reversals of traverse if the yarn is not sufficiently tensioned to form a stable package or if the traverse guide is at the wrong distance from the surface of the package. The fault involves yarn at the end of the package taking a short-cut from one point on the circumference to a point further round, instead of following the curved circumferential path. Such a fault can cause tension peaks or end-breakages during unwinding.

1.3.9.3 Bulging

The soft inner layers may be squeezed out at the ends of the package due to different hardness of layers from the inside to the outside of a package.

1.3.9.4 Cauliflower effect

The fault identifies the distortion produced on the yarn at the intermediate layers of a package, brought about by the pressure exerted on them by the outer layers, if the tension in these layers drops to zero, this leads them to buckle [Wegener 69].

1.3.9.5 Sloughing-off

Too low a yarn tension or drum pressure may permit the yarn to fall off the edge of the package during unwinding causing the fault known as sloughing off. This is more of a problem in the case of continuous filament yarns.

1.4 Types of winding

There are two main methods for producing cross wound packages; random winding and precision winding. These have different specifications and have certain advantages and disadvantages. There are also some relatively recent winding techniques that combine the best features of precision winding and random winding, such as Step Precision Winding (Digicone) and Ribbon Free Random Winding (RFR). The two basic winding processes are described below.

1.4.1 Precision winding

The layout of a precision winder is given by Fig. 1.5. The package is mounted on a spindle which is positively driven. The traversing of the yarn is provided by a yarn guide which is driven by cylindrical cam, which is coupled to the package spindle at a constant ratio. The package spindle in precision winding normally has a constant speed, which causes the surface speed of the package to gradually increase, as the package becomes larger.

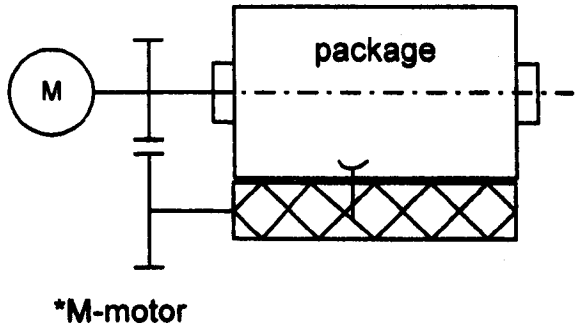

Fig 1.5 Layout of the precision winder

The package rotates a certain number of times during each double traverse of the yarn guide. Hence the traverse ratio (w) for precision winding remains the same. However it can be seen from Fig 1.6 that the wind angle progressively decreases from A1 to A2 as the diameter of package increases during winding.

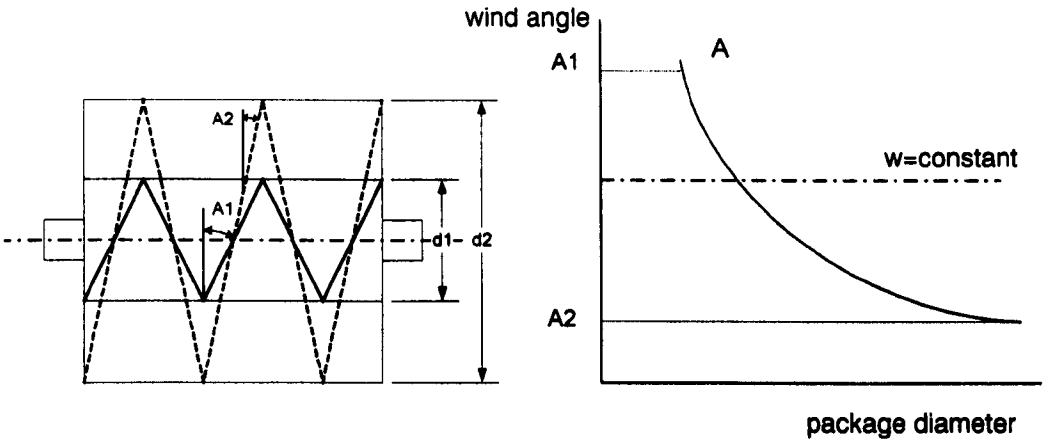

Fig 1.6 The variation of wind angle with package diameter for precision winding

The main advantage of precision winding is that, the gain in this type of winding is a constant which when adjusted to a suitable value, enables the production of a cross-wound package with no ribboning. Integer values of wind ratio are of course avoided.

1.4.2 Random winding

The other main method of producing cross wound packages is random winding. In random winding, the package spindle is not positively driven. Instead, the package is driven by surface friction from the winding drum, which incorporates an endless groove to provide traverse to the yarn.

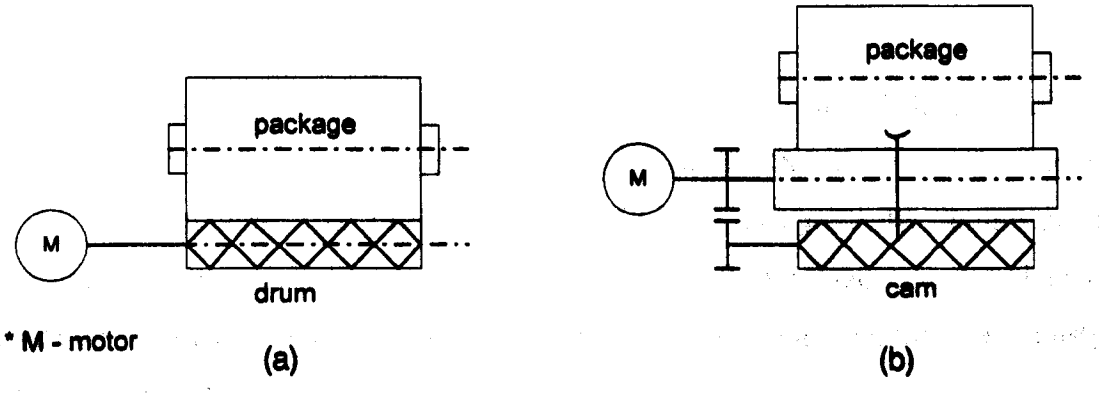

Fig 1.7 Layout of the random winder

The simplicity of the above arrangement is that a cam type traverse arrangement is not required. However considerable rubbing is caused on the yarn by the groove, so this type of winder is only suitable for spun yarns.

The construction of Fig. 1.7b is sometimes employed. Here the package is driven by a smooth cylinder which is rotated at a constant speed. A separate cam drive is coupled to the driving drum as shown. This mechanism behaves in an identical manner to the basic random winder shown by Fig. 1.7a.

One further advantage of the grooved drum is that the yarn being wound, due to the winding tension, falls readily into the groove, without the need for any threading action to be carried out. This is a distinct advantage in such operations as yarn clearing where defective portions of yarn have to be cut off, the yarn rejoined, and the winder set in motion again. The freedom from having to repeatedly rethread the yarn through the yarn guide has therefore resulted in the use of the grooved drum winder in the construction of automatic winders.

As the package is driven by frictional contact with drum, the surface speeds of drum and package are equal. As the drive speed is constant, this enables a constant winding speed to be maintained during the whole period of winding a package.

The wind angle of the yarn on the package remains the same at all points, as this is decided by the resultant velocity of yarn on the surface of the package, which is constant. This also contributes to a uniform package density.

On the other hand, the traverse ratio decreases from the core to full diameter of the package as seen in Fig 1.8. This has a great significance for the random winding process. As the traverse ratio (which is twice the wind ratio) gradually diminishes, it passes through a series of integer values. How long the number lingers on at an integer depends on the rate of change of package diameter as winding continues. Obviously, this rate is higher at small package diameters.

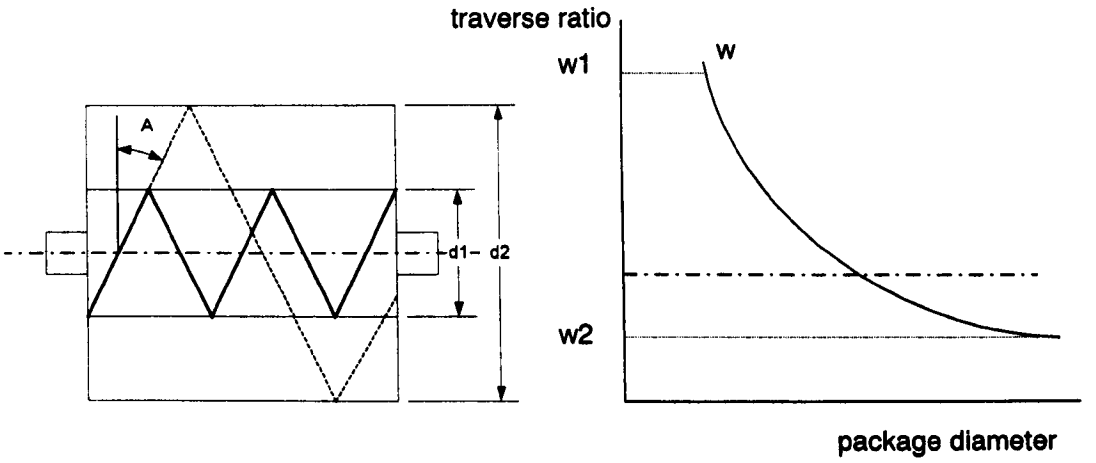

Fig 1.8 The variation of wind ratio with package diameter for random winding

The significance of the traverse ratio attaining integer values is that at these intervals, successive yarn coils are coincident, giving rise to overwinding of yarn turns known as ribboning or patterning as identified before. This effect will be explained in greater detail in Chapter 5.

Ribboning or patterning affects the package unwinding characteristics and the consistency of dyeing in subsequent manufacturing processes. Avoidance of ribboning is of utmost importance in random winding. Thus, all random winding machines incorporate some method of ribbon avoidance.

1.4.3 Comparison of the two package winding methods

	Precision winding		Random winding	
Pattern zones	+	Free of pattern zones	-	Anti-patterning is necessary
Package density	-	Package density is not constant	+	Uniform package density
Wind angle	-	Decreases from core to outer radius	+	constant
Density of wind	+	High package density	-	Low package density
Package geometry	+	Precise yarn displacement	-	Irregular yarn laying from layer to layer
Unwinding property	+	Good unwinding properties	-	Problem of pattern zones
Technically	-	Complicated system	+	Simple system

1.4.4 Modern techniques of ribbon free winding

As indicated in the previous section each winding method has some advantages and disadvantages. With the introduction of microprocessor based control, superior types of winding machines have been realised by combining the better features of the two basic winding processes. These methods are known as Stepped Precision Winding (Digicone) and Ribbon Free Random winding (RFR).

These are described below.

1.4.4 1 Stepped precision winding

The digicone is the name given to a type of precision wound package which is produced by a process termed stepped precision winding. The main positive characteristic of random winding is the constant wind angle and that of precision winding is constant winding ratio which prevents pattern formation. These positive characteristics of random and precision winding are combined in the digicone process (stepped precision winding) which achieves a pattern free package with a near-constant winding angle.

Fig. 1.9 shows the arrangement used in a Digiconer. The drum is driven at a constant speed by the motor so that a constant winding speed is achieved. The motor also drives the variable ratio drive V which is used to vary the speed of the traverse cam. At the beginning of winding a package, the traverse ratio is high and set at a value (w1) which gives the required amount of gain. As winding begins the wind angle has the value A1 corresponding to curve 1. As winding proceeds, the traverse ratio is held at this value but the wind angle gradually increases to the value A2 corresponding to the curve 2. At this point, which is determined using the shaft encoders placed on the two spindles as shown, the ratio of the coupling is changed so that the wind angle is again set at the lower value A1. This results in a lower value of traverse ratio (w2), which avoids winding at an integer value of traverse ratio, and still ensures the same gain as required. Winding at this traverse ratio continues, as the wind angle becomes excessive again. The above procedure is repeated till the package is wound to the required diameter. Thus package consists of several intermeshed concentric layers, each wound with a different traverse ratio but with very little variation in wind angle.

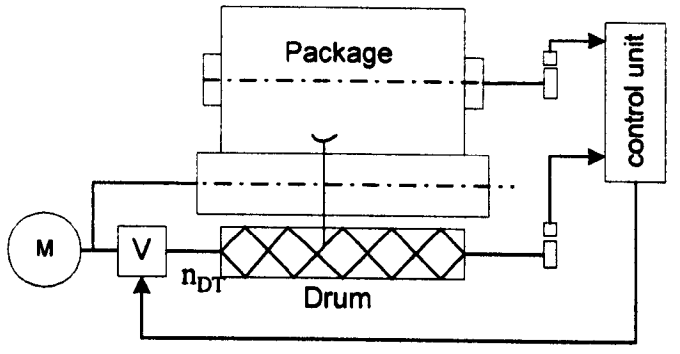

V - variable ratio drive

Fig 1.9 Digicone Winder

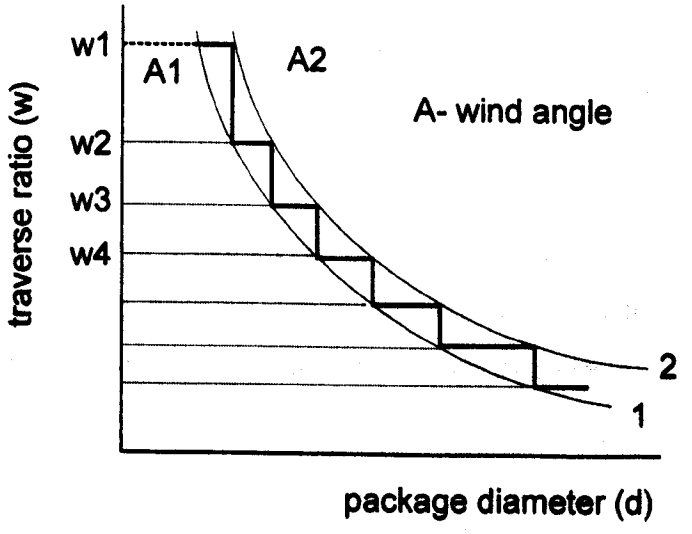

Fig 1.10 Principle of the Digiconer

1.4.4.2 Ribbon Free Random winding (RFR)

This method is rather similar to the basic random winding method. The only difference is in changing the wind ratio, so as to avoid winding at critical values of traverse ratio.

The RFR winder is very similar in construction to that used in the digiconer as shown by Fig 1.11. The difference in operation is achieved by the manner in which the control unit varies the variable ratio drive (V) to achieve two traverse cam speeds, n_{DT1} and n_{DT2}. The ratio of package speed (n_{pac}) to one of the double traverse speed supplies a constant wind angle as in normal random winding. As a result the yarn package produced has two wind angles. The winding is switched between them so as to avoid winding at integer values of traverse ratio. As shown by Fig 1.12, winding is started with wind angle A2. As the package diameter increases, the traverse ratio reaches the critical value w2. At this stage, the speed of yarn guide is instantaneously changed by the control unit and the traverse ratio drops to w3, corresponding to wind angle A1 at this diameter. The package is built up at the same wind angle until the new critical point (w4) is reached. The control unit incorporating microprocessor technology checks the speed of package and yarn guide at all times, and under software control, determines the points of change.

As in the Digiconer a package with intermeshed layers is produced, but in this case the layers have the two alternating values of wind angle.

The development of the microprocessor control has meant that the above design is further simplified by dispensing with the mechanical variable ratio drive altogether, as the desired speeds can be obtained now directly through frequency controlled motor drives.

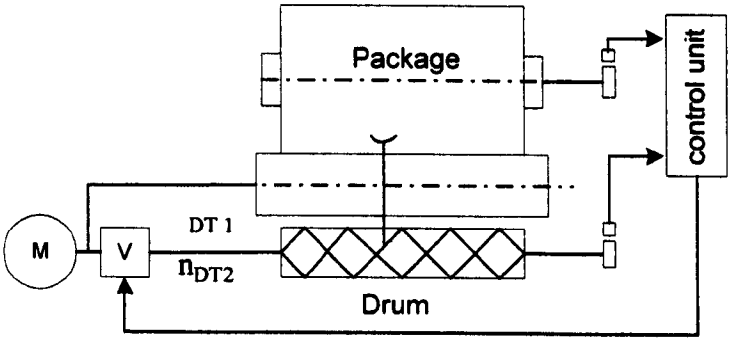

Fig 1.11 RFR Winder

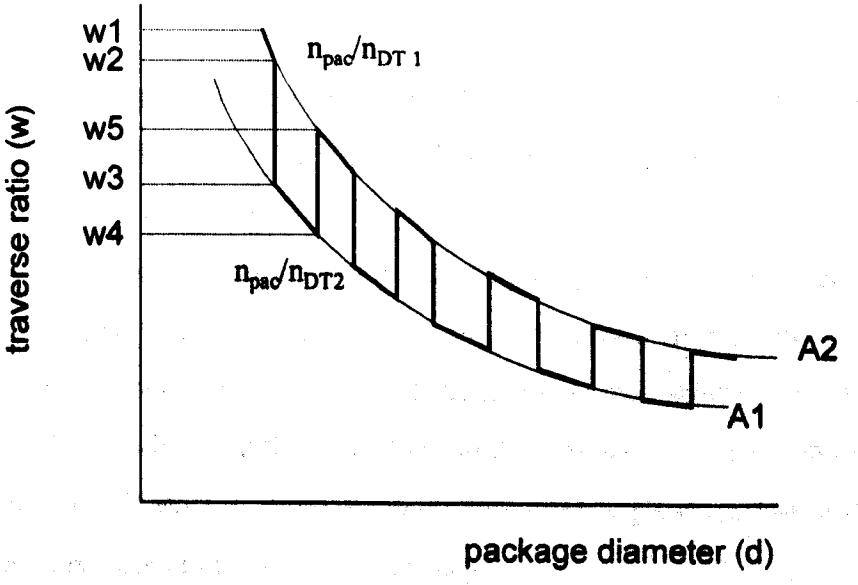

Fig 1.12 Principle of RFR

1.5 The wind angle at the reversal point of cylindrical package

The problem of hard edges on cross wound packages is caused by the inability of the traversing mechanism to sharply reverse the direction of traverse at the edges of the package. As such the change of direction of the yarn involves a lower speed of traverse, and hence more yarn is deposited at the reversal points than is ideally required. It appears that if a cam were available which is capable of very fast reversal of traverse, the problem will be solved.

However the problem also depends on the behaviour of yarn at a point of reversal of traverse, as it is the tension of the yarn that holds it on the package surface and keeps it from slipping from the position it is deposited at by the yarn guide. At a point of reversal of traverse, the tension of the yarn tends to straighten the yarn, which in other words means that the yarn slips back some distance behind the yarn guide as the latter changes direction. So it is evident that, even if a perfect traverse reversal is achievable, the stability of the yarn at the reversal point will anyway lead to the formation if a curvature in the yarn at the point of reversal.

The following section considers this on the basis of yarn tension and frictional forces between the yarn and the package surface at a point of reversal of traverse.

The calculations involved are based on the equilibrium of forces acting on the yarn curve at the reversal point [Hebberling 69]. Two distributed loads act on the yarn at a reversal point on the package surface

- Normal load due to the friction between the yarn and the package surface
- Tangential load as a component of the yarn tension at the turn

As the wind angle is increased, the radius of the turn becomes smaller. The wind angle has an upper value at which equilibrium is no longer possible. The last wind angle at which equilibrium still exist is called the maximum wind angle α_{max}. The corresponding radius of yarn curvature at the reversal point is ρ_{min}.

The following assumptions are made for simplifying the calculation.

- The package is cylindrical (cheese).

- The yarn tension is assumed to be constant along the reversal curve and yarn path is assumed to be circular at the reversal.

The yarn reversal is in equilibrium until the radius of curvature ρ reaches its minimum value at the point of reversal. In this condition the product of normal tension load P and coefficient of fibre friction μ must equal the tangential load Q.

$$\mu \, . \, P = Q \tag{1.4}$$

The geometric relations are shown in Fig 1.13 and Fig 1.14. All notations used in this calculation are given below.

α	-	wind angle	degree
α_{max}	-	maximum wind angle	degree
T	-	yarn tension	g
P	-	distributed normal load	g/cm
Q	-	distributed tangential load	g/cm
l	-	length of the yarn	cm
θ	-	radial angle	degree
φ	-	peripheral angle	degree
ρ	-	radius of curvature	cm
μ	-	coefficient of friction	-
ϵ	-	stroke ratio	-
D	-	diameter of the package	cm

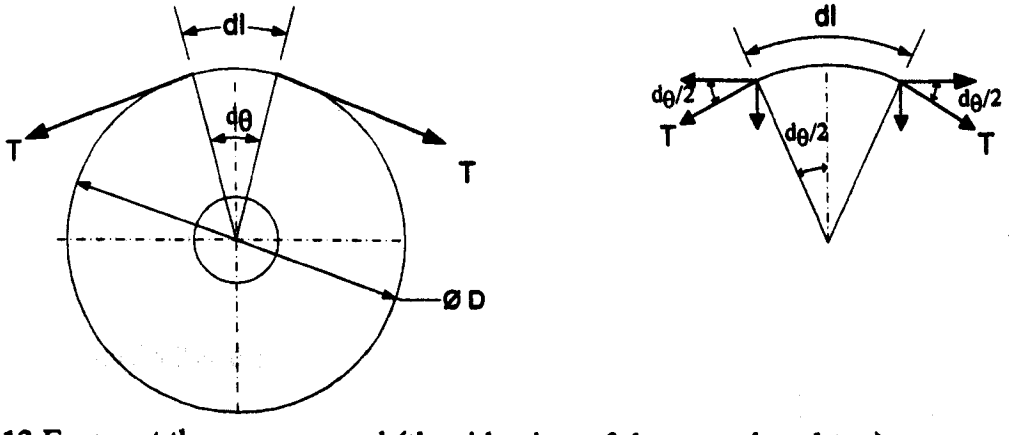

Fig 1.13 Forces at the yarn reversal (the side view of the wound package)

Normal tension load P can be calculated considering the reversal arc with reference to Fig 1.13.

$$2.T.\sin(d\theta/2) = P.dl \qquad (1.5)$$

$$dl = (D/2).d\theta \qquad (i)$$

$$\sin(d\theta/2) = d\theta/2 \qquad (ii)$$

$$P = [2.T.\sin(d\theta/2)]/dl \qquad (iii)$$

Substituting (i) and (ii) in Equation (iii)

$$P = 2.T/D \qquad (1.6)$$

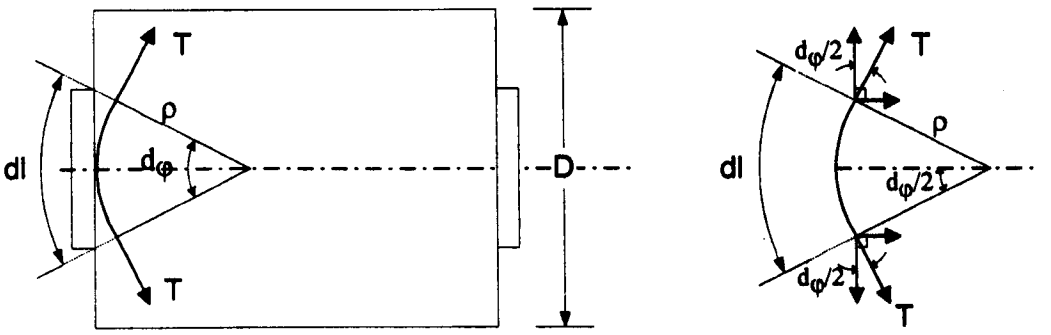

Fig 1.14 - Forces at the yarn reversal (top view of the wound package)

The tangential load Q can be calculated using the geometric relations of Fig 1.14.

$$2.T.\sin(d\varphi/2) = Q.dl \qquad (1.7)$$

$$dl = \rho.d\varphi \qquad (iv)$$

$$\sin(d\varphi/2) = d\varphi/2 \qquad (v)$$

$$Q = [2.T.\sin(d\varphi/2)]/dl \qquad (vi)$$

Substituting (iv) and (v) in Equation (vi);

$$Q=T/\rho \tag{1.8}$$

As mentioned before, the reversal is in equilibrium and ρ is a minimum, so

$$\rho=\rho_{min}$$

Substituting Equation (1.6) and Equation (1.8) in Equation (1.4),

$$\mu\,[2.T/D]=T/\rho_{min} \tag{vii}$$

$$\rho_{min}=D/(2.\mu) = R/\mu \tag{1.9}$$

Under the assumed conditions, the minimum reversal radius depends on the radius of package and the fibre friction as seen by Equation 1.9 whereas yarn tension does not affect the minimum reversal radius.

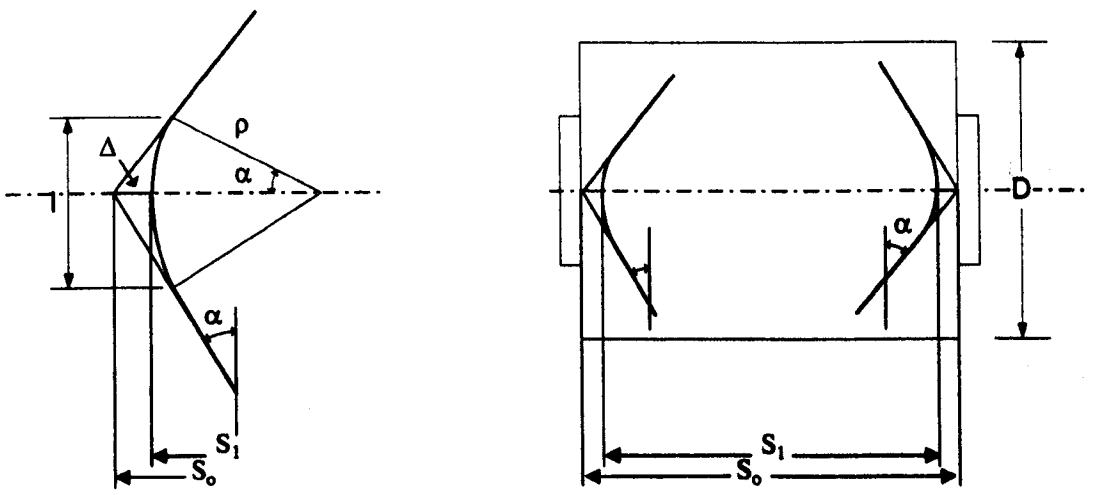

Fig 1.15 - Reversal geometry and stroke at the package

In the following solution, yarn reversal is assumed to be a circular arc.

Referring to Fig 1.15, cos α can be written as

$$\cos\alpha = \frac{\rho}{\rho + \Delta} \tag{1.10}$$

The stroke ratio is a measure of the reduction of the traverse stroke. It can be defined as;

$$\epsilon = \frac{S_1}{S_0}$$

where

S_0 – theoretical length of package

S_1 – actual length of package

$$\Delta = \frac{S_0 - S_1}{2} = \frac{S_1}{2}\left(\frac{1-\epsilon}{\epsilon}\right) \tag{1.11}$$

Substituting Equation (1.11) in Equation (1.10) and solving for ρ,

$$\rho = \frac{S_1}{2}\left(\frac{\cos\alpha}{1-\cos\alpha}\right)\left(\frac{1-\epsilon}{\epsilon}\right) \tag{1.12}$$

Substituting Equation (1.9) in Equation (1.12) and solving for μ when $\alpha=\alpha_{max}$ and $\rho=\rho_{min}$.

$$\mu = \frac{D}{S_1}\left(\frac{1-\cos\alpha_{max}}{\cos\alpha_{max}}\right)\left(\frac{\epsilon}{1-\epsilon}\right) \tag{1.13}$$

$$\alpha_{max} = \cos^{-1}\left[\frac{1}{\frac{\mu S_1}{D}\left(\frac{1-\epsilon}{\epsilon}\right)+1}\right] \tag{1.14}$$

In conclusion, Equation (1.14) shows that the maximum wind angle is a function of μ, S_1, D and ϵ. If the wind angle were over the maximum wind angle, it would cause yarn to slip over package surface at the reversal. Therefore, the yarn traverse stroke at the

package decreases. Speed of winding does not count in this calculation. It is assumed that winding speed is low.

1.6 The random winding machine

1.6.1 Conventional winding machine

The basic construction of the random winder has not changed much over the years. The path of the yarn on the machine is very much the same as before. New developments have been made on individual sections, like different types of yarn guide and improved compensation of yarn package holder pressure as package builds up. The winding head of a winding machine has generally the same arrangement of features for handling the yarn on the way to the package. These are supply spindle, unwinding accelerator, tension assembly, yarn guide cylinder (with lap guard, traverse displacement and anti-patterning), package cradle (with package weight compensation device, and package size control), linkage housing (with performance control, and linkage of all stop and start motions) as shown by Fig 1.16.

1.6.2 Modern Developments in random winding machines

The new developments in random winding machine are aimed at improving yarn properties (i.e. by clearing), package quality, unwinding behaviour of package and winding speed. The winding machine has clearly benefited from microprocessor technology. The information about the process taken from various points of the winding machine is evaluated by the microprocessor, and then the necessary action will be taken automatically.

Yarn tension is maintained at a constant level in order to minimize variation of density at the package. Companies that produce winding machines use different methods for maintaining constant tension. A new winding machine by the Schlafhorst company [Schlafhorst] has a tension sensor connected to the winding head control unit for ensuring uniform yarn tension during process. It is situated in the yarn path after the clearer to register the actual yarn tension at the package (Fig 1.17). The measured values

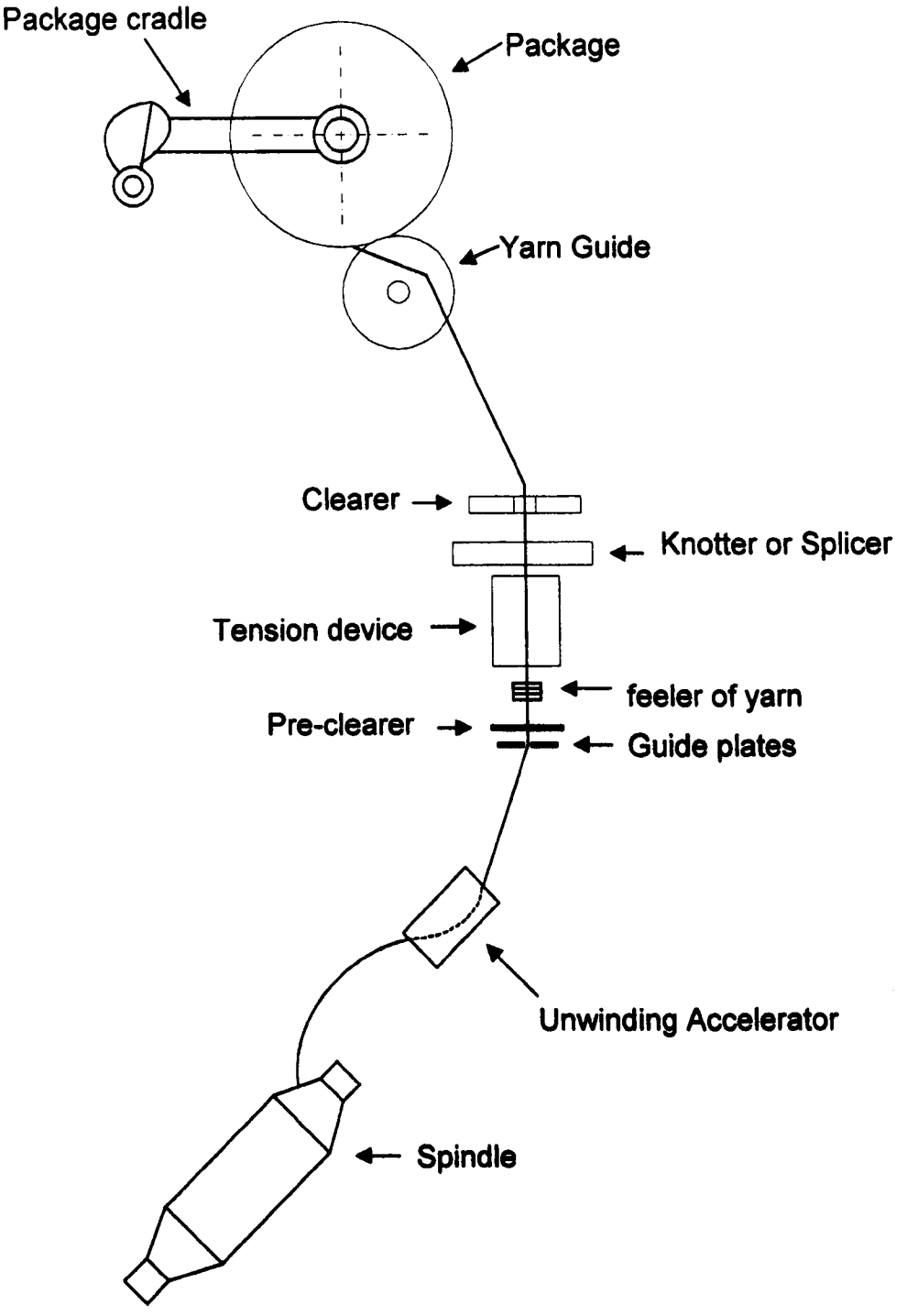

Fig 1.16 Conventional random winder

are transmitted to the tensioner, where the pressure is increased or lowered according to the information received. Some winders incorporate double section yarn tensioner [SSM]. It is believed that the double section yarn tensioner supplies a uniform winding tension, since tension is applied at two points.

Today, on most machines the yarn guide drum of the individual heads is directly driven by a dedicated servomotor. The motor runs under the electronic control as seen in Fig 1.17. These bring some advantages to the modified random winding machine. It is claimed that the combination of winding head computer and direct drum drive facilitates smooth, absolutely jerk-free start-up, slip-controlled acceleration, high winding speeds and improved anti-patterning. Obviously, the effectiveness of anti-ribboning can be improved due to slip control. As one of the well known anti-ribboning methods is the fluctuation of the drive to cause slippage between package and drum, electronically controlled direct drum drive can achieve such slippage under greater control.

In one type of precision winding machine produced by SSM, the package is directly connected to a drivemotor, and a servomotor as shown by Fig 1.18 which drives the yarn guide. They are connected to a control unit which collects all information about the process. At the beginning of winding, the information about speed and wind ratio is collected by the control unit.

Fig 1.19 shows the direct drive system of the drum of the Schlafhorst Autoconer 338. Each winding head is equipped with the servomotor for the drum drive in this machine. The drum is mounted directly on the shaft of the drive motor, so that the motor transmits the torque directly.

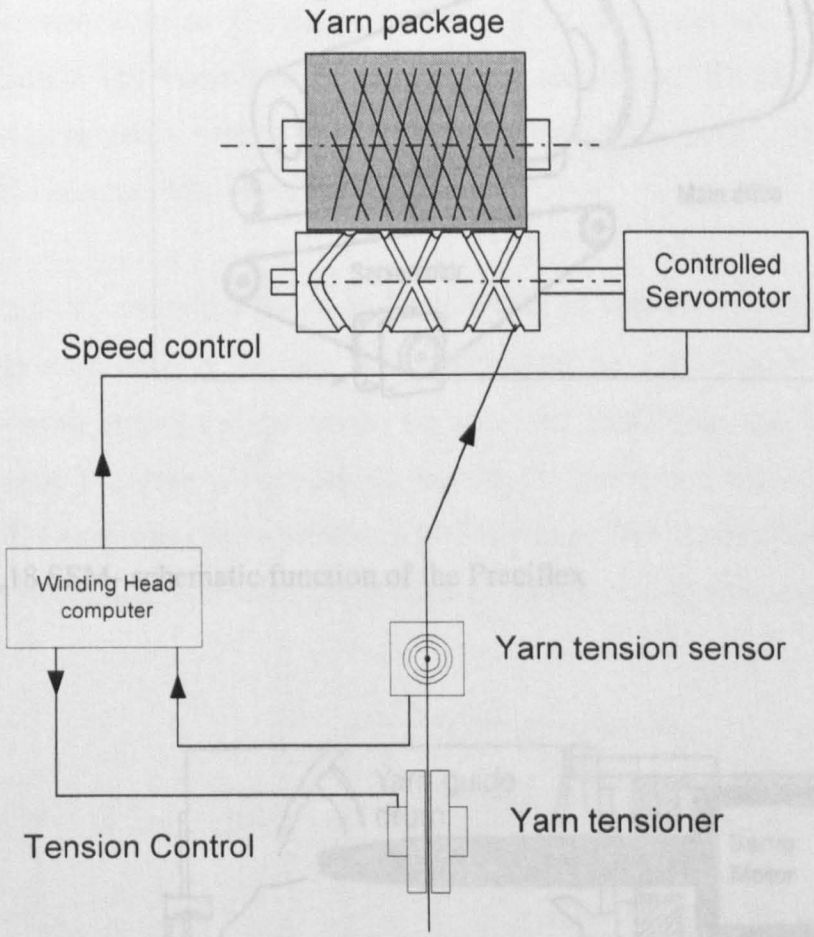

Fig 1.17 Autoconer 338 – Schlafhorst Autotense yarn tension regulator

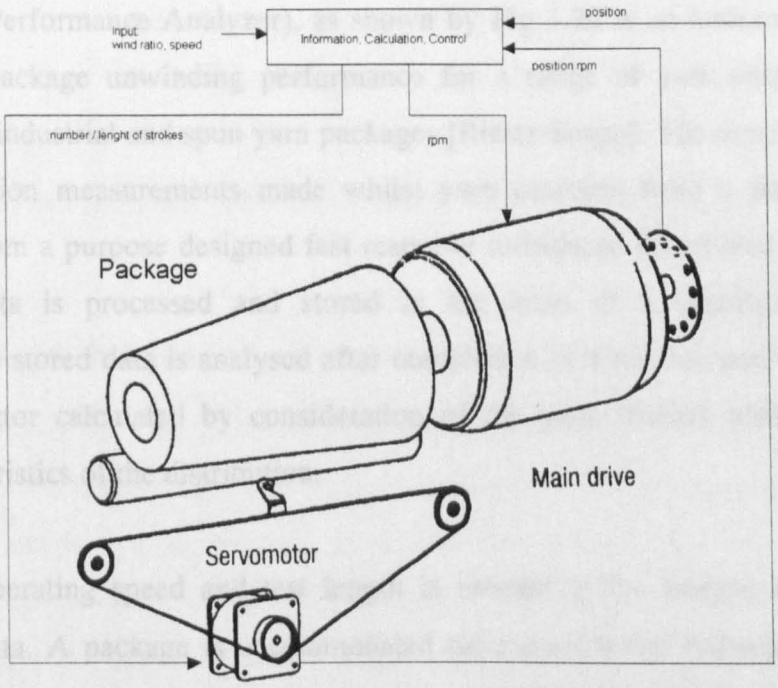

Fig 1.18 SSM- schematic function of the Preciflex

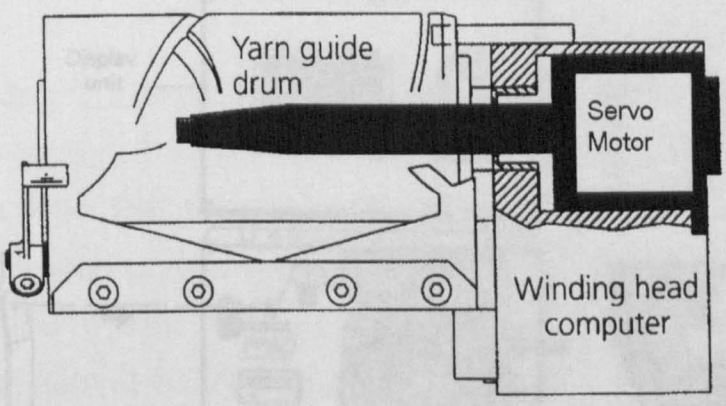

Fig 1.19 Schlafhorst Autoconer 338 with ATT direct drive (ATT :Auto Torque Transmission)

1.7 Package Performance Analyser

PPA (**P**ackage **P**erformance **A**nalyzer), as shown by Fig 1.20 is an instrument for the assessment of package unwinding performance for a range of yarn package types, including many industrial and spun yarn packages [Rieter-Scagg]. The assessment is an analysis of tension measurements made whilst yarn unwinds from a package. The output signal from a purpose designed fast response transducer is sampled at 1000Hz. The tension data is processed and stored in the form of a cumulative tension distribution. The stored data is analysed after completion of a test run and the package performance factor calculated by consideration of the peak tension with respect to general characteristics of the distribution.

The required operating speed and test length is entered at the keypad with sample identification data. A package is accommodated on a creel while balloon length and guide wrap angles can be set to simulate the unwinding conditions of subsequent processes. The yarn is threaded throughout the instrument into waste suction and test started. The results can be printed as PPF (Package Performance Factor), mean and peak tensions with the probability distribution of 100 equal subsections of the test.

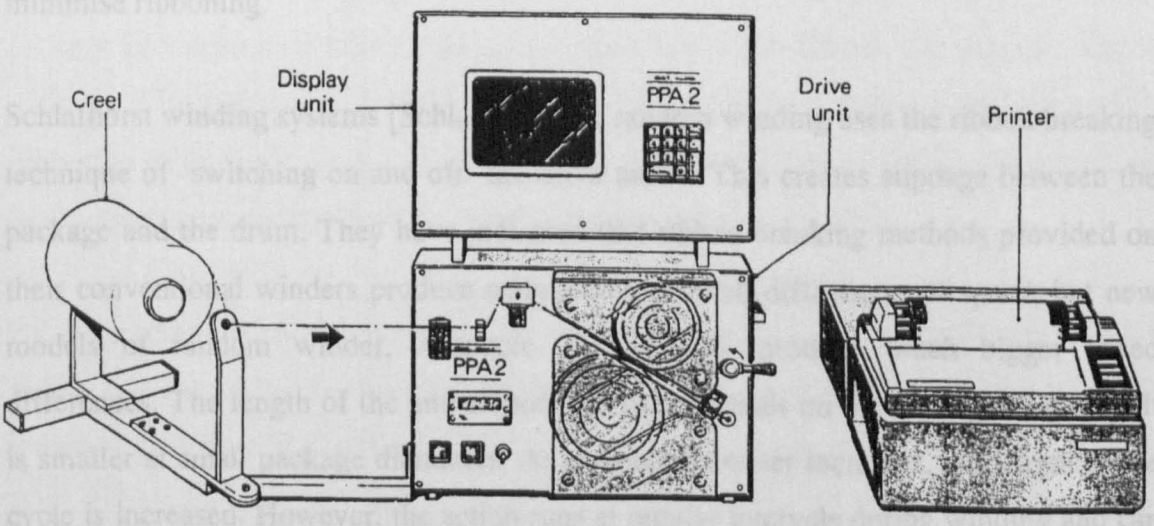

Fig 1.20 Package Performance Analyser (PPA)

CHAPTER ONE

PART II

LITERATURE REVIEW AND AIMS OF THE RESEARCH

1.8 Anti-ribboning techniques

As mentioned briefly in Part I, the random winding process is prone to producing ribboning on the wound package. The traverse ratio attained at any particular stage of winding determines the spacing between successive double traverses of yarn. When the wind ratio becomes an integer, yarn coils produced over a number of double traverses coincide, and cause the defect known as major ribboning. Similar overwinding occurs when the wind ratio is 0.5 ,0.33, 0.25 etc, but the amount of ribboning is less intense (minor ribboning).

Commercial random winding machines combat ribboning by creating abrupt slippage between the package and the winding drum. This helps to disperse the yarns and minimise ribboning.

Schlafhorst winding systems [Schlafhorst] for random winding uses the ribbon breaking technique of switching on and off the drive motor. This creates slippage between the package and the drum. They have indicated that ribbon breaking methods provided on their conventional winders produce comparatively small differences of speed, but new models of random winder, Autocore 238 or 338, produce much bigger speed differences. The length of the anti-ribboning cycle depends on the package diameter. It is smaller at small package diameters. As package diameter increases, the length of the cycle is increased. However, the action runs at regular intervals during winding and can hence be called 'passive'. Other winding machine manufacturing companies also use similar methods of ribbon breaking.

Kyoto [Kyoto,89] reported another method for winding packages called super winding The method is based on using a new type of grooved drum called the 'super drum'. The super drum has one groove in one direction and two grooves in the other direction. Yarn can be selectively guided into one or the other of these grooves as necessary. It was claimed that the method provides packages of even density and favourable shape which are the advantages of the conventional random winding. During winding, yarn is by-passed to the additional groove, when approaching the package diameter at which major ribboning is expected. A yarn-path switching device is used on the machine for changing the number of windings. Packages produced by this method were compared with those produced by conventional random winding, using unwinding trials. The number of yarn breaks experienced on the packages wound with the new method were very few compared with those experienced with conventionally wound packages. It was claimed that the packages produced by the new method do not have any ribboning. However there is no evidence of the industry having adopted this new concept of random winding.

1.9 Deformation of yarn packages

A wound yarn package has a number of specifications associated with it. The wind angle is of basic importance. While for parallel wound packages this angle is practically zero, for cross wound packages it may be about 16^0. In the present work, cross-wound package produced by random winding are specifically considered. The random wound package is investigated in terms of its behaviour during the winding operation, and its properties after being wound to full size. The instrumentation of the winding machine facilitates the understand how the package behaves during winding.

A yarn package is an assembly of a yarn on a suitable tube or bobbin. A cross wound package is considered in this context, and hence there are no flanges, which constrain the yarn being wound in any way.

The yarn is associated with elastic properties in its length direction as well as its transverse direction. However the elastic moduli in these two directions are different due to the structure of the yarn. The 'tensile' modulus in the axial directional is usually greater than the 'compressional' modulus in the transverse direction.

Although a cross wound package is built up by adding a single yarn with traverse, it is convenient to think of 'layers' of yarn which are added up to form the final package. The layer concept is easier to adopt in the case of a precision package. This can be the taken as the set of yarn turns involved in the number of double traverses which is numerically equal to the reciprocal of the *gain* used. The package can be considered the collection of such layers required to complete the package to its full size.

This concept is still useful for the consideration of a random wound package, but there is the difficulty that spaces between successive double traverses of yarn are not constant. This is on account of the constantly diminishing wind ratio. However the wind ratio only changes by a small amount over a small increment of diameter of the package. So if the package is divided into a number of annuli, each of a small thickness, it is possible to assume the traverse ratio to have a constant (mean) value corresponding to a given annulus. An effective ribbon breaking technique will help maintain some reasonably even spacing between the turns, so in practice, it seems useful if the number of double traverses of yarn required to cover each such annulus from the core to the surface of the package could be determined.

In winding a package, yarn is supplied to the winder at a constant tension. It is desirable to have a constant residual tension in yarn inside the package. This is on account of viscoelasticity of textile yarns, as the tension of the yarn within the package influences how the yarn relaxes once it is unwound from the package. Uneven relaxation of yarns may cause such problems as variation of check width in a woven fabric.

A yarn package can be considered as having been formed by adding layers of yarn on top of the previously wound layers. Each added layer will impose pressure on the layer beneath it. The layer that is subjected to this pressure is compressed radially towards the centre of the core and moves to a position of smaller circumference. Thus, each layer of yarn deforms radially. Also the movement of the layer due to the pressure causes the yarn in that layer to contract (i.e. undergo a reduction of radius compared to its value as it is wound) and hence its tension to drop. So as each new layer is added at the outer radius of the package, the pressure inside the package will increase. However every layer from core to outer radius will not be under the same pressure, since number of

layers existing above and below it are different, depending on its radius within the package. The amount of radial movement towards the core will be different for every layer and so will the amount of reduction of yarn tension in every layer. It is possible that a layer at a certain radius inside the package may lose all its tension and will begin to be under compression. The layer next to the core of the package will not undergo radial movement and not lose its tension, as the core is generally incompressible. These layers can only lose some of their tension due to Poisson's effect. However for a cross wound package the Poisson's effect is likely to be much smaller than for a parallel wound package.

This basic concept of deformation has been used by several researchers for cheese packages which are precision wound. A random wound package is more complex than a parallel wound or precision wound package, because it involves more variables.

Catlow and Walls [Catlow 62] have derived equations for determining the stress distribution in a pirn formed by parallel winding. In the solution, the pirn is considered as having layers of yarn of infinitesimal thickness. It is assumed to be isotropic and homogenous. Another assumption is that it is parallel winding so that winding tension is acting perpendicular to the axis of the package. A layer at the outer radius is considered to impose additional pressure to the layers below. The changes in radial and circumferential stress caused by this are obtained as second order differential equations. The necessary boundary conditions are that the core is incompressible so the radial deformation of the pirn at the core is zero and the pressure imposed by the added layer at the radius of pirn is known from the yarn tension and the thickness of that layer. The equation can be integrated analytically to give the expressions of incremental, radial and circumferential stresses at any radius of the pirn for each layer added at the outside. The total changes at any radius for final outer radius of the pirn are obtained by integrating contributions of all the layers added.

The values of the ratio of residual circumferential stress to the winding stress at the different pirn radii for different size of the pirn and for different values of Poisson's ratio were obtained as outlined above. If the Poisson's ratio is zero, the minimum value occurs in the mid-radius and the residual tension at the core is equal to the winding tension. By increasing the Poissons's ratio, the minimum value is found to move close

to the core radius. Finally, the minimum value occurs at the core radius, when Poissons's ratio increases up to 0.5.

Beddoe [Beddoe 67] used the same approach to establish a theory of winding anisotropic elastic yarn on a thick-flanged tube in order to predict pressures on the tube and its flanges. He found that the modulus ratio, which he has defined as the ratio of Young's Modulus in the circumferential direction to that for radial and axial direction in the wound yarn, could be as high as 20. He calculated and constructed graphs with several different modulus ratios in the range 1-20. One of the graphs shows the variation of yarn radial pressure against to radius, the other is variation of yarn tension against radius. The pressure imposed by the wound yarn in the isotropic case(modulus ratio=1) is twice as much as when the modulus ratio is 20. Additionally, the maximum pressure at the tube to the minimum pressure at the outside of the completed beam in the case of high modulus ratio (20) is also twice as much as in the isotropic case. He found that the tension in the yarn, or distribution of circumferential stress, changes as the modulus ratio is increased. In the isotropic case, yarn tension increases linearly from a minimum value at the tube radius to the maximum value at the outer radius of the beam. At a modulus ratio of 20 (non-isotropic), the value of the ratio of the residual circumferential to the winding stress varies from 0.12 to 1. The minimum value (0.12) occurs at the radius of 1.3. The value of the ratio at the tube radius is about 0.75. The Poisson's ratio chosen for these calculation is 0.3. The yarn loses its tension at the tube radius due to Poisson's effect if the tube cannot be deformed radially. In the isotropic case, the pressure at the tube is highest, therefore the loss of yarn tension at the tube is also highest.

Nakashima et al [Nakashima 68] used a similar approach to Beddoe to find the stress distribution inside a flanged beam. They assumed that the yarn layer is a anisotropic elastic body. The modulus ratio is defined as the ratio of Young's modulus for the layer in the circumferential direction to that in radial direction. They calculated forces on the core and flanges of beam, tension distribution in the yarn package and the distribution of radial stress in the beam. These results were similar to those obtained by Beddoe.

Jhalani [Jhalani 70] carried out a computer simulation by combining the approach of Catlow and Walls with the geometry of the precision wound package. There are certain clear differences between a cross wound package and a parallel wound pirn. In a parallel wound package the axial component of the tension in the yarn is fairly small and can be considered to be zero. The circumferential stress of the added layer at the outer radius is constant regardless of the radius. In the cross wound package the tension in the yarn has two components, the circumferential and the axial due to the wind angle. In his study, he assumed that the cheese consisted of yarn layers of small thickness. Each layer is supported by a similar layer beneath it. Interlacing of the two layers is ignored and the contact between two layers is established at a multitude crossing points made by the threads of the two layers thus forming a cylindrical trellis. Two ends of the cheese are different from the central part of cheese due to the direction of thread at the two ends. Hence his theoretical solution was aimed at the central part of the cheese.

He considered the yarn package as anisotropic and nonhomogenous. Poisson's ratio is assumed negligible because the yarn is not close-packed as in parallel winding. Yarn is treated as elastic. The tension in the yarn is the only force acting on the yarn and acts along a tangent to the cheese. He made the solution in two stages. On the first stage, he assumed the modulus of compression of the cheese E and the elasticity of yarn in extension EY as constant, but in second stage, he treated them as variable particularly when the interyarn pressure is small.

A second order differential equation was developed to give the radial deformation of the cheese due to the pressure imposed by the added layer at the outer radius of the package. The equation was numerically integrated to give radial deformation at any radius of the package from core to outer radius. The boundary conditions for the solution are that the compression at the core which is assumed to be incompressible is zero and the pressure imposed by the added layer at the outer radius is known. As a new layer is added to the package, a new solution is made on the computer using the equation. The total compression of the cheese at any radius is equal to the combined compression of the cheese at that radius due to the addition of all the layers.

He plotted graphs of the dependent variables pressure within the package, tension in the yarn layers and the movement of layers for each of the independent variables considered. The variables used are winding tension, spacing at the adjacent wraps of threads, traverse per wind, the modulus of the compression E and the elasticity of yarn EY. The value of modulus ratio which is the elasticity of yarn in extension EY to the modulus of compression of the cheese E is a measure of the anisotropy of the yarn. The modulus ratio has a considerable effect on the behaviour of the cross wound package. A high value of the ratio brings about smaller values of the pressure, greater changes in the tension of the yarn, and the yarn may acquire 'negative tension'. Packages produced from low modulus ratio yarn showed a continuous increase in pressure with the increase in outer radius of the package and the value at the core is considerably higher than with the high modulus type. The tension would not reduce so much as in the former type and is not likely to acquire negative values.

He also found that the residual tension in the yarn, like pressure, depends on the modulus ratio of the yarn. With a high modulus ratio of yarn, the residual tension in the yarn falls sharply with radius near the core and quickly becomes negative showing the yarn in compression. After the initial fall it changes little with radius till it rises again near the outside of the package. With a low modulus ratio of yarn it falls gradually with radius till it starts rising from near mid radius of the cheese. Changes in the tension are comparatively smaller and the yarn tension is not likely to become negative.

In the second stage of simulation, the value of compression modulus and of elasticity modulus in extension are not constant especially when the loads are small, though at high loads the variation in them may be small. He took into account the variation of them in his modified theoretical solution. First he determined the relation between modulus of compression and pressure in the cheese and between the modulus of elasticity and the tension in the yarn. The second order equation was integrated numerically using a different computer program which was written in KDF 9 Algol.

His results in this stage were divided into three sections, each containing three solutions for three values of the winding tension. First, the modulus of compression E is assumed to be constant and the modulus of elasticity in extension EY is variable with winding

tension. The value of the modulus ratio at a given inner radius reduces as outer radius increases from the inner radius and reaches its minimum value as the tension in the yarn continues to fall. Then the modulus ratio at inner radius increases for some increases in outer radius due to the yarn acquiring negative tension as the compression of the cheese at inner radius continues with outer radius. Finally the modulus ratio becomes constant as further increase in outer radius does not effect the cheese at inner radius.

Next, a solution was obtained as the modulus of compression and the modulus of elasticity were assumed variable with pressure and tension respectively. He admitted that the program ran very slowly due to many trial solutions required. Quadratic interpolation was used instead of linear interpolation which was used in all previous solutions in the program. Another reason for slow progress was that many trial solution fail due to the value of the modulus of compression becoming very small or the value of incremental deformation becoming very large. He attempted to improve the solution by reducing the thickness of added layer, but a different solution to the problem resulted. He accepted that there were errors, which might be procedural rather than mathematical. And also the modulus of compression was set to a lower limit in the program in order to avoid the situation with near-zero force acting on near-zero resistance due to the lower values of pressure and the compression modulus at outer radius. The staring value of modulus ratio was very high and therefore the effect of the added layer was limited to fewer layers immediately beneath it. This prevented the build up of high values of pressure, the modulus of compression and radial compression, the tension in the yarn would not become negative at higher radius.

Last, he made solution, starting with a low initial value of the compression modulus. The starting values of the compression modulus were raised and this reduced the starting modulus ratio (EY/E) causing the tension to persist further into the package but then to change more rapidly and become negative. Also the values of pressure in the package, the radial compression and the variation in yarn tension inside the package are not proportional to the winding tension in the yarn due to the change in modulus ratio with increased in winding tension.

Jhalani commented that the theoretical analysis is not applicable to a random wound cheese because of basic differences in the two types of packages. The differences are that winding angle, the number of yarn in a given axial width, therefore the number of crossing points in the element which does not vary with a radius for the precison wound cheese. He added that it is not also applicable to a conical package, whether precision wound or random wound due to different geometrical shape and to a parallel wound package. In a parallel package, the contact between the wraps of yarn is line contact and changes to a surface contact in the deformed state.

Wegener and Schubert [Wegener, 68,69] give expressions for determining the pressure on the cores for precision and random wound cheese. The expression give the pressure at the some intermediate radius of the cheese. They assumed the tension in the yarn at that radius is the same. Adding a layer at the outer radius did not changed the tension at the particular element of the layer. But this assumption would be possible if there was no compression of the cheese at that radius. To find the pressure at the core radius, the expression is integrated between the limits of the core radius and the final outer radius of the cheese. The expression gave a rough idea of the pressures for calculation of the deformation at the cylindrical package.

Ursiny [Ursiny 86] attempted a calculation of the deformation of the package at a cross wound cylindrical packages produced on rotor open-end spinning machines. The package can be considered idealised as a compact pressure vessel so that the laws of linear elasticity apply and can be characterised by means of the constant average Young's modulus elasticity and the constant coefficients of lateral contraction (Poisson's effect). He assumed a constant package tension in the yarn to calculate the relative radial tension and the relative tangential tension which are a function of the radius according to the equation he derived.

He defined a degree of anisotropy which is square root of the young's modulus of elasticity in the tangential direction to that in the radial direction.

$$k = \sqrt{\frac{E_t}{E_r}}$$

where E_t – the Young's modulus of elasticity in tangential direction.

E_r – the Young's modulus of elasticity in radial direction.

The results were plotted and this showed that radial tension increases from zero at the outer radius of package to the maximum at the core. On the other hand, the tangential tension falls at certain intervals from the core down to negative values and increases to the outer radius of the package. The results are similar to those reported by other researchers.

While the above researchers have tried to find a suitable theoretical approached for pressure and deformation at a cylindrical package, some of them have designed methods for measuring radial and axial deformation of a cross wound package.

Wegener and Schubert [Wegener 69] inserted aluminium foil strips inside the package at different chosen radii when the package was prepared for measuring the radial deformation of a cheese. They measured the position of each foil strip and recorded them. This is repeated during winding and then during unwinding. Analysing the record gave the total and permanent deformation at the cheese. When the radial deformation of the cheese plotted against the radius of the cheese, the maximum total deformation of about 1.4% occurs at a radius of about 9 cm. The permanent deformation of about 0.7% at the radius of 9 cm is more than half of the total deformation.

Jhalani [Jhalani 70] has also used similar method but in a different way for measuring the radial deformations of the package. A resistance strain gauge wire placed on the circumference of the cheese shortens along with the circumference of the cheese at a radius chosen on his experiment as the cheese built up. The change in the length of the wire was estimated by the change in the resistance of the wire. A slotted paper which has different crimping behaviour comparing the ordinary paper was wrapped around the central region of the package. The gauge wire was wound on top of it. Two strips of copper foil were soldered to the ends of the gauge wire as the leads to be connected to the measuring unit. The winding was continued, the resistance of the gauge was measured after 10 mm increase in radius of the package. The change in resistance of the gauge was calculated and it corresponded to the amount of compression received at that particular radius where the gauge was placed. Measurement were taken for both winding and unwinding of the package. The results showed that permanent radial

deformation of the cheese at any radius is nearly half of the total radial deformation of the cheese at that radius as the cheese was built up to a given outer radius. Initial winding at that radius gives a quick, large initial compression of the package. As winding continued further, there is little increase of compression and there is a tendency for it to stay constant. These results were in agreement with Wegener and Schuber's results. They used a different method to find radial deformation, and different yarn materials. Both above investigations agree that permanent radial deformation at any radius is approximately half the total deformation at that radius.

Law [Law 80] set up similar methods with Wegener and Schubert for measuring the radial and axial deformation of the cheese during the winding. In his research, several kinds of yarn were used and their properties such as the modulus ratio were measured. His results from the radial deformation tests for types of yarn were of similar nature. For any radius of the package, initial winding at that radius gave a quick initial compression, this compression became very little as the winding carried on. The magnitude for radial and axial deformation varied with different types of yarn. The greatest deformation took place at the region about midway between the core and the outer radius. These results were of similar shape as those by Jhalani. Finally, he claimed that the radial deformation always shows a reduction in radius. The greatest value of it occurs at any radius soon after initial winding at that radius, then gradually becoming constant. The axial deformation mostly concentrated near the package ends.

1.10 Slippage between the drum and the package

As mentioned before, a random wound package is driven by a winding drum. The package is rotated solely by virtue of friction which is present at the area of contact between the two bodies. It seems that some slippage between these two bodies in contact is inevitable. Very few researchers have reported study of slippage in random winding.

Osawa and Koyama [Osawa 72] studied the slippage between grooved drum and forming packages while cotton yarns were wound into a cylindrical cheese. They measured the slippage on their experimental random winding machine by varying the yarn tension, the pressure between drum and package etc.

They admitted that there is slip between them and the slip is usually within 5%. The slip is caused by the resistance against the driving torque of the drum. It is affected by the yarn tension, the friction at the spindle-bearing, the air resistance, the resistance of the inertia of the package and the deforming resistance of the package.

Their finding was that yarn tension during winding affects the slippage when comparing the slippage between with feeding the yarn to the package and without feeding any yarn. The slippage was also dependent on the pressure between the drum and the package. At the very low value of pressure (less than 0.5 kg), slippage is more. They also indicated that the deformation of the package, which is the decrease in the radius of package at the point of contact, should affect the slippage. Their later work [Osawa 76], concerned two types of slippage, sliding slip and elastic slip, that occur simultaneously. Sliding slip is the relative speed when two rigid bodies contact each other and their surfaces move at different speed. Elastic slip is the other type of speed difference that occurs between two bodies moving in contact because of their elastic deformation. On the random winding, the drum is accepted as a rigid body but the yarn wound package is a deformable cylinder of fibrous material. They set up an apparatus and method of experiment for analysing slippage and resistance torque of the package. There is relation ship between resistance torque and slip. As the resisting torque increases, the slip between the drum and the package increases. Moreover, there is relation between resisting torque (M) of package and slip rate(η) at different values of RPM of drum. This was plotted on a graph. The inclinations of M-η lines change at M=30 g.cm(=M1). Torque M1 is the transient point from elastic to sliding slip They claimed that the package deformation at the contact point would be maximum at that M1 of resistance torque. When the value of the resistance torque is below M1, the slippage would be elastic slip and when the resistance torque is above M1 , the slippage would be sliding slip.

1.11 Aims of the present research

The different winding processes are quite important for the subsequent processes of the textile industry. Better quality of wound packages are aimed at by researchers and winding machine manufacturers. Most of the reported work has been on the precision wound package perhaps because the structure of the random wound package is more

complex than that of the precision wound package. As the random wound package is used widely, there is a case for carrying out research on it.

The project was started with the intention of applying mechatronic control to the basic random winder to realise a system which achieves 'active' ribbon breaking as identified in the following chapters. As the apparatus conceived was capable of carrying out considerable measurements concerning the winding process, a number of objectives were identified as part of the study.

Aims of the present work :

- analysis of the structure of random wound packages
- investigating the slippage between drum and package
- evaluation of ribboning or patterning during winding
- active avoidance of ribboning
- examining the effectiveness of different anti-ribboning procedures
- computer simulation of the random wound package.

The structure of the package relates to the manner in which successive turns of yarn are deposited and such physical properties as the resulting density distribution within the package. The rotation of the yarn package by friction by the grooved drum naturally poses the question about the nature of any slip that exists between the elements during the progress of winding of a package. Once the experimental winder was equipped with shaft encoders and these were interfaced to the PC, it was realized that the above determinations could be carried out with considerable ease under program control. So the first two objectives above arose out of preliminary work with the apparatus.
The next three objectives may be considered of primary interest as the work was mainly directed at achieving a better ribbon breaking method. During this early work it was also clear that the apparatus could be used to determine the number of double traverses of yarn wound at each layer (thickness) of the package. This information would make it possible to extend the work on the simulation of package winding carried out by an earlier worker applicable to precision winding, to the case of random winding. This is how the last objective was identified.

CHAPTER TWO

INSTRUMENTATION OF THE RANDOM WINDER

2.1 Introduction

To be able to effectively analyse a random wound packages, it is important to be able to wind such packages under controlled conditions. The basic winder as described below has hardly any instrumentation provided on it as standard. This project therefore required the addition of a range of sensors and actuators to configure the winder into an apparatus that was capable of carrying out the planned experiments as described in the following chapters.

This additional instrumentation provided includes some equipment that are mounted directly on the winder, and some that are stand alone or of an auxiliary nature

The instrumentation that was devised is described in this chapter. Additional details on the electronics used are provided in Appendix A.

2.2 The Random winding machine

General information about random winding and random winding machines are given in Chapter 1. The winding machine used in this work is Autoconer type GKN produced by Schlafhorst. The machine had been acquired by the School of Textile Industries in 1967. The machine basically has a winding unit and a tensioner assembly.

2.2.1 Winding unit

The winding unit consists of a grooved drum, a control housing and a package holder. The drum is driven from the main shaft of the machine through an intermediate roller and can be displaced laterally to give soft edges to the packages. The drum is 90 mm in diameter and its length is 125 mm, and the drum constant (number of drum rotations per double traverse) is 3. This machine avoids patterning by changing the speed ratio between the grooved drum and the package at random intervals. Basically, the intermediate roller is pulled away from the drive shaft roller in order to interrupt the

drive to the drum every 2 seconds. The drum loses speed during this, and the slippage that occurs between the drum and the package as the drive is re-engaged disperses turns of yarn, thereby effectively diminishing the intensity of any patterning.

The package cradle holds the tube, and keeps it in contact with the grooved drum under some pressure. Increasing package weight is compensated by a relief system on the package holder for uniform and constant pressure throughout the winding process. The pressure between the package and the winding drum is one of the factors that determine the package hardness, the other being the yarn tension. There is a screw for the adjustment of the pressure used.

The winder had been originally equipped to wind cones. For this work, the package cradle was modified to allow the mounting of cylindrical tubes, so as to be able to produce cylindrical packages. This modification mainly amounted to the provision of an adapter to enlarge the tail side of the tube holder. The control housing contains the controls for the stop motion, lateral displacement, anti-patterning and performance control. Mostly the system runs mechanically.

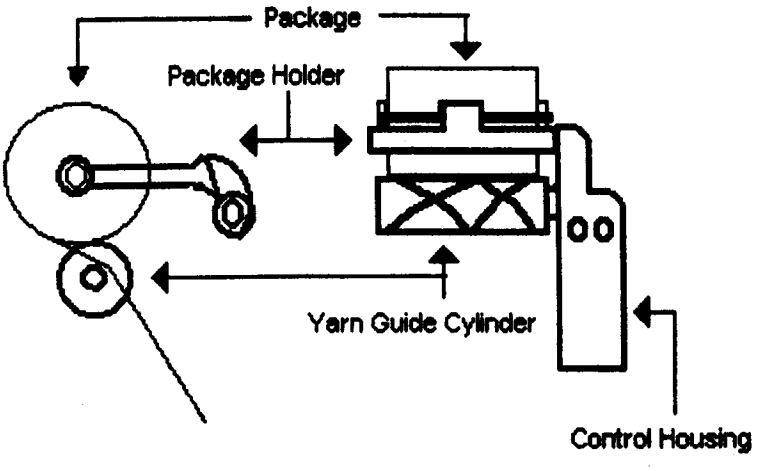

Fig 2.1 Configuration of the winding unit

2.2.2 Tension Assembly

The tension assembly consists of the following parts in the yarn path as shown by Fig. 2.2: threading plate, pre-clearer, gate feeler, tension device, yarn guide plate. The threading plate assists the yarn to be guided through the other elements of the tension assembly. The pre-clearer strips coarse and loose impurities from the yarn without damaging it. The slot width in the pre-clearer is adjustable from 0.5 mm to 1.5 mm. The gate feeler feels the presence of the yarn. The tensioner is important in that it applies sufficient tension to the yarn so as to break weak places of it, and give the desired package density. The tension is created by pressing the tension shoe that holds the yarn against a tension disc under the predetermined pressure of the spring to suit the yarn being wound. There is a small electric motor that drives the tension disc at a speed of roughly 375 rpm to achieve self cleaning of the tensioner during winding.

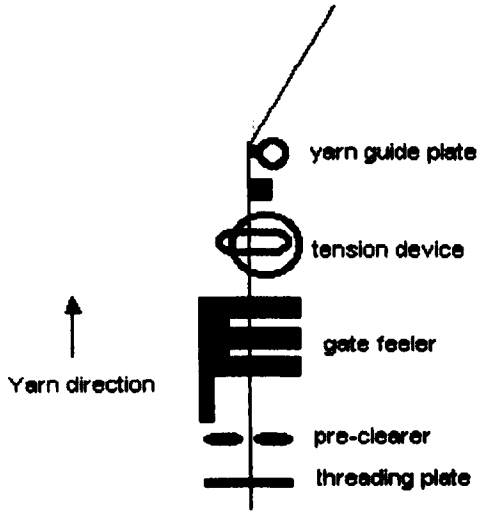

Fig 2.2 the tension assembly

2.3 Description of the apparatus

2.3.1 Yarn compression (thickness) tester

Early in this work, it was intended that a computer simulation of yarn package formation would be carried out, and this necessitated knowing the transverse modulus of the yarn, in addition to its longitudinal modulus. However the transverse modulus is

dependent of the transverse pressure acting on the yarn, and hence required the construction of a suitable apparatus to measure it.

A yarn thickness tester constructed using a linear eddy current proximity sensor was used to measure the thickness of layers of yarn so placed on the tester as to provide a number of intersecting points. The results of the measurements were used to obtain the relationship of load per intersecting point vs. deformation from which yarn transverse modulus can be determined over a range of loading values.

2.3.1.1 Description of the yarn thickness tester

The thickness tester was constructed using an inductive proximity sensor [Distec Instr.], which was readily available. The sensor has an associated amplifier module giving a voltage output which varies directly as the distance between the face of the sensor and a steel target placed before it. The sensor used has a measuring range of 2 mm, and this was considered adequate for the purpose.

The tester as shown by Fig. 2.3 has the proximity sensor mounted on the top surface of a die-cast metal box, chosen for convenience of use and its sufficient rigidity. To prevent the sensitivity of the probe from being reduced by the metal of the housing itself, the sensor was placed at the centre of a 25 mm diameter hole made at the centre of the top of the housing. This necessitated the adoption of a loading plate 'target', shaped as shown in the figure. The rectangular bearing surfaces of the plate give two equal areas of 10 cm^2 each. The actual area is not of consequence for yarn thickness measurement, but simply the yarn intersections concerned should lie within these areas.

2.3.1.1.1 Non-contact displacement measuring system

The proximity sensor is a device [Distec Instr.], supplied by Graham&White Instruments Ltd, consisted of two parts, probe and signal conditioning unit. The probe measures the gap between its tip and the surface of the target plate. The signal-conditioning unit provides the probe with a constant high frequency signal. The output could be fed into a readout equipment such as an oscilloscope or a voltmeter. The necessary power for the signal-conditioning unit is –18 V. The specifications of probe involved, type 375-1, is given in Table 2.1

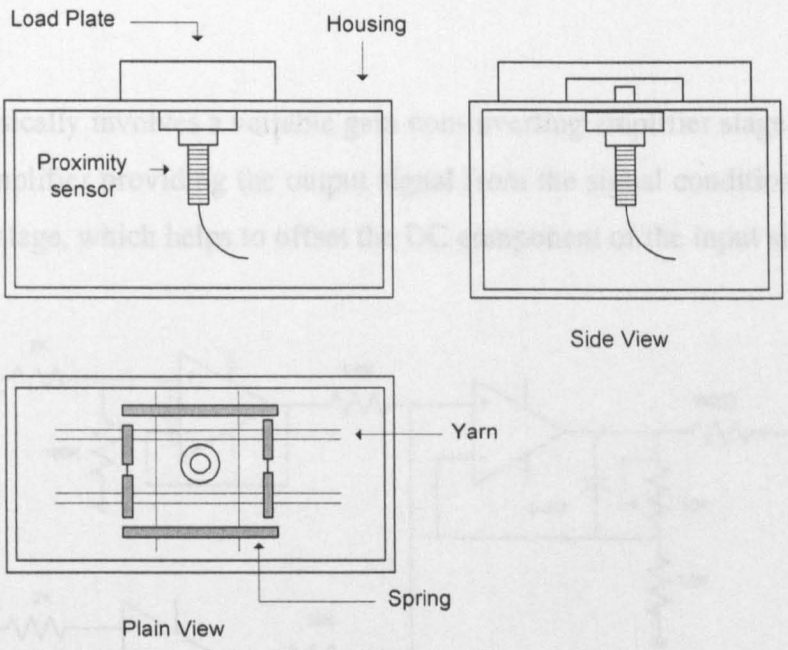

Fig. 2.3 Configuration of the Tester

Specification of probe	Type 375-1
Typical Displacement Range	0.006"
Temperature Range	-29 ^{0}C to +80 ^{0}C
Coil Material	Copper
Probe Tip Diameter	0.300"
Face Material	Fibreglass
Body Material	Stainless Steel
Thread Size	3/8" U.N.F.
Probe Length	1" standard

Table 2.1 Specifications of the probe

2.3.1.1.2 Circuit Diagram

The output of the signal conditioning unit required further amplification for measurement purposes, so an additional amplifier was built around the LM348 operational amplifier. This IC consists of four independent, low power operational amplifiers which are similar to the familiar 741 operational amplifier. The IC requires a

bipolar power supply giving +15 , 0 and –15 volts. The circuit diagram adopted is given by Fig. 2.4.

The circuit basically involves a variable gain non-inverting amplifier stage, which is fed by a buffer amplifier providing the output signal from the signal conditioner, and a DC level shifting stage, which helps to offset the DC component of the input signal.

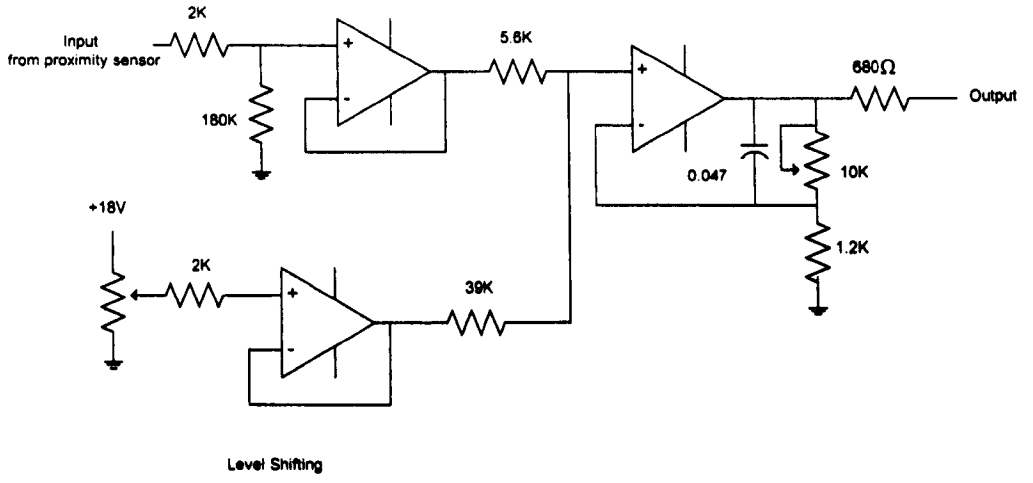

Fig 2.4 Circuit diagram of the yarn thickness tester

2.3.1.1.3 Power Supply

A power supply was built to provide the necessary power to the signal conditioning unit and the amplifier circuit. It produces +15 V, -15 V, 0 V and –18 V. The circuit diagram of power supply is given in Fig.2.5. The –18 V line is for the signal conditioning unit whereas ±15 volts are for LM348.

2.3.1.2 Calibration of the yarn thickness tester

The output signal voltage is level shifted and amplified so as to give the calibration curve given by Fig. 2.6. The calibration was carried out using a number of steel shim strips of precise thickness placed under the target plate. A number of steel shim strips in the range of No. 5 (0.05 mm) to No. 45 (0.45 mm) were employed to give different separations between the sensor and the target plate. The output corresponding to each shim strip assembly was read four times using a digital voltmeter, and the average taken. Using linear regression, the equation of the relationship between thickness and

Power Supply for Compression tester

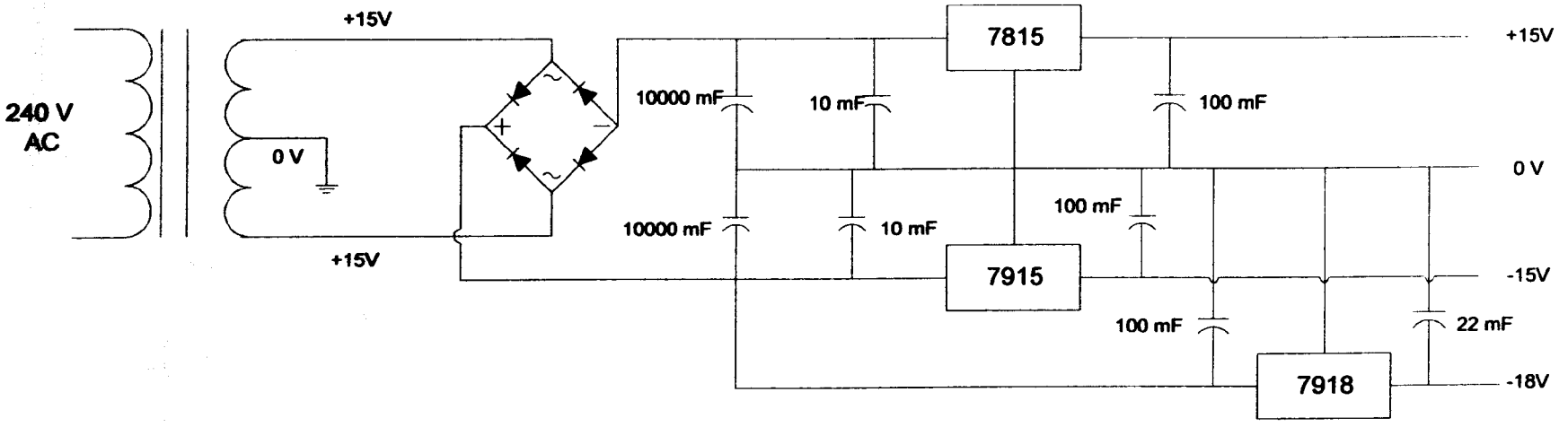

Fig 2.5 Power supply for the yarn thickness tester

the output voltage was obtained. This formula is valid for all yarn thickness experiments carried out.

The formula is as follows.

Thickness (mm) = 0.006 + 2.9363E-2 * Voltage (volt)

The thickness of shimmy (1mm=100)	The average output voltage (volt)	The thickness (mm)	The average output voltage (milivolt)
45	15.325	0.45	15325.0
40	13.7025	0.4	13702.5
35	11.545	0.35	11545.0
30	9.7175	0.3	9717.5
25	8.17	0.25	8170.0
20	6.4675	0.2	6467.5
15	4.8975	0.15	4897.5
10	3.1175	0.1	3117.5
5	1.5925	0.05	1592.5
0	0.05	0	50.0

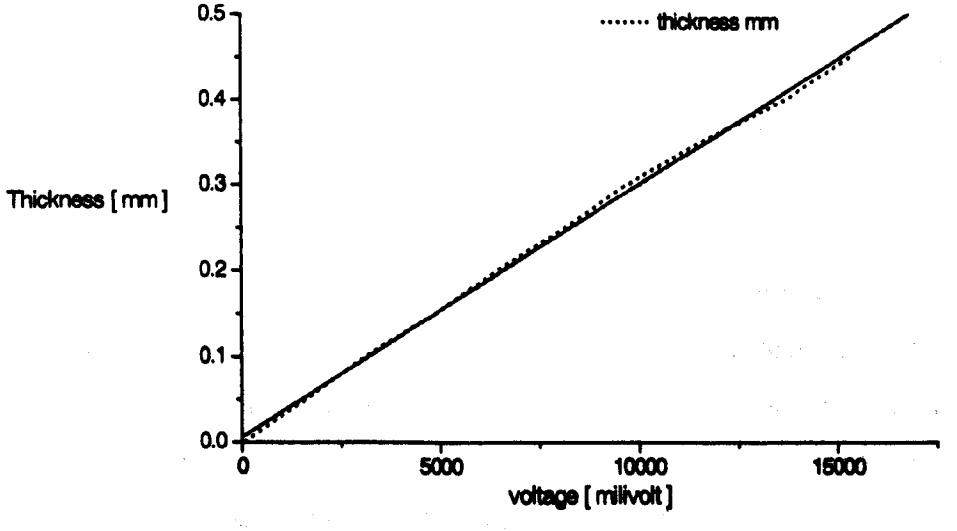

Fig 2.6 The calibration curve of tester

2.3.2 Yarn Tension Measurement

Yarn tension is of essential importance in yarn winding. A single yarn tension probe was used to measure yarn tension as yarn was wound on the package. The device used employs a strain gauge based cantilever arrangement, and has a natural frequency of 2.5 kHz. It is therefore capable of measuring rapid variations of yarn tension that occur in the yarn during winding.

2.3.2.1 Yarn tension probe

The single yarn tension probe used in this work is a strain gauge based device. It uses a short cantilever made of duralumin. The cantilever is rigidly clamped to the body of the instrument at one end, and carries a 1.5 mm dia. ceramic pin. The cantilever tapers towards its outer end in order to minimise its mass and to retain the high degree of stiffness. Four strain gauges are bonded to the cantilever close to its base so that two of them undergo extension in response to yarn tension, while the other two undergo compression. The ceramic pin works in conjuction with two fixed ceramic guides so as to load the cantilever under yarn tension according to the well known 3-point loading principle.

The gauges are connected in a full Wheatstone bridge arrangement so as to achieve maximum sensitivity to yarn tension variations. This is important as the deflection of the cantilever under the low values of yarn tension involved (2-50 g) will be quite small. The signal produced by the bridge is only a few millivolts, and is required to be amplified with a gain of the order of 1 k, so that a large enough signal is produced for measurement using a standard multimeter or oscilloscope.

Since the gauges are in thermal balance by virtue of there being bonded to the same metal body (cantilever), the main problem in amplification is keeping electrical noise pickup to a minimum. This is achieved to a satisfactory degree by the use of screened cabling, whereby the case of the probe is electrically earthed. A standard DC amplifier specially made for use with strain gauge bridges is used for this purpose (RS 435-692]. The amplifier also powers the bridge. In fact the electrical gain of the bridge can be set by adjusting the bridge supply voltage. Once this is set at a suitable value, the load

calibration of the probe is done using a variable resistor which directly sets the gain of the amplifier.

Using the storage oscilloscope the natural frequency of the probe was found to be about 2.5 kHz. Since the tension fluctuations of yarn involved are generally of a much lower frequency, this ensures that the output signal of the probe are free of gauge resonance effects.

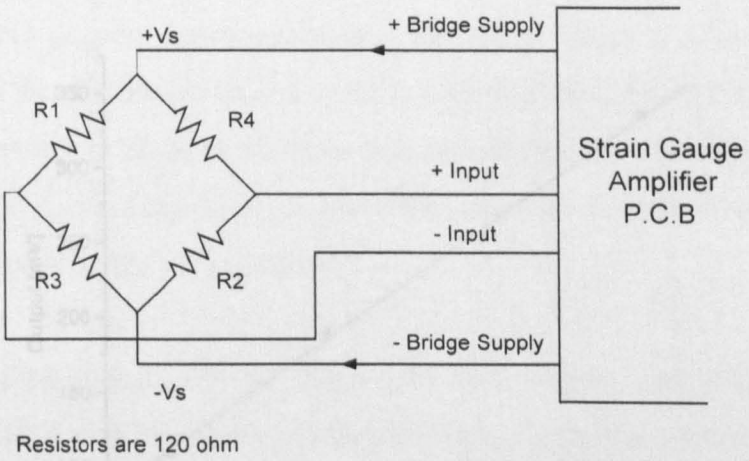

Fig 2.7 Wheatstone bridge arrangement of the tension probe

2.3.2.2 Calibration of the yarn tension probe

The probe, as shown by Fig. 2.8, has a central ceramic pin, which senses the tension of the yarn which is guided by the two ceramic guides on each side of the pin. The probe was mounted on a stand so as to place it in the yarn path. The probe was calibrated as shown by hanging weights from a yarn placed in the probe as shown by the figure. The output voltage of the device was measured on the oscilloscope as shown by Fig. 2.9.

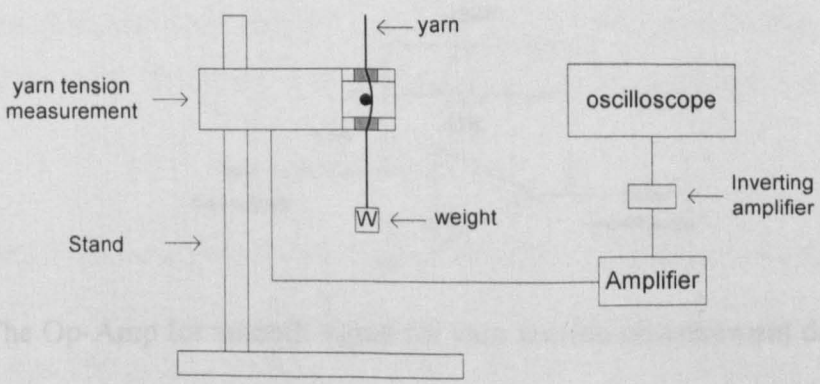

Fig 2.8 Set-up to calibrate the single yarn tension measurement device

Weight (g)	Output (mV)
25	110
50	190
75	255
100	335

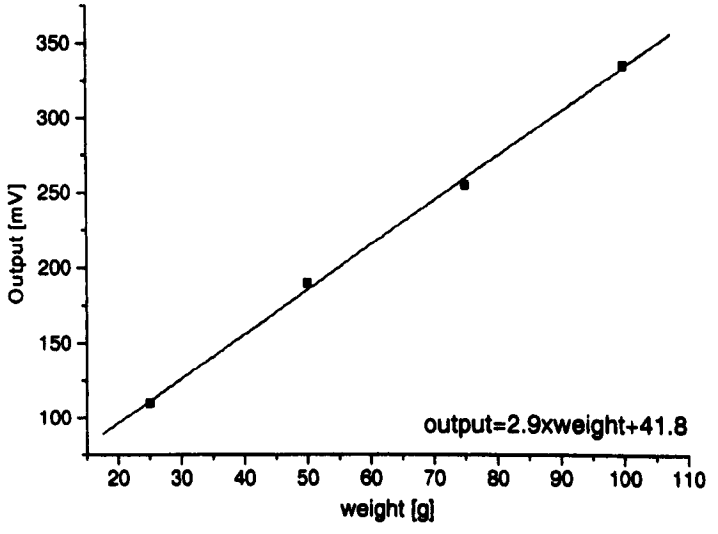

Fig 2.9. Calibration of yarn tension measurement

When the device is used for measuring winding tension it was found that the yarn tension was in fact of a fluctuating nature. Since only the mean tension of the yarn is mostly of interest, the small additional circuit was added to the output of the main amplifier, so that a smoother output proportional to the mean tension was obtained.

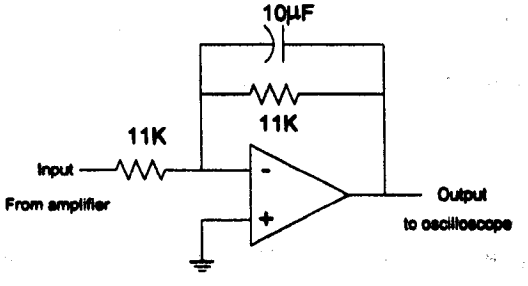

Fig 2.10 The Op-Amp for smooth signal for yarn tension measurement device

2.3.3 Shaft Encoder

In order to follow the progress of the winding of a yarn package, it is very useful to be able to track the rotational positions of the drum and the package continuously when required. It is therefore necessary to introduce shaft encoders on the drum and package axes.

Optical shaft encoders are the most convenient for this purpose, and they produce information about angular displacement in digital form. There are two main types of encoder device; the absolute encoder and the incremental encoder. In this project, it was considered necessary to place an absolute type encoder on the drum shaft. For reasons of simplicity and also greater freedom from false readings, it seemed better to place an incremental encoder on the package shaft.

The principle of the optical shaft encoder is as follows. A glass disk is rigidly connected to the input shaft. A precise pattern of concentric rings is printed on the disk. Each ring is divided into alternate dark and clear segments equal to 2^n, where n is the number of the ring counted from the innermost. A light source is collimated, focused and projected through the disk from one side and is detected by a photo sensor place behind each ring. The pattern of illumination of the sensors depends on the angular orientation of the disk. As the shaft rotates the light source faces different patterns and the photo sensors produce a binary output depending on this pattern. A shaft encoder with 8 concentric rings will provide an 8-bit output of its position and hence resolve a revolution of its shaft into 256 parts [Sternheim 89].

2.3.3.1 Absolute Shaft Encoder

An absolute-shaft encoder provides a unique binary word corresponding to the angular position of its shaft. The output signal produced is in straight binary or in grey code form.

The absolute encoder chosen to determine the position of the groove drum is an 8-bit device. A full cycle of shaft rotation gives readings in the range 0-255 (i.e. divide a revolution into 256 parts). On the winder the encoder was so fitted as to give a 0 reading

when the yarn is on the extreme left side of the grooved drum, as this gave a convenient reference as the start of a double traverse.

A difficulty associated with an absolute encoder is that, when a microprocessor reads its output, the reading may contain some inaccuracy due to the simultaneous changing of one or more bits. There are various encoding patterns that are normally incorporated on the disc to minimise errors.

The specifications of the particular device used are given in Appendix A.1.

2.3.3.2 Incremental Shaft Encoder

An incremental shaft encoder is basically similar in construction to the absolute type device discussed above, but is simpler in that it provides a single bit output as its shaft is rotated. The encoder disk is again divided into a number of segments which is a power of two. Thus an incremental encoder may divide a complete rotation of its shaft to 256 or 512 divisions. However an external counter is necessary to be incorporated with an incremental encoder, so that the amount of rotation undergone by it can be determined. The total count of this counter can be zeroed at any arbitrary position of the shaft encoder, hence the incremental nature of the reading obtained with this device. However an incremental shaft encoder normally has two other outputs; one to indicate the completion of each rotation and the other which is similar to the normal output as indicated about, but in quadrature with it.

A 512 count incremental shaft encoder was attached to the package shaft on the experimental winder. The device was however used to produce an 8 bit reading of its position by feeding its output into a divide by two counter, and reading only the Q2 to Q9 outputs of it, as shown by Fig. 2.23. The particulars of this device are also given in Appendix A.2.

2.3.4 Measurement of package diameter and compression

2.3.4.1 Linear variable differential transformer

A Linear Variable Differential Transformer (LVDT) was used to measure the package diameter while the package was on the drum. LVDT consists of one primary winding and two identical secondary windings connected in series opposition. A movable magnetic armature attached to a brass push road takes place between the primary and secondary windings. When the primary winding is excited by AC supply voltage the combined output of the two secondaries represent the difference between the voltage induced in them. The relative position of the magnetic armature in the coils shows the radial displacement of the wound package. Fig. 2.11 shows the electrical diagram of the LVDT used in this work.

Fig. 2.14 and Fig. 2.15 also show the circuit diagram of LVDT.

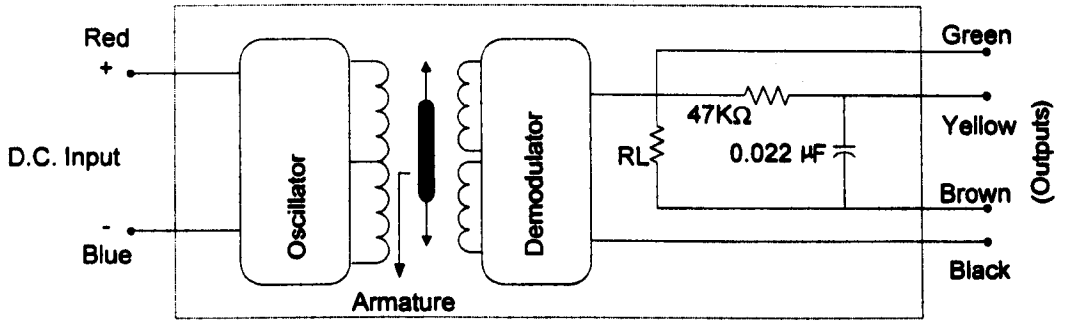

Fig 2.11 Schematic diagram of the LVDT

The LVDT was mounted on a plate on the machine frame as shown Fig 2.12, so that its probe sensed the height of the package centre. As a result, what it actually measures is the compresses radius of the package on the grooved drum. As the package undergoes some compression against the grooved drum due to the pressure imposed on it during winding, knowing the compressed radius of the package is of importance.

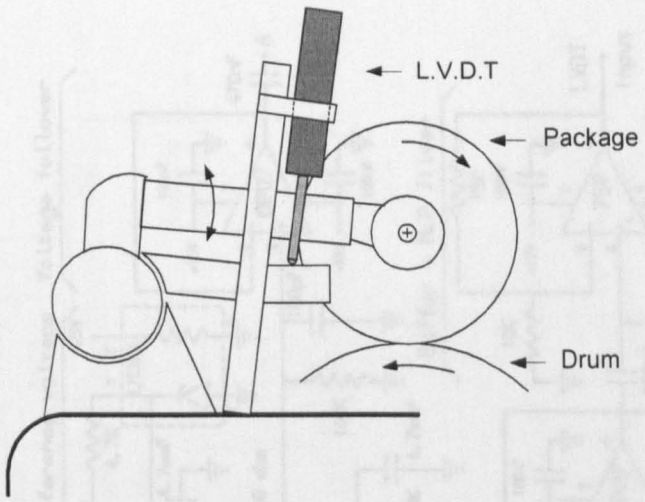

Fig 2.12 The method of measuring deformed wound package radius

2.3.4.2. Potentiometer

A potentiometer (POT) was adopted for measuring the un-deformed radius of the yarn package by sensing the outside surface of the package using a wide aluminium roller. The roller is attached to a light radius arm mounted on the potentiometer shaft. The potentiometer is mounted as shown in Fig. 2.13, so that it rides on the package surface without deforming it. The potentiometer chosen requires very little torque to turn it, and hence does not cause the roller to compress the package.

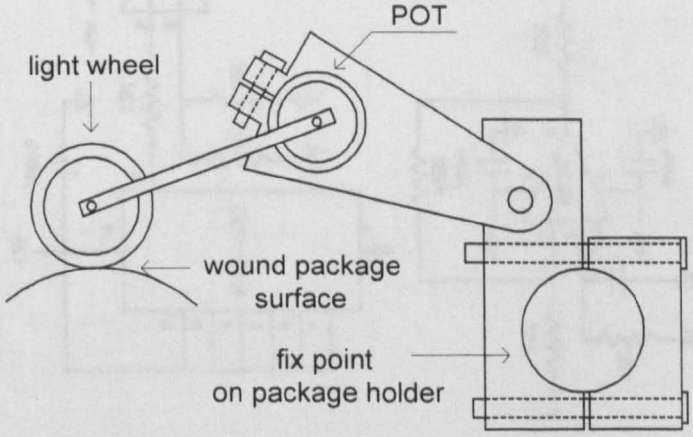

Fig. 2.13 The method of measuring un-deformed wound package radius

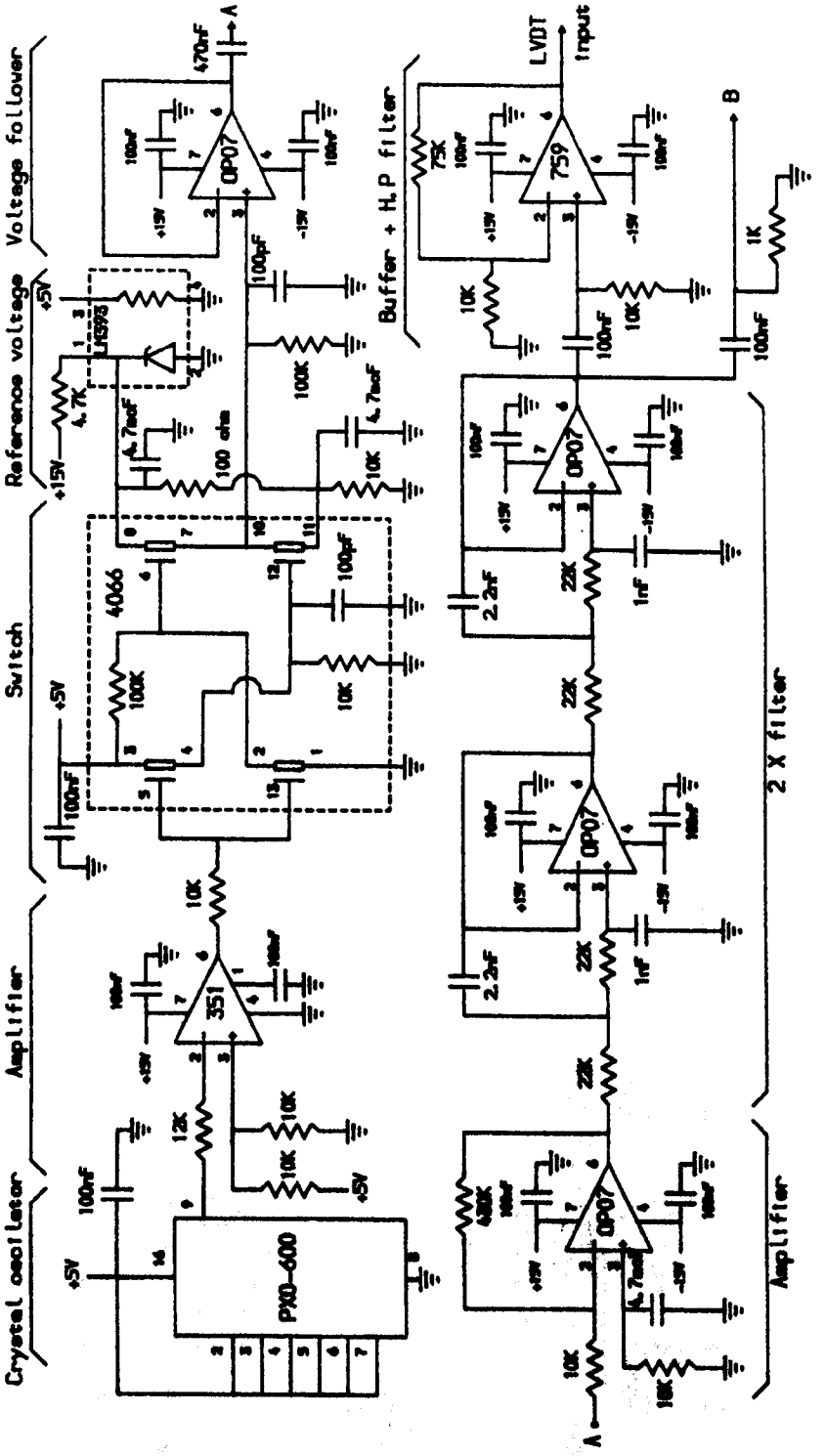

Fig 2.14 L.V.D.T excitation and summing junction circuit diagram (I)

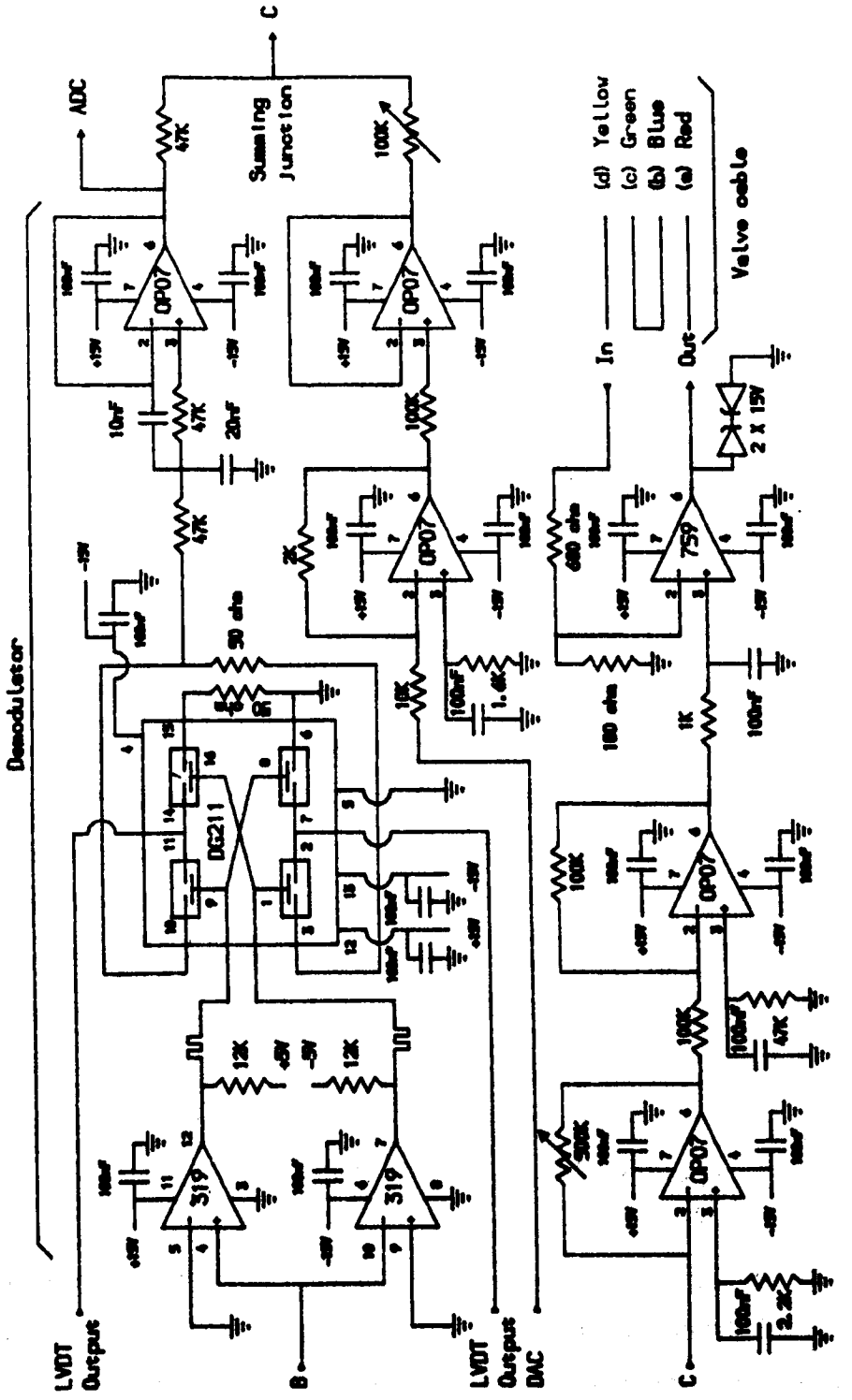

Fig 2.15 L.V.D.T. excitation and summing junction circuit diagram (II)

There are three terminals on the POT. A constant voltage of 5.0 V is applied to the main terminals of the POT. The central terminal, connected to the slider, provides a signal proportional to the position of the roller, and hence a measure of the undeformed radius of the package.

2.3.5 Interface Card

The interface card enables the connection of the signals produced from the different sensors and amplifiers provided on the winder. It fits into one of the expansion slots in the mother board of the PC. There are two common types of signal, analogue and digital. Analogue signals vary continuously in amplitude and time, and can be carried by a single conductor. Digital signals are usually in binary, which means each such signal will have a number of bits (binary digits), and requires a corresponding number of conductors to carry them.

The interface circuit is based on the IBM prototype board [RS 435-686].The circuitry on the board is provided to buffer and decode relevant signals to simplify the interfacing of the board circuitry to the PC system and a grid matrix area is provided to facilitate the development and construction of electronics circuits. The signal from shaft encoders are available in binary form. Their 8 output lines are connected to port A of the interface card. The computer can read the shaft encoders directly by addressing port A. The L.V.D.T and the POT signals are sent to the Analogue Digital Converter (A/D). The A/D circuit is based on chip ZN448 in a bi-polar configuration with an input range of ± 5V. The outputs from Brushless motor and the stepper motor are taken from a Digital to Analogue converter (D/A); based on chip AD558N and latch 74LS373. The D/C gives an output of 0-5V for converted number of a 8-bit number 0-255.

The computer receives information from the system through the channels of the interface circuit, for controlling the operation of the system; mainly the absolute and the incremental shaft encoder, LVDT and POT, stepper motor and brushless servo motor as shown in Fig 2.16a and Fig 2.16b.

In this work, the output of both shaft encoders was connected to the interface card. The data were buffered and can be read by the computer on the specific addresses. The

outputs of the LVDT and the POT were also connected to the interface card. Both output signals were converted from analogue into digital by two eight-bit A/D converters on the board. Moreover, when necessary the output from the computer can be converted into analogue by the D/A converter chip. Each device connected to the card has a specific address used by the microprocessor in addressing it. The interface circuit diagram is given in Fig 2.17 and the actual addresses assigned to devices is given in Table 2.2.

HEXADECIMAL	DECIMAL	CHIP OPERATION
300	768	Start conversion of A/C
301	769	Read POT A/C
302	770	Write brushless motor D/A
303	771	Write stepper motor D/A
304	772	Read absolute SE A/C
305	773	Read incremental SE A/C
306	774	Read L.V.D.T A/C

Table 2. 2 Addresses used by the interface card

2.3.6 Calibration of the LVDT and the POT

Several methods of calibrating the above two devices were considered before adopting the method described below. Several wound packages were prepared to a number of different outside diameters, which fitted snugly inside a rigid card board tube of a corresponding diameter, cut to the same length as the package. A metal sleeve was attached to a normal winding tube as shown by Fig. 2.18. This together with the 4 larger tubes provided 5 'gauges', using which the LVDT and the POT could be calibrated. The hard surfaces provided on each gauge minimised the oscillation of the POT as the grooved drum was rotated during calibration.

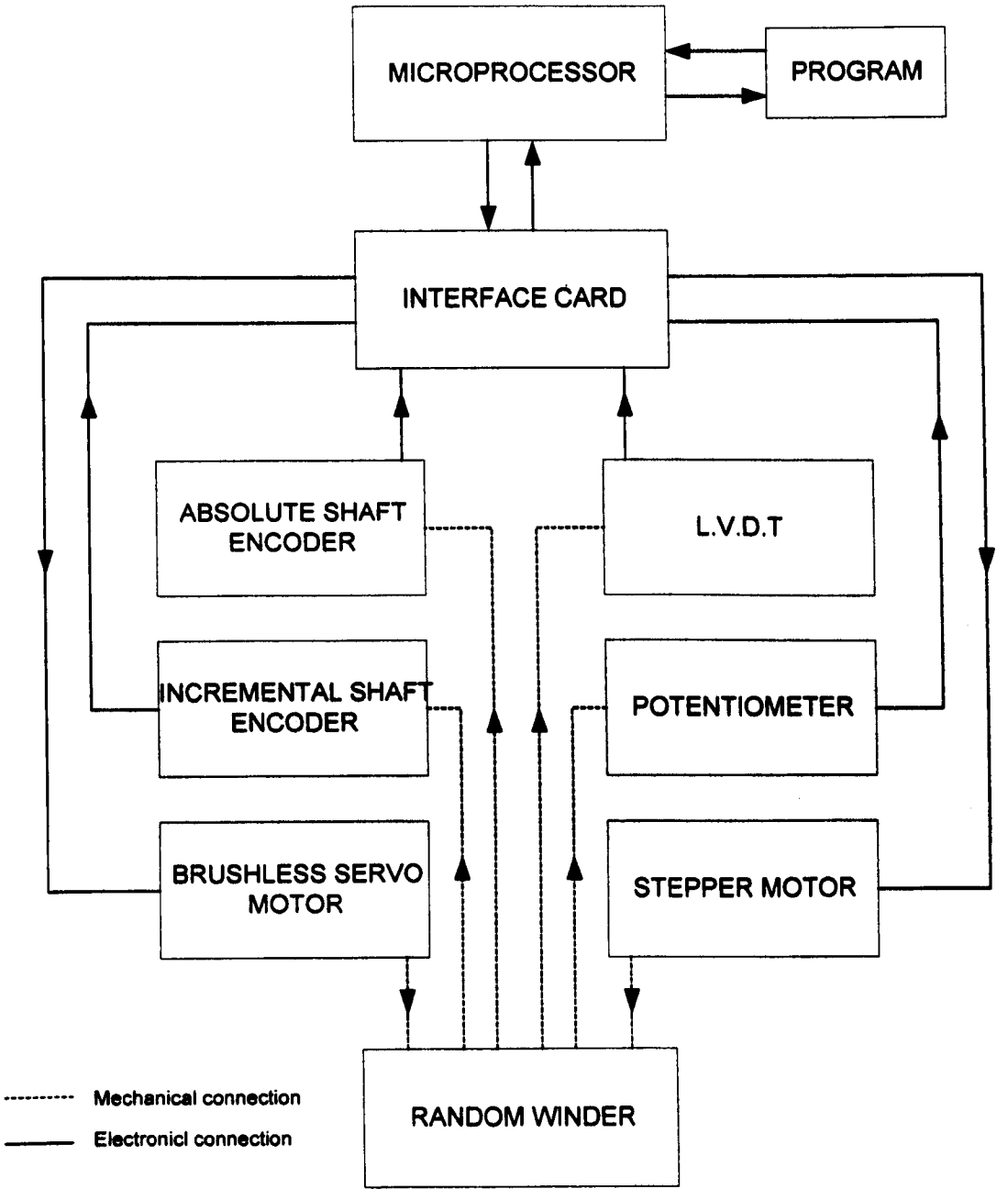

Fig 2.16a Electronic and Mechanical connections of devices

Fig 2.16b A view of winding machine

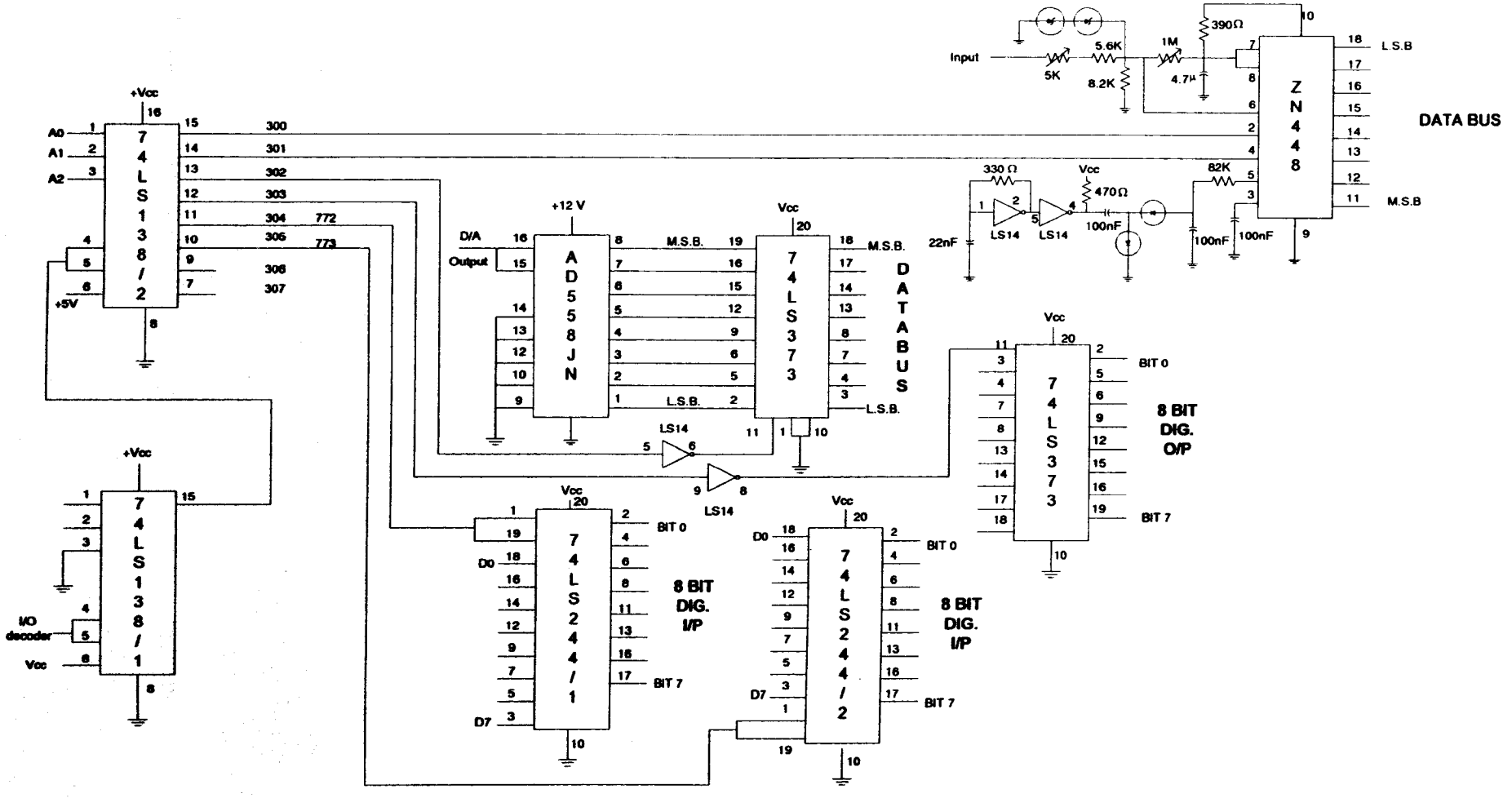

Fig 2.17 Computer interface circuit diagram

The calibration of the POT and the LVDT were done together as the grooved drum was allowed to run slowly. A program was written in 'C' to read the position of LVDT and POT and display the results on the monitor of the PC. The program is given in Appendix C.1. All readings taken were saved and plotted on the graphs.

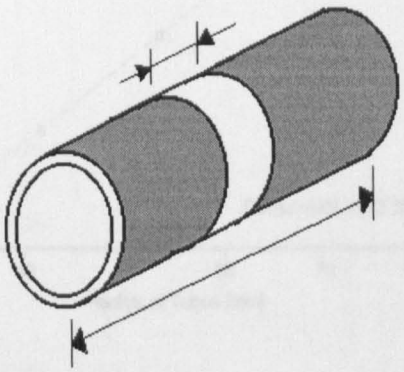

Fig 2.18 The original tube with a metal sleeve

The results of the calibration procedure are given below in Table 2.3. The corresponding graphs are shown in Fig. 2.19a and 2.19b.

	LVDT reading (binary value)			**POT reading (binary value)**		
Radius	**2 kg**	**1.25 kg**	**0.7 kg**	**2 kg**	**1.25 kg**	**0.7 kg**
30	24.3	24.7	25	16.3	16	15.9
41.8	65.7	66.1	66.6	59	58.5	59.2
53.8	109.7	110.2	111.2	97.8	97.1	97
62.6	142.6	142.9	143.9	127.9	127.5	127.5
77.9	200.9	201.9	202	175.4	175.6	175.9

Table 2.3 Calibration data of LVDT and POT read from computer

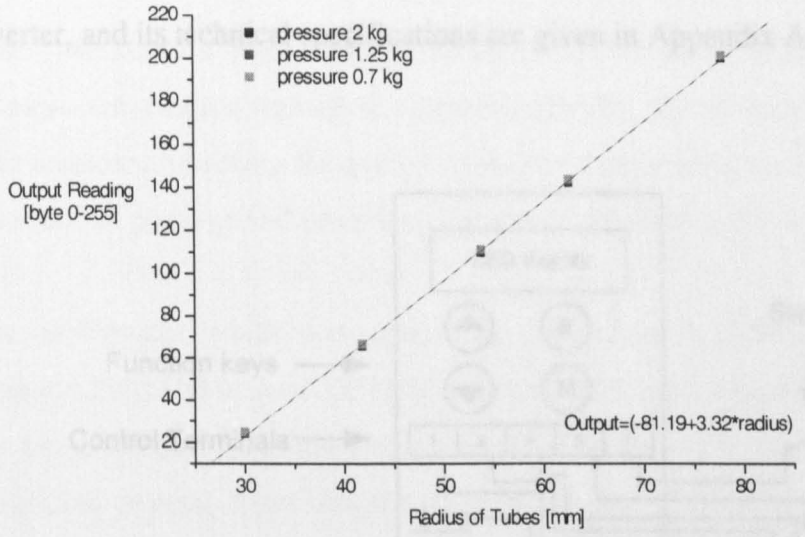

Fig. 2.19a Calibration graph of LVDT

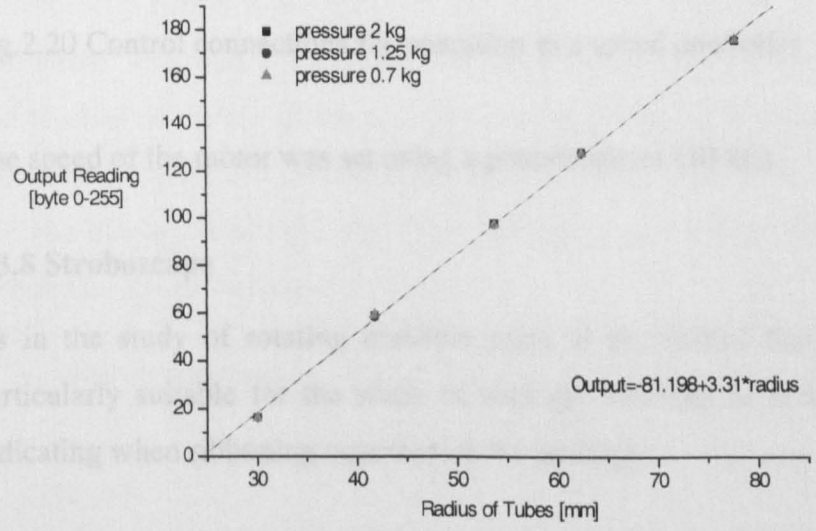

Fig. 2.19b Calibration graph of POT

2.3.7 Frequency Inverter

The winding machine was originally fitted with a 3 phase fixed speed motor. By supplying the motor from a frequency inverter drive, it could be run as a variable speed motor. This enabled the grooved drum to be run at different speeds as required. The inverter allows the speed of the motor to be set from its front panel. The motor could be

enabled or disabled from a simple switch. Fig. 2.20 shows the connection diagram of inverter, and its technical specifications are given in Appendix A.3.

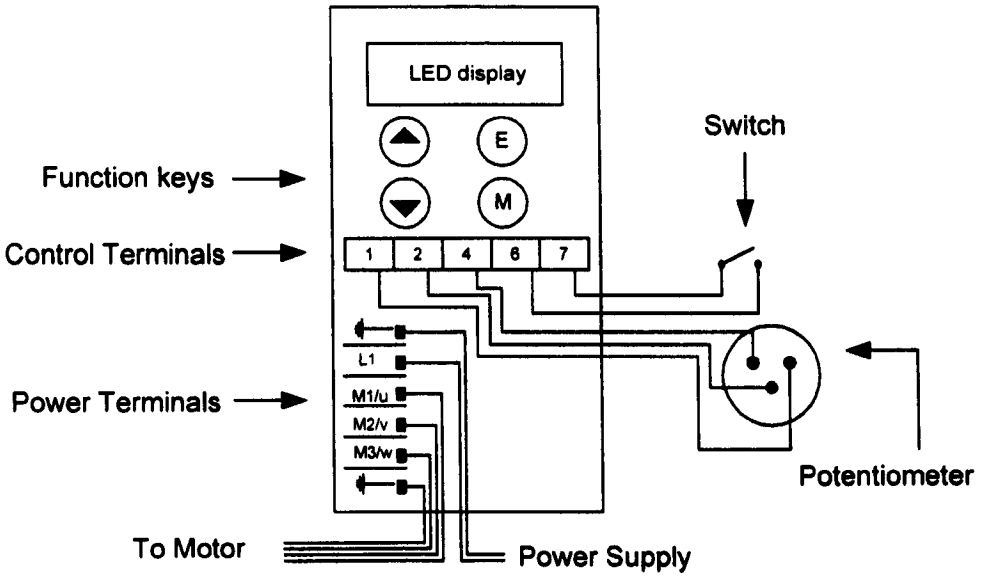

Fig.2.20 Control connections for operation as a speed controller

The speed of the motor was set using a potentiometer (10 kΩ).

2.3.8 Stroboscope

As in the study of rotating machine parts, it as realised that a stroboscope will be particularly suitable for the study of package winding, as it seemed to be useful for indicating when ribboning occurred on the package.

A Genrad Strobolume Type 1540 stroboscope was available, and it was controlled through the interface card using one bit from the digital output port. The bit was activated when ribboning was detected by the control programme, and the flash occurred each time the package arrived at a chosen orientation. This enabled the package to be visually 'frozen', to facilitate the observation of the ribboning or the ribbon breaking actions.

2.3.9 Oscilloscope

Extensive use of a digital storage oscilloscope was made in this work to observe and measure the various signals of electronic circuits. For example the calibration of the yarn tensioner, checking the quality of signals from shaft encoders, the determination of the speed of package and drum were greatly facilitated by the use of this instrument.

The oscilloscope which was used in the research is a 60 MHz digital storage device made by PHILIPS (model 3331). It has two input signal channels, therefore two signals can be simultaneously shown on its screen. The signal displayed on the screen can be magnified several times on the time scale for ease of measurement, as well as waveforms saved for comparison or printout purposes.

2.3.10 Tachometer

A tachometer is another essential basic instrument in a study such as this, to conveniently measure the speed of the motor, the drum etc. A digital photo / contact tachometer was used in this work. This tachometer has an integrated optical transmitter and receiver at the top of the unit and a mechanical contact assembly at the base of the unit. The 5-digit LCD automatically inverts when switched from optical to contact so that the display is always the right way up when viewed. The specifications of the tachometer are given below.

- Photo tachometer - direct reading rpm
- Contact tachometer - direct reading, ranges rpm, m/min, ft./min.
- Memory recall of last reading

Measurement range	5 to 19999 rpm (optical) 0.5 to 19999 rpm(contact)
Resolution	0·1 rpm
Accuracy	±0·05% +1 digit (depend on ambient light conditions)
Sensing range	50 to 150mm
Overall dimensions	H. 215×W. 65×D. 38
Battery	4 × AA Cells

Table 2.4. Technical specifications of the tachometer

2.3.11 Electronic circuits

A number of basic electronic circuits were built to perform a number of different functions of measurement and to enable the interfacing of the different sensors used on the winder.

2.3.11.1 Frequency to Voltage converter for checking yarn package speed

Much of the measurements carried out on the winding operation were based on the assumption of constant speed of drum rotation. Initial measurements of drum and package speed indicated significant fluctuations, which were difficult to explain. Since the output of the shaft encoders were in the form of pulses, it was not too easy to use them to determine any fluctuation of drum speed taking place within each revolution of its rotation. Therefore it was decided to build a frequency to voltage converter, which would be fed from the least significant bit from a shaft encoder, which could be used to display any fluctuation of the drum or the package on the oscilloscope.

The circuit constructed was based on the LM2917 chip which is a monolithic frequency to voltage converter with a high gain op amp/comparator designed to operate a relay, lamp, or other load when the input frequency reaches or exceeds a selected rate [National Semi.]. The circuit diagram employed is given in Fig. 2.21. A single bit (bit 0) from either of shaft encoder connected to pin no. 1 as input while the oscilloscope was connected to the V_{out}. As the machine runs, the analogue voltage, which is proportional to the speed of the shaft encoder concerned is displayed on the oscilloscope.

It should be mentioned that the shaft encoders are connected using bellows type couplings which are rotationally rigid. Hence they follow the speed of the drum or the package without error.

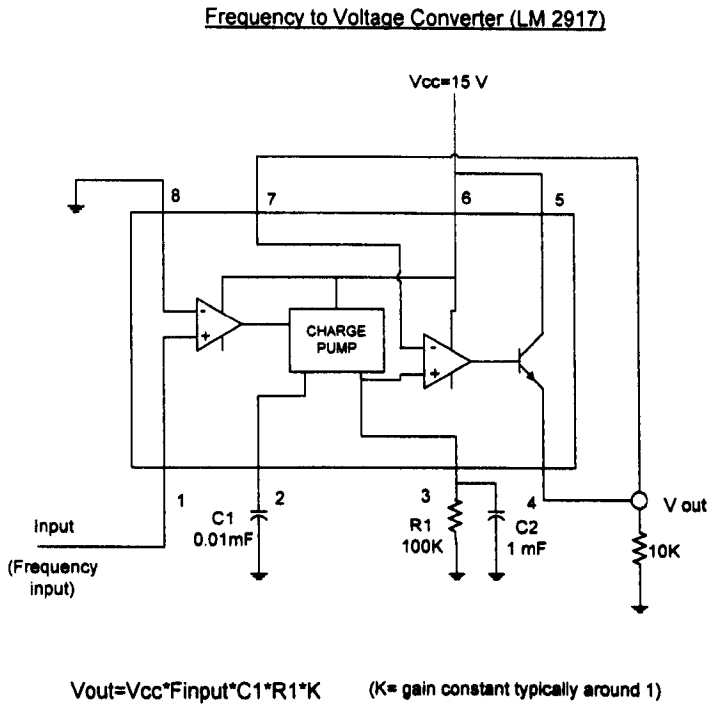

Fig. 2.21 The connection of F/V converter

2.3.11.2 Amplifier card

2.3.11.2.1 Zero adjustment and level shifting for POT and LVDT

As seen in Fig. 2.22, two op-amps (operational amplifier) are used to adjust the amount of gain and level shifting for signals provided by the LVDT and the POT. The op-amps are basically differential amplifiers, and are hence capable of amplifying the difference between the signal levels impressed on their inverting and non-inverting terminals. The negative feed back applied between the output terminal and the input determines the gain of an op-amp. The variable resistor is to adjust the $Vout_1$ to a required. LM348 analogue amplifier chip employed is a quad 741 type op-amp. Two of these are used for the POT and the other two for the LVDT.

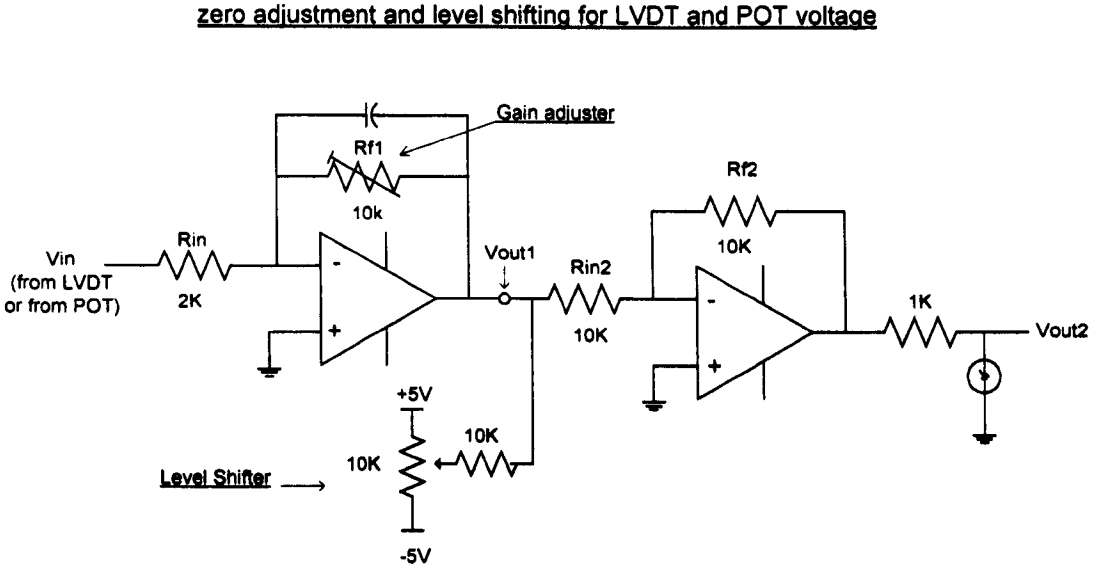

Fig. 2.22 The schematic diagram of amplifier for POT and LVDT

With reference to Fig 2.22 the gain of amplifiers is obtained from the following relations:

$$Gain_1 = \frac{Rf1}{Rin} \qquad \text{and} \qquad Vout_1 = -Vin\frac{Rf1}{Rin}$$

$$Gain_2 = \frac{Rf2}{Rin2} \qquad \text{and} \qquad Vout_2 = -Vout_1\frac{Rf2}{Rin2}$$

2.3.11.2.2 Counter for incremental shaft encoder

A 12- stage binary ripple counter , HCF4040BE , was used to count the pulses from the incremental shaft encoder. The output signal (A signal) was fed to the counter as shown. As the incremental encoder of the 512 count/revolution type, to obtain an 8 bit output which moved through values 0 to 255 each revolution, the bits Q2 to Q9 from the output of the counter were employed as shown by Fig. 2.23.

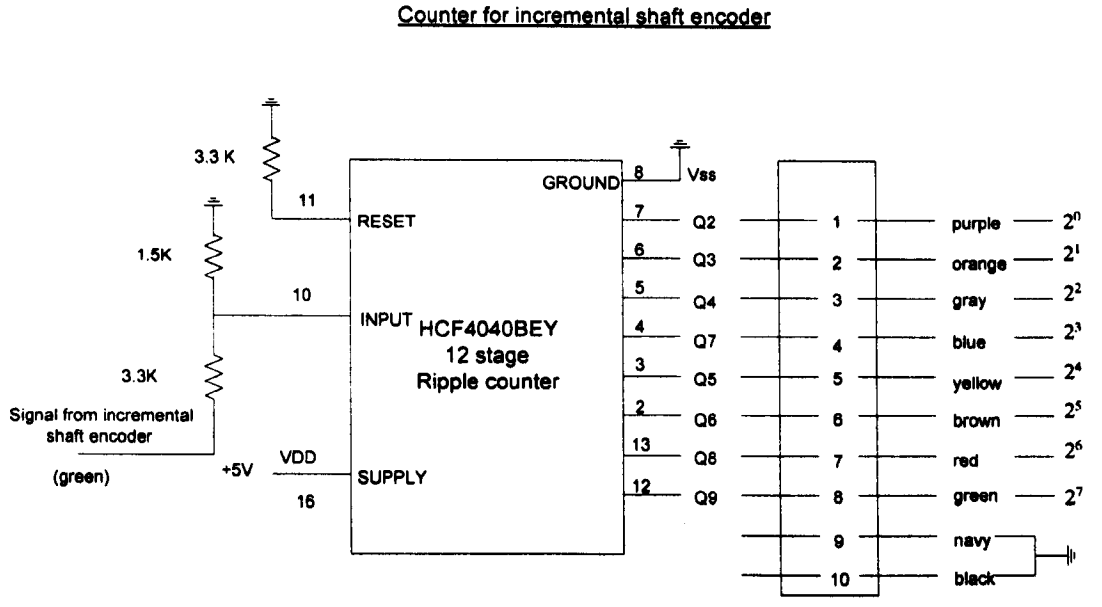

Fig.2.23. Conversion of signal from the incremental shaft encoder to 8 bit binary code

2.3.11.2.3 Voltage regulator for POT

The switching action of the PC power supply and the frequency inverter for the motor, and the mains 50 Hz power supply being all present together, the winder was found to have a noisy electrical environment which conflicted with having clean analogue signals to be available for feeding to the amplifier circuits. So it was necessary to provide the voltage for supplying the POT by deriving it from +15 V from the main power supply. A 5V positive regulator was available and was used for this purpose as shown by Fig 2.24. The high level of regulation provided by the chip and its very low output impedance permitted the noise level in its output to be very low.

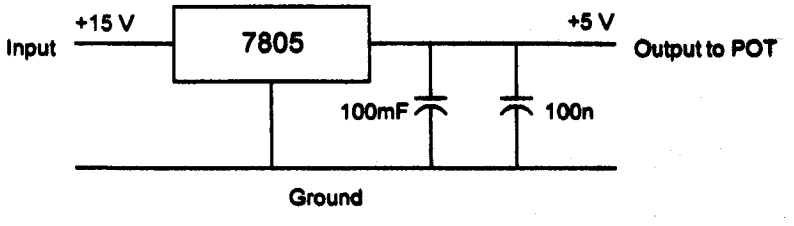

Fig.2.24 The voltage regulator

2.3.11.2.4 Stepper motor drive card for lifting the package

Action of the lifting the package discussed in Chapter 5 required a special card to drive the stepper motor used. A proprietary stepper motor control card type supplied by RS Components was used for the purpose. The configuration of the card is given in Fig 2.25. The card basically requires 3 signals from the PC through the interface card described above. These are a single bit pulse train which decides the speed of the motor, a single bit for enabling the drive card, and a single bit for deciding the direction of rotation. Of these the pulse train is provided by a frequency generator on the motor control card itself. The other two signals are generated under programme control by the PC. The circuit diagram of computer card and stepper motor and all connection for the action of lifting package are given in Appendix A.5.

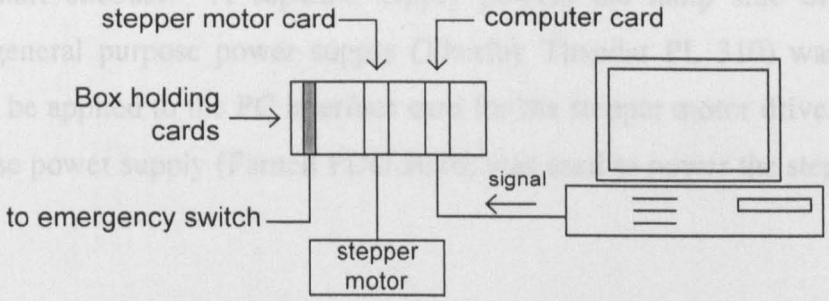

Fig 2.25 Basic configuration for the lifting the package

The more information about the action is given in Chapter 5.

2.3.12 Brushless Servomotor and controller card

The initial operation of the winder indicated the inadequacy of the power of the standard motor fitted on it, to carry out all the experiments planned in this research. A DC brushless motor was available, and was considered greatly superior in its power rating and versatility of control compared with the standard motor powered from the frequency inverter. The motor has its own microprocessor controlled power supply, and can be run so as to provide a variable speed profile under program control. The latter stages of experiments were carried out by using this motor to replace the standard motor.

This motor is of the BRU-200 series supplied by Robbin & Myers. The motor directly replaces the old motor by direct connection to the grooved drum shaft of the winder.

2.3.13 Low Voltage Power Supply

On the system several different power supplies were used to provide the necessary DC power for the electronic circuits. The separate power supplies are important, as they greatly reduce the chance of electrical noise being created in the signals, if all circuits were supplied with power derived from one source. The circuit diagram concerned is shown by Fig 2.26.

One of these was built to provide a highly regulated dual rail 15V and a +5V supply for the amplifier circuitry for the LVDT, the POT and the divide by two counter for the incremental shaft encoder. A separate supply powers the lamp side of the shaft encoders. A general purpose power supply (Thurlby Thandar PL 310) was used to obtain +5V to be applied to the PC interface card for the stepper motor drive. A further general purpose power supply (Farnell PDD 3010) was used to power the stepper motor drive.

2.3.14 Actuators

2.3.14.1 Stepper motor drives

In order to implement the anti-ribboning method by lifting the package, a geared stepper motor was used to operate the arm as shown by Fig 5.8 in Chapter 5. Technical details of the stepper motor are given in Appendix A 5.1. The motor is controlled through the computer.

2.3.13.2 Safety Switches

The safety switches were used to disconnect the power supply of the stepper motors if the package lifting arm were to lose control when the anti-ribboning was in progress. This could be reset again by positioning the arm under the package and then the operation would start again. Safety switches connection are shown in Appendix A 5.2.

Regulated Power Supply for Shaft Encoder and Potentiometer for measuring the undeformed package radius

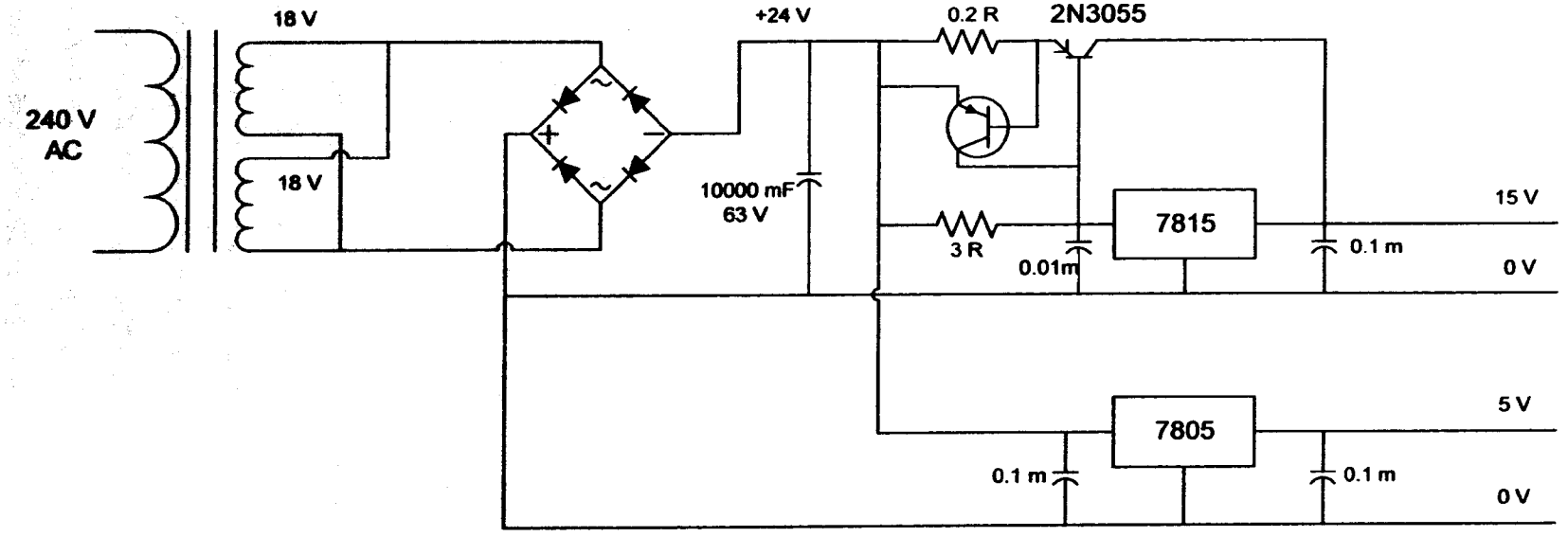

Fig 2.26 Low voltage power supply

2.4 PC Hardware

A standard PC type computer was used as the controller of the experimental winder. The specifications of PC are

- 14" monitor VDU, resolution 480 x 640 (Elonex SuperVGA)
- Motherboard with 200 Mhz. processor,
  Motherboard in PC has 3 ISA (Industry Standard Architecture) and 2 PCI (Peripheral Component Interconnect) slots.
- 32 Mbytes RAM
- 518 Mbytes Hard disk
- 3 1/2" floppy disk drive
- Keyboard, Mouse, Printer (Panasonic KX-P1180 Multi-mode printer)

2.5 Software

The PC has installed in it MS-DOS version 6.20, Windows 3.11, and the programming language Borland C++ version 3.1(Borland International inc. 1992) .
All programs in this project were written in the C language. For analysing data, the Microcal™ Origin™ version 4.10 16 Bit and Microsoft™ Excel were used on a separate computer.

2.6 Noise on the signals and other problems

The modified winder has a number of electrical and electronic circuits associated with it. Some of these handle analogue signals and others digital signals. Some involve small currents while others such as the stepper motor control card handle high currents.

One of the problems experienced in the operation of all these together is the possibility of one circuit affecting another, as seen by the noise content of the various signals. The main supply at 230 v and 50 Hz, causes considerable noise in the signals as a 50 Hz component riding on the DC level of the signal. An even greater problem was found to be caused by the electrical switching (EMI) within the PC power supply and the frequency inverter used to drive the winder motor. EMI causes noise by inducing voltages to appear on the high impedance input segments of circuitry.

These problems were experienced at the beginning of the experiments and a number of measures were taken to reduce the problem to a tolerable level. The oscilloscope was very useful for observing noise on the signals as well as for checking the effectiveness of the various noise reduction measures that were implemented.

- The frequency inverter was separated from the junction box where many of the signal carrying wires meet, by as much as 1 metre, and ferrite sleeves were put on the mains cable that supplies the inverter. This produced some easing of the noise.
- The 3 core power cable between the motor and the inverter was replaced with a screened type and a ferrite sleeve was added. This provided some further relief.
- It was recognised that the motor had not been directly earthed. The inverter and the motor were separately earthed and this contributed to a considerable reduction of noise. The lids of die-cast housing used to contain the circuit boards boxes were properly closed.
- Shaft Encoder was earlier powered by the same transformer that powered the LVDT circuits. As the shaft encoder seemed to be was drawing a considerable current the supply to the shaft encoder was separated. The board which has amplifier circuit for POT and LVDT was powered with that separated power(+15 V and +5 V).
- All mains plugs were checked to ensure they were properly grounded.
- There is a small motor which runs a pressure shoes for yarn tension, which operated from 415 V, 3 phase supply. It was thought that that three phase supply caused some noise, but careful checking indicated that it was not so.

These measures finally achieved an acceptable noise level in the various signals. As indicated above, the separation of the power supplies enabled some measure of noise reduction by reducing 'cross talk' due to feedback between circuits across power supply lines.

CHAPTER THREE

MEASUREMENT OF PACKAGE DENSITY, SLIPPAGE AND DEFORMATION

3.1 Introduction

The Study of the random winding process should lead to the determination of such aspects as the distribution of yarn in the package, deformation of the package at the contact point between the drum and the package, and the nature of slip between the package and the drum. The drum surface is hard and non-deformable, but the wound package surface is relatively soft, deformable and non-homogenous in its construction depending on the yarn tension and the pressure maintained between the package and the drum. Density distribution of a cheese packages shows differences depending on the type of winding used. Generally it is known that the density of the cheese depends on the cradle pressure, the winding tension and the wind angle. In random winding, the wind angle is constant throughout the package. In precision winding the wind angle diminishes with increasing diameter of the package.

According to Wegener and Schubert [Wegener 68], the density distribution in a cheese wound package produced by precision winding shows a sharp reduction near the core, accompanied by a gradual increase of the density with increasing radius. Finally the density falls again sharply near the final outer radius of the cheese, as shown by Fig.3.1.

In this chapter, preparation of yarn packages for each of the experiment will be explained and the results will be given.

3.2 Physical properties of Yarn

The parameters of the yarn used for winding were tested in the testing laboratory under standard testing conditions. Tensile properties were tested on the Statimat at 100 mm/min on a sample length of 200 mm. Yarn twist was measured on a twist tester and its count was measured by winding 100 m of it on the yarn count reel and weighting on a sensitive balance. Yarn specifications are given in Table 3.1.

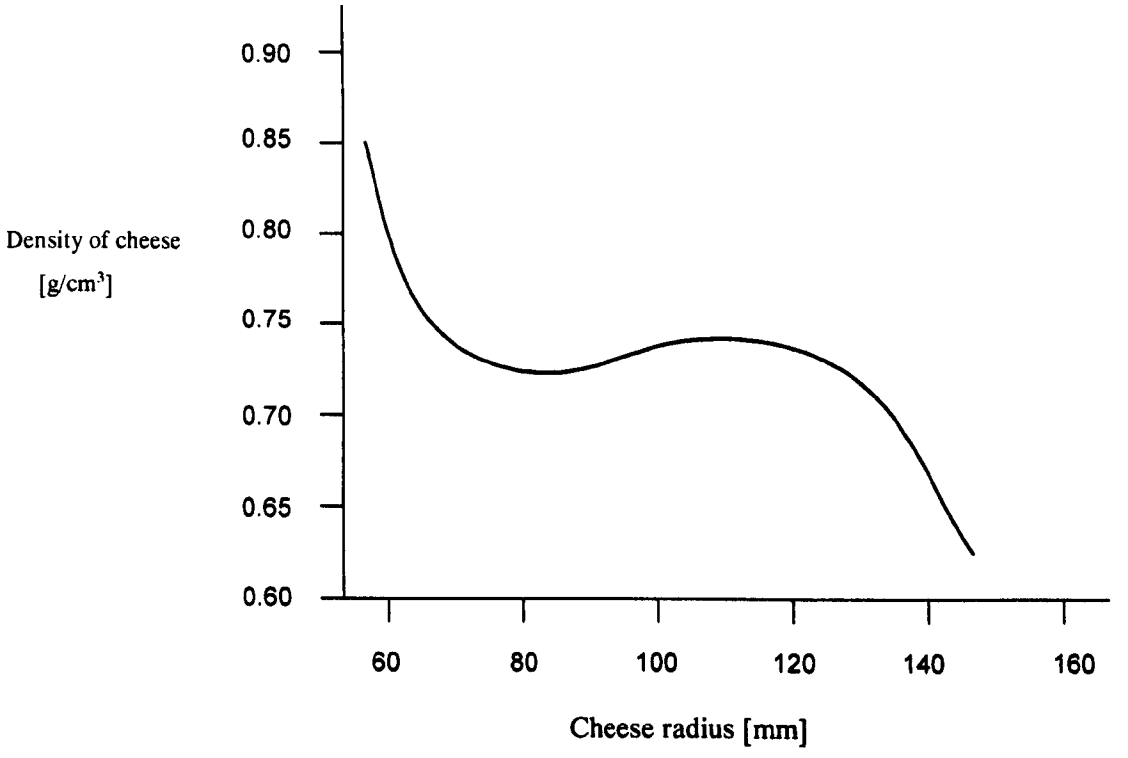

Fig 3.1 Variation of the density of cheese with radius in precision winding

Parameters of Yarn	
Type of yarn	Worsted
Yarn colour	Ecru
Yarn count	R42/2 tex
Yarn twist	544 t/m
Twist direction of yarn	S
Average Elongation	18.44%
Average tenacity	8.38 cN/tex
Average work to rupture	884.95 cN/tex
Breaking Force	309.21 cN
Modulus (0-3%)	115.29 cN/tex
Modulus (0-5%)	117.87 cN/tex

Table 3.1 Yarn specifications

3.2.1 Elastic Modulus of Yarn

Elastic Modulus of Yarn, EY, is defined as the force or tension required in the yarn to produce a unit strain in the length of the yarn. It is expressed in grammes. It was found by using the Instron Testile Tester, Model 1122.

The Instron Tensile tester consists of a recording unit, acrosshead unit and a control panel. There are two jaws in the crosshead unit that allow a specimen to be clamped in the vertical direction. The upper jaw is suspended from a load cell which is fixed centrally in the stationary crosshead and driven upwards and downwards by screwed rods on each side, whereas the lower jaw was fixed at the surface of the tester. The load-extension curve was obtained on the chart in the recording unit. The movement of the chart was proportional to the extension of the sample. A pen on the chart unit moved across the chart when the tensile force applied to the sample of yarn. The speed of the chart and crosshead could be adjustable due to the best-proportioned curve. The adjustments necessary can be made on the control panel.

The specifications below were used in the test:

- The length of the yarn was 150 mm.
- The speed of the crosshead was 5 mm/min.
- The speed of the chart was 200 mm/min.
- Maximum load applied was 100 g.

Therefore, 4 cm of chart paper represented 1 mm extension of the yarn sample.

The test was repeated 3 times on a sample. The tester was set to automatic reversing movement. When the load reached the maximum load, 100 g, the upper jaw was stopped and driven in opposite direction until the original point of the sample. Therefore the extension and recovery curves were both obtained on the chart. The modulus of elasticity could be calculated from the curves on the chart.

3.2.1.1 Results

The curve in Fig. 3.2 was obtained for yarn used in the experiment. The extension of yarn is significantly different for low loads, as compared with that for higher loads. However, the tension of the yarn during the winding test was between 10-50 g. The modulus of the yarn could be obtained in two regions, 10-20 g and 20-50 g, by constructing tangents to the curves as shown.

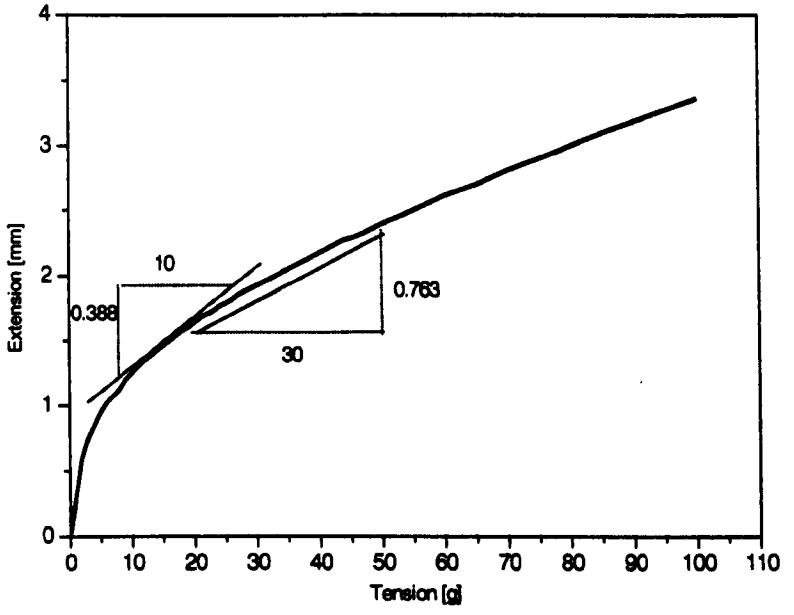

Fig. 3.2 Instron Load-Extension curve

Elastic Modulus at the region of 10-20 g.:

$$EY = \frac{\text{tension gradient}}{\text{corresponding strain}} = \frac{10}{0.388/150} \cong 3866 \text{ g}$$

Elastic Modulus at the region of 20-50 g.:

$$EY = \frac{\text{tension gradient}}{\text{corresponding strain}} = \frac{20}{0.763/150} \cong 5898 \text{ g}$$

3.2.2 Transverse Modulus of Yarn

3.2.2.1 Measurement of Yarn Thickness

In this test, it was necessary to measure the compression of yarn under varying loads and with different numbers of intersecting yarn layers. To ensure a good accuracy in the measurement, it was important to place the yarns sufficiently close to each other with equal spacing between them. Actually the angle between the direction of yarn layers should be equal to that between intersecting yarns in the package which is about 60°. However, 90° was considered not an unrealistic value in the first instance.

The yarns in each layer were placed in the coils of four close coiled springs, placed as shown by Fig. 2.3 in Chapter 2 using suitable wire hooks. This ensured an equal and close spacing of yarns in each layer. When pressure is applied using the load plate, the outermost layers of yarn will have contact along their full length on the metal surfaces, whereas those that are held within the layers have yarn that bear on each other at intersections.

Tests were carried out with different numbers of yarn layers placed under the loading plate. It was ensured that there were equal numbers of yarn intersections on each side of the plate. Different numbers of yarn intersections were formed by laying the yarn under a low tension , of which the overall thickness was measured with a digital voltmeter. The measurement was repeated under different loads.

Table 3.2 gives the results of the testing carried out on a Tex R42/2 worsted yarn. The results were used to obtain the relationship between the thickness of yarn under different pressure levels.

	LOAD (g)	LOAD/POINT (g)	THICKNESS (mm)		
			2 LAYER(t_2)	3 LAYER(t_3)	6 LAYER(t_6)
Number of Intersections = 8	130.5*	16.32	0.31	0.45	--
	155.5	19.44	0.30	0.42	0.86
	180.5	22.57	0.29	0.40	0.82
	230.5	28.82	0.28	0.37	0.72
	280.5	35.07	0.27	0.34	0.66
	330.5	41.32	0.26	0.33	0.60
	380.5	47.57	0.26	0.31	0.57
	430.5	53.82	0.25	0.30	0.54
	480.5	60.07	0.25	0.30	0.52
	530.5	66.32	0.24	0.29	0.50
	580.5	72.57	0.24	0.28	0.49
Number of Intersections = 18	130.5	7.25	0.34	0.50	--
	155.5	8.64	0.33	0.48	--
	180.5	10.03	0.32	0.45	--
	230.5	12.81	0.31	0.42	0.92
	280.5	15.59	0.30	0.39	0.92
	330.5	18.36	0.29	0.37	0.85
	380.5	21.14	0.28	0.35	0.80
	430.5	23.92	0.28	0.33	0.76
	480.5	26.70	0.27	0.33	0.73
	530.5	29.47	0.27	0.32	0.70
	580.5	32.25	0.26	0.32	0.68
Number of Intersections = 32	130.5	4.08	0.39	0.52	--
	155.5	4.86	0.38	0.50	--
	180.5	5.64	0.37	0.47	--
	230.5	7.20	0.35	0.44	0.96
	280.5	8.77	0.34	0.41	0.93
	330.5	10.33	0.33	0.38	0.85
	380.5	11.89	0.32	0.37	0.81
	430.5	13.45	0.31	0.36	0.77
	480.5	15.02	0.30	0.35	0.74
	530.5	16.58	0.29	0.34	0.71
	580.5	18.14	0.29	0.33	0.69

* Note : Weight of load plate = 130.5 g.

Table 3.2 Thickness measurements

3.2.2.2 Results

On the tester, the outermost yarns of two or more layers placed on the tester contact with the flat metal surfaces on the one side, and make yarn to yarn contact on the other. All yarn in between bear on other yarns lying in a transverse direction. What is basically required is to determine is the thickness of a yarn, when compressed transversely between two similar yarns.

Let x = thickness of an intermediate yarn, and
y = thickness of an outer yarn,

These will be ideally constant for a given level of load

Thus the measured thickness of n layers

$$T = (n-2).x + 2y$$

If t is the measured thickness of n layers then (t-T) is a measure of the error in any one measurement. As the measurement is repeated for a number of values of n, it is possible to calculate $\bar{x}$ and $\bar{y}$, the best estimates of x and y, based on the method of least squares.

The errors of measurement are $(t_i - T_i)$

$$(t_i - T_i) = t_i - 2y - (n_i - 2)x$$

With the method of least squares, defining,

$$s = \sum_{i=1}^{N} (t_i - 2y - (n_i - 2)x)^2$$

S= Sum of squares of errors

$$\frac{\partial S}{\partial y} = \frac{\partial S}{\partial x} = 0$$

$$\frac{\partial S}{\partial y} = \sum_{i=1}^{N} 2(t_i - 2y - (n_i - 2)x)(-2) = 0$$

$$\sum_{i=1}^{N} (t_i - 2\bar{y} - (n_i - 2)\bar{x}) = 0$$

$$\sum_{i=1}^{N} t_i - 2N\bar{y} - \sum_{i=1}^{N} (n_i - 2) = 0 \qquad (3.1)$$

Also $$\frac{\partial S}{\partial x} = \sum_{i=1}^{N} 2(t_i - 2y - (n_i - 2)x)(-(n_i - 2)) = 0$$

$$\sum_{i=1}^{N} (t_i(n_i - 2) - 2\bar{y}\sum_{i=1}^{N} (n_i - 2) - \bar{x}\sum_{i=1}^{N} (n_i - 2)^2 = 0 \qquad (3.2)$$

Solving equation 1 and 2. Firstly, $\bar{y}$ is taken from equation 1.

$$\bar{y}' = \frac{\sum_{i=1}^{N} t_i - \bar{x}\sum_{i=1}^{N} (n_{i-2} - 2)}{2N}$$

Substitute $\bar{y}$ into Equation 2

$$\sum_{i=1}^{N} t_i(n_i - 2) - 2\left[\frac{\sum_{i=1}^{N} t_i - \bar{x}\sum_{i=1}^{N} (n_i - 2)}{2N}\right]\sum_{i=1}^{N} (n_i - 2) - \bar{x}\sum_{i=1}^{N} (n_i - 2)^2 = 0$$

$$N\sum_{i=1}^{N} t_i(n_i - 2) - \left[\sum_{i=1}^{N} t_i - \bar{x}\sum_{i=1}^{N} (n_i - 2)\right]\sum_{i=1}^{N} (n_i - 2) - \bar{x}N\sum_{i=1}^{N} (n_i - 2)^2 = 0$$

$$N\sum_{i=1}^{N} t_i(n_i - 2) - \sum_{i=1}^{N} t_i\sum_{i=1}^{N} (n_i - 2) + \bar{x}\sum_{i=1}^{N} (n_i - 2)\sum_{i=1}^{N} (n_i - 2) - \bar{x}N\sum_{i=1}^{N} (n_i - 2)^2 = 0$$

$$N\sum_{i=1}^{N} t_i(n_i-2)-\sum_{i=1}^{N} t_i\sum_{i=1}^{N}(n_i-2)=\bar{x}\left[N\sum_{i=1}^{N}(n_i-2)^2-\sum_{i=1}^{N}(n_i-2)\sum_{i=1}^{N}(n_i-2)\right]$$

$$\bar{x}=\frac{N\sum_{i=1}^{N} t_i(n_i-2)-\sum_{i=1}^{N} t_i\sum_{i=1}^{N}(n_i-2)}{N\sum_{i=1}^{N}(n_i-2)^2-\sum_{i=1}^{N}(n_i-2)\sum_{i=1}^{N}(n_i-2)} \tag{3.3}$$

$$\bar{y}=\frac{\sum_{i=1}^{N} t_i}{2N}-\frac{\sum_{i=1}^{N}(n_i-2)}{2N}\bar{x} \tag{3.4}$$

where N = Number of 'stacks' tested each with a different value of n

Once $\bar{x}$ is obtained, the transverse elastic modulus E may be defined as follows.

$$E=\frac{\Delta load}{\frac{\Delta\bar{x}}{\bar{x}}} \tag{3.5}$$

For this case $\bar{x}$ and $\bar{y}$ were calculated for a given load at each intersection. Results are given in Table 3.3.

The results of the above calculations, for a range of load values, are given in Table 3.3 below.

load/point (g)	$\bar{x}$ (mm)	$\bar{y}$ (mm)	$\frac{\Delta\bar{x}}{\bar{x}}$	Δload (g)	E (g)
7.20	0.16	0.16	0.02	1.56	63.90
8.77	0.15	0.15	0.10	1.56	15.27
10.33	0.14	0.15	0.06	1.56	27.73
11.89	0.13	0.14	-0.21	0.92	-4.37
12.81	0.16	0.14	0.23	0.65	2.77
13.45	0.12	0.14	0.05	1.56	28.63
15.02	0.11	0.14	-0.41	0.57	-1.39
15.59	0.16	0.13	0.32	0.99	3.08
16.58	0.11	0.13	0.04	1.56	39.46
18.14	0.10	0.13	-0.40	0.22	-0.55
18.36	0.15	0.13	0.03	1.08	42.52
19.44	0.14	0.15	0.07	1.70	25.91
22.57	0.13	0.14	0.07	1.35	20.74
23.92	0.12	0.12	0.05	2.78	59.29
26.70	0.12	0.12	0.05	2.12	42.49
29.47	0.11	0.12	0.04	2.78	71.02
32.25	0.11	0.12	0.08	2.82	34.27
35.07	0.10	0.13	0.15	6.25	42.76
41.32	0.08	0.13	0.06	6.25	99.89
47.57	0.08	0.12	0.06	6.25	104.49
53.82	0.07	0.12	0.06	6.25	103.46
60.07	0.07	0.12	0.04	6.25	146.15
66.32	0.07	0.12	0.04	6.25	168.55

Table 3.3 Results of Analysis

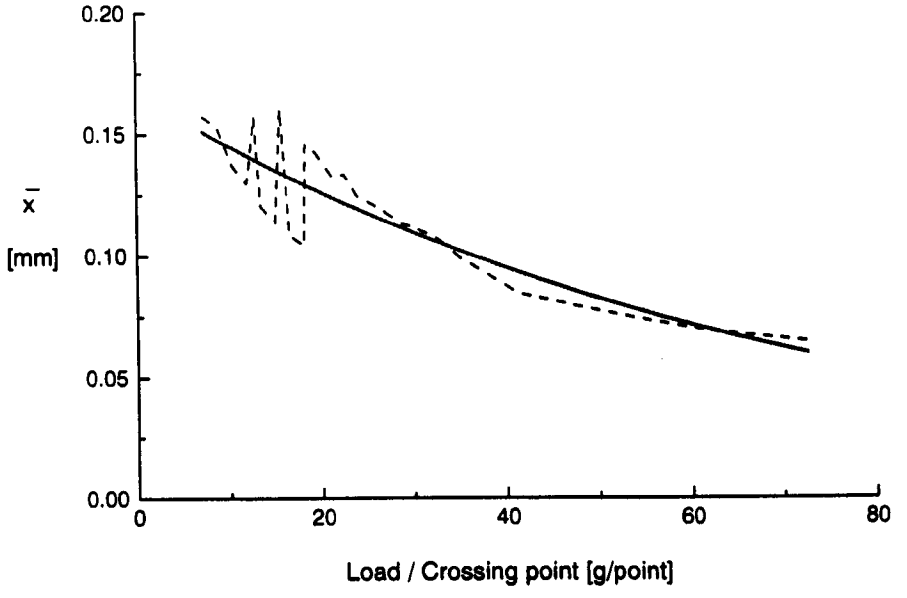

$$\bar{x} = -0.00287 + 0.15383e^{\left(\frac{-(load/point-72)}{72.78}\right)}$$

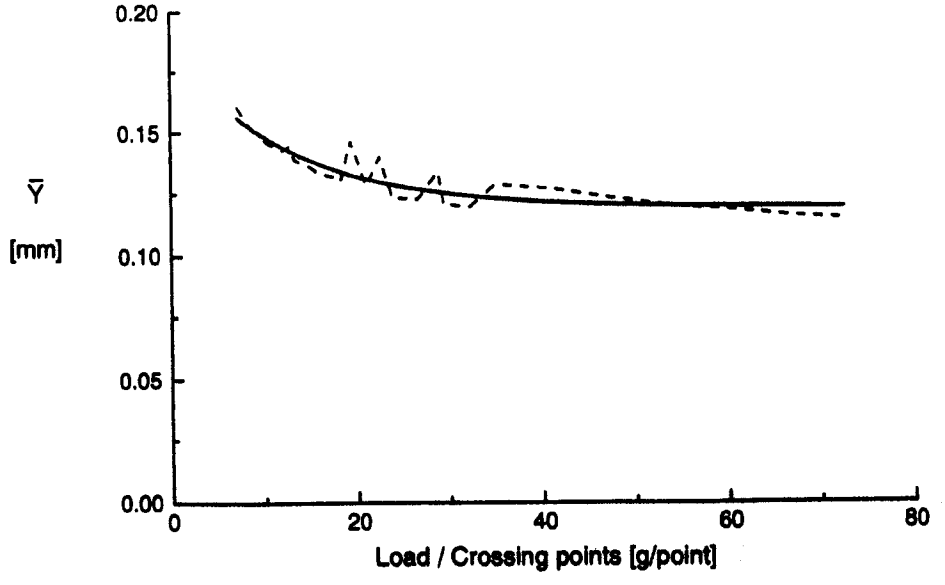

$$\bar{y} = 0.11966 + 0.0362.e^{\left(\frac{-(load/point-72)}{1184}\right)}$$

Fig 3.3 Variation of $\bar{x}$ and $\bar{y}$ with load

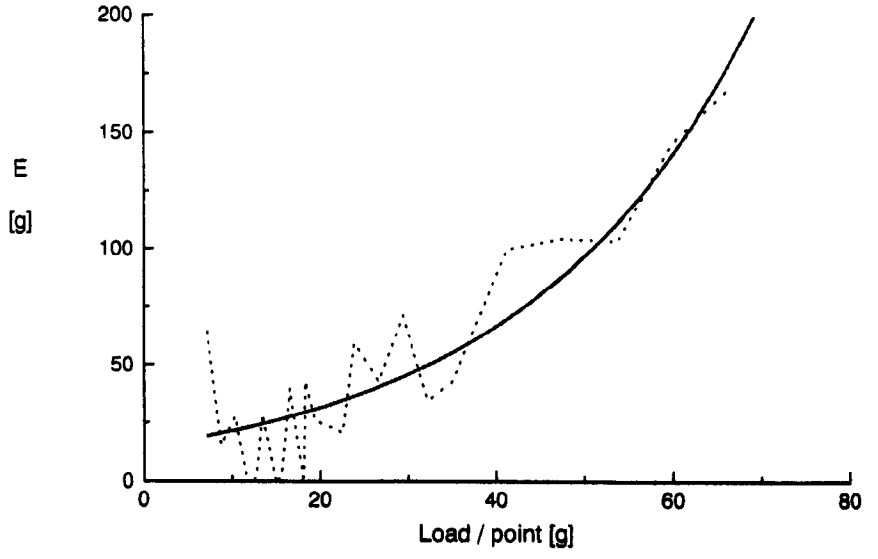

Fig 3.4 Variation of E with load

$$E = 14.8.e^{\left(\frac{load/point}{26.65}\right)}$$

3.3 Preparing yarn packages

Random wound package was prepared to different diameters by varying the winding tension and pressure values applied in each case.

The pressure settings chosen were 2 kg, 1.25 kg and 0.7 kg. The winding tension settings applied to the yarn were maximum, medium and minimum, which correspond to 30 g, 19 g and 8 g respectively. The diameters of package chosen were 80 mm, 120mm, and 160 mm. The experiment are based on all the combinations of tension, pressure and diameter values given above.

3.3.1 Pressure

On the winder, the pressure to be applied on the package can be set to a desired value. This pressure is provided by a spiral spring in a way that it can also compensate for the growing weight of the package [Schlafhorst 67]. The initial tension of the clock spring is adjustable. The range of setting available for the spring are from 1 to 6. The scale position 1 gives the maximum pressure, whereas the position 6 gives the minimum pressure. If necessary an additional weight can be put on the package cradle by means of the moveable weight. The effect of this additional weight of 1 kg can be changed by moving it upwards or downwards.

The pressure can be checked by means of a spring balance before starting any experiment. The pressure settings chosen for this experiment are the following:

2 kg (maximum) – the scale was 1 and additional weight on the package cradle is on and it was placed at full length.

1.25 kg (medium) – the scale was 3.5 and additional weight on the package cradle and it was place full length.

0.7 kg (minimum) – the scale was 4.5 and no additional weight on the package cradle.

It was observed that the yarn could not be wound to the package with under 0.7 kg pressure. Below this setting, the tube will not remain on the drum with sufficient pressure Hence the minimum pressure chosen was 0.7 kg.

3.3.2 Yarn winding tension

The winder has an adjustable tensioner which was identified in Chapter 2. As checked by the electronic tension probe (described section 2.3.2 in Chapter 2), the maximum and minimum tensions that could be obtained by adjusting the tensioner amounted to 30 g and 8 g respectively. Therefore the medium tension setting was chosen as 19 g. The setting was facilitated by the colour coding of tension values marked on the tensioner adjustment.

As a rule of thumb, on a winder the winding tension used should be about 10-15 % of the mean yarn-breaking load [Oxtoby 87]. Weak places on the yarn can be removed under this tension in the case of natural fibres, while strong synthetics and blends do not necessarily follow this. Too high a winding tension may permanently impair the elastic properties of a yarn and cause fabric faults. According to this rule, the maximum tension applied to chosen worsted yarn should be 35 g due to the mean breaking load of the yarn.

3.3.3 Oscillation of drum

On the winder, the grooved drum can be given an axial oscillatory motion that displaces the yarn laterally on the edges of the package. This enables soft edges on the package which are important for certain operations such as pressure dyeing. The lateral displacement motion moves the yarn guide cylinder sideways 30 times per minute. 3 different displacements are provided; 2 mm, 3 mm and 4 mm. If necessary, it can be cancelled completely. For producing the packages for experiments, the maximum displacement of 4 mm, was used. Use of the lateral displacement of the package prevented the formation of hard edges, and allowed the package to contact the drum properly along its full length.

3.3.4 Package diameter

The wound package diameters chosen for experiment were 80 mm, 120 mm, and 160 mm. A computer program was written in the C-language to check the diameter of the package by means of the LVDT during winding of yarn to the package [Appendix C. 1]. Only one variable had to be changed on the programme, namely the package diameter. For example, when 120 mm package diameter was required to be produced, the variable was assigned the value 120.

3.3.5 Speed of winding drum

The speed of the drum was set 1800 rpm, corresponding to a yarn speed of 510 m/min approximately. This corresponded to a speed setting of Decimal 215 on the motor drive controller.

There are several ways to check the accuracy of the drum speed. One way is to count the number of revolution of the drum in a time using the absolute shaft encoder connected to the drum shaft. A program was written for this purpose [Appendix C.2]. It was found that the maximum value 255 of the byte gives 2133 rpm. But this speed was not chosen because in any case the maximum speed would be needed for another purpose. The particular speed of 1800 rpm was also the speed used with the original motor fitted on the winder using the frequency inverter.

Table A.4 in the Appendix A gives the speeds reached for different values of speed command signal applied to the BRU 200 controller.

The other way of the checking the speed is to use the optical tachometer. A small piece of retro reflective tape was stuck on the drum, to enable the tachometer count the each revolution of the drum. There was additionally the possibility of using the V/F converter circuit given in section 2.3.11.1 in Chapter 2 using any of the bits output from the absolute shaft encoder. All these methods applied to check the drum speed gave the same result. As the drum diameter is 0.09m., the surface speed of the drum is closely 510 m/min.

3.4 Density of random wound packages

3.4.1 The method of finding the density of random wound packages

The investigation of the density distribution of the package is one of the important aspects of the study of the random wound package. It was intended to measure a number of packages prepared under different pressure, winding tension and diameter for this purpose. In order the obtain information on the distribution of yarn weight with package diameter, it was necessary to find the volume and the weight of the packages, as they were wound from the minimum size to the final size. The weight readings were obtained on an accurate weighing scale. The gross weight of the package minus the weight of the tube gave the total weight of yarn on the package at each stage of completion of it.

Packages shape is cylindrical except the side faces of it. During winding each new layer produced pressure on the previous one. At increasing package diameter, more pressure was being applied to the inner layers of the package. One of the results of this is the two outer faces of the package becoming convex.

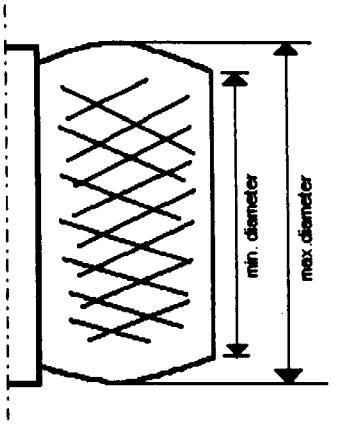

Fig 3.5 side view of a package

To calculate the package volume, the diameter and length of the package should be measured. The diameter is relatively easy to measure. The length of the package was taken as the average of the sum of the maximum and minimum lengths of the package. The equation for density of the package was taken as the following:

$$\text{Density}(g/cm^3) = \frac{w}{\frac{\pi}{4}.(D^2 - d^2).l} \qquad (3.6)$$

Where

w – the net weight of the yarn on the wound package in gram.

(w= the weight of the package – the weight of the tube*)

* the mean weight of the tube is 54.7 g.

D – the diameter of the package in cm included the tube diameter

d – the diameter of the package in cm subtracted tube diameter

l – the averaged length of the package in cm

3.4.2. The results of the density of the random wound packages

Random wound packages produced under different winding tension and pressure values were measured for weight and volume to determine their density. All results obtained are shown in the Appendix B.1.

The distribution above naturally depends on the type of yarn involved. The yarn used in this experiment R42/2 worsted. However with a different yarn, the results are unlikely to deviate to any large degree.

The density of packages was averaged over 3 packages for each of pressure and yarn tension. They are tabulated in Table 3.3.

YARN TENSION (g)	PRESSURE (kg)		
	2 kg	**1.25 kg**	**0.7 kg**
30 g	0.478	0.457	0.444
19 g	0.435	0.414	0.4
8 g	0.381	0.36	0.351

Table 3.4 Density of random wound packages

The results of Table 3.4 were plotted yarn tension against density of package in Fig 3.6. According to the Fig.3.6, when more tension applied to the yarn, the package density increases in the manner shown, under a constant pressure. It is also clear that the pressure of package cradle influences the density. An increase of yarn tension from 8 to 30 g has been observed to increase package density from 0.381 to 0.478 g/cm^3 at the maximum pressure of 2 kg. The difference in density is 0.097 g/cm^3. Although an increase of pressure from 0.7 kg to 2 kg has been observed to increase package density from 0.444 to 0.478 g/cm^3 at the maximum yarn tension applied, the difference in

density brought about is 0.034 g/cm$_3$. It is clear that changing yarn tension has a greater effect on package density than pressure applied to the package holder.

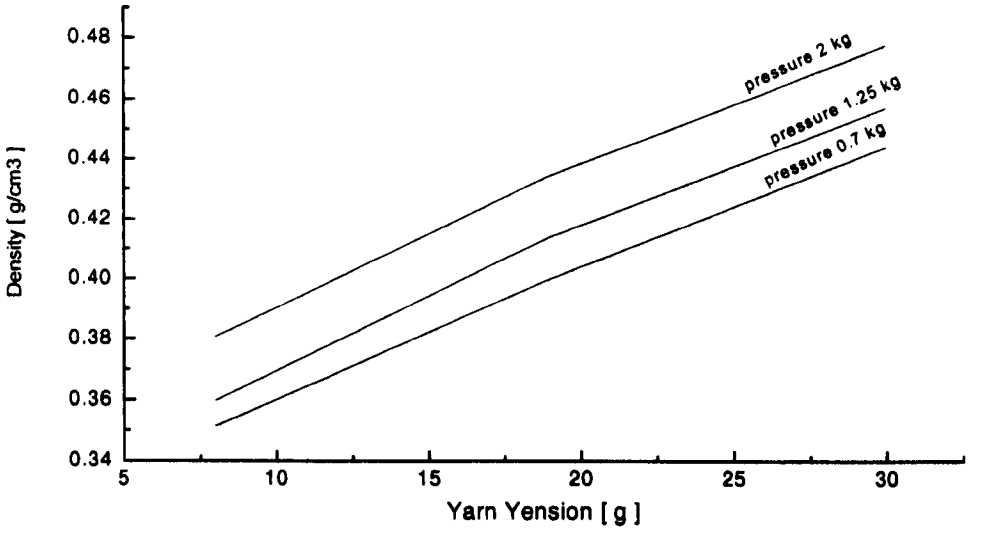

Fig 3.6 The density distribution in terms of yarn tension and pressure

For a better understanding of the variation of density of wound yarn packages, they can be plotted in a 3D representation. Using the graphic software Origin, the graphs were prepared as given below. The X, Y, and Z-axis show the radius of the package, yarn tension and density of the package respectively. Each graph has been drawn for a constant pressure setting, and they show a similar density distribution. If pressure is kept constant, a lower winding tension makes soft packages; and a higher winding tension makes hard packages.

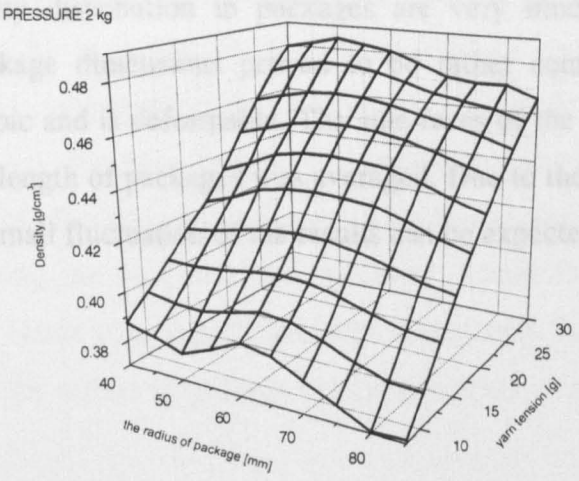

Fig 3.7 the density distribution at the pressure 2 kg

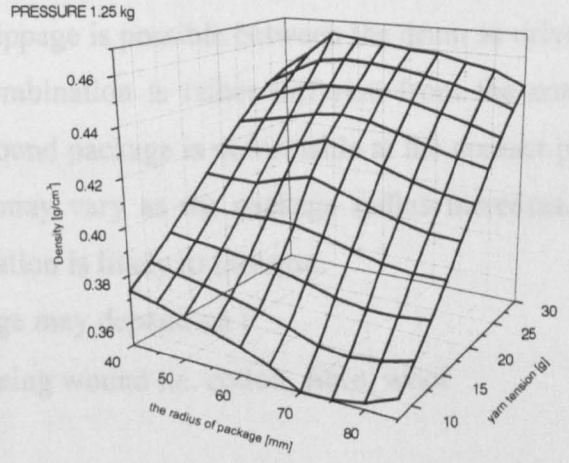

Fig 3.8 the density distribution at the pressure 1.25 kg

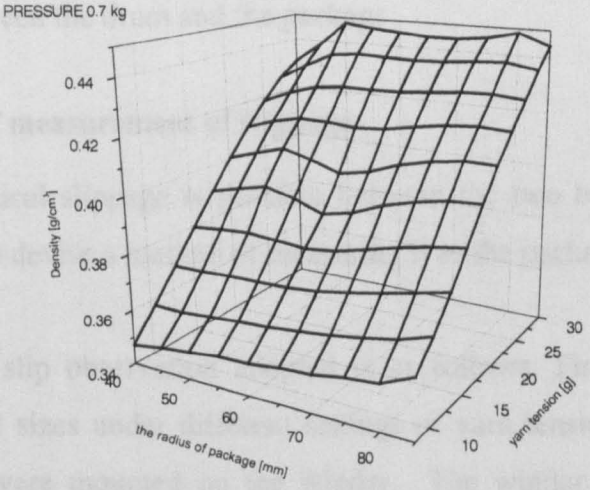

Fig 3.9 the density distribution at the pressure 0.7 kg

3.4.3 Discussion of Density

The results of density distribution in packages are very much as expected. The measurement of package dimensions proved to be rather complicated. The wound package is not isotropic and is deformable. The side faces of the edges are not flat and that is why the axial length of packages was averaged. Due to the difficulty of accurate measurement, some small fluctuation of the results can be expected.

3.5 Slippage

3.5.1 Introduction

As a round body drives another such body by frictional contact, there will be some opportunity for slippage between them to occur. In random winding, while yarn is wound as a cheese, slippage is possible between the drum as driver and the package as a driven body. This combination is rather different from the combination of two hard bodies because the wound package is deformable at the contact point. Due to a number of reasons, slippage may vary as the package radius increases. As package diameter increases, the deformation is likely to increase.

The amount of slippage may depend on :

- type of yarn being wound i.e. cotton, fibro, wool
- yarn count
- yarn tension
- surface of the driving drum (steel, bakelite, chromium plate etc.)
- pressure between the drum and the package

3.5.2 The method of measurement of slippage

While some mechanical slippage is possible between the two bodies concerned, it is extremely difficult to devise a method of measuring it as the package rotates.

The method of the slip observation adopted is as follows. First the packages were prepared in different sizes under different settings of yarn tension and pressure. The prepared packages were mounted on the winder. The winder was run without any addition of yarn. The effect of the yarn drag was neglected. The package pressure

applied during experiment was the same as that used for preparing the package i.e. If a package was produced with 2 kg pressure, the pressure used during the measurement of slippage was 2 kg for that package. The number of package revolutions produced was counted for a fixed number of drum revolutions. 2000 drum revolutions were considered adequate for the measurement. A computer program was written in C language to count the package and drum revolution, at the same time the drum revolution is comparing the fixed number indicated [Appendix C.3]. A loop in the program ran 3 times while counting the package revolutions for the fixed number of drum revolutions and the results of package revolutions were averaged.

One of the points to be noted is that during the preparation of the packages the maximum oscillation of winder, 4 mm, was employed in order to obtain soft edges to the package. This would allow package contact with the drum over the full axial length of the package.

3.5.3 Provision of the drag effect

3.5.3.1 The pulley

To give a same effect of yarn drag to the winding package when a package was rotated with no yarn winding, an aluminium pulley was mounted on the package shaft, on which a weighted cord was added to provide a controlled amount of frictional drag. The details of the pulley are shown by Fig 3.10.

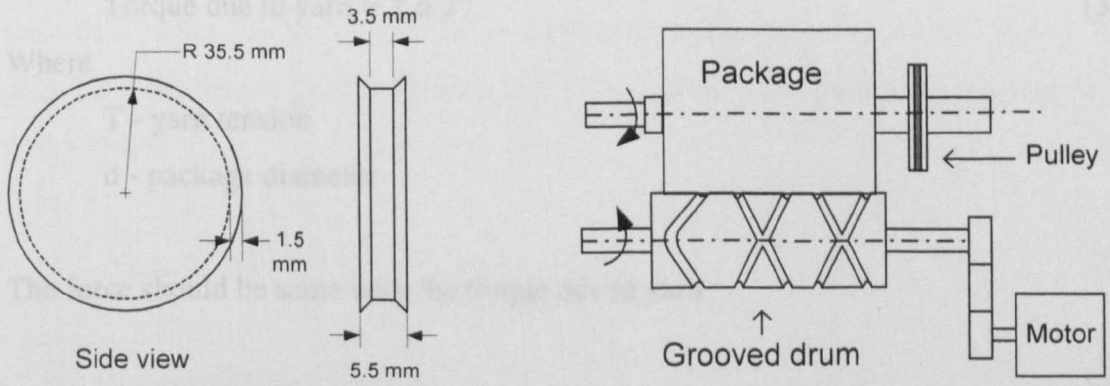

Fig 3.10 a) the dimension of the pulley b) the pulley on the machine

3.5.3.2 The calculation of weight hung

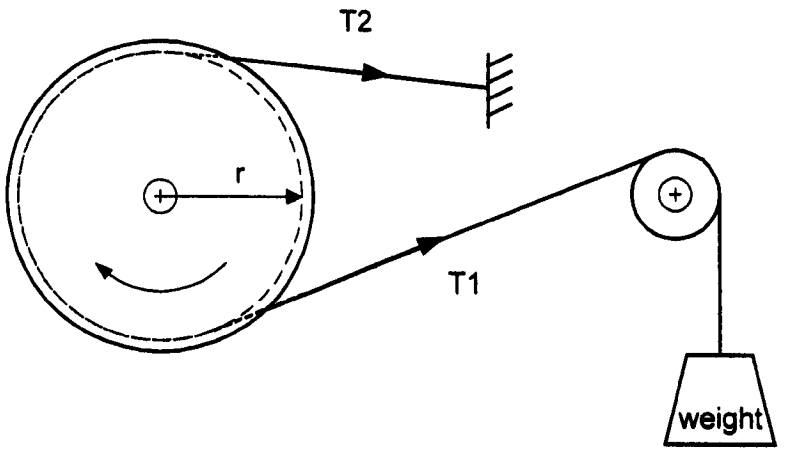

Fig. 3.11 The drag due to cord with weight

With reference to Fig 3.11 , the following equation can be written;

$$\frac{T_2}{T_1} = e^{\mu.\alpha}$$

$$T_2 = T_1.e^{\mu.\alpha} \qquad (3.7)$$

Where

T_2 - tension on the cord at the left hand side of the pulley

T_1 – tension due to the weight on the cord at the right hand side of the pulley

μ - Coefficient of the friction between the cord and the pulley

α - the angle which cord covers the pulley

Torque due to yarn = T.d/2 (3.8)

Where

T - yarn tension

d - package diameter

The force should be same with the torque due to yarn

$$(T_2-T_1).r = T.d/2 \qquad (3.9)$$

where

r is the radius of the pulley

Substituting for T_2 from equation (1)

$$(T_1.e^{\mu.\alpha} - T_1).r = T.d/2$$

$$T_1 = \frac{T.d/2}{(e^{\mu.\alpha} - 1).r} \qquad (3.10)$$

T_1 is the weight that is hung from the cord to suit the package diameter and tension applied to the yarn. The coefficient of friction (μ) between the cord and the pulley is approximately 0.25 and the angle of the wrap cord on the pulley (α) is $4/3\pi$. The chosen package diameter is 120 mm on this calculation. The results are approximately same when the diameter is chosen 80 and 160 mm. The 120 mm package diameter was chosen because it is close to the mid value of package diameters that can be handle on the winder. The inner radius of the pulley is 35.5 mm.

Substituting all values to the equation (4),

Weight = T_1 = 0.9.T

The weight depends on what winding tension is applied to the yarn.

Maximum tension applied is 30 g, the weight will be 27 g - in practice 30 g.

Medium tension applied is 19 g, the weight will be 17.1 g - in practice 20 g.

Minimum tension applied is 8 g, the weight will be 7.2 g - in practice 10 g.

3.5.4 Results of Slippage

The results of slippage are as tabulated in Table 3.5. The radius indicated on the table is the actual radius reading i.e. the deformed package radius, from the LVDT. All individual results are given Appendix B.2. The method of calculation of slippage is given below.

$$V_{drum} = 2.\pi.N.R \qquad (3.11)$$

$$V_{package} = 2.\pi.n.r \qquad (3.12)$$

$$\Delta V = V_{drum} - V_{package} = 2.\pi.(N.R - n.r) \qquad (3.13)$$

$$\text{slippage}(\%) = \frac{\Delta V}{V}.100 = \frac{2.\pi.(N.R - n.r)}{2.\pi.N.R}.100 = [1 - \frac{n.r}{N.R}].100$$

$$\text{slippage}(\%) = [1 - \frac{n.r}{2000.45}].100 = 100 - \frac{n.r}{900} \quad (3.14)$$

To find the loss of the package revolution:

Assuming no slip, the velocity of the package should be the same as the velocity of the drum at the contact point.

$$V_{drum} = V_{package}$$

$$2.\pi.N.R = 2.\pi.n.r$$

$$n_{teo.rev} = N.\frac{R}{r_{act.radi}}$$

$$\text{Lost revolution} = n_t - n_m \quad (3.15)$$

where

n_t – theoretical revolutions of package

n_m – measured revolutions of package

DIA. (mm)	PRESSURE (kg)	2	2	2	1.25	1.25	1.25	0.7	0.7	0.7
	Yarn tension(g)	Max (30 g)	Med (19 g)	Min (8 g)	Max (30 g)	Med (19 g)	Min (8 g)	Max (30 g)	Med (19 g)	Min (8 g)
80	Rev	2229.3	2222.9	2194.5	2234	2224.7	2205.2	2220	2216.1	2213.3
	Radius	39.9	39.8	39.8	39.8	39.9	39.9	39.9	39.9	39.9
	Density	0.4564	0.4033	0.3632	0.4323	0.3954	0.3558	0.4201	0.3847	0.3325
	Slip(%)	**1.17**	**1.7**	**2.95**	**1.21**	**1.62**	**2.24**	**1.58**	**1.75**	**1.88**
	Lost Rev.	26.34	38.41	66.81	27.31	36.61	50.44	35.64	39.54	42.34
120	Rev	1486	1484.3	1463.6	1489.8	1500.3	1483	1495.6	1492.5	1487.4
	Radius	59.9	60.0	59.9	60.3	59.7	59.8	60.0	60.1	60.1
	Density	0.4599	0.4207	0.3700	0.4547	0.4233	0.3451	0.4336	0.3847	0.3415
	Slip(%)	**1.1**	**1.05**	**2.59**	**0.18**	**0.48**	**1.46**	**0.29**	**0.33**	**0.67**
	Lost Rev	16.5	15.7	38.9	2.74	7.24	22.02	4.4	5.0	10.1
160	Rev	1120.1	1118.9	1102.3	1120.4	1117.3	1109.8	1123.5	1119.4	1115.1
	Radius	79.7	79.6	79.7	79.8	80.0	80.0	79.8	80.1	80.1
	Density	0.452	0.4060	0.3432	0.4405	0.4028	0.3448	0.4367	0.4009	0.3461
	Slip(%)	**0.81**	**1.04**	**2.39**	**0.66**	**0.68**	**1.35**	**0.38**	**0.37**	**0.76**
	Lost Rev	9.13	11.75	26.93	7.42	7.7	15.2	4.32	4.2	8.5

- Density g/cm^3, Radius mm, revolution rev as drum count 2000 rev

Table 3.5. the results of the slippage test

Slippage is usually calculated as a percentage. The results were plotted as 3D graphs of package diameter and density against slippage. There are three different graphs drawn in terms of package cradle pressure. In Figure 3.12, the pressure is maximum, 2 kg. The maximum slippage was found to occur when the packages are soft and radius is small.

As the radius of package increases, the amount of slippage slightly decreases, whereas when a package is harder, the slippage decreases very much. In general, as the density of a package ranges from soft to hard, the slippage is slightly reduced. For the pressure of 0.7 kg, as the radius of packages increases, the slippage decreases rapidly until the radius of 60 mm, after which there is no significant reduction. In Fig 3.14 the graph plotted with medium pressure of package cradle. It can be noticed that the pattern is the middle of two graphs, one is with minimum pressure, and the other is maximum. Increasing either package density or package radius make a small drop on the slip.

It can be said that the deformation on the contact line in axial direction between the drum and the package depends on the package holder pressure applied and the density of package produced. The radius of the package at the contact line is smaller than the normal package radius. The small radius depends on the deformation. When the slippage is calculated, the deformed radius has been considered. It might be thought that the explanation of the slippage depends on what happens on the contact line between package and drum. The pressure applied affects the area of contact of the package on the drum. A higher pressure produces more contact area depending on the package density. When the package turns, the material in the area of contact is likely to stretch. As material of the package deforms as it meets the drum during rotation, sufficient torque should be applied to the drum to supply the work of this deformation.

As material so compressed leaves contact with the drum, it recovers its normal shape and releases the energy earlier stored in it due to compression. When packages just leave the drum, it starts covering original radius. As some of this energy will be simply dissipated in the material against internal friction, the effect may contribute to some lost revolutions of the drum.

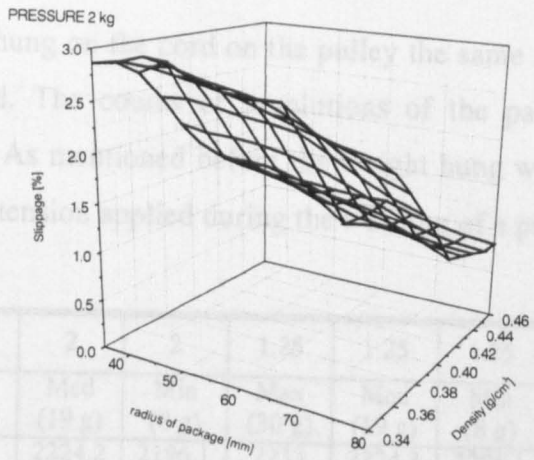

Fig 3.12 the slippage at pressure 2 kg

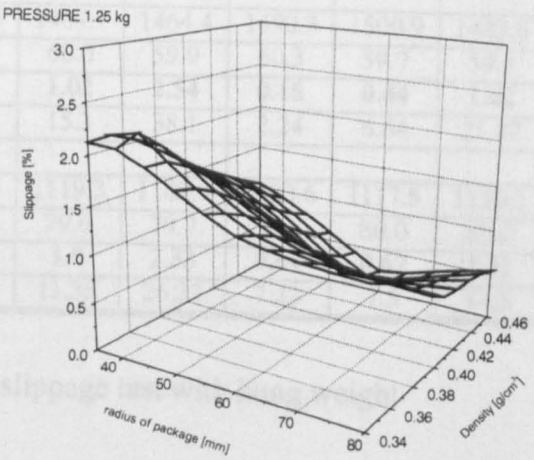

Fig 3.13 the slippage at pressure 1.25 kg

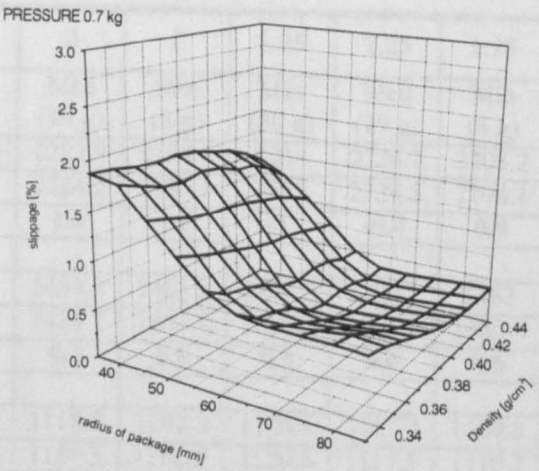

Fig 3.14 the slippage at pressure 0.7 kg

3.5.4.1 Results of Slippage with Yarn Drag Effect

With suitable weights hung on the cord on the pulley the same tests that were done for slippage were repeated. The counts of revolutions of the package were saved and tabulated in Table 3.6. As mentioned before the weight hung was so as to produce the same effect as the yarn tension applied during the winding of a particular package.

DIA. (mm)	PRESSURE (kg)	2	2	2	1.25	1.25	1.25	0.7	0.7	0.7
	Yarn tension(g)	Max (30 g)	Med (19 g)	Min (8 g)	Max (30 g)	Med (19 g)	Min (8 g)	Max (30 g)	Med (19 g)	Min (8 g)
80	Rev	2230	2224.2	2196.1	2233	2224.3	2206.1	2214	2211.1	2212.2
	Radius	39.9	39.8	39.8	39.8	39.9	39.9	39.9	39.9	39.9
	Slip(%)	**1.14**	**1.64**	**2.88**	**1.25**	**1.64**	**2.2**	**1.85**	**1.97**	**1.93**
	Lost Rev.	25.64	37.11	65.21	28.31	37.01	49.54	41.64	44.54	43.44
120	Rev	1486.5	1484.7	1464.4	1490.3	1500.9	1483.6	1494.9	1492.3	1487.6
	Radius	59.9	60.0	59.9	60.3	59.7	59.8	60.0	60.1	60.1
	Slip(%)	**1.07**	**1.02**	**2.54**	**0.15**	**0.44**	**1.42**	**0.34**	**0.35**	**0.66**
	Lost Rev	16	15.3	38.1	2.24	6.64	21.42	5.1	5.2	9.9
160	Rev	1120.4	1119.3	1102.9	1120.6	1117.5	1110.2	1123.6	1119.6	1115.4
	Radius	79.7	79.6	79.7	79.8	80.0	80.0	79.8	80.1	80.1
	Slip(%)	**0.78**	**1.0**	**2.33**	**0.64**	**0.67**	**1.32**	**0.37**	**0.36**	**0.73**
	Lost Rev	8.83	11.35	26.33	7.22	7.5	14.8	4.22	4	8.2

Table 3.6 The results of slippage test with hung weight

3.5.5 Comparison of the two experiments

DIA. (mm)	PRESSURE (kg)	2	2	2	1.25	1.25	1.25	0.7	0.7	0.7
	Yarn tension(g)	Max (30 g)	Med (19 g)	Min (8 g)	Max (30 g)	Med (19 g)	Min (8 g)	Max (30 g)	Med (19 g)	Min (8 g)
80	Rev	2229.3	2222.9	2194.5	2234	2224.7	2205.2	2220	2216.1	2213.3
	Drag Rev	2230	2224.2	2196.1	2233	2224.3	2206.1	2214	2211.1	2212.2
	Subtracted	**0.7**	**1.3**	**1.6**	**-1**	**-0.4**	**0.9**	**-6**	**-5**	**-0.9**
120	Rev	1486	1484.3	1463.6	1489.8	1500.3	1483	1495.6	1492.5	1487.4
	Drag Rev	1486.5	1484.7	1464.4	1490.3	1500.9	1483.6	1494.9	1492.3	1487.6
	Subtracted	**0.5**	**0.4**	**0.8**	**0.5**	**0.6**	**0.6**	**-0.7**	**-0.2**	**-0.2**
160	Rev	1120.1	1118.9	1102.3	1120.4	1117.3	1109.8	1123.5	1119.4	1115.1
	Drag Rev	1120.4	1119.3	1102.9	1120.6	1117.5	1110.2	1123.6	1119.6	1115.4
	Subtracted	**0.3**	**0.4**	**0.6**	**0.2**	**0.2**	**0.4**	**0.1**	**0.2**	**0.3**

Table 3.7 The results of comparing two tests of slippage

$$\chi^2 = \sum \frac{(\text{Observed Freq.} - \text{Expected Freq.})^2}{\text{Expected Freq.}}$$

Effect of drag on revolutions of package at 120 mm

	Observed frequencies F_0	Expected frequencies F_e	Deviations F_0-f_e	$(F_o-f_e)^2/f_e$
Press. 2 /ten. 30 g	1486.5	1486.94	-0.444	1.32578E-4
Press. 2 /ten. 19 g	1484.7	1486.94	-2.244	0.00339
Press. 2 /ten. 8 g	1464.4	1486.94	-22.544	0.3418
Press. 1.25 /ten. 30 g	1490.3	1486.94	3.356	0.00757
Press. 1.25 /ten. 19 g	1500.9	1486.94	13.956	0.13099
Press. 1.25 /ten. 8 g	1483.6	1486.94	-3.344	0.00752
Press. 0.7 /ten. 30 g	1494.9	1486.94	7.956	0.04257
Press. 0.7 /ten. 19 g	1492.3	1486.94	5.356	0.01929
Press. 0.7 /ten. 8 g	1487.6	1486.94	0.656	2.8941E-4
Total	**13385.2**	**13382.496**	**2.704**	**0.5535**

- Observed frequencies are the revolutions of package with drag effect (from Table 3.6)
- Expected frequencies are the mean of the revolution of package without drag effect (from Table 3.5)

$\chi^2_{9,0.05} = 16.92$

$0.5535 << \chi^2_{9,0.05}$

So the drag effect does not cause any significant change of slippage.

Effect of drag on revolutions of package at 80 mm

	Observed frequencies F_0	Expected frequencies F_e	Deviations F_0-f_e	$(F_o-f_e)^2/f_e$
Press. 2 /ten. 30 g	2230	2217.77	12.23	0.06744
Press. 2 /ten. 19 g	2224.2	2217.77	6.43	0.01864
Press. 2 /ten. 8 g	2196.1	2217.77	-21.67	0.21174
Press. 1.25 /ten. 30 g	2233	2217.77	15.23	0.10459
Press. 1.25 /ten. 19 g	2224.3	2217.77	6.53	0.01923
Press. 1.25 /ten. 8 g	2206.1	2217.77	-11.67	0.06141
Press. 0.7 /ten. 30 g	2214	2217.77	-3.77	0.00641
Press. 0.7 /ten. 19 g	2211.1	2217.77	-6.67	0.02006
Press. 0.7 /ten. 8 g	2212.2	2217.77	-5.57	0.01399
Total	19951	19959.93	-8.93	0.52351

Effect of drag on revolutions of package at 160 mm

	Observed frequencies F_o	Expected frequencies F_e	Deviations F_o-f_e	$(F_o-f_e)^2/f_e$
Press. 2 /ten. 30 g	1120.4	1116.31	4.09	0.01499
Press. 2 /ten. 19 g	1119.3	1116.31	2.99	0.00801
Press. 2 /ten. 8 g	1102.9	1116.31	-13.41	0.16109
Press. 1.25 /ten. 30 g	1120.6	1116.31	4.29	0.01649
Press. 1.25 /ten. 19 g	1117.5	1116.31	1.19	0.00127
Press. 1.25 /ten. 8 g	1110.2	1116.31	-6.11	0.03344
Press. 0.7 /ten. 30 g	1123.6	1116.31	7.29	0.04761
Press. 0.7 /ten. 19 g	1119.6	1116.31	3.29	0.0097
Press. 0.7 /ten. 8 g	1115.4	1116.31	-0.91	7.41819E-4
Total	10049.5	10046.79	2.71	0.29334

3.5.6 Discussion of Slippage

There are a few references about the slippage of cheese packages in winding. One of these was published by Osawa and Koyama [Osawa 72]. Their experiment is somewhat different from the experiment performed in this project as some of the settings used were unrealistically high. Their result was that slippage increases when increasing pressure or yarn drag is applied to a cheese package. In this project, the conditions of winding were the same as those normally used in the textile industry. Packages were produced under limited values of tension and pressure and slippage determined.

3.6 Deformation of a wound package at the contact point

3.6.1 Introduction

The deformation occurs at the contact point between the drum and the package due to package cradle pressure and the own weight of the package. As mentioned before, the drum is hard and is not deformable. The package is relatively soft and is non-isotropic due to the yarn. Besides, the surface of the package consists of yarn laid at a constant wind angle. The winding creates spaces between successive turns of yarn wound.

3.6.2 The Method of Measuring Package Deformation

Experiments were conducted at different diameters, pressure and yarn tension values in order to determine package deformation at the point of contact with the drum. The LVDT, located on the package cradle gives the deformed radius of the package; the POT which is located on the top of the package gives the non-deformed radius of the package. The difference of the two readings is therefore the amount of deformation.

However, on account of the fact that the wound package is not quite cylindrical, the deformation shows variation at different points on the package.

Therefore it was decided to measure deformation while the package is rotated on the winder, and the average of a sufficient number of such readings will give a better estimate of deformation.

However, it was found that the reading from the POT had considerable jitter due to the light cylinder connected to its arm jumped excessively on the package while the winder was operated. Another solution was needed to measure the undeformed radius of the package.

The solution adopted was to use a screw and nut arrangement to gently raise the package arm till the package just cleared the drum surface. As this point the LVDT should give the un-deformed radius of the package. First, the package was allowed to rotate normally, and the LVDT was read to obtain its deformed radius as described in the previous paragraph. After that, the screw was located between the flat surface under package cradle and the package cradle arm. The nut on the screw was turned slowly by hand to lift the package arm while running the winder. The point of stopping was when the package only just touched the drum. At this point, the package speed was almost zero. The reading at that point from the LVDT gives the un-deformed radius of the package. The difference of the two reading gave the deformation of the package. A program in C language was written to follow the LVDT reading on the monitor for both deformed radius and un-deformed radius. The program gives the average reading of 10 revolution of the package [Appendix C.4].

3.6.3 Results of deformation measurement

The reading of the LVDT was obtained for different values of package diameter, pressure between drum and package, and winding tension. The calculation of deformation was done and tabulated below in Table 3.8. More information about the results of deformation is given in Appendix B. The results are shown by Fig 3.15, 3.16, 3.17.

The amount of deformation depends on the package cradle pressure as mentioned before. At the same pressure, the deformation depends on the package radius. Generally, increasing package radius caused the greater deformation contact point as shown by each graph.

At the pressure of 1.25 kg as in Fig 3.16, the deformation generally shows a decrease with increasing density, and an increase with increasing package radius. The behaviour

is similar at the lower pressure of 0.7 kg, but is more complex at the higher pressure of 2 kg.

DIA. (mm)	PRESSURE (kg)	2	2	2	1.25	1.25	1.25	0.7	0.7	0.7
	Yarn tension (g)	Max (30 g)	Med (19 g)	Min (8 g)	Max (30 g)	Med (19 g)	Min (8 g)	Max (30 g)	Med (19 g)	Min (8 g)
80	Radius	39.9	39.8	39.8	39.8	39.9	39.9	39.9	39.9	39.9
	Density	0.4564	0.4033	0.3632	0.4323	0.3954	0.3558	0.4201	0.3847	0.3325
	Def	**0.32**	**0.44**	**1.35**	**0.34**	**0.43**	**0.75**	**0.18**	**0.18**	**0.4**
120	Radius	59.9	60.0	59.9	60.3	59.7	59.8	60.0	60.1	60.1
	Density	0.4599	0.4207	0.3700	0.4547	0.4233	0.3451	0.4336	0.3847	0.3415
	Def	**0.9**	**1.02**	**1.67**	**0.45**	**0.57**	**1.14**	**0.28**	**0.37**	**0.55**
160	Radius	79.7	79.6	79.7	79.8	80.0	80.0	79.8	80.1	80.1
	Density	0.452	0.4060	0.3432	0.4405	0.4028	0.3448	0.4367	0.4009	0.3461
	Def	**0.8**	**1.27**	**2.2**	**0.41**	**0.76**	**1.11**	**0.53**	**0.53**	**0.79**

- Density [g/cm^3], Radius [mm], deformation [mm]

Table 3.8. Deformation of packages

3.7 Discussion

The deformation of the package on the winding drum is of interest in random winding. The amount of compression which depends on the basic winding parameters as given in the previous section will have a direct influence on the speed of package rotation. When other things are constant, slippage increases with increase of package cradle pressure. It can be seen for example by comparing Fig.3.14 and 3.17 that while the amount of compression increases with increasing package radius, other things being constant, the slippage shows a decrease. This could be partly due to the increase of surface area of contact for the same amount of compression (depth of penetration) as the package radius increases.

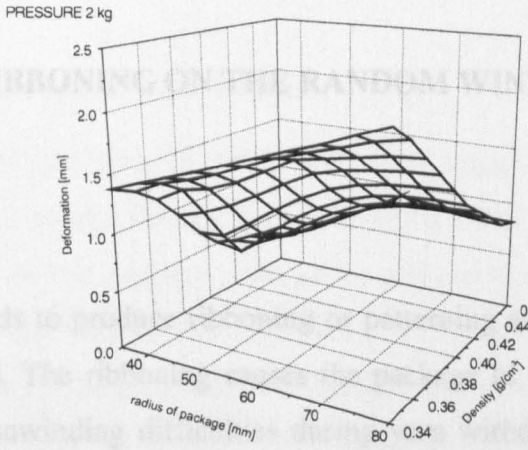

Fig 3.15 Deformation of package at pressure 2 kg

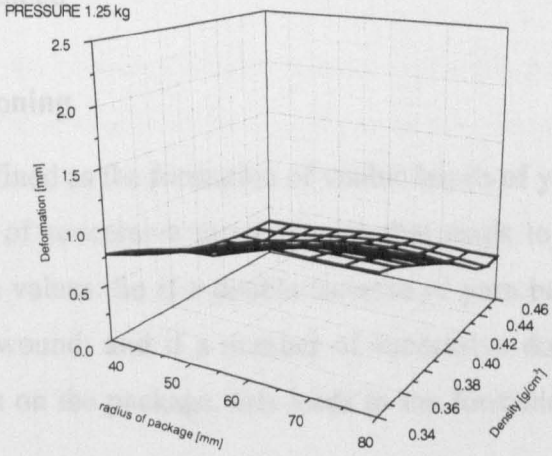

Fig 3.16 Deformation of package at pressure 1.25 kg

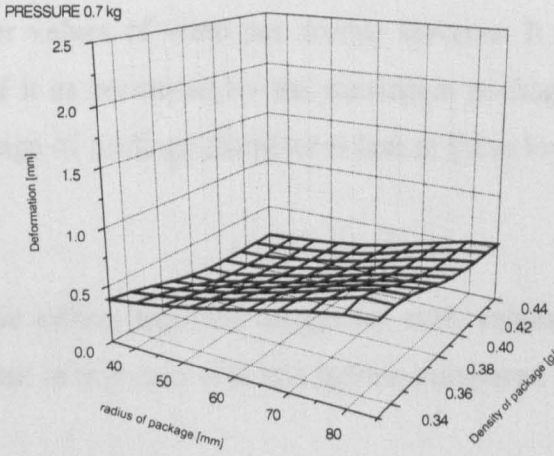

Fig 3.17 Deformation of package at pressure 0.7 kg

CHAPTER FOUR

RIBBONING ON THE RANDOM WINDER

4.1 Introduction

A random winder tends to produce ribboning or patterning at certain diameters of the package being wound. The ribboning causes the package to deviate from the desired shape as well cause unwinding difficulties during yarn withdrawal from the package. Where packages are dyed it causes the package to dye non-uniformly. In this chapter, ribboning will be defined and controlling the random winding operation by the use of electronics will be explained

4.2 Definition of Ribboning

Ribboning has been defined as the formation of visible bands of yarn by the overlapping or very close winding of successive turns of yarn that tends to occur as the package diameter attains certain values. So if a double traverse of yarn begins at a certain point on the package being wound; and if a number of successive double traverses of yarn begin at the same point on the package, this leads to the formation of a visible band or ribbon of yarn.

As explained before, ribboning is most intense (major ribboning)at points where the package reaches integer values of wind per double traverse. It persists longest at the lower integer values of it as permitted by the maximum package size wound. This is because the rate of change of package diameter is less at these lower values of wind per double traverse.

Where the traverse ratio differs from an integer by such values as 0.5 and 0.333 etc, ribboning still occurs, but in this case it is less intense compared to major ribboning.

4.3 Analysis of ribboning on the random winder

4.3.1 Configuration of experimental winder

Fig 4.1 shows the configuration of the experimental apparatus. There are two shaft encoders located on the winder. One of these is attached to the drum shaft of the winder. The other is mounted on the package shaft at the same side of the winder. Both were connected to interface card via junction box so that their angular position can be read as an 8-bit digital number by the computer. The cables from the shaft encoders are lead to a pair of D-type connectors, to facilitate checking of all the signals provided by them. The 8 bit angular position reading is fed to the PC interface card using screened wire. A program was written in the C language to read both shaft encoders.

The constant speed motor provided on the winder was replaced with a DC brushless motor [Electro-craft] whose speed can be directly controlled by an external DC voltage. The motor is capable of any speed from 0-3000 rpm, as well as very rapid speed fluctuation under external control. More information about the shaft encoders and the motor was given in Chapter 2. The function of the pulley shown is covered on page 96.

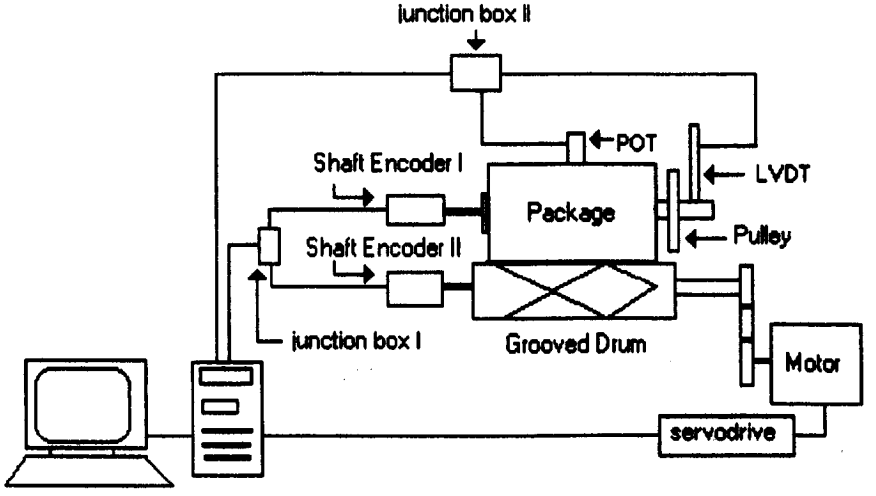

Fig 4.1 Configuration of the winder

4.3.2 The method of following yarn on the drum and the package

On the experimental winder the shaft encoder on the drum was set to read to zero when the yarn is at the left hand end of the groove. As the grooved drum has a drum constant of 3, by reading the package shaft encoder reading at every third zero crossing of the drum, a convenient reference is obtained to identify the beginning of a double traverse.

4.3.2.1 The program for reading shaft encoder on the drum

The program written for this purpose enables the PC to read the shaft encoder when the drum is made to rotate at the required speed. It writes the 0-255 value of shaft position on the VDU. At any constant speed of the drum, each value of shaft position should be written very closely the same number of times, for one rotation of the drum. For instance, the number of reading between 1 and 2 should be as same as the number of reading between 244 and 245.

The operation of both shaft encoders was painstakingly checked for correct operation, before experiments were started. When tested as above, the incremental shaft encoder was quite well behaved, but the absolute shaft encoder occasionally provided solitary rogue values. There were two possible causes of this. One was electrical noise, as described in Chapter 2. The other was the intrinsic problem with absolute shaft encoders, in that if a reading was taken at a time one or more bits were changing, a faulty reading could be obtained. This problem was far less severe with the incremental encoder, as the error was no more than one least count. As confirmed by observations over a number of hours, the spurious values provided by the absolute encoder were always single, and these were comparatively rare in the readings obtained in each revolution.

4.3.2.2 Experiments to observe ribbon formation in winding

The observation or detection of ribboning is based on the following procedure. Each time a new double traverse begins, the reading of the package shaft encoder is taken. As this procedure is repeated, the reading of the package shaft encoder is compared with its previous reading. If the difference is zero or very close to zero, this indicates major

ribboning. If the difference is 180^0, 90^0(or 270^0), 45^0(or 315^0) etc. diminishing magnitudes of minor ribboning is indicated.

Since the beginning of a double traverse was chosen as when the drum shaft encoder reads zero, it is first necessary to detect when the grooved drum is at this position, in every 3 revolutions (as the drum constant is 3). Since the reading of 0 from this shaft encoder will last in the duration between angle reading of 255 and 1, it was arbitrarily chosen to detect the transition from 0 to 1 as the reference, so that the package shaft encoder reading can be obtained with the best accuracy. However since the drum shaft encoder involves the occasional rogue numbers, a procedure is necessary to avoid any difficulties that can be caused by such numbers.

The program was modified to be able to eliminate such false values. Two methods of achieving this were tried. The first method is to use two stages of nested loops as shown by Fig 4.2. The routine is not disturbed by false numbers, and exits only when a reliable transition of the reading from 0 to 1 occurs.

The second method consists of taking 4 successive readings, and comparing them to check that they are all the same. This is repeated till the reading of 0 is achieved. The routine then waits till the reading of 1 has reliably arrived. Both these methods were tried and were found to work reliably. The program is given in Appendix C.5.

4.3.3 Graphic representation of progress of winding

The yarn starts winding at the left hand side of the drum, and goes back to the same point, after the drum has made 3 revolutions. Ribboning is expected each time the package shaft encoder recorded the same reading over a number of successive arrivals of the drum at the beginning of a double traverse. Therefore it appeared useful to plot on the VDU the value of the package shaft encoder, each time a new double traverse began.

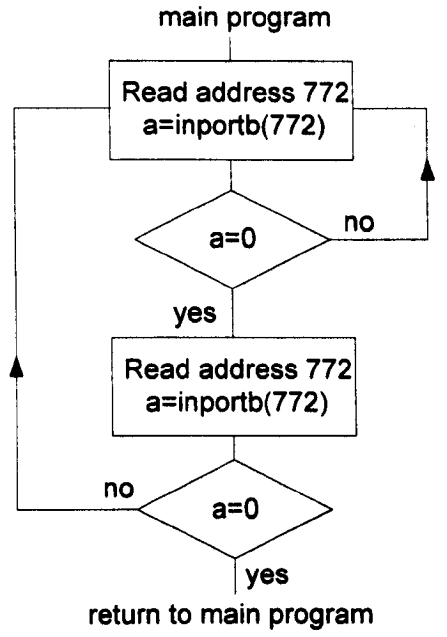

(a)

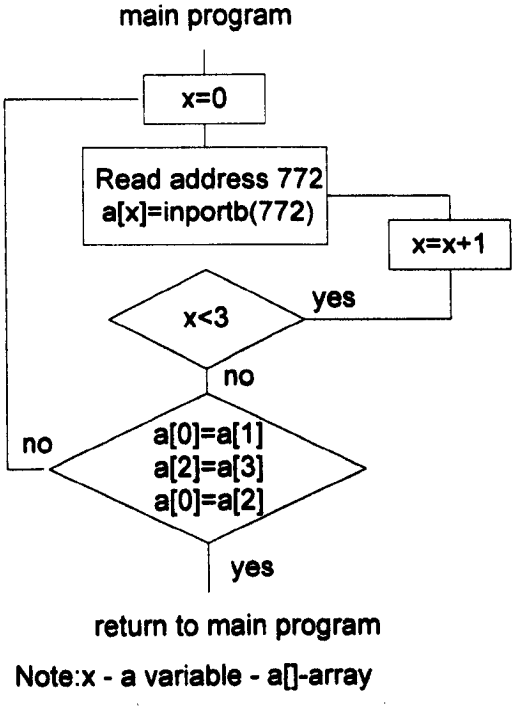

(b)

Fig 4.2 Flowchart for eliminating false values

a) nested loops b)comparing four readings

A programme was written to perform this in real time as winding progressed, as the resulting diagram will visually present advance indication of the occurrence and the conclusion of each stage of ribboning. This was done by detecting the 0 point of the drum shaft encoder as described in the previous section, and then immediately reading the package shaft encoder. The next point was obtained at the occurrence of the next double traverse and so on. So the successive readings of the package shaft encoder at each third occurrence of zero crossing of the drum are plotted on the VDU as winding proceeds.

The plot obtained on the VDU was called the **ADT** (**A**ngle at **D**ouble **T**raverse) diagram. The diagram is based on 500 successive double traverses on the horizontal axis and the angle of the package at the beginning of each double traverse (0-255) on the vertical axis in Fig 4.3. The software was written to create the diagram on the VDU. Each reading of double traverse locates a dot on the diagram. It corresponds to the start of one double traverse on the package. After completing of 500 double traverses, the diagram is cleared and the next 500 points will be plotted by the program. In addition, to aid following the progress of winding, the diameter of the package was read from LVDT to calculate traverse ratio. The program is given in Appendix C.6. The pattern of points was found to aid the understanding the formation of the random wound package. Several examples were studied under various conditions of winding.

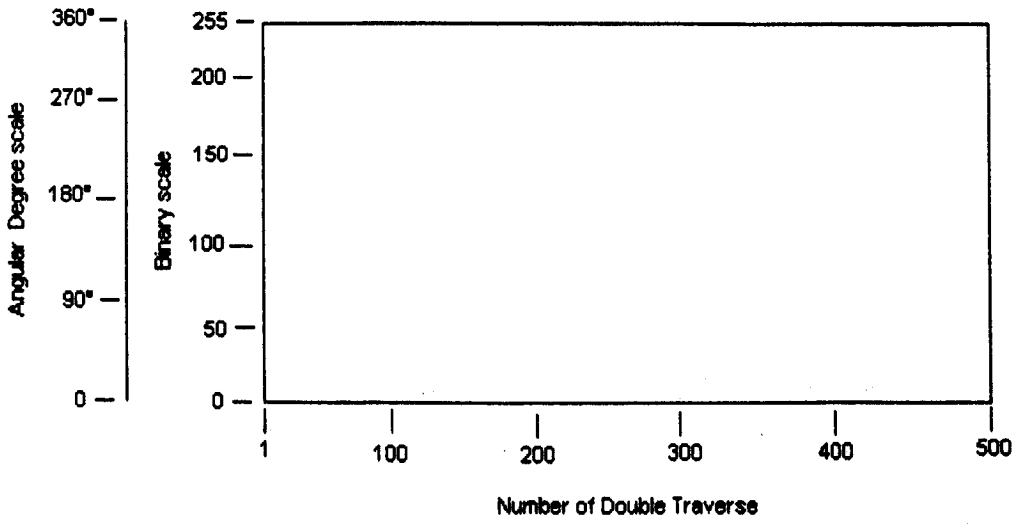

Fig 4.3 ADT diagram

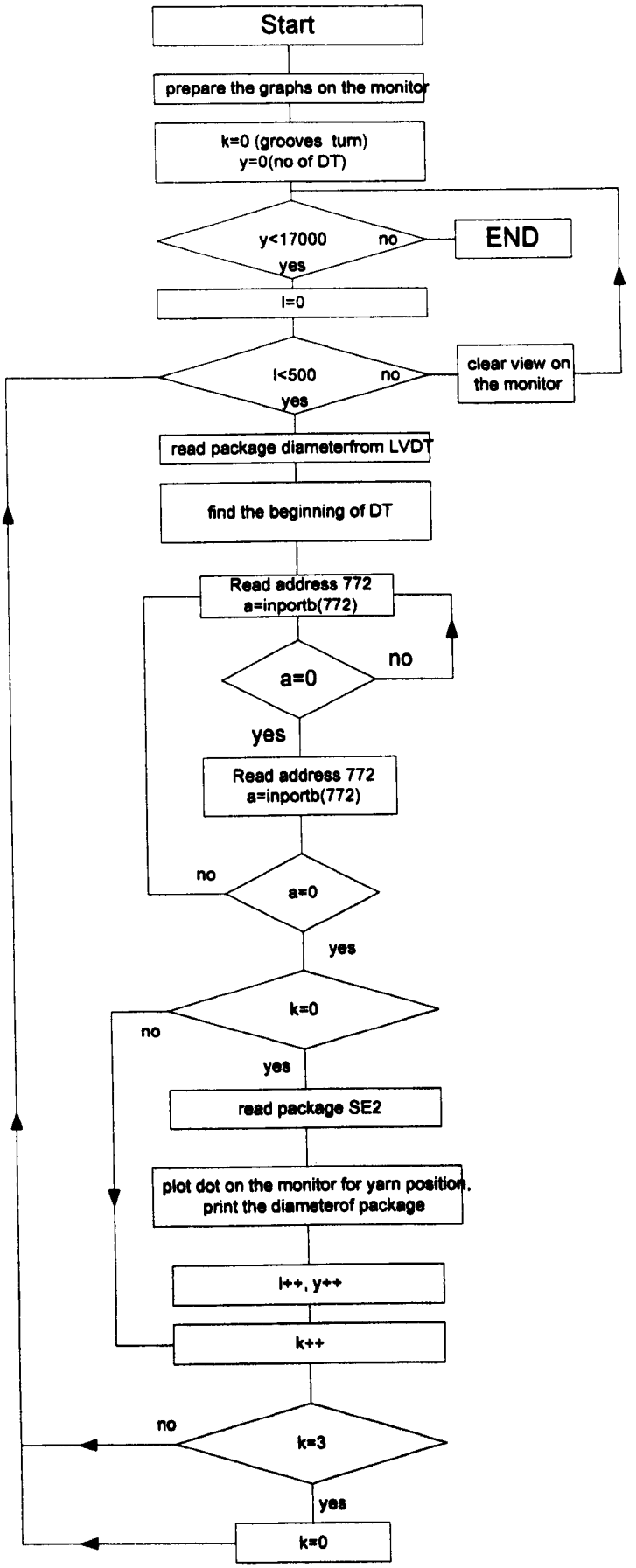

Fig 4.4 Flowchart of the program of ADT diagram

4.3.4 Package formation

Random winding produces ribboning on a package. Yarn was wound without the use of ribbon breaking and the ADT diagram was plotted during winding. Some examples of these trials are given in Figs 4.5 and 4.8. These very effectively show how yarn is added on to form the surface of the package. Ribboning or patterning depends on the traverse ratio, which is the ratio of drum diameter to package diameter. The decimal part of the traverse ratio at a given package diameter gives the corresponding number of the curves on the ADT diagram. It can be seen that when the decimal part is zero or traverse ratio is integer, there is only one curve, as seen Fig 4.7. If it is 0.5, the number of curves is 2 as seen in Fig 4.5. The rather sudden change in the single curve of Fig. 4.7 can be explained on account of the rather large asymmetry brought about on the package due to the 'single' and dense ribbon caused, which causes some instability to the driving of the package, perhaps due to the interference from the groove of the drum. When the ribboning is other than major, the two or more ribbons that form help the package to be more symmetric and the driving is likely to be less disturbed.

Decimal of traverse ratio	Number of curves	Decimal of traverse ratio	Number of curves
0	1	0.15	7
0.5	2	0.12	8
0.33	3	0.11	9
0.25	4	0.1	10
0.20	5	0.09	11
0.17	6	0.08	12

Table 4.1 Relation of decimal of traverse and number of curves

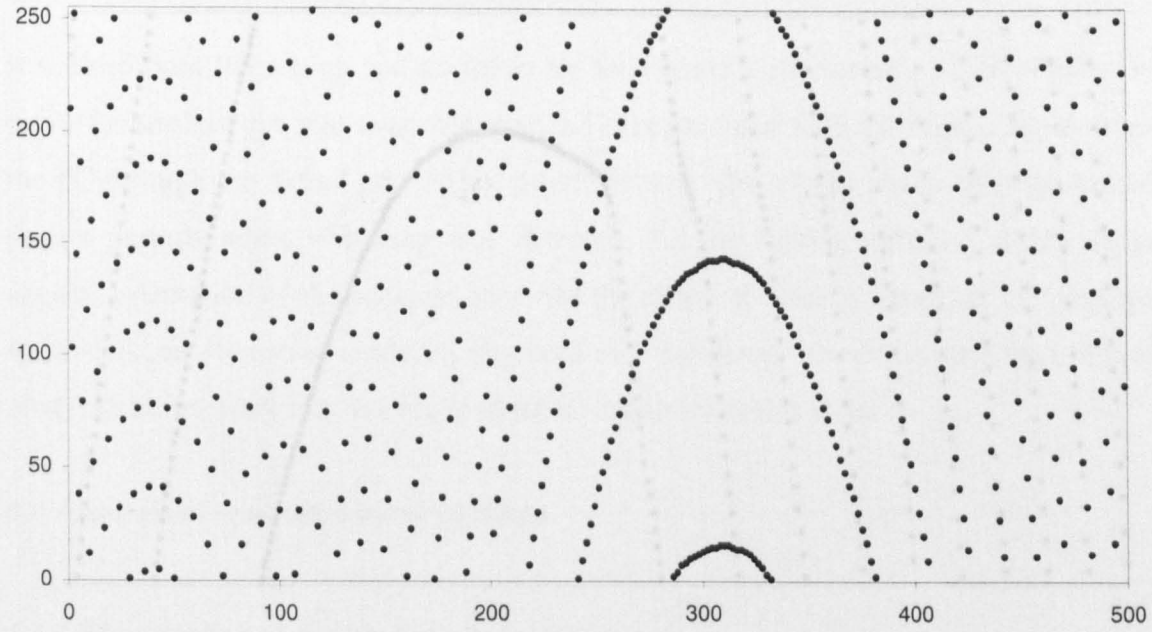

Fig 4.5 Traverse ratio 3.5 (3.60 – 3.48)- no ribbon breaking

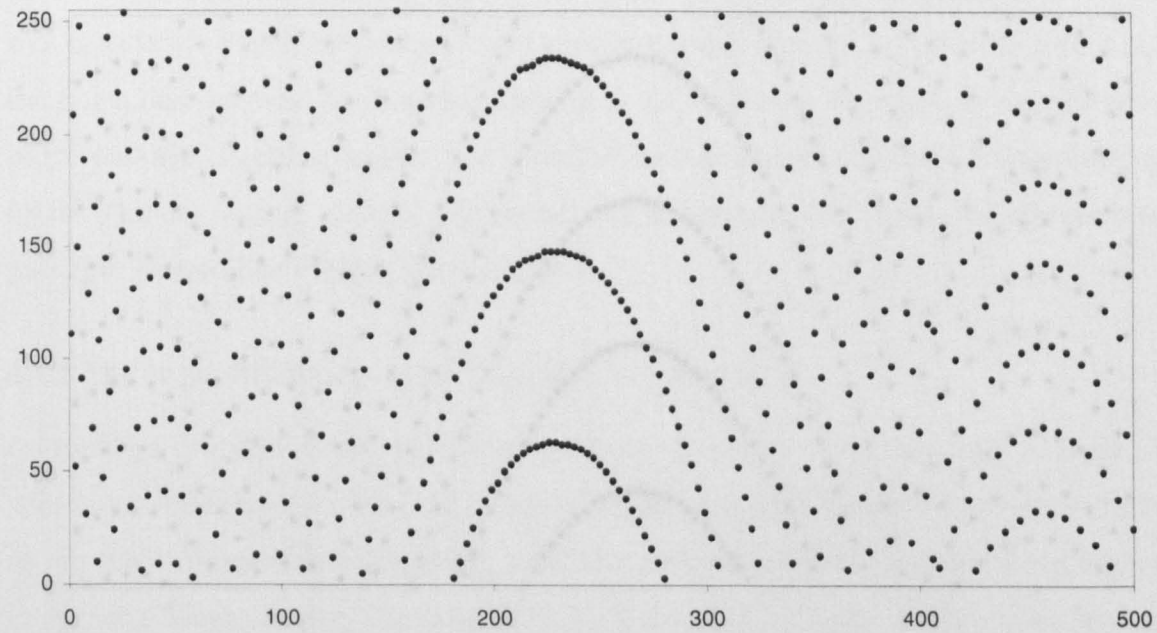

Fig 4.6 Traverse ratio 3.3 (3.41-3.31)- no ribbon breaking

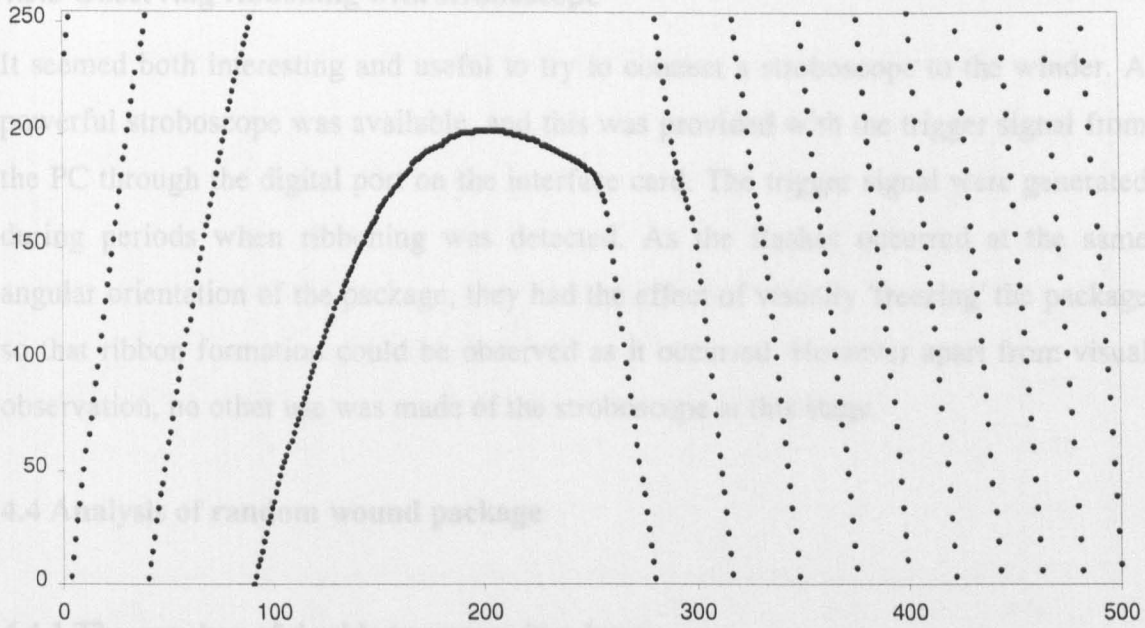

Fig 4.7 Traverse ratio 3.0 (3.06-2.97) – no ribbon breaking

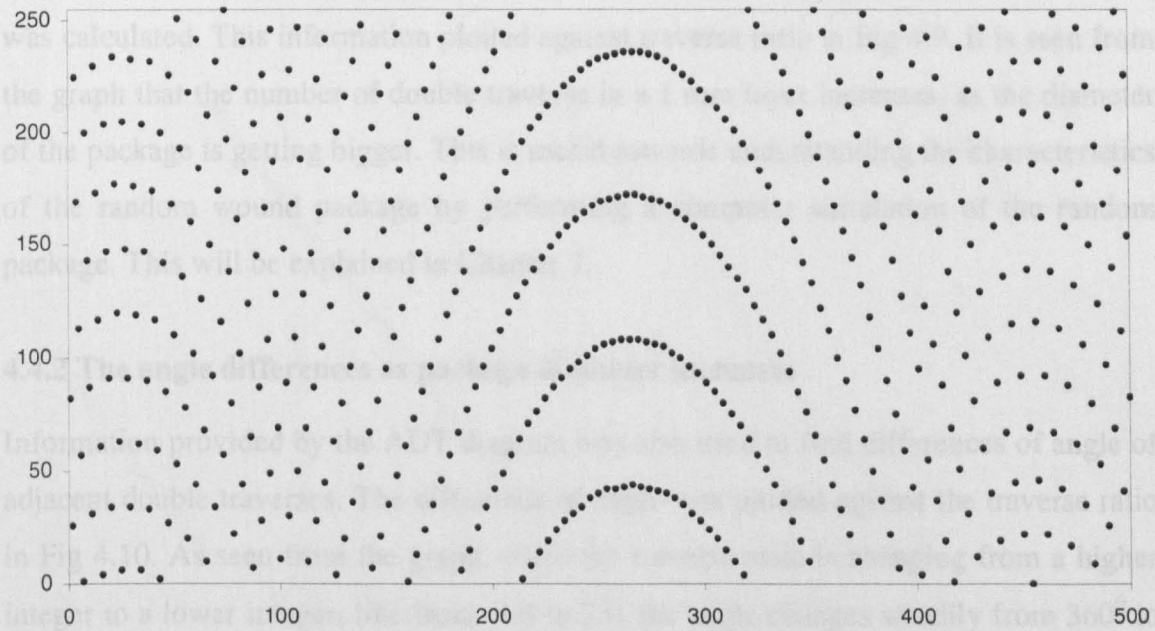

Fig 4.8 Traverse ratio 2.75 (2.80-2.73) – no ribbon breaking

4.3.5 Observing ribboning with stroboscope

It seemed both interesting and useful to try to connect a stroboscope to the winder. A powerful stroboscope was available, and this was provided with the trigger signal from the PC through the digital port on the interface card. The trigger signal were generated during periods when ribboning was detected. As the flashes occurred at the same angular orientation of the package, they had the effect of visually 'freezing' the package so that ribbon formation could be observed as it occurred. However apart from visual observation, no other use was made of the stroboscope at this stage.

4.4 Analysis of random wound package

4.4.1 The number of double traverses in a layer

By winding yarn to form a package from tube diameter of 57 mm to a maximum radius of 160 mm, the winding process was followed using the PC to record the radius of package and the angle of the double traverse on the package. Using this information, the number of double traverses deposited in successive layers of package of thickness 1 mm was calculated. This information plotted against traverse ratio in Fig 4.9. It is seen from the graph that the number of double traverse in a 1 mm layer increases, as the diameter of the package is getting bigger. This is useful towards understanding the characteristics of the random wound package by performing a computer simulation of the random package. This will be explained in Chapter 7.

4.4.2 The angle differences as package diameter increases

Information provided by the ADT diagram was also used to find differences of angle of adjacent double traverses. The difference of angle was plotted against the traverse ratio in Fig 4.10. As seen from the graph, when the traverse ratio is changing from a higher integer to a lower integer, like from 4.0 to 3.0, the angle changes steadily from 360^0 to 0^0 (binary 255-0). This shows that when the traverse ratio is 0, or 0.5; the angle of difference is 0^0 or 180^0 respectively. The other differences indicate stages of minor ribboning on the package.

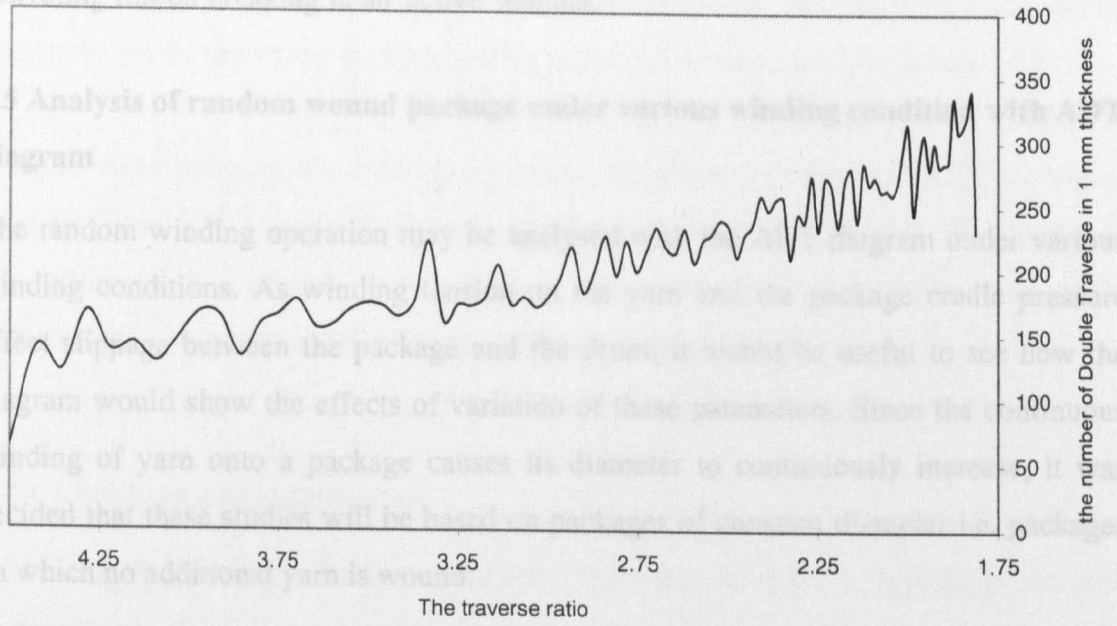

Fig 4.9 the number of double traverse in 1 mm thickness of diameter against traverse ratio.

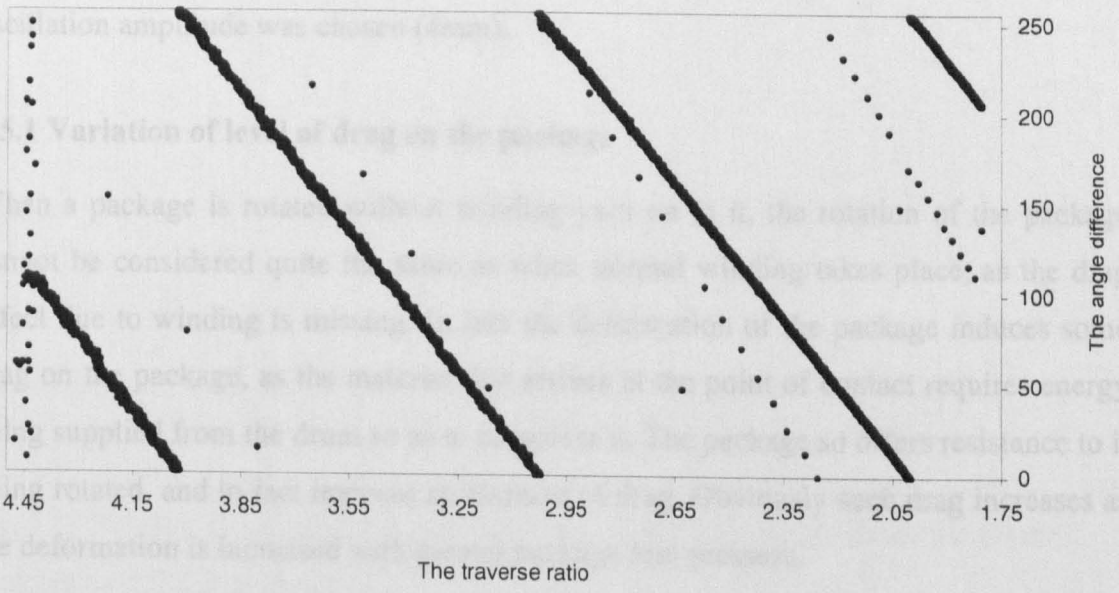

Fig 4.10 the angle differences between each double traverse against traverse ratio

This information is useful for both knowing the form of a random package and activating ribbon breaking in an 'active' manner.

4.5 Analysis of random wound package under various winding condition with ADT diagram

The random winding operation may be analysed with the ADT diagram under various winding conditions. As winding tension on the yarn and the package cradle pressure affect slippage between the package and the drum, it would be useful to see how the diagram would show the effects of variation of these parameters. Since the continuous winding of yarn onto a package causes its diameter to continuously increase, it was decided that these studies will be based on packages of constant diameter i.e. packages on which no additional yarn is wound.

Package diameters of 80 mm and 120 mm were chosen for the experiments. The packages were prepared in the normal manner by winding until the required diameter was reached. The winding conditions applied were scale 3 of the pressure (1.5 kg) and 19 g of yarn tension. The speed of the drum was set at 255 binary (2133 rpm). Drum oscillation was activated in certain experiments as indicated, where the maximum oscillation amplitude was chosen (4mm).

4.5.1 Variation of level of drag on the package

When a package is rotated without winding yarn on to it, the rotation of the package cannot be considered quite the same as when normal winding takes place, as the drag effect due to winding is missing. In fact the deformation of the package induces some drag on the package, as the material that arrives at the point of contact requires energy being supplied from the drum so as to compress it. The package so offers resistance to it being rotated, and in fact imposes an element of drag. Obviously such drag increases as the deformation is increased with greater package arm pressure.

So in the study of the rotation of packages of fixed diameter, the yarn drag effect can be accounted for by use of the cord and pulley arrangement described in section 3.5.3.1.

Weights were hung on the cord on the pulley for giving the drag effect. The weights used are 50 g, 100 g and150g. Normal winding tension is no more than 30 g acting at the surface of the package. It was thought that lateral oscillation of the drum would induce some (circumferential) slippage of the package on the drum.

4.5.1.1 Without drum oscillation

By running the package of 80 mm diameter, and using different drag weights but with no oscillation, ADT diagrams were obtained as shown by Fig. 4.11 to Fig 4.14.

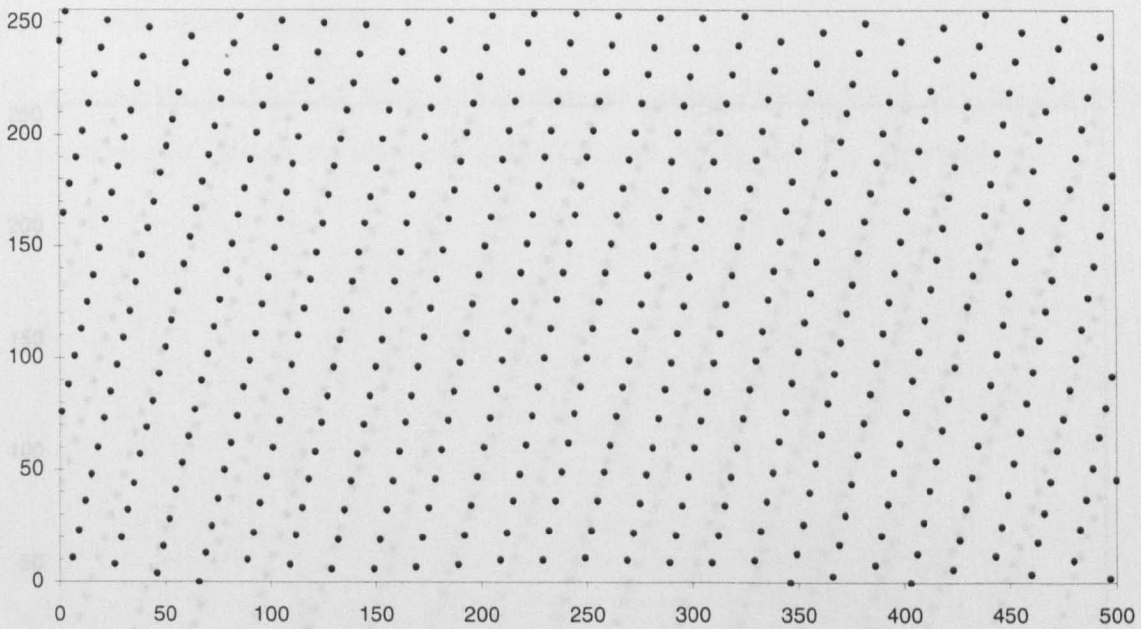

Fig 4.11 Rotation of constant diameter package at increased drag (diameter :80 mm, traverse ratio:3.4, no-weight)

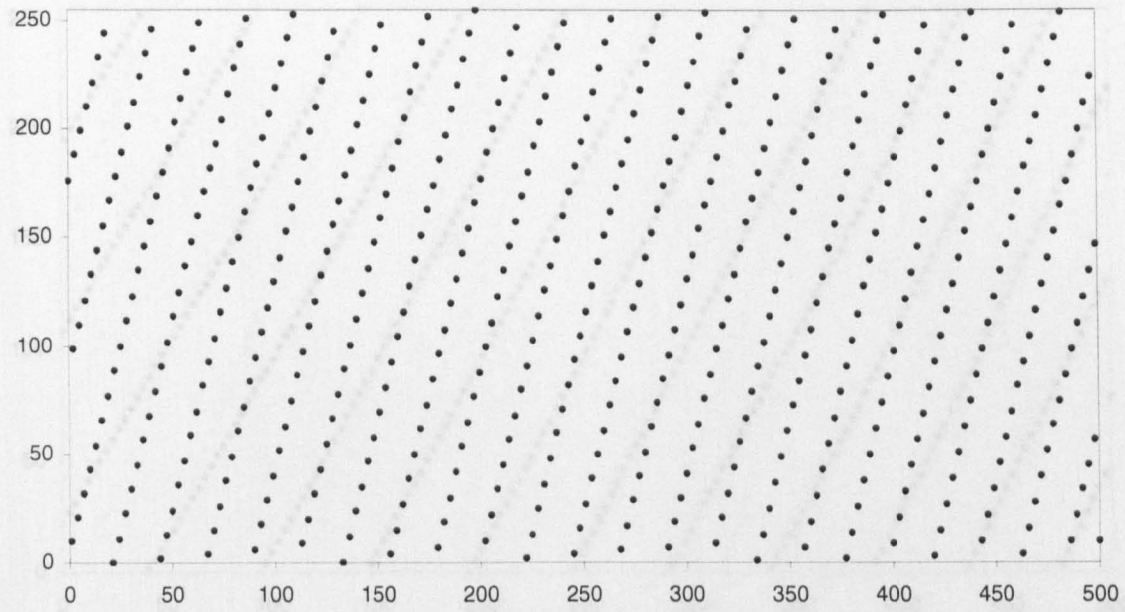

Fig 4.12 Rotation of constant diameter package at increased drag (diameter :80 mm, traverse ratio:3.4, weight 50 g)

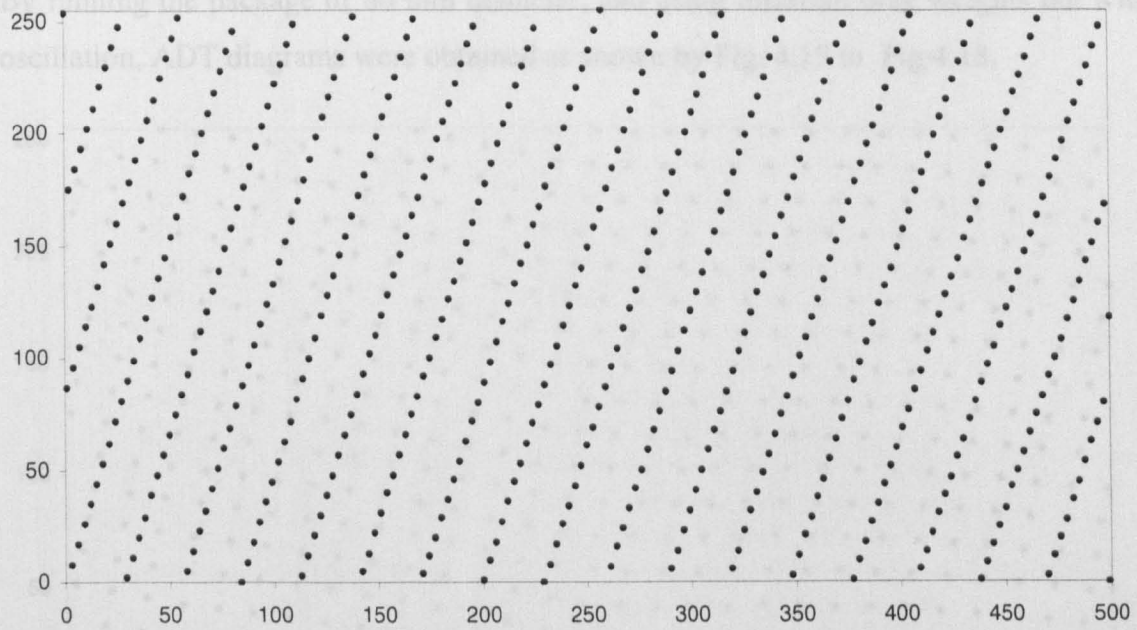

Fig 4.13 Rotation of constant diameter package at increased drag (diameter :80 mm, traverse ratio:3.4, weight 100 g)

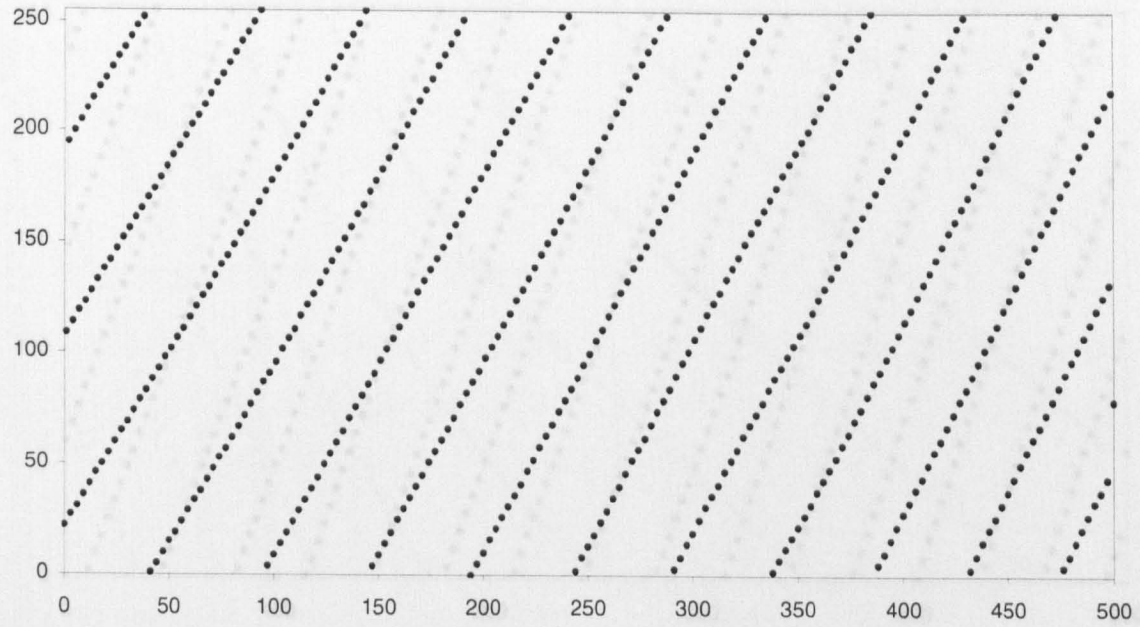

Fig 4.14 Rotation of constant diameter package at increased drag (diameter :80 mm, traverse ratio:3.4, weight 150 g)

4.5.1.2 with drum oscillation

By running the package of 80 mm diameter, and using different drag weights but with oscillation, ADT diagrams were obtained as shown by Fig. 4.15 to Fig 4.18.

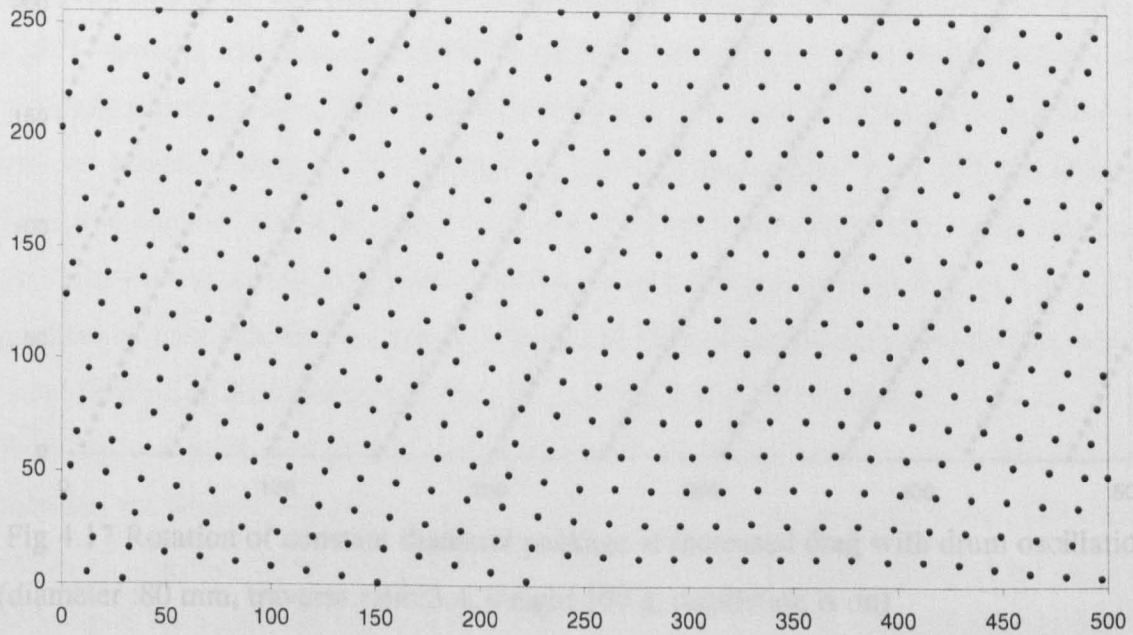

Fig 4.15 Rotation of constant diameter package at increased drag with drum oscillation (diameter :80 mm, traverse ratio:3.4, no-weight, oscillation is on)

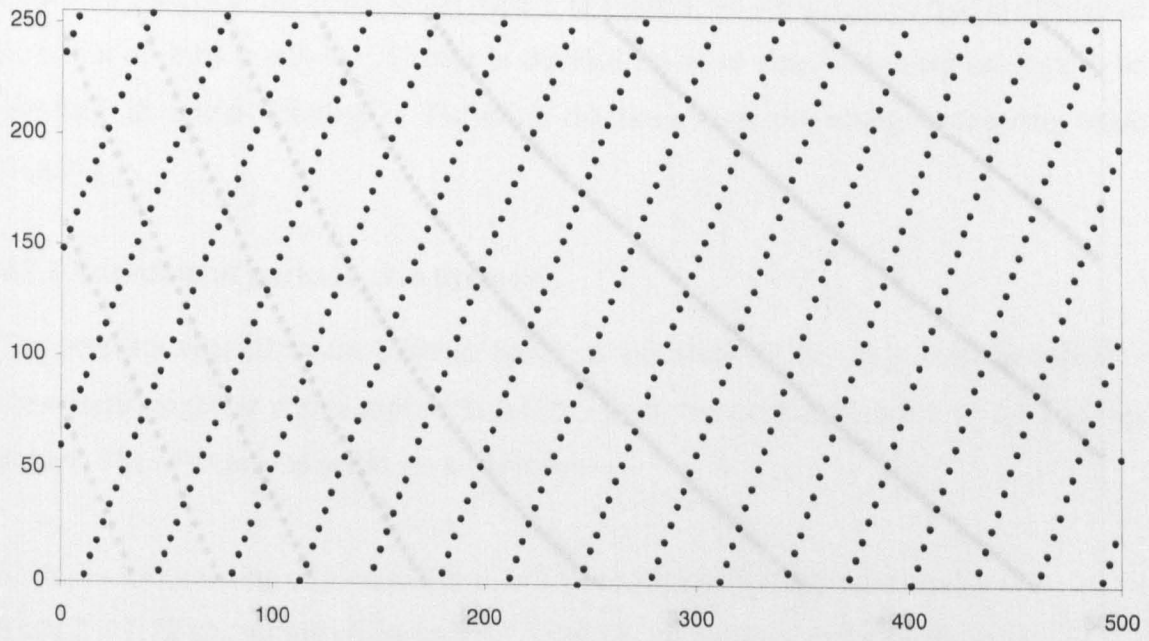

Fig 4.16 Rotation of constant diameter package at increased drag with drum oscillation (diameter :80 mm, traverse ratio:3.4, weight 50 g, oscillation is on)

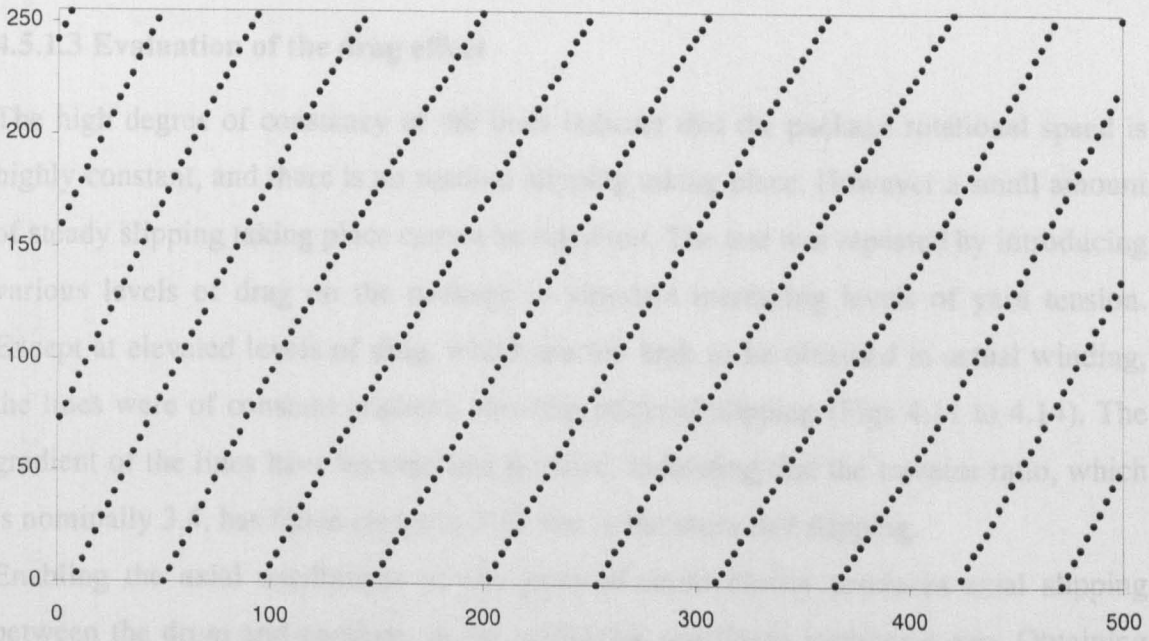

Fig 4.17 Rotation of constant diameter package at increased drag with drum oscillation (diameter :80 mm, traverse ratio:3.4, weight 100 g, oscillation is on)

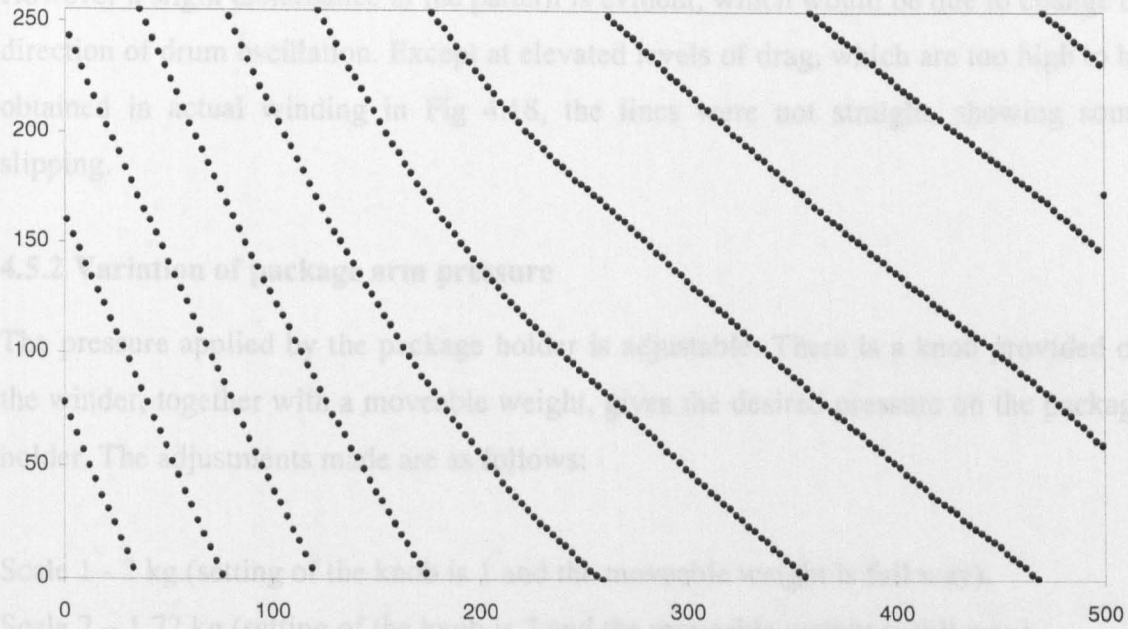

Fig 4.18 Rotation of constant diameter package at increased drag with drum oscillation (diameter :80 mm, traverse ratio:3.4, weight 150 g, oscillation is on)

4.5.1.3 Evaluation of the drag effect

The high degree of constancy of the lines indicate that the package rotational speed is highly constant, and there is no random slipping taking place. However a small amount of steady slipping taking place cannot be ruled out. The test was repeated by introducing various levels of drag on the package to simulate increasing levels of yarn tension. Except at elevated levels of drag, which are too high to be obtained in actual winding, the lines were of constant gradient, showing minimal slipping (Figs 4.11 to 4.14). The gradient of the lines have become less positive, indicating that the traverse ratio, which is nominally 3.4, has fallen closer to 3.33 due to the increased slipping.

Enabling the axial oscillations of the grooved drum clearly produces axial slipping between the drum and package, as the oscillation amplitude is about 4 mm. Obtaining the ADT diagram under this condition (Figs 4.15 to 4.17)still indicates no random slipping in the rotational movement of the package. The similar slope of lines to that in Figs 4.15 to 4.17 also show that no increased level of slipping is occurring either.

However a slight disturbance in the pattern is evident, which would be due to change of direction of drum oscillation. Except at elevated levels of drag, which are too high to be obtained in actual winding in Fig 4.18, the lines were not straight, showing some slipping.

4.5.2 Variation of package arm pressure

The pressure applied by the package holder is adjustable. There is a knob provided on the winder, together with a moveable weight, gives the desired pressure on the package holder. The adjustments made are as follows:

Scale 1 - 2 kg.(setting of the knob is 1 and the moveable weight is full way).
Scale 2 – 1.72 kg.(setting of the knob is 2 and the moveable weight is full way).
Scale 3 – 1.5 kg.(setting of the knob is 3 and the moveable weight is half way).
Scale 4 – 1.1 kg.(setting of the knob is 4 and the moveable weight is full way).
Scale 5 – 0.7 kg.(setting of the knob is 4.5 and the moveable weight is moved out).

4.5.2.1 Without oscillation

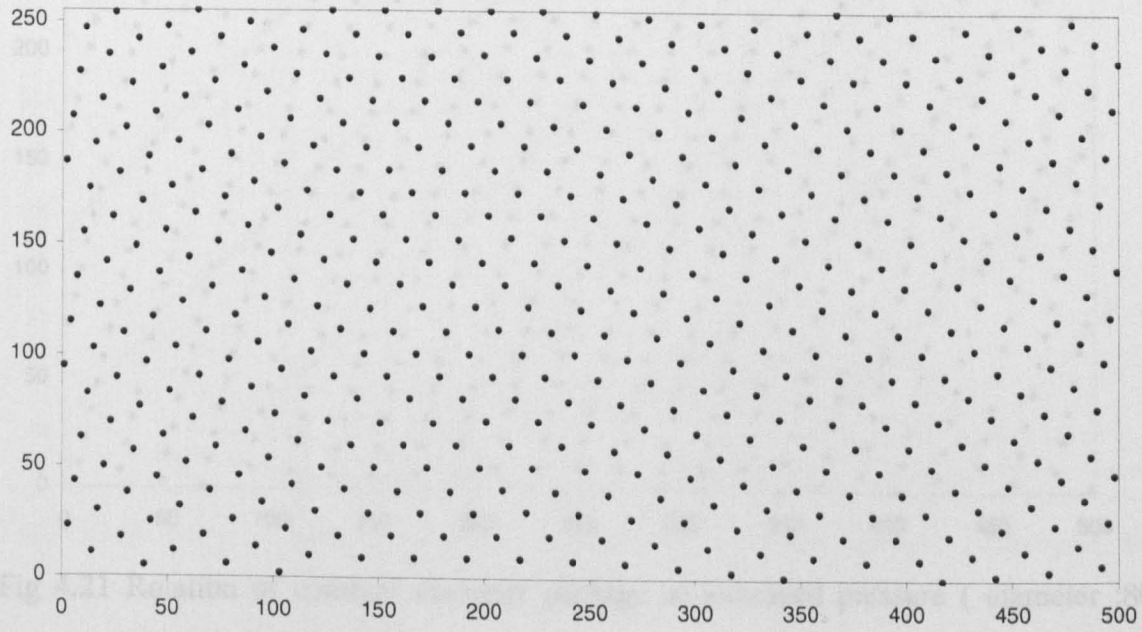

Fig 4.19 Rotation of constant diameter package at increased pressure (diameter :80 mm, traverse ratio:3.4, scale 1)

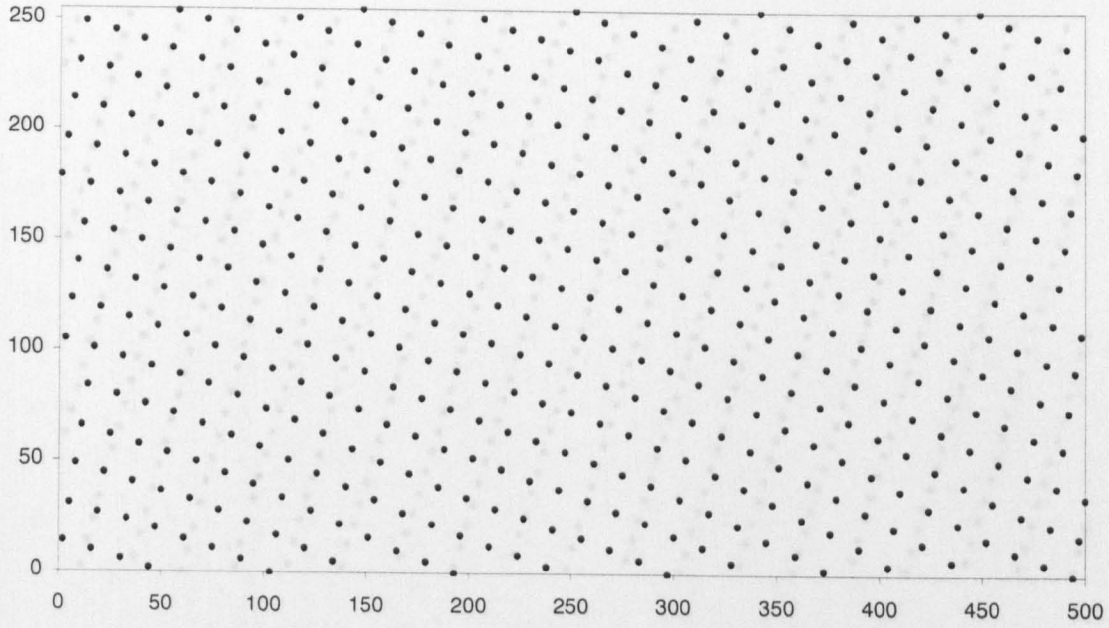

Fig 4.20 Rotation of constant diameter package at increased pressure (diameter :80 mm, traverse ratio:3.4,scale 2)

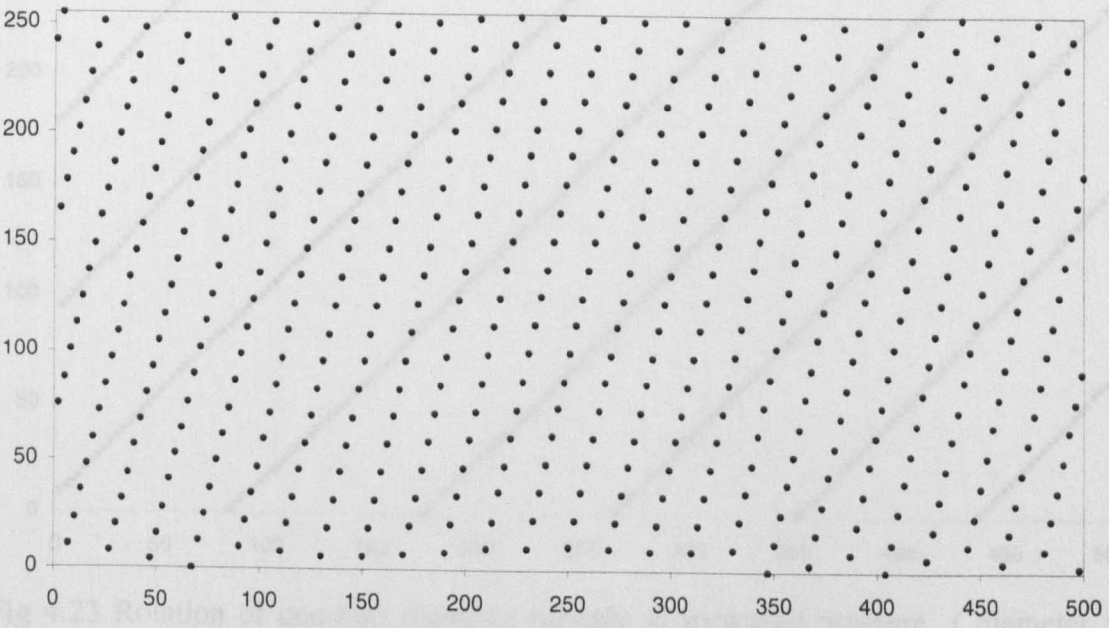

Fig 4.21 Rotation of constant diameter package at increased pressure (diameter :80 mm, traverse ratio:3.4,scale 3)

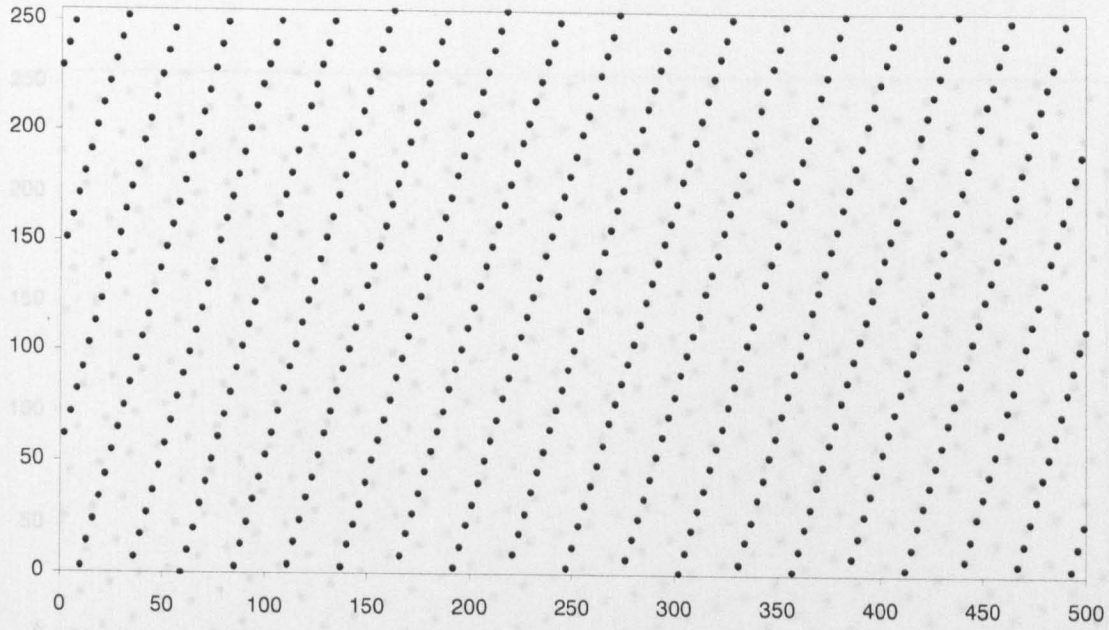

Fig 4.22 Rotation of constant diameter package at increased pressure (diameter :80 mm, traverse ratio:3.4,scale 4)

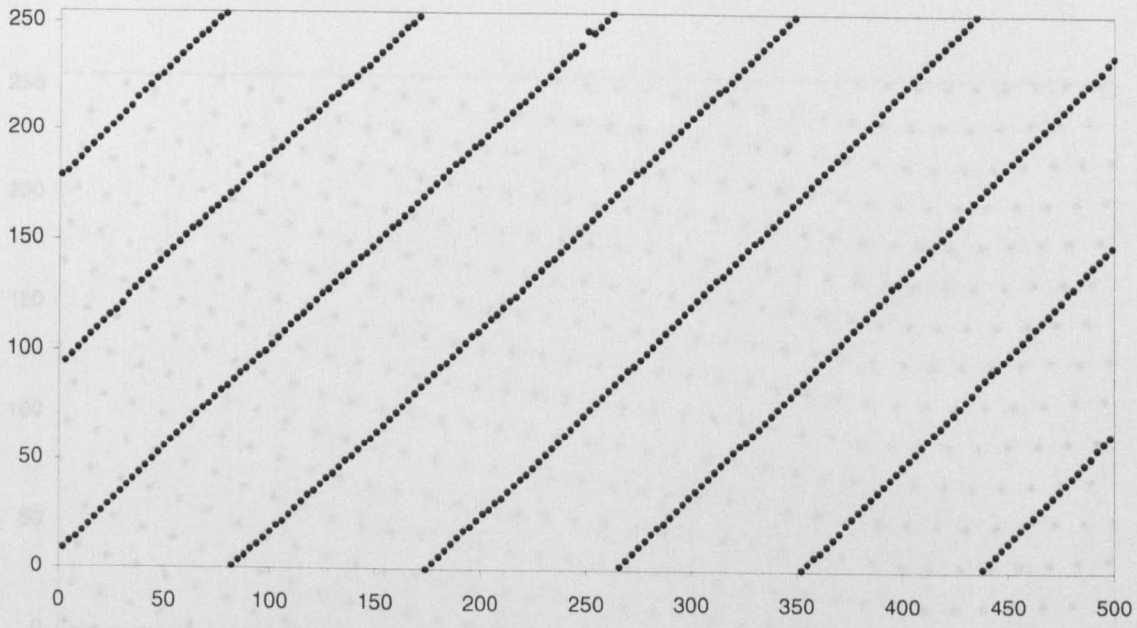

Fig 4.23 Rotation of constant diameter package at increased pressure (diameter :80 mm, traverse ratio:3.4, scale 5)

4.5.2.2 With oscillation

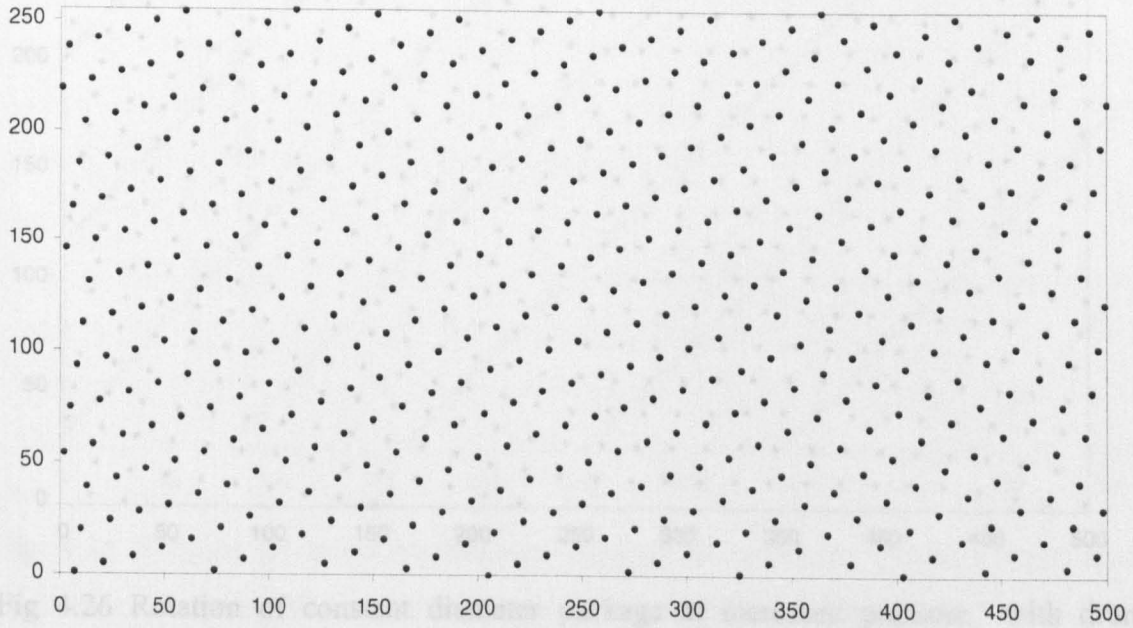

Fig 4.24 Rotation of constant diameter package at increased pressure with drum oscillation (diameter :80 mm, traverse ratio:3.4, scale 1, oscillation is on)

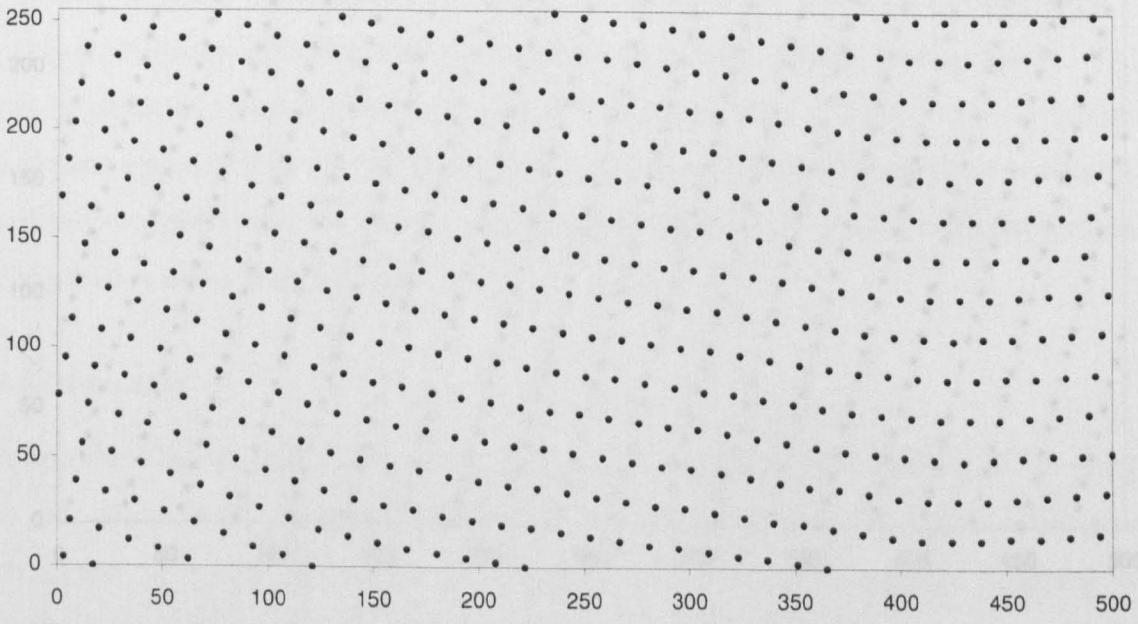

Fig 4.25 Rotation of constant diameter package at increased pressure with drum oscillation (diameter :80 mm, traverse ratio:3.4, scale 2, oscillation is on)

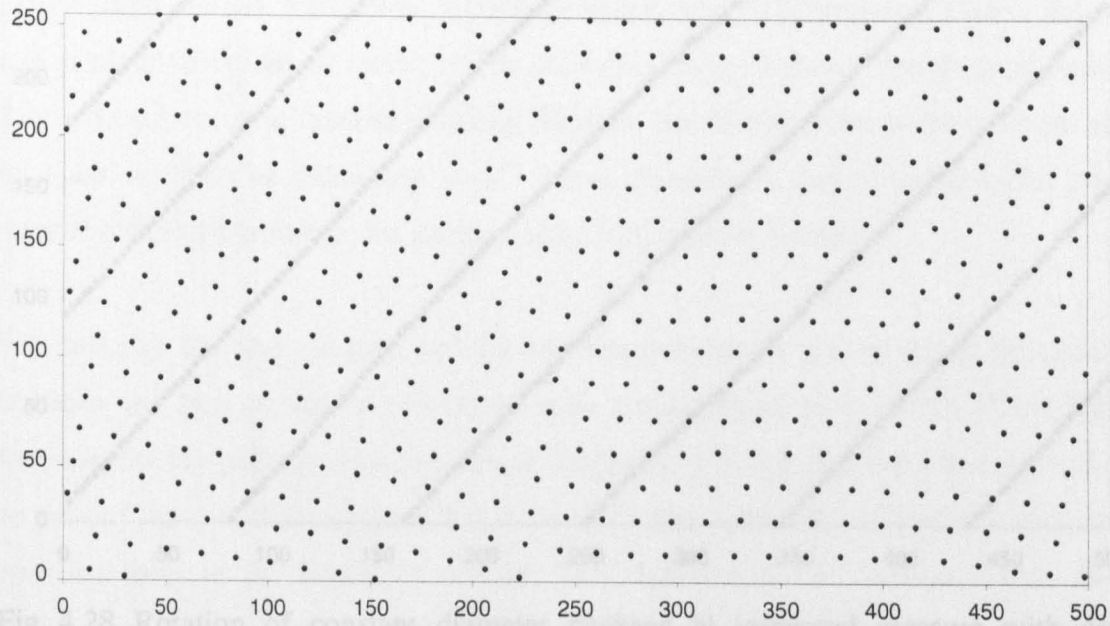

Fig 4.26 Rotation of constant diameter package at increased pressure with drum oscillation (diameter :80 mm, traverse ratio:3.4, scale 3, oscillation is on)

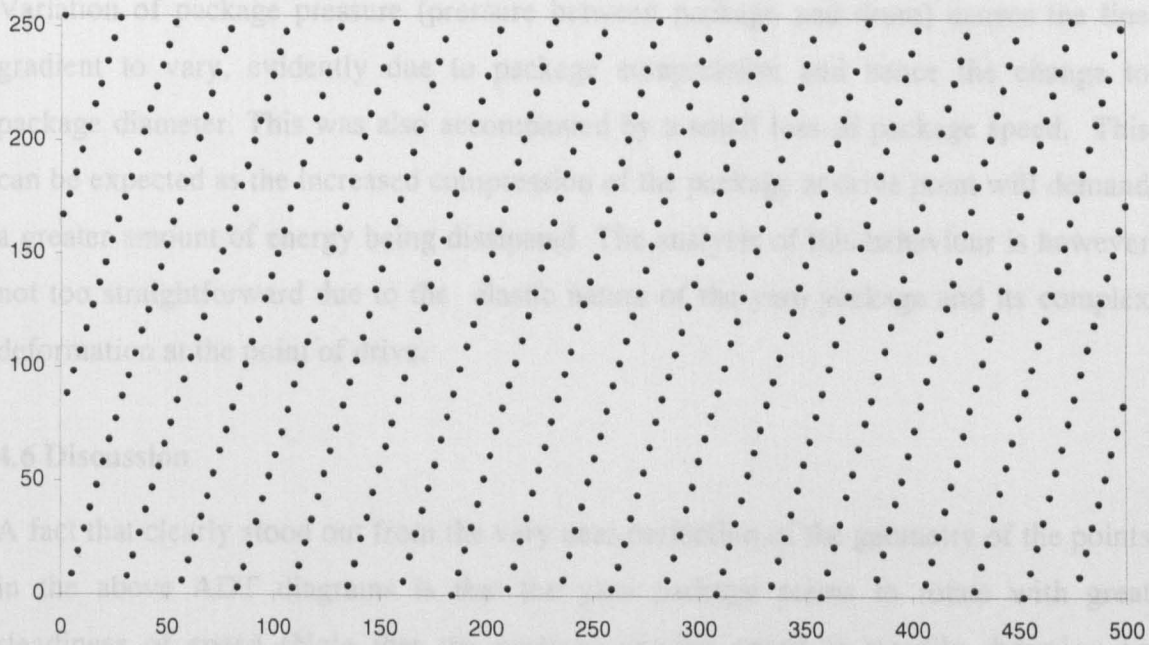

Fig 4.27 Rotation of constant diameter package at increased pressure with drum oscillation (diameter :80 mm, traverse ratio:3.4, scale 4, oscillation is on)

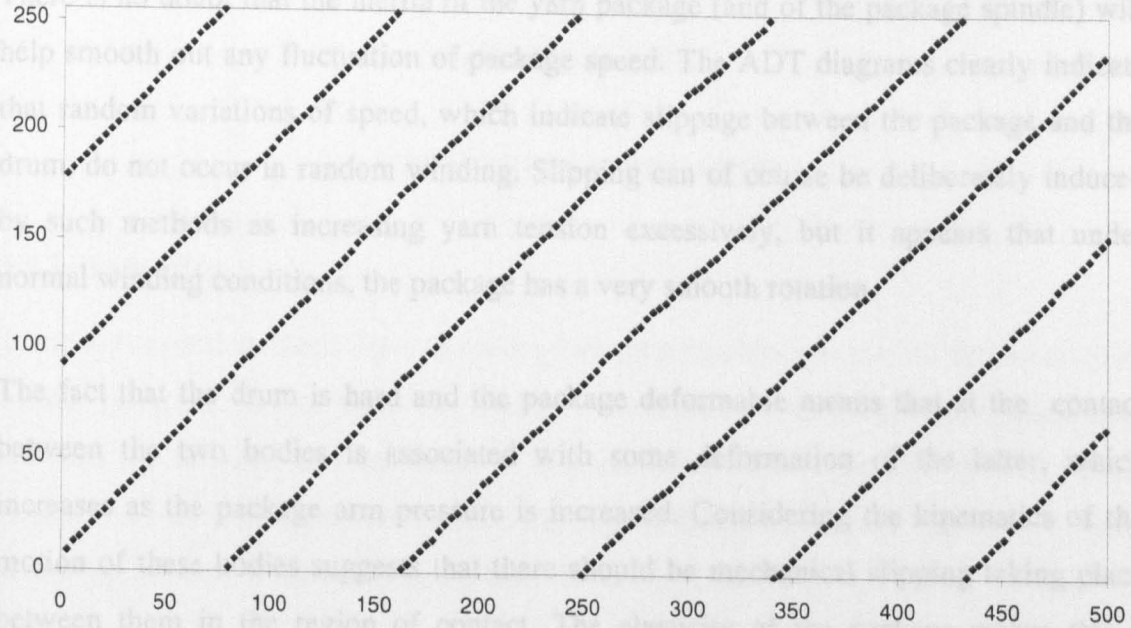

Fig 4.28 Rotation of constant diameter package at increased pressure with drum oscillation (diameter :80 mm, traverse ratio:3.4, scale 5, oscillation is on)

4.5.2.3 Evaluation of pressure effect on the ADT diagram

Variation of package pressure (pressure between package and drum) causes the line gradient to vary, evidently due to package compression and hence the change to package diameter. This was also accompanied by a small loss of package speed. This can be expected as the increased compression of the package at drive point will demand a greater amount of energy being dissipated. The analysis of this behaviour is however not too straightforward due to the elastic nature of the yarn package and its complex deformation at the point of drive.

4.6 Discussion

A fact that clearly stood out from the very near perfection of the geometry of the points in the above ADT diagrams is that the yarn package seems to rotate with great steadiness of speed (Note that the package angular speed is steadily dropping on account of its increasing diameter. Given that the package rotates in contact with the drum, this suggests, at a first glance, little or no slip between the two bodies. If there is any slip between them, then it has to be small, and of a very constant nature.

There is no doubt that the inertia of the yarn package (and of the package spindle) will help smooth out any fluctuation of package speed. The ADT diagrams clearly indicate that random variations of speed, which indicate slippage between the package and the drum, do not occur in random winding. Slipping can of course be deliberately induced by such methods as increasing yarn tension excessively, but it appears that under normal winding conditions, the package has a very smooth rotation.

The fact that the drum is hard and the package deformable means that at the contact between the two bodies is associated with some deformation of the latter, which increases as the package arm pressure is increased. Considering the kinematics of the motion of these bodies suggests that there should be mechanical slipping taking place between them in the region of contact. The elasticity of the package makes this a difficult problem to analyse. However it promises to be an interesting problem to tackle.

CHAPTER FIVE

ACTIVE RIBBON BREAKING

5.1 Introduction

There are several methods used on random winding machines to disturb the intensity on wound packages. All of them are based on intermittent changing of the speed ratio between the package and the drum to displace yarn position on the random wound package. These procedures are activated at regular intervals without regard to whether ribboning is actually occurring at the time the action is taken.

PC control of the experimental winder provides the means of adopting a better method of ribbon breaking, by allowing efficient detection of the moments when significant ribboning takes place on the wound package. A suitable ribbon breaking technique can then be brought into action, and repeatedly applied till the intensity of ribboning reduced to a harmless degree. Such a system can be considered a 'positive' ribbon breaking system. Achieving this was one of the objectives of this work.

5. 2 Standard ribbon breaking methods

5.2.1 The system for ribbon breaking originally provided

The Schlafhorst auto-coner used during this study incorporates a ribbon breaking mechanism, which basically interrupts the drum speed. The motion to the drum is obtained from motor roller via the intermediate roller, which has a smooth surface as shown by Fig 5.1. The motor roller is driven at a constant speed by the motor. Any position change on the intermediate roller affects the drum roller speed. A rod on the shaft of the intermediate roller pulls the intermediate roller away from the drum roller by an eccentric cam at once in 2 seconds. Thus, the drive to the grooved drum is interrupted as a result of which both the drum and the package lose speed. When the intermediate roller is brought back into the driving position, the cylinder is accelerated

faster than the package. The slippage between the package and cylinder, resulting from this acceleration, can break up the formation of ribboning or patterning [Schlafhorst 67]. The ribbon breaking mechanism is active throughout the winding process.

Yarn winding was carried out using the original ribbon breaking method in this experiment. The ADT diagram was plotted on the VDU during the winding process.

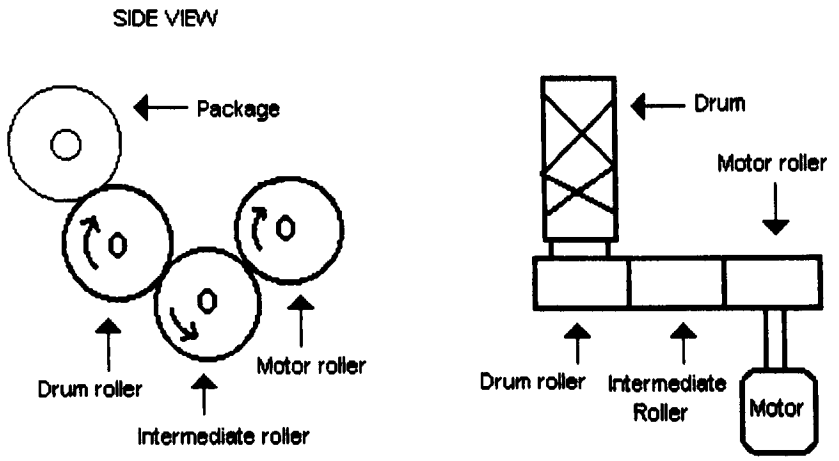

Fig 5.1 Original ribbon break mechanism

5.2.2 Effect of normal ribbon breaking

The ADT diagram was plotted normally on the VDU and the data generated during the winding were saved on the hard disk. The wind ratio 2 was reached at the package diameter of 135 mm. Fig 5.2 is the ADT which includes this wind ratio. It is seen that the original ribbon breaking method has a rather limited effectiveness in ribbon breaking. By examining the package at this point, some remnant ribboning was clearly visible. This experiment made use of the DC brushless motor which was much superior to the original 3-phase motor, due to its greater torque capability. So the lack of effectiveness of ribbon breaking is not due to the limitation of the motor.

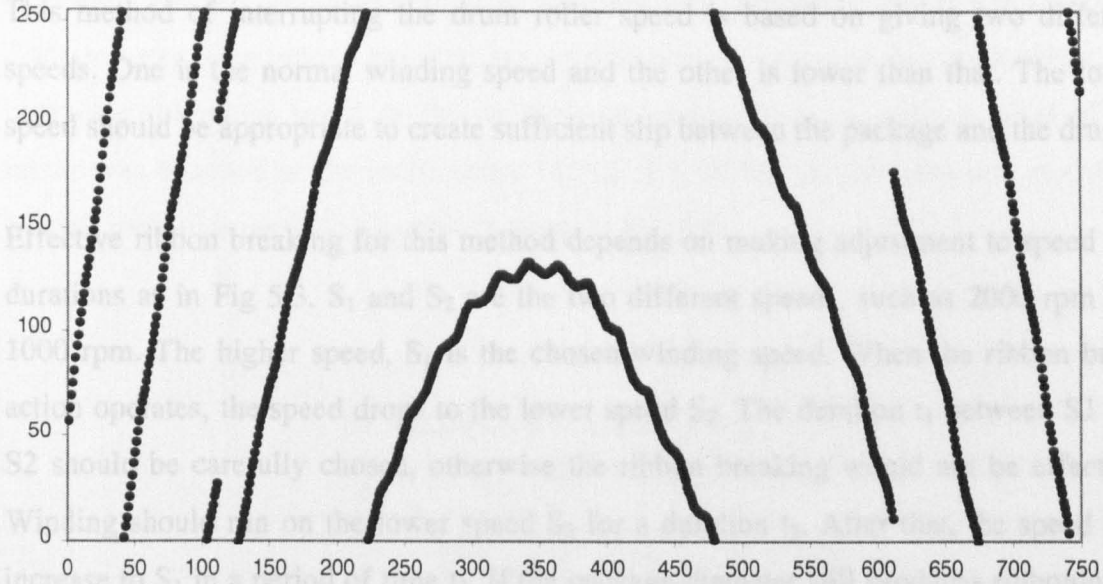

Fig 5.2 the effect of original ribbon breaking method at wind ratio 2

5.3 The method of interrupting motor speed

5.3.1 System set up

The speed of the DC brushless motor can be controlled by an external DC command voltage. As this motor is basically a high response servomotor, it is capable of producing sharp interruptions to its speed when so commanded. The necessary DC command signals can be easily generated by the PC through the D/A converter in the interface card. A program written in C language was used to provide the motor speed. Any speed between 0 (0 rpm) and 255 (2133 rpm) can be applied.

The program continuously checks for the occurrence of ribboning. The decision as to whether ribboning is occurring is decided by comparing successive readings of the package shaft encoder to see if they come within 5 decimal counts of one another. If ribboning is present, the ribbon breaking action takes place. The action is repeatedly applied till the ribbon breaking that results and the increasing package diameter automatically leads to a period of no ribbon breaking activity, till the next phase of ribbon formation arrives.

5.3.2 Choice of speeds

This method of interrupting the drum roller speed is based on giving two different speeds. One is the normal winding speed and the other is lower than that. The lower speed should be appropriate to create sufficient slip between the package and the drum.

Effective ribbon breaking for this method depends on making adjustment to speed and durations as in Fig 5.3. S_1 and S_2 are the two different speeds, such as 2000 rpm and 1000 rpm. The higher speed, S_1 is the chosen winding speed. When the ribbon break action operates, the speed drops to the lower speed S_2. The duration t_1 between S1 and S2 should be carefully chosen, otherwise the ribbon breaking would not be effective. Winding should run on the lower speed S_2 for a duration t_2. After that, the speed will increase to S_1 in a period of time t_3. If the package diameter still produces ribboning in order to have an integer wind ratio, same step of the speed variations will continue in a period of time t_4, before the sequence is made to repeat.

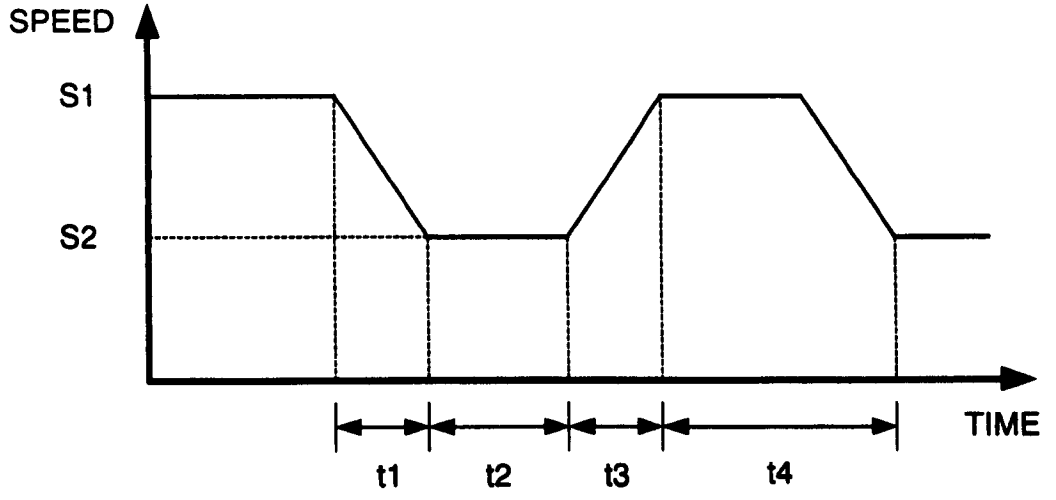

Fig 5.3 the speed –time graph for motor speed interruption

Speed variation on the motor changes the speed ratio between the package and drum speed. Acceleration and deceleration of the package speed change the position of the yarn in order to reduce the ribboning in the package. The flowchart of the program is given in Fig. 5.4a and b. The program appears in Appendix C.7.

Motor speed, package speed and drum speed were observed on the oscilloscope to compare them. Bit "0" from both shaft encoders was connected (one at a time) to the F/V converter as an input. Output from converter was connected to the oscilloscope. For observing the motor speed on the oscilloscope, output from the control panel of the motor was attached to the oscilloscope in Fig. 5.5. While the program was run, both outputs were observed. An example is given in Fig. 5.6.

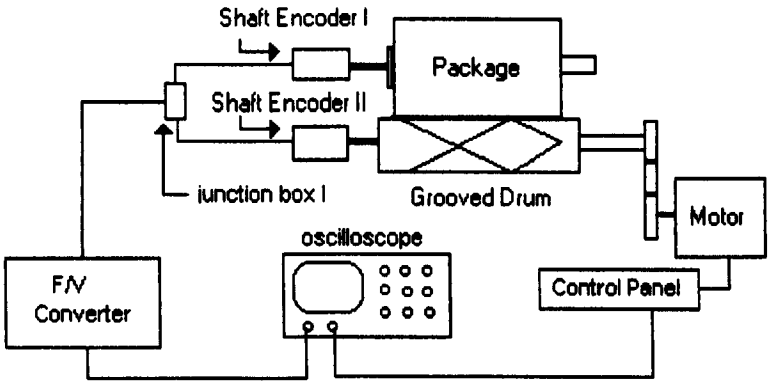

Fig. 5.5 Checking of package and drum speeds under motor speed control

Key to Symbols used in flowchart:

k : drum rotations within double traverse (0-2)

y : number of double traverses produced

l : number of double traverses for diagram (0-500)

rib : variable to indicate stage of ribbon breaking

(0 = no action required)

(1-3 = stages of interrupting motor speed)

stepforlow_speed, stepforhigh_speed : time duration of motor speed expressed in double traverses

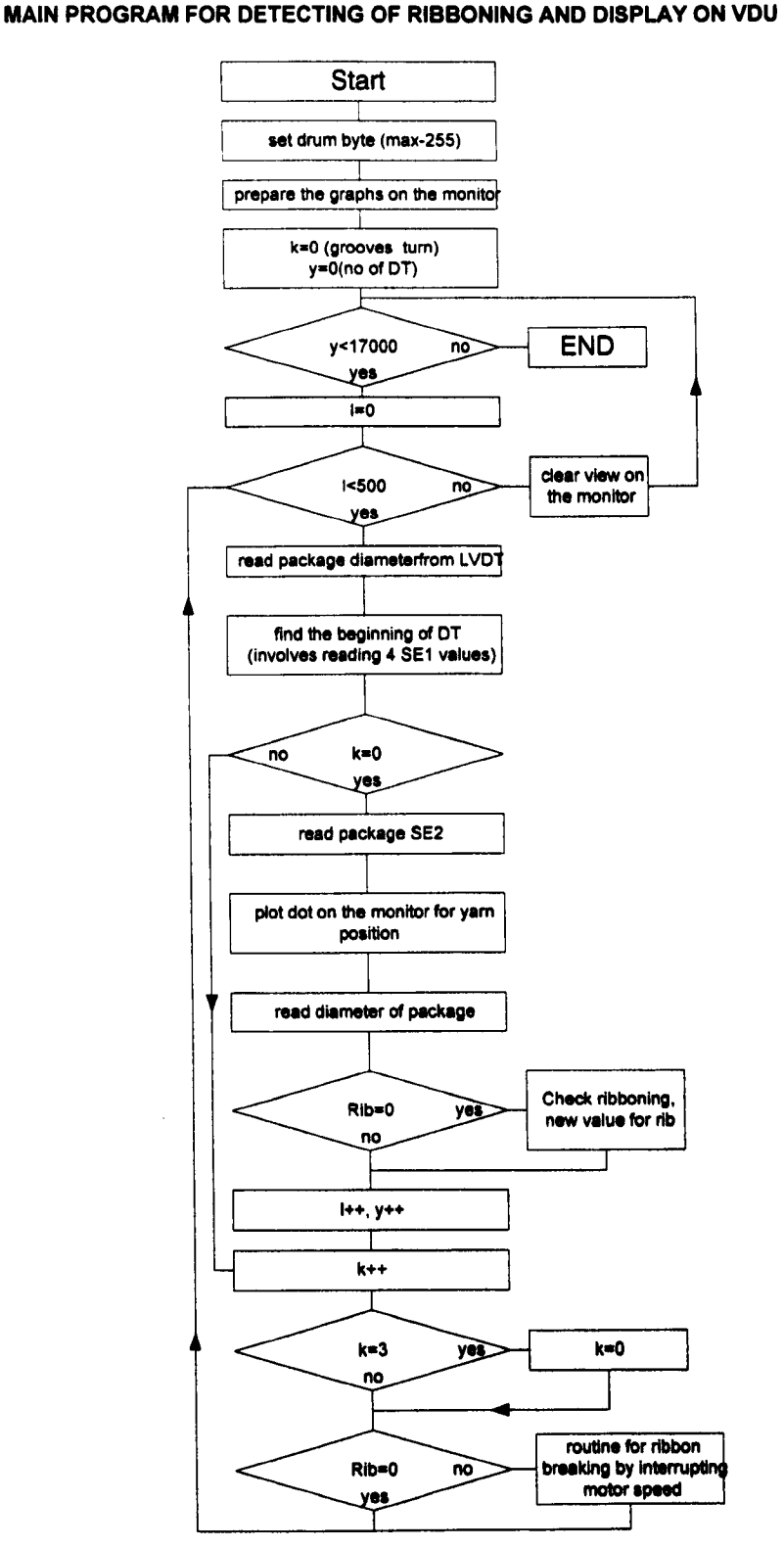

Fig 5.4a Flowchart of the program for interrupting motor speed

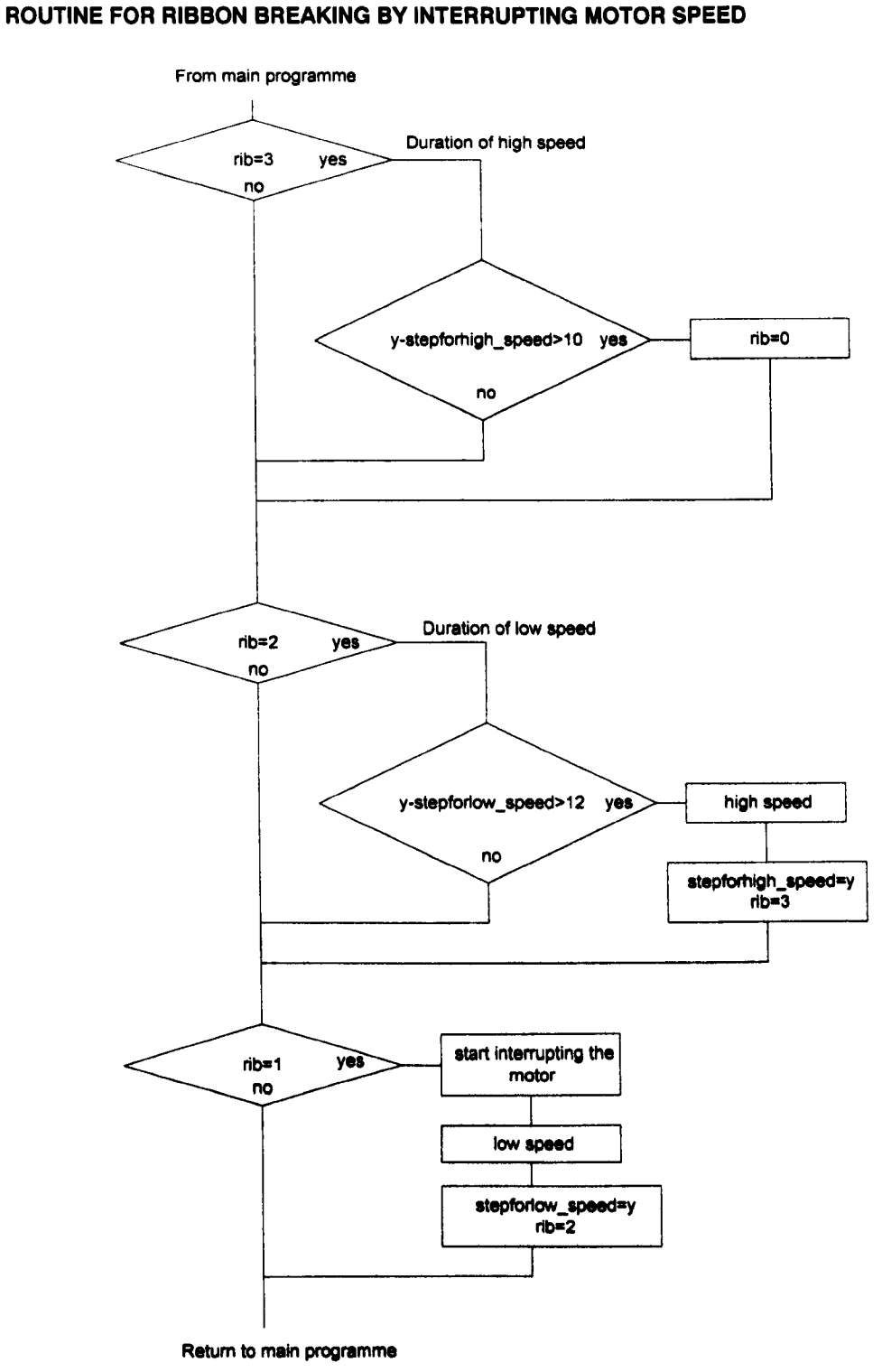

Fig 5.4b Flowchart of the program for interrupting motor speed

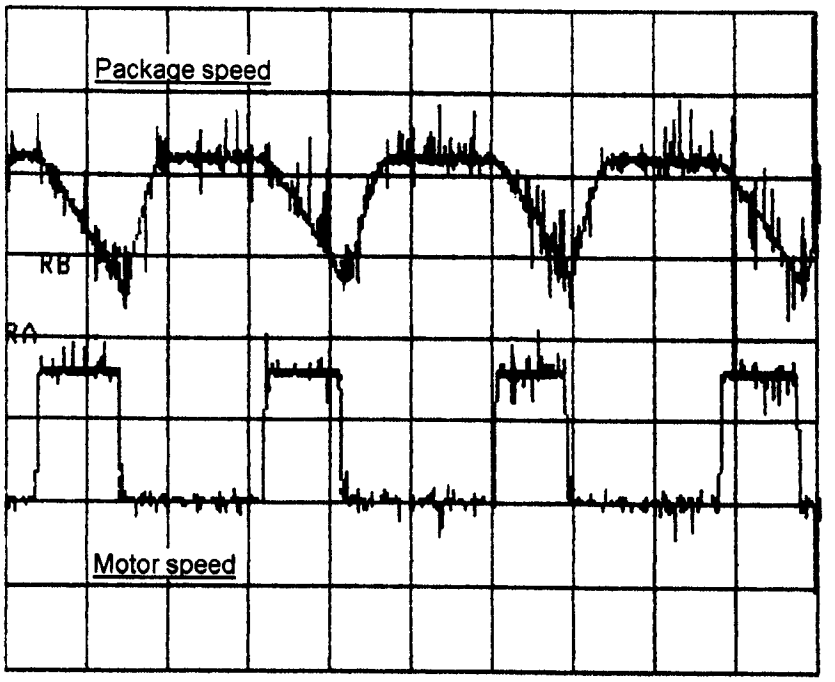

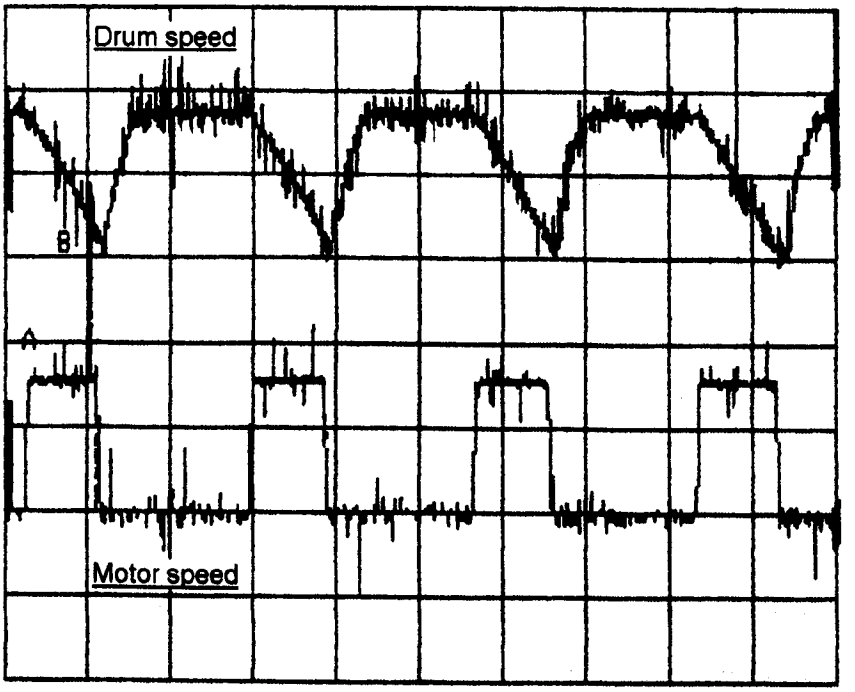

Fig 5.6 Output of package speed and winding drum speed

5.3.3 Results

The speed chosen for the experiment are decimal 255 for the high speed and decimal 100 for the low speed. The number of double traverses was chosen for duration of time either high speed or low speed. Duration for high speed was 12 double traverses, for low speed was 10 double traverses. The program is given in Appendix C 7 and C.8.

The ADT diagram obtained is shown by Fig. 5.7. This graph shows a part of the winding process. It is taken at the wind ratio 2. The important thing to note is the greater effectiveness of ribbon breaking realised by this method.

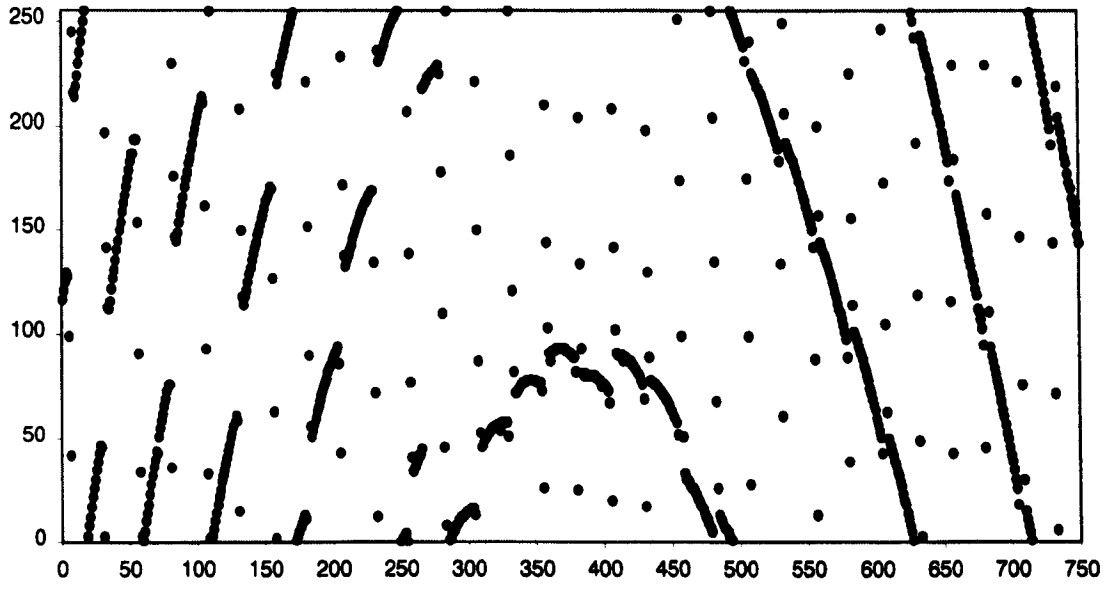

Fig 5.7 Effect of disturbing motor speed at wind ratio 2

5.4 Method of ribbon breaking by lifting the package

5.4.1 System set up

The other method of ribbon break investigated was that of lifting the package intermittently. During preliminary testing, this method was seen to be distinctly more effective than the method of interrupting drum speed. It was therefore decided to add a motor controlled arm that could raise or lower the package spindle under the control of the PC. The system adopted is shown schematically by Fig. 5.8.

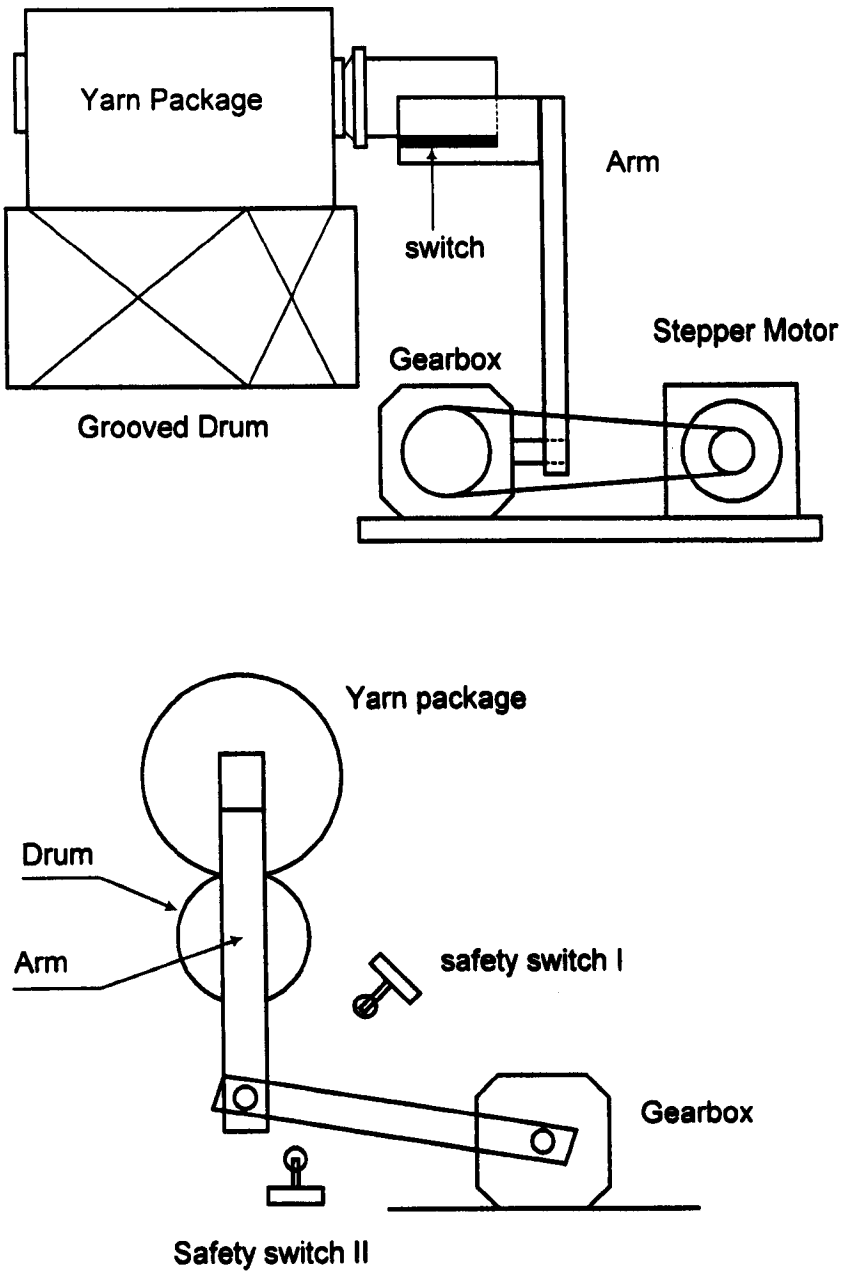

Fig 5.8a Arrangement for lifting the package

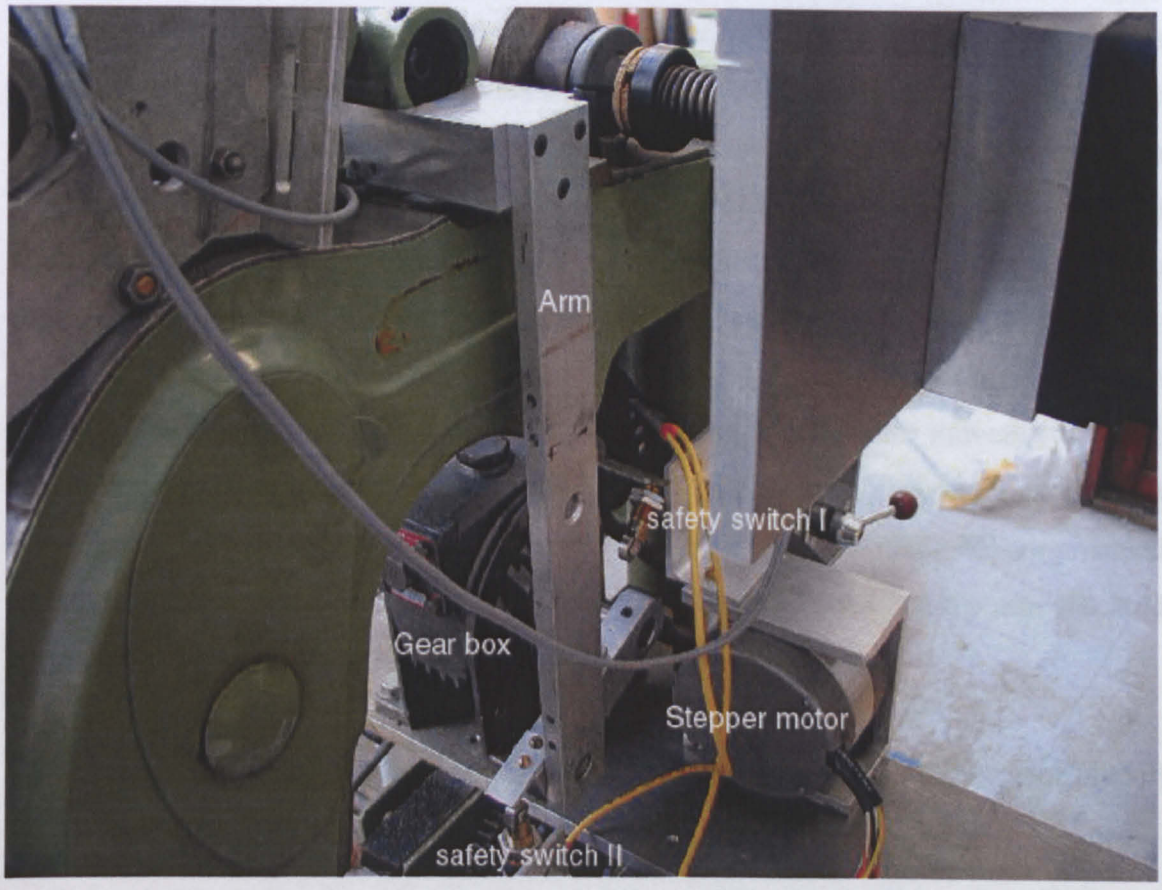

Fig 5.8 b Package lifting arrangement

The arm was mounted on a worm type reduction gearbox, driven from a stepper motor through a toothed belt. The motor is controlled through its own driver card, that is interfaced to the PC. Two safety switches are provided, so that the arm cannot be moved out of the range it is normally expected to be in.

One of the problems in using a lifting arm is that the arm should normally maintain itself very slightly below the hub of the package shaft, which continuously moves up as the yarn package increases in size. This is so, in order that the arm contacts and lifts the package swiftly upon the initiation of a lifting command. Further, when the arm is to lower the package, it should deposit the package on the drum, and then come to a stop after a slight further movement. This ability was realised by incorporating a microswitch on the part of the arm that contacts the package spindle hub, as shown by Fig. 5.9. The switch signals the PC when it makes contact with the package during an upward movement, and when it leaves contact during a downward movement. These responses can be programmed in software, so that the desired movement of the arm takes place. The fact that the stepper motor is holding its position when not commanded to move, and the reduction available through the gearbox ensures that the arm can hold its position during periods of inaction of the arm.

Technical details of the stepper motor, the gear box, and the stepper motor control card are given in Appendix. The wiring details are provided in Appendix A 5.2.

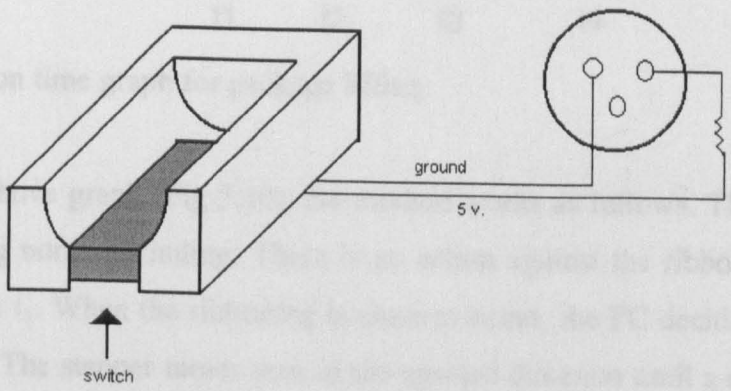

Fig 5.9 Connection of switch

5.4.2 Running and programming

After setting up the system for lifting the package, a programme in C language was written to control the ribbon break. This system works in principle the same as the method of disturbing the motor speed. While yarn being wound on the package, its progress is constantly monitored by the PC. When ribboning occurs, the arm is lifted until the package is lifted slightly clear of the drum. This separation distance should be kept very small so as to just disconnect the package from the drum. Otherwise it will lead to lack of control in winding the yarn. Once lifted, the package should be kept up for long enough so that an adequate amount of ribbon breaking takes place. On the other hand, the period of lift should not be too long to prevent loss of yarn traverse. The process of lifting and lowering of the package will be repeated quickly several times till the ribboning disappears.

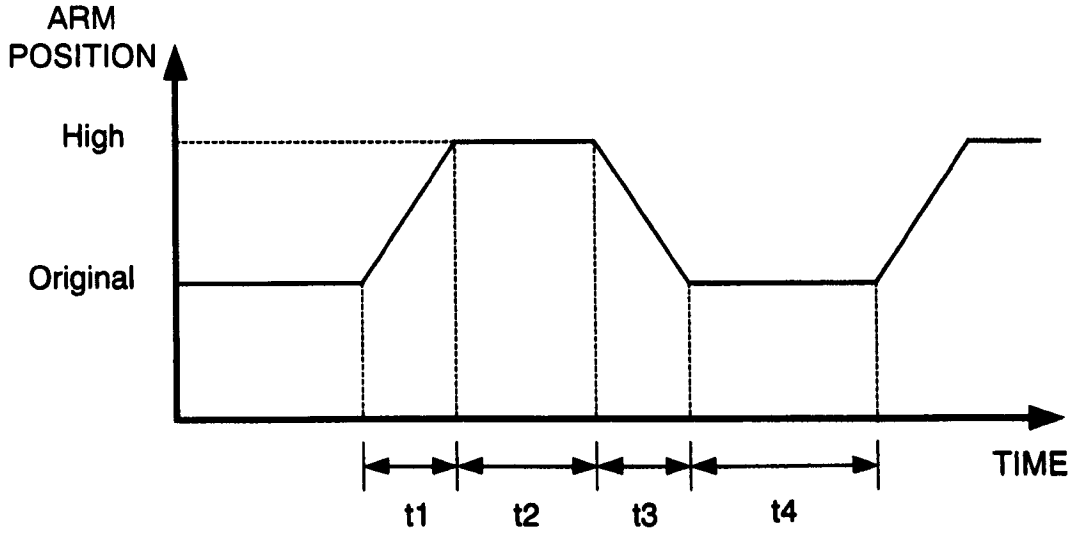

Fig. 5.10 Position time graph for package lifting

As seen from above graph (Fig 5.10), the method works as follows. The package is on the drum during normal winding. There is no action against the ribboning until at the start of duration t_1. When the ribboning is close to occur, the PC decides to start lifting of the package. The stepper motor runs in the upward direction until a couple of double traverses pass. The duration of lifting time t_1 depends on the number of double traverses chosen (Since each double traverse is detected by the PC, it is a convenient way of timing events). The package stays on the top position for a while (duration t_2). After that, the arm comes back to the original position. That duration t_3 is completed when the

switch on the package holder closes. The package remains at original position a period of time t_4, before checking for ribboning. This process is repeated until ribboning is eliminated. The flowchart of the program is given in Fig 5.11a and b. The program appears in Appendix C.9.

Key to Symbols used in flowchart:

k : drum rotations within double traverse (0-2)

y : number of double traverses produced

l : number of double traverses for diagram (0-500)

rib : variable to indicate stage of ribbon breaking

(0 = no action required)

(1-6 = stages of arm movement)

lift_step, stop_step: time duration of arm movements expressed in double traverses

MAIN PROGRAM FOR DETECTING OF RIBBONING AND DISPLAY ON VDU

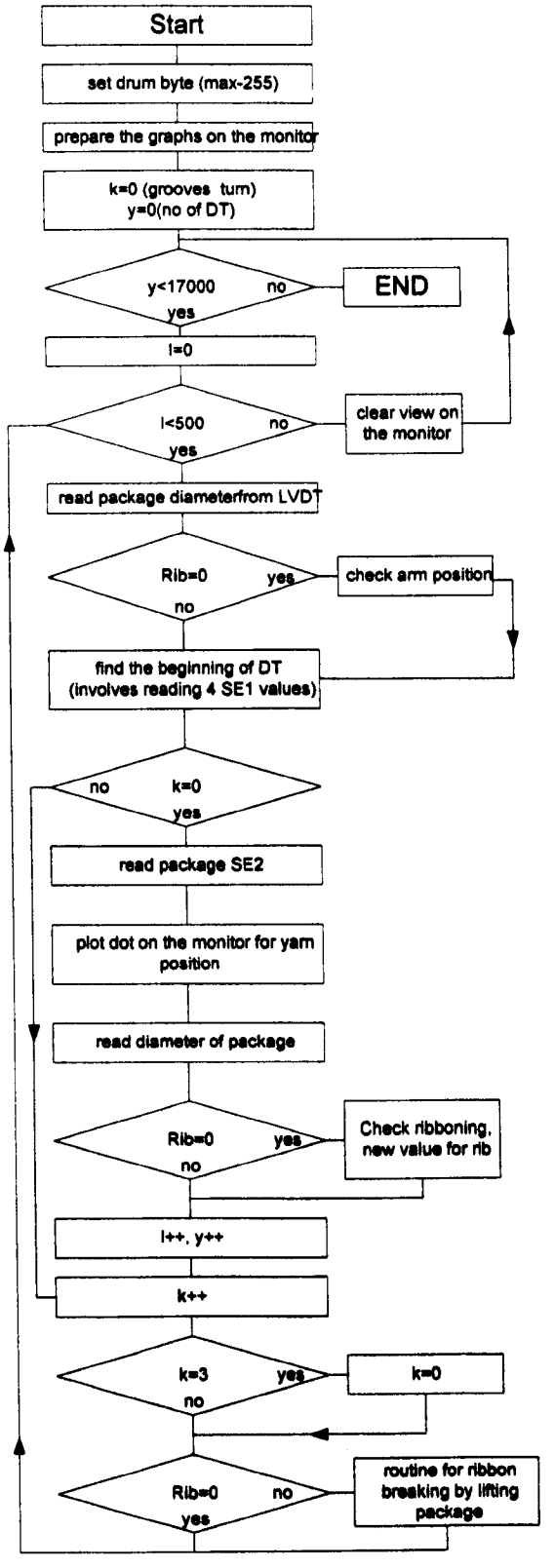

Fig 5.11a Flowchart of the program

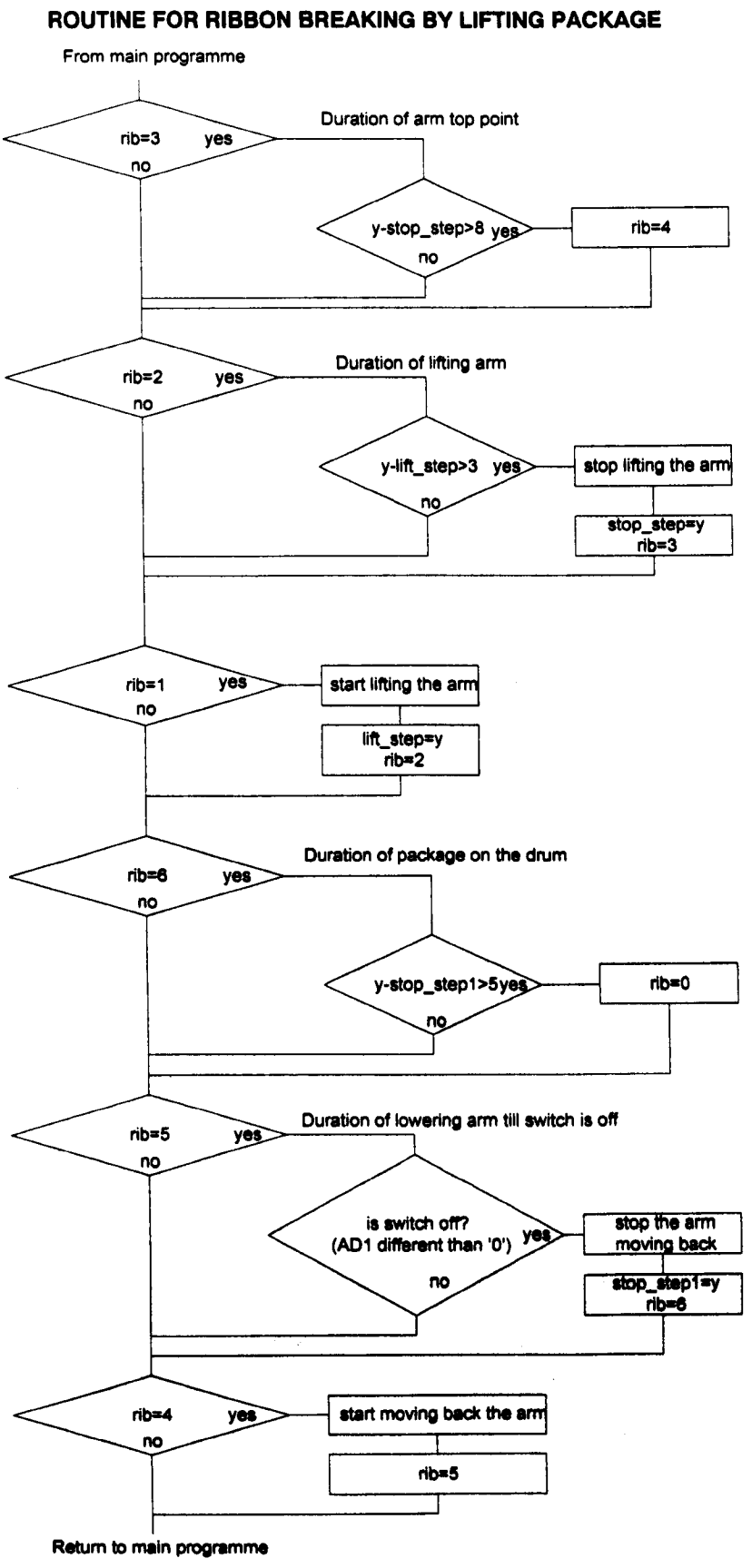

Fig 5.11b Flowchart of the program

5.4.3 Results

The appropriate durations of time chosen, in multiples of double traverse, were 3,8 and 5 for t_1, t_2 and t_4 respectively. The address of the outport for the stepper motor is 771. As the "0" is written to that address, the motor runs upwards, and "8" moves the arm downwards.

Yarn was wound from the core radius to the required package diameter while observing the winding on the ADT diagram. All data were saved on the hard disk. 750 double traverses were plotted on the ADT diagram as shown by Fig. 5.12 at the wind ratio of 2, which is one of the major ribboning events. Fig. 5.13 is based on 1500 double traverses.

5.5 Comparison of ribbon breaking methods

Three methods of ribbon breaking were compared in the above experiments. These methods were applied at the same wind ratio to compare them easily. It can be seen that the method of the lifting the package is more effective than the others. Ribboning is more effectively spread out by this method as shown by the ADT diagrams and in visual observation of the package. The method of the interrupted motor speed gives better results than the original ribbon breaking method, but it is still not effective enough to spread out the yarn position on the package. It can be expected that better ribbon breaking will enable more even unwinding tension for a random wound package. Results of such unwinding tension analysis are given in Chapter 6.

One of the disadvantages of the method of lifting the package is that yarn might be out of control particularly at the small diameter of the packages. To reduce this problem the separation between the drum and the package should be kept to a minimum, and the duration of each lifting operation carefully chosen. The slight loss of traverse during ribbon breaking by this method is not really a problem if it is kept in control, as random winders normally incorporate some form of package or drum oscillation to achieve softer edges.

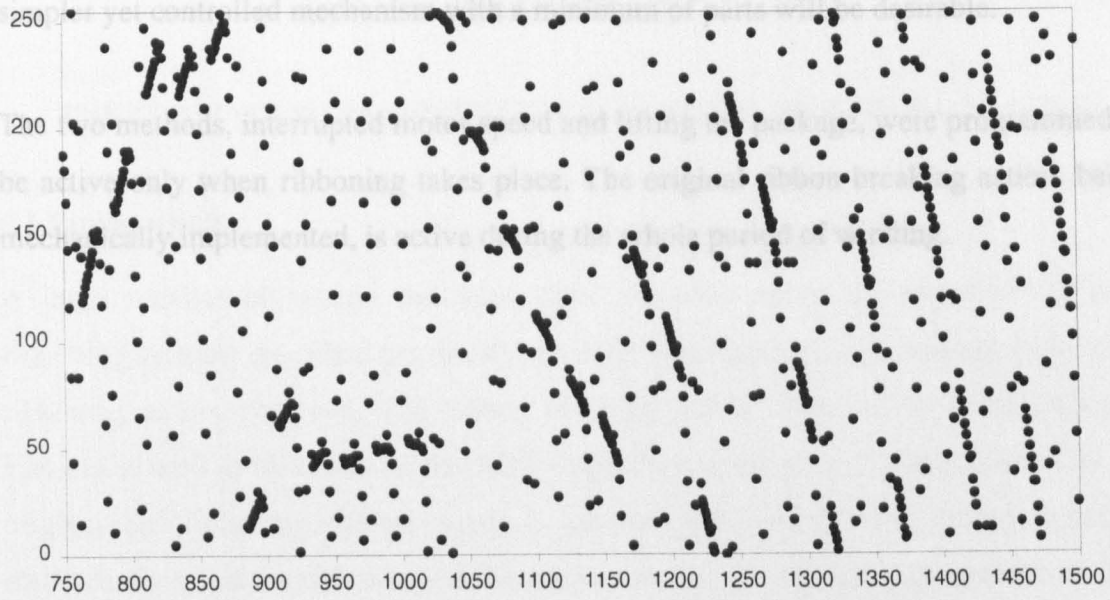

Fig 5.12 ADT diagram of 750 double traverses around wind ratio of 2

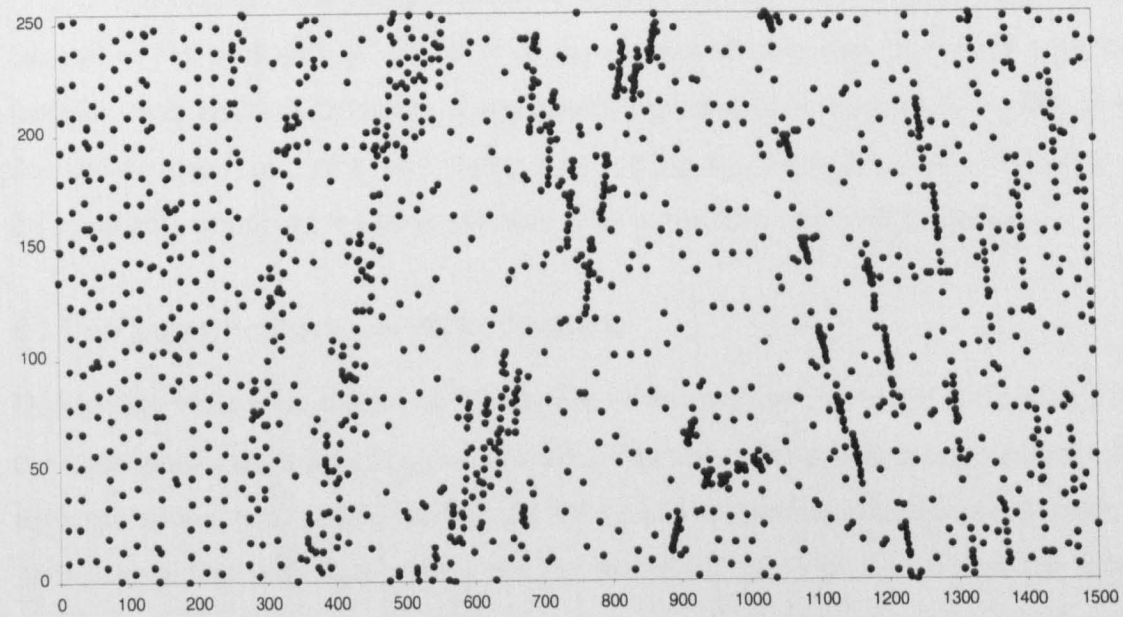

Fig 5.13 ADT diagram of 1500 double traverses around wind ratio of 2

The package lifting arrangement devised in this work was rather cumbersome, and a simpler yet controlled mechanism with a minimum of parts will be desirable.

The two methods, interrupted motor speed and lifting the package, were programmed to be active only when ribboning takes place. The original ribbon breaking action, being mechanically implemented, is active during the whole period of winding.

CHAPTER SIX

THE UNWINDING PROPERTIES OF RANDOM WOUND PACKAGES

6.1 Introduction

A large number of wound packages were produced using the experimental anti-ribboning systems described previously, to study the degree of improvement in the anti-ribboning action achieved. The ribbon breaking action observed on these packages visually as well as by means of the ADT diagram, was superior to that produced by the original anti-ribboning system used. It appears that experimental ribbon breaking methods disturbed the ribboning on the random wound packages to a greater extent. It is necessary to quantify the effectiveness of the ribbon breaking in terms of not only how effectively ribboning is dispersed, but more importantly how this affects the unwinding tension of the packages.

It is known that the unwinding tension of yarn in the ribboning zone is higher than in the rest of the package. A reduction of the amount of ribboning present in a package therefore will enable a reduction in the unwinding tension of the yarn. Therefore it was decided to carry out yarn unwinding trials using the packages produced using the different anti-ribboning methods and measure the resulting unwinding tension.

6.2 Unwinding Performance of the Packages

Unwinding trials as indicated above require withdrawal of yarn from the package at a constant speed, and measuring the unwinding tension experienced using a suitable high response single yarn tension probe. As the yarn is withdrawn, the measured tension is partly due to the ballooning of the yarn, the magnitude of which varies from the front to the back of the package, and partly any drag on the package surface as the yarn is peeled off it. It is customary to incorporate a tensioner just after the package in order that a minimum tension is maintained in the yarn. As the yarn is withdrawn, the measured unwinding tension will fluctuate, and will show higher levels when passing through regions of ribboning.

By recording the unwinding tension continuously from the beginning to the end of unwinding of a package, the results can be analysed so as to give an index of unwinding performance.

Yarn unwinding performance provides a useful indication of the suitability of a wound package for a given purpose, and in fact standard instruments are available for the routine testing of yarn packages for this purpose. An example is the Package Performance Analyser (PPA) produced by Rieter [Rieter-Scragg].

6.2.1. Apparatus for Yarn Unwinding Trials

The PPA is ideally suited for analysing the unwinding performance of the packages produced in this work, but such an instrument was not readily available. However after carefully considering the basic arrangement of the PPA it became evident that Schlafhorst winder could be modified for the purpose of measuring the tension of the yarn during the unwinding of packages. The drum on the winder can be set to a constant speed. As seen from the Fig 6.1 a creel was horizontally set up for holding the wound package. Two ceramic guides were placed, one for adjusting the length of the balloon, and the other for giving direction to the yarn for the tension measurement device. A tensioner was positioned between two guides for steady withdrawal of yarn from the package. The yarn after tension measurement was wound normally through the tension assembly of the winder.

It was observed that the yarn in fact undergoes a small fluctuation of velocity due to the traversing action of the drum. However this was calculated to be less than 4.2% of the surface speed of the drum, and could be considered acceptable.

The tensioner used between the yarn guides was of the leaf type. The reason of this choice was that pulling yarn through it is easy and stable. The disc tensioner was tried before, but it had a disadvantage in that moving the yarn through it led to incorrect tension readings due to excessive vibration of the plate under the fluctuation of tension undergone by the yarn.

The tension measuring device is that described in Chapter 2. Its natural frequency is sufficiently high to enable the tension peaks that occur during yarn unwinding to be recorded accurately.

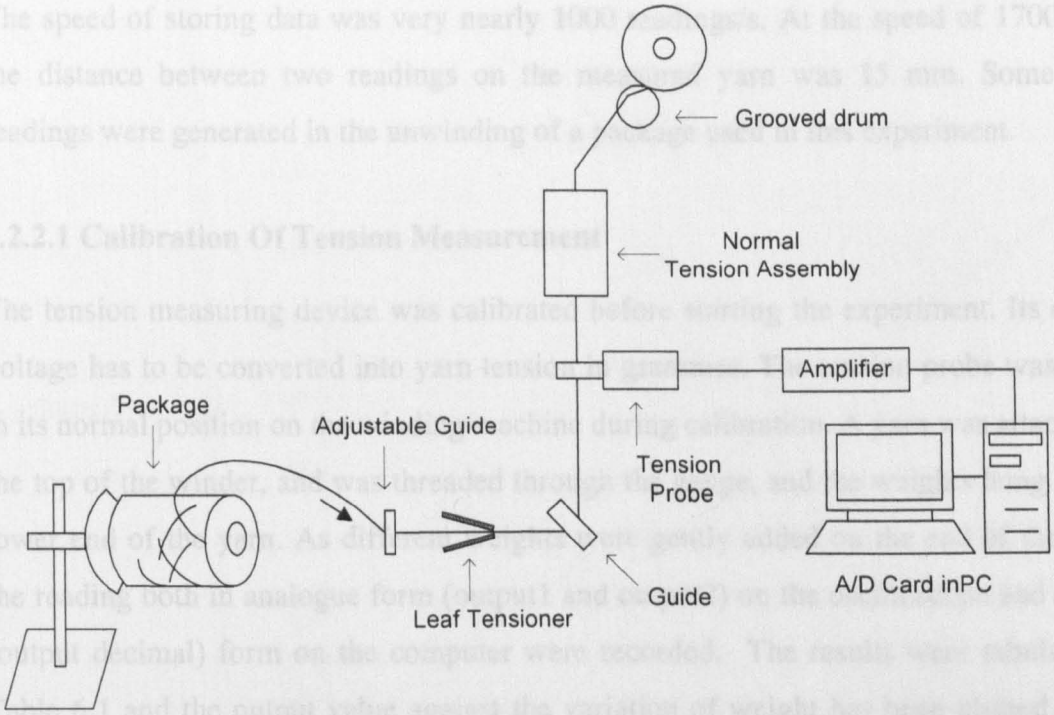

Fig 6.1 Configuration of the unwinding apparatus

6.2.2 Tension Measurement and Recording of Data

The output of the tension measuring device was connected to the A/D converter of the PC interface card. A program written in the C language used to read the tension values and store the data directly on the hard disk of the computer. Due to the very large number of data values produced in the unwinding of a package, sufficient memory was not available to save data in the memory itself. During the test, the computer was made to read the data and write it to the hard disk at maximum speed in order to not miss any data.

The oscilloscope was used to observe the unwinding tension throughout the unwinding of a package. An integrating amplifier was additionally employed to generate a second trace giving the mean value of unwinding tension. These two traces were constantly

monitored to ensure that the unwinding operation was satisfactory from the beginning to the completion of the unwinding operation.

The speed of storing data was very nearly 1000 readings/s. At the speed of 1700 rpm, the distance between two readings on the measured yarn was 15 mm. Some 1 M readings were generated in the unwinding of a package used in this experiment.

6.2.2.1 Calibration Of Tension Measurement

The tension measuring device was calibrated before starting the experiment. Its output voltage has to be converted into yarn tension in grammes. The tension probe was fitted in its normal position on the winding machine during calibration. A yarn was attached at the top of the winder, and was threaded through the gauge, and the weights hung on the lower end of the yarn. As different weights were gently added on the end of the yarn, the reading both in analogue form (output1 and output2) on the oscilloscope and digital (output decimal) form on the computer were recorded. The results were tabulated in Table 6.1 and the output value against the variation of weight has been plotted in Fig 6.2.

Weight [g]	Output1 [mV]	Output2 [mV]	Output binary [Decimal]
0	160	720	40
5	240	960	60
10	280	1240	72
20	440	1920	97
30	560	2480	126
40	720	3200	161

Table 6.1 Calibration data of tension measurement

From the Table 6.1, the relation between weight and output signal is seen to be linear. To convert the tension to binary, the following equation can be used.

$$B = 2.9*T + 41.8$$

Where B is the output value and T the yarn tension in grammes.

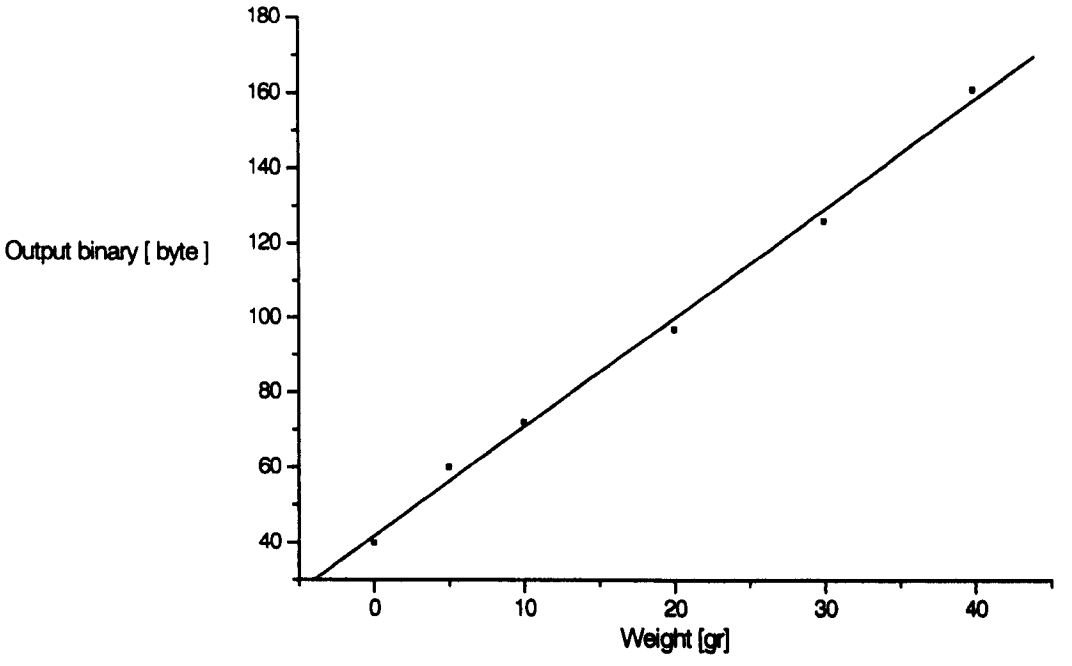

Fig 6.2 Calibration graph of tension measurement

6.2.3 Preparation Of Packages

Four similar packages were prepared for the measurement of unwinding tension. Of these one did not incorporate any anti-ribboning procedure. The other three involved ribbon breaking action by disconnection of the intermediate roller (the original method), direct interruption of drive motor speed, and of lifting the package.

Yarn used in the packages was 2/42 Ne_W white worsted. The tubes were initially wound to a diameter of 100mm using a similar yarn but black in colour. One reasons for doing this was to avoid loss of control of yarn on the drum at the small package diameters when the package lifting was applied. The other reason is that the length of the yarn wound on the package at the chosen starting diameter was quite sufficient for the analysis.

The first major ribboning started at diameter 135 mm. Approximately 10 km of yarn was wound till the package diameter reached 160 mm. The number of double traverses involved was 17000. The actual final diameter of the package depended on this.

Each of the settings of the winder viz. speed, pressure and winding tension, were kept the same except the way of anti-ribboning when preparing the packages. The actual values set were drum speed of 1700 rpm, yarn tension of 30 g and the package holder pressure of 1 kg.

6.2.4 Testing

The tension setting on the winder was adjusted to the medium position and the pre-clearer was open wide. The tension measuring system was adjusted to read zero with no yarn inserted. The yarn was placed in the creel and threaded up as in Fig.6.1. The leaf tensioner was carefully adjusted to ensure a small tension in the yarn downstream to prevent yarn through the tension probe losing control. The program written for reading and storing data (Appendix C.10.1 and C.10.2) was started, which also started the motor to start the yarn moving.

Fig. 6.3 is the oscilloscope trace of the yarn tension variation observed. Some of the periodicity of the signal is due to the fluctuating balloon tension which repeated over the unwinding of one double traverse of yarn. The component of signal amplitude due to yarn drag on the package surface will be superimposed on this. This component will be influenced by the remnant ribboning present in the package.

The ballooning of the yarn during unwinding will facilitate the removal of the yarn, due to it effectively being 'peeled off' from the yarn surface. At a lower withdrawal speed, there will be an increased amount of drag acting on the yarn.

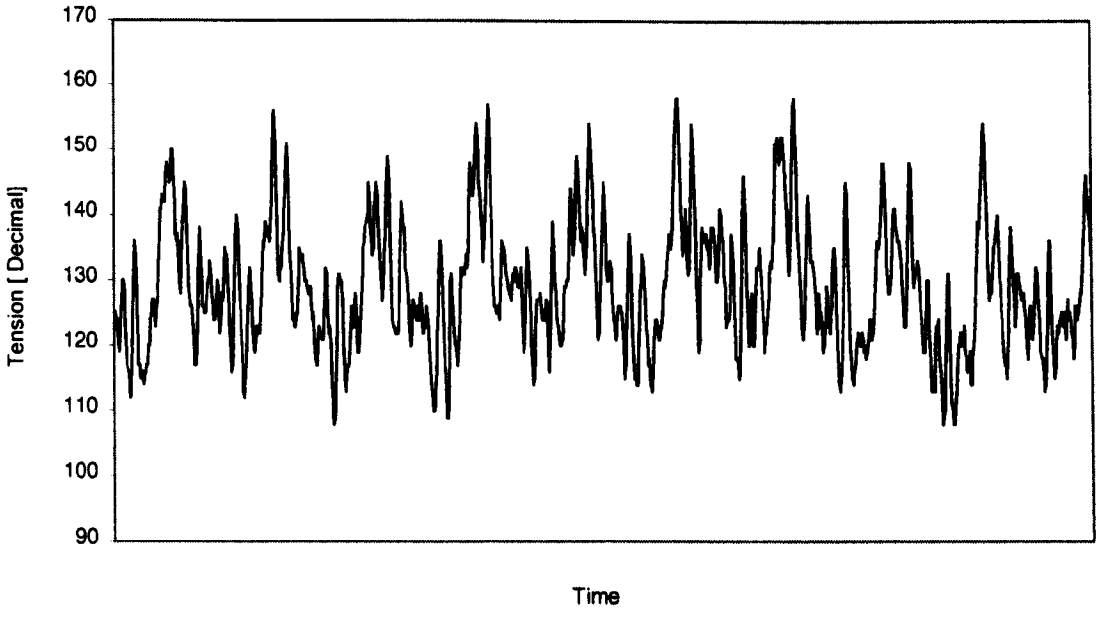

Fig 6.3 A periodic course of yarn tension signal

6.2.5 Test Results

The stored data has to be analysed for each packages to compare the anti-ribboning system in terms of the unwinding tension values recorded. A program was written in the C language to obtain the frequency distribution of unwinding tension. The diagram is plotted by classifying the tension readings into a number of contiguous classes of tension, and finding the frequency of each class. The results are plotted as tension against the frequency using Origin technical graphics software.

The four curves of tension analysis are shown by Fig 6.4a and b. It can be seen that the curve at the right hand side of graph belongs to the package which was wound with no ribbon breaking. This has highest peak tension and as such the overall tension distribution is more biased to the right on the tension scale. The curve at the left hand side of the graph shows tension distribution for the package which wound with "lifting the package" action. This has lowest peak tension and overall tension distribution is lower than the others with respect to unwinding yarn tension. The peak tension and overall tension of package which was wound with "interrupted the motor speed" is slightly higher than the wound package with "lifting the package" whereas it is

considerably lower than packages with a no-ribbon breaking and with original ribbon breaking.

The area under the curves is proportional to the number of reading on which they are based. This number is the same for each curve (1 M), and hence they are understandably of the same size. The leaf tensioner setting used was the same for all four packages, and therefore it simply would have imposed a constant positive shift on all readings obtained, and hence it has no influence on the comparison.

The diagram may be slightly confusing in that attention is immediately drawn to the peaks of the tension distributions. The tension corresponding to the peaks simply is the most frequently occurring unwinding tension for the corresponding package. The peak tension caused are represented by the right hand tail of the graph. So it is clearly seen that the package with no ribbon breaking produced the highest tension values. The package having ribbon breaking by lifting the package does not produce peak tensions as high as that.

It is often the case that the tension values of importance are those that are the occasional high peaks that occur in the unwinding of a package. It is such peak tensions that cause difficulties, as yarn breakages are directly influenced by them. The experiment above did not show such peak tensions however. The tension probe used was capable of recording any tension peaks that would have occurred. As the yarn was unwound at a constant speed, at which speed the yarn balloon was constantly present, high peaks of yarn tension seem to have been unlikely. Such peaks are more likely to occur in intermittent withdrawal of yarn such as encountered on a weft package on a shuttleless loom.

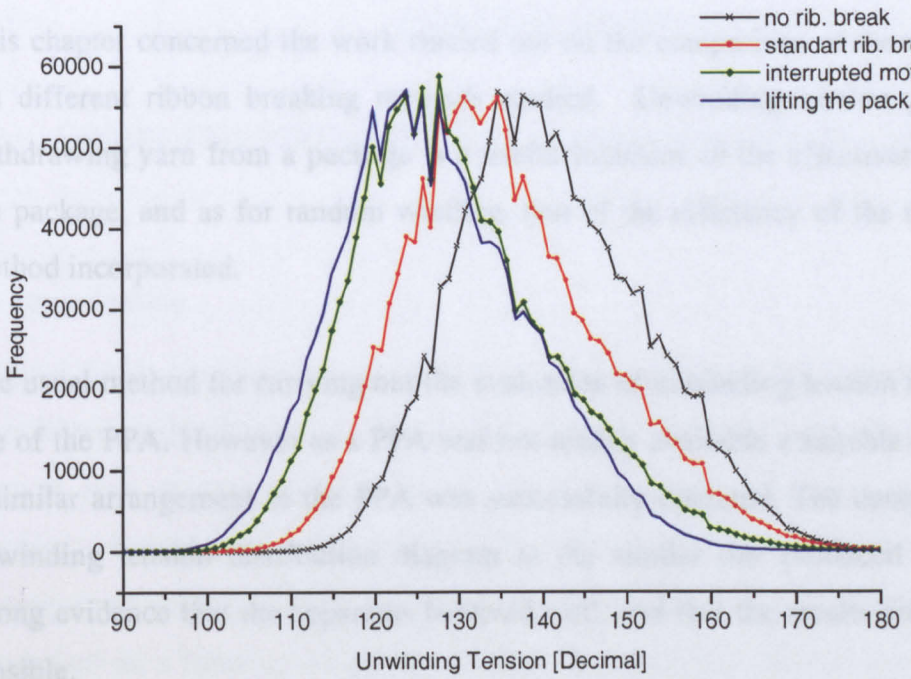

Fig 6.4a The basic results of analysis of stored tension data obtained with the 3 different anti-ribboning methods

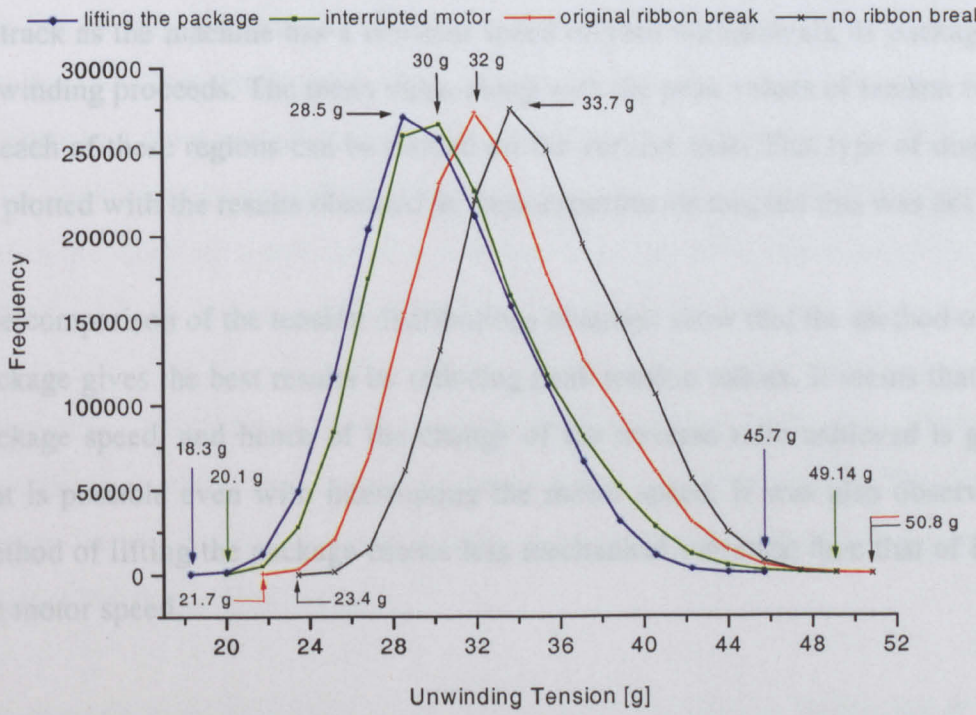

Fig 6.4b The results of analysis of stored tension data obtained with the 3 different anti-ribboning methods.

6.3 Discussion

This chapter concerned the work carried out on the comparison of the effectiveness of the different ribbon breaking methods studied. Unwinding tension produced when withdrawing yarn from a package is a useful indicator of the effectiveness of winding the package, and as for random winding, that of the efficiency of the ribbon breaking method incorporated.

The usual method for carrying out the evaluation of unwinding tension nowadays is the use of the PPA. However as a PPA was not readily available a suitable apparatus using a similar arrangement to the PPA was successfully operated. The compatibility of the unwinding tension distribution diagram to the similar one produced by the PPA is strong evidence that the apparatus behaved well, and that the results provided by it are sensible.

In fact the PPA can present its results in an alternative way, which is very useful for understanding how the unwinding tension varies as the package is gradually exhausted. This uses as the horizontal axis, each 1000 m 'section' unwound from the package (easy to track as the machine has a constant speed of yarn withdrawal), or package radius as unwinding proceeds. The mean value along with the peak values of tension encountered in each of these regions can be plotted on the vertical axis. This type of diagram could be plotted with the results obtained in these experiments too, but this was not attempted.

The comparison of the tension distributions obtained show that the method of lifting the package gives the best results by reducing peak tension values. It seems that the loss of package speed, and hence of the change of the traverse ratio achieved is greater than that is possible even with interrupting the motor speed. It was also observed that the method of lifting the package causes less mechanical vibration than that of interrupting the motor speed.

CHAPTER SEVEN

COMPUTER SIMULATION OF A RANDOM WOUND PACKAGE

7.1 Introduction

Stresses within a wound package and the layer movement within it during its formation were introduced in Chapter 1, Part II. As such it is useful to know these parameters for a given type of yarn package. Some research carried out on this subject has been reported where practical and theoretical studies have been made on parallel wound packages and precision wound packages for the analysis of stress distribution and layer movement as a function of package radius. However the case of the random wound package has not been studied similarly. A random wound package is more irregular compared to a precision wound package or a parallel wound package, and is comparatively more difficult to model.

The deformation of packages can vary depending on the type of winding involved. In a parallel wound package such as a pirn or a beam, the yarn has a zero wind angle, whereas in a cross wound package, the yarn is wound obliquely so that the yarn tension has a component in the axial direction of the package. Despite certain similarities, this makes the study of a cross wound package more complex than for one that is parallel wound.

Simulation studies carried out on the precision wound model have been helpful in arriving at a method of modelling the random wound package. The simulation of random wound cheese described in this chapter is based on the method used by Jhalani [Jhalani 70] for precision winding.

The main differences between random winding and precision winding are in the traverse ratio and wind angle. The traverse ratio is constant for precision winding while it decreases with increase of diameter in random winding. In addition, the wind angle of the yarn is changed from the core radius to outer radius of the package for precision

winding but it remains constant for random winding. The traverse ratio implies the number of wraps of yarn wound on the package for each double traverse of the yarn from one end of the package back to the same end. In random winding, the yarn does not have the same orderly arrangement as in precision winding. However, immediately in the neighbourhood of a given radius within the package, the yarn can be considered as being wound at a near constant traverse ratio. For a random wound package, the gain between successive double traverses depends on the decimal part of the traverse ratio. For precision winding the gain is set at a chosen constant value. These are the main differences between precision and random winding.

In precision winding, a number of double traverses equal to the reciprocal of the gain will cover the surface of the package completely. This can be considered as a double layer of turns of yarn, which produces a corresponding number of crossing points at which the top layer of yarns can be considered as bearing on the layer below.

This is a simplified way of considering the build up of a precision wound package. As each double layer has the same number of double traverses, the number of crossing points also remains the same. A similar idea would be useful for analysing the construction of a random wound package.

A difficulty however is that the traverse ratio varies with diameter in a random wound package. When the traverse ratio differs only slightly from an integer, there will be many double traverses wound covering the circumference of the package, as in the case of precision winding. But when it has a value midway between two integers, the idea of the double layer does not work so well, as the gaps between successive double traverses is too large to prevent yarns from successive double traverses moving into these spaces.

It was decided to overcome this problem by measuring the number of double traverses that go into making the package as a function of package radius. Since the experimental winder is equipped with shaft encoders, and LVDT based diameter measurement, this can be done relatively easily by winding a package under software control. The results of the measurement are given in section 7.3.1.

7.2 The approach to theoretical solution of the random wound cheese

The added layer at the outer radius of the cheese package imposes a pressure on the previous layer and causes it to deform. This pressure can be calculated. A second order differential equation was developed to give the radial deformation of the cheese package due to the pressure imposed by the added layer. The equation is integrated numerically by Euler's modified method to give radial deformation at any radius of the cheese from the core radius to the outer radius. The boundary conditions for the solution of the equation are that the compressibility of the core is assumed to be zero and that the pressure imposed at the outer radius by the added layer is known, as this is a function of the winding tension. The differential equation is solved with the added layer from the core to the newly added layer, at the outer radius.

The package is not isotropic because the loading between layers takes place at crossing points which are isolated and the yarn compression that occurs at the crossing points does not involve the whole length of the yarn concerned [Jhalani 70]. The Poisson's ratio for the cheese is assumed to be negligible because yarn compressed in the radial direction on the package can expand sideways without causing a change of the length of the yarn.

7.3 The equation of compression of the random wound cheese

As each outer layer of yarn bears on the layer immediately within, a wedge shaped section of the package can be considered due to the symmetry of the package as shown by Fig 7.1. The different layers of the package within the wedge are actually the elements involved. The section considered is assumed to be at the mid section of the package, so that due to symmetry there will be no net axial forces on any element considered.

An element at a radius φ within the section is considered. This element is considered as having had a radius r when it was initially wound. As the cheese was wound from this radius r to its present outer radius R, the layer deformed to the radius ρ. Total deformation of the element can be called U, where $U = \rho - r$. This gives negative values for U, as it is a radially inward deformation.

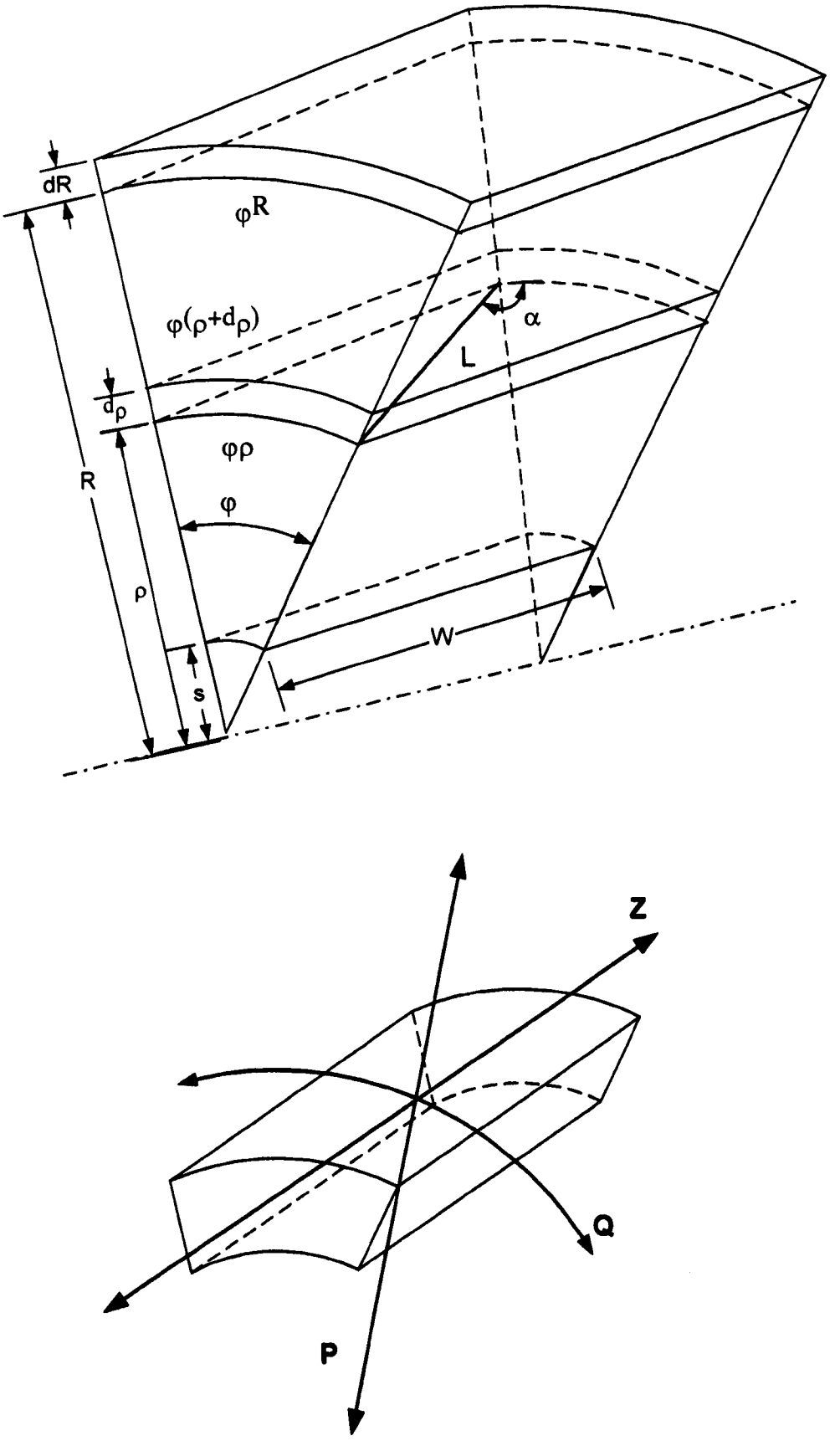

Fig 7.1 An element of the cross wound package

The element subtends an angle φ at the centre of the cheese. Dimensions of the element are φρ, dρ and W in the circumferential, radial and axial directions respectively. W is determined so that the diagonal length of the element at ρ is L and it is in the yarn direction. α is the wind angle of the yarn. This element can be considered as formed by a number of layers of yarn.

7.3.1 Number of double traverses as a function of package radius

The winder was set to wind a package, and the computer was programmed to record the number of double traverses wound and the radius of package, as provided by the LVDT. Considering a layer of 1 mm thickness as shown by Fig. 7.2.

$$D_2-D_1=2r_2-2r_1=1 \text{ mm}$$

$$r_2-r_1=1/2 \text{ mm}$$

$$r_1 = r_2-1/2 \text{ mm}$$

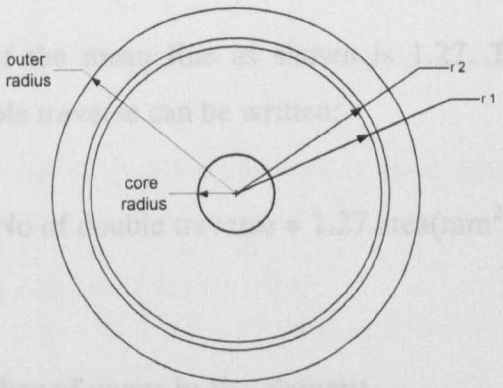

Fig 7.2 Layer of yarn 1 mm thick

The area in radial direction between r_2 and r_1 can be calculated as,

$$\text{Area } (mm^2)=\pi.(r_2^2-r_1^2)=\pi.(r_2+r_1).(r_2-r_1)$$

Substituting $r_2-r_1=1/2$ mm,

$$\text{Area } (mm^2)=\pi/2.(r_2+r_1)$$

By substituting for r_1

$$\text{Area } (mm^2)=\pi/2.(r_2+ r_2-1/2)=\pi/2.(2r_2-1/2)=\pi.(r_2-1/4) \quad (7.1)$$

The area calculated and the numbers of double traverses is known in that area. A graph is plotted of the area against no of double traverses as shown by Fig 7.3.

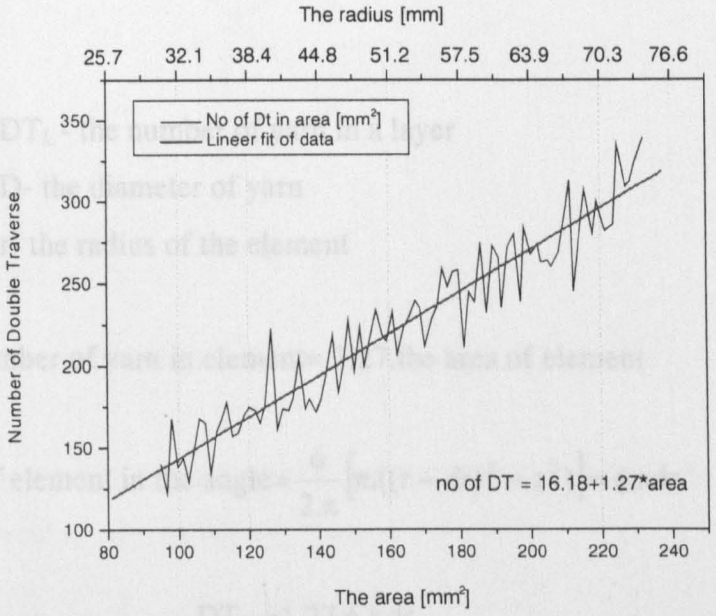

Fig 7.3 The measured number of double traverses as a function of area

The gradient of the mean line as shown is 1.27. The expression between area and number of double traverse can be written:

$$\text{No of double traverse} = 1.27.\text{area}(mm^2) \quad (7.2)$$

7.3.2 The number of yarns in the element

The number of yarn segments in the element can be calculated using the above information. When the area of the element is known, the number of double traverses is calculated using equation 7.2. The yarn wound covers the surface of the package with the different space between them in random wound package. A layer of yarn is considered as having the same thickness as that of a yarn.

$$\text{The number of yarns in layer} = 1.27 \text{ x area of layer within angle } \phi \quad (7.x)$$

Area of layer $= \frac{\phi}{2.\pi}\left[\pi.((r + D)^2 - r^2)\right] = \phi.r.D$

$$DT_L = 1.27.\phi.r.D \qquad (7.3)$$

where

DT_L - the number of yarn in a layer

D- the diameter of yarn

r- the radius of the element

The number of yarn in element= 1.27.the area of element

Area of element in the angle$= \frac{\phi}{2.\pi}\left[\pi.((r + dr)^2 - r^2)\right] = \phi.r.dr$

$$DT_E = 1.27.\phi.r.dr \qquad (7.4)$$

where

DT_E - The number of yarns in an element

As such the number of crossing points in an element will be

$$\text{crossing point} = 2[\ 1.27.\phi.r.D]^2 \qquad (7.5)$$

All units are mm in this equation. A layer is supported by the layer beneath at a number of crossing points from the construction of the element. The pressure imposed by any layer is carried by the next lower layer on these crossing points. The total number of crossing points at a random package depends on the radius concerned. As the radius increases, the total number of crossing points will increase.

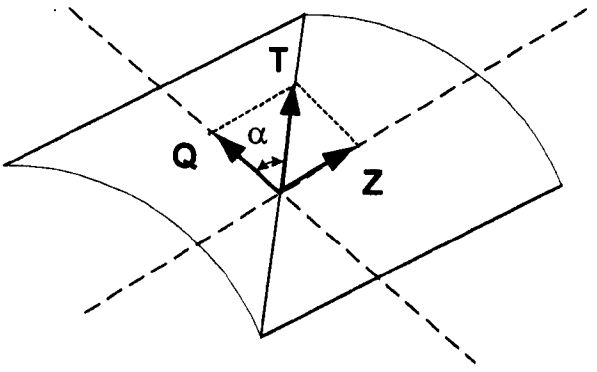

Fig 7.4 Forces on the yarn

Let Q and Z be the net circumferential and axial components of the force thought the face of the element as seen in Fig 7.4, then

$$Q=DT_E.T.\cos\alpha \tag{7.6}$$

$$Z=DT_E.T.\sin\alpha \tag{7.7}$$

The wind angle is constant in random winding. Q and Z will be change with the radius of element due to the change of the number of yarns involved.

7.3.3 The Addition of a layer at R

A layer of thickness dR added at the outer radius R of the cheese imposes pressure over the cheese as a result of which the element at ρ deforms.

$$\cos\alpha = \phi\rho / L$$

differentiating with respect to R;

$$0 = \frac{(\phi\rho)'.L - \phi\rho.(L)'}{L^2}$$

or $$0 = \frac{(\phi\rho)'}{L} - \frac{\phi\rho}{L^2}.\frac{\partial L}{\partial R}dR$$

$$\frac{\varphi\frac{\partial\rho}{\partial R}dR}{L} = \frac{\varphi\rho}{L^2}.\frac{\partial L}{\partial R}dR$$

But $\frac{\partial\rho}{\partial R}dR = u$ and $\frac{\partial L}{\partial R}dR = l$

$$\frac{\phi u}{L} = \frac{\phi\rho}{L^2}I$$

By multiplying both sides of the above equation by L and dividing by $\phi\rho$, the equation will be

$$\frac{I}{L} = \frac{u}{\rho} \qquad (7.8)$$

Due to the addition of the layer of thickness dR at the outer radius R the tension in the yarn has changed by t from T to (T+t). The change in the circumferential component of the force through the face of the element is

$$q = DT_E.[\,(T+t).\cos\alpha - T.\cos\alpha]$$

$$q = DT_E.t.\cos\alpha \qquad (7.9)$$

Similarly the change z in the axial component of the force through the face of the element can be given as

$$z = DT_E.[\,(T+t).\sin\alpha - T.\sin\alpha]$$

$$z = DT_E.t.\sin\alpha \qquad (7.10)$$

The element is under equilibrium and by resolving the changes in the forces along the axis of the symmetry of the element

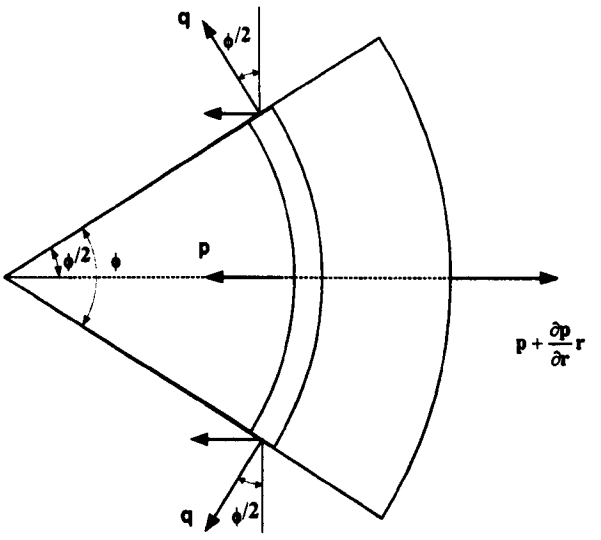

Fig 7.5 Pressure and circumferential forces at the element

From Fig 7.5,

$$p + \frac{\partial p}{\partial r} r - p = q.\phi$$

$$\frac{\partial p}{\partial r} = \frac{q.\phi}{dr} \tag{7.11}$$

The change in the circumferential strain of the element is u/r where u is the $(\partial U/\partial R).dR$ and the change in the radial strain of the element is $\partial u/\partial r$. Eliminating q from equation 7.9 and 7.11,

$$\frac{\partial p}{\partial r} = DT_E.t.\cos\alpha.\frac{\phi}{dr} \tag{7.x$_1$}$$

The change in the radial strain of the element, $\partial u/\partial r$, is related to the change of pressure per crossing point, therefore

$$p = \frac{\partial u}{\partial r}.E.[\text{crossing point}] \tag{7.12}$$

E is the modulus of compression of the cheese. The value of E is assumed as constant in the present situation.

Differentiating equation 7.12 with respect to r

$$\frac{\partial p}{\partial r} = [\text{crossing point}].E.\frac{\partial^2 u}{\partial r^2} \qquad (7.x_2)$$

Eliminating $\partial p/\partial r$ from equation $7.x_1$ and $7.x_2$

$$DT_e.t.\cos\alpha.\frac{\phi}{dr} = [\text{crossing point}].E.\frac{\partial^2 u}{\partial r^2}$$

$$\frac{\partial^2 u}{\partial r^2} = \frac{DT_E.t.\cos\alpha.\frac{\phi}{dr}}{[\text{crossing point}].E} \qquad (7.13)$$

t is the change in the tension T of the yarn due to change I in the length L of the yarn as a result of addition of the layer at the outer radius R,

$$t = EY.I/L \qquad (7.x_3)$$

Where EY is the elasticity of the yarn in extension.

Substituting the value of I/L from equation 7.8

$$t = EY.u/\rho \qquad (7.14)$$

substituting the value of t from equation 14 in equation 13.

$$\frac{\partial^2 u}{\partial r^2} = \frac{DT_E.EY.\frac{u}{\rho}.\cos\alpha.\frac{\phi}{dr}}{[\text{crossing point}].E} \qquad (7.x_4)$$

The difference between ρ and r is small and may be neglected, though in numerical solution it can be taken account of.

$$\frac{\partial^2 u}{\partial r^2} = \frac{DT_E.EY.\frac{u}{r}.\cos\alpha.\frac{\phi}{dr}}{[\text{crossing point}].E} \tag{7.15}$$

7.4 Values of q, z, Z, Q

Replacing ρ by the original value r and substituting the values of t in the equation 7.9 and 7.10.

$$q = DT_E.EY.(u/r).\cos\alpha \tag{7.16}$$

$$z = DT_E.EY.(u/r).\sin\alpha \tag{7.17}$$

When the element itself was wound at r, i.e. when R=r, the axial component of the force Z_{or} throught the face of the element is given by the following equation

$$Z_{or} = DT_E.T_o.\sin\alpha$$

However as the cheese is built up from this radius to any other radius R, the axial component of the force through the face of the element has changed. If z is the change in Z due to the addition of a layer at the outer radius the total change is Zor when the outer radius is R is given by integral ∫ z. Therefore the current or the residual axial component of the force through the face of the element is given by the expression

$$Z = Z_{or} + \int_r^R \frac{\partial Z}{\partial R} dR \tag{7.18}$$

Similarly the residual circumferential component Q of the force through the face of the element is given by the expression

$$Q = Q_{or} + \int_r^R \frac{\partial Q}{\partial R} dR \tag{7.19}$$

7.5 Integration of the differential equation

7.5.1 Boundary conditions

Equation 7.15 is a second order partial differential equation in u and r. Hence two boundary conditions are necessary to solve the equation and the equation is to be integrated numerically.

The necessary boundary condition for numerical solution follows:

1-At the core radius, the deformation in r is zero, as the core is assumed to be incompressible. U, total compression of the cheese at the core radius is also zero.

$$r = s \qquad u = 0 \quad U=0$$

2-At the outer radius R, the change in the pressure of the element caused by the winding of a layer is the pressure imposed by the element of the layer added. This pressure is given by the expression.

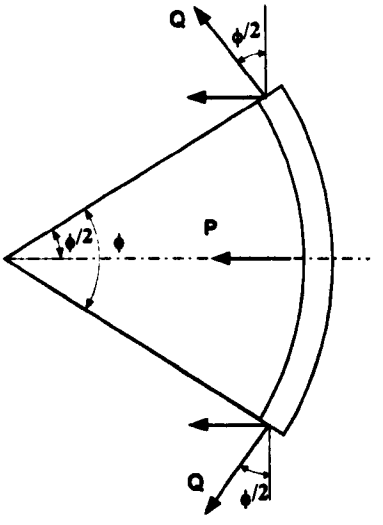

Fig 7.6 Pressure at the outer radius

$$P_{OR} + 2.Q.\sin(\phi/2) = 0$$

$$P_{OR} + Q\phi = 0$$

$$p_{OR} = -Q\phi$$

$$P_{OR} = -DT_E.T.\cos\alpha.\phi \qquad (7.20)$$

Therefore at r=R

The equation 7.12 and 7.20 give same pressure, so

$$\frac{\partial u}{\partial r}.E.[\text{crossing point}] = -DT_E.T.\cos\alpha.\phi$$

$$\frac{\partial u}{\partial r} = \frac{-DT_E.T.\cos\alpha.\phi}{E.[\text{crossing point}]} \qquad (7.21)$$

7.5.2 Procedure for solving the equation

The equation 7.18 is integrated numerically using the modified method of Euler for integration. The calculation is carried up to the radius when r=R. The value of $\partial u/\partial r$ is obtained by linear interpolation from the two previous set values of $\partial u/\partial r$ at r=s and at r=R. The linear interpolation is repeated until the value of $\partial u/\partial r$ is sufficiently close to the correct value of $\partial u/\partial r$ at r=R. The last calculation is the solution of the equation. This gives the value of u at any radius.

7.5.3 Interpolation of the value $\partial u/\partial r$ at the core radius

The method of interpolation used was the same as that Jhalani used. The value of $\partial u/\partial r$ is calculated from the two previous sets of values of $\partial u/\partial r$ at r=s and at r=R. The formula is

$$ndu = sdu+((sdu-C)/(du-D1))*(cdu-du) \qquad (7.22)$$

where

ndu – is the new value of $\partial u/\partial r$ at r=s

C - is the first guess of the value of $\partial u/\partial r$ at r=s

D1 - is the first calculated value of $\partial u/\partial r$ at r=R obtained from C

sdu – is the second guess of the value of $\partial u/\partial r$ at r=s

du – is the second calculated value of $\partial u/\partial r$ at r=R obtained from sdu

cdu – is the correct value of $\partial u/\partial r$ at r=R obtained from the second boundary condition.

7.5.4 Euler's modified method for integrating the equation

The method is as follows. The integration is carried out starting from the known values at the core radius and values at the beginning of the second layer are calculated. This is repeated for next layer and continued until the cheese is solved up to the given radius when r=R.

tu, tdu, and td2u represent the values of u, $\partial u/\partial r$, and $\partial^2 u/\partial^2 r$ respectively at the radius denoted by [k]. "dr" is the thickness of the layer as known the step length. Then at (r+dr)

u = tu+ tdu.dr

du = tdu+td2u.dr

d2u= F(u, r[k+1]) , where F stands for 'function of'

The values obtained are projected values; these values are averaged and the new values are calculated and suffixed by "a".

ua = tu+ (tdu+dua).dr/2

dua = tdu+(td2u+d2u).dr/2

d2ua= F(ua, r[k+1])

u and ua are compared and if the value is not close to each other, process is repeated until the value is sufficiently close.

The calculation gives the value of u, $\partial u/\partial r$, and $\partial^2 u/\partial^2 r$ at r[k+1].The calculation continues from r=s to r=R.

7.5.5 Error in the values of R and U at r

The addition of the layer at the outer radius causes the radius r of the cheese to shorten by u. As the new layer is added the value of u should be read off at (r+u) and not r to get the correct value U at r. However for keeping the computer program simple the value of u is read at r. The difference is very small.

7.6 Theoretical results

7.6.1 Values of the variables

The software program given in Appendix D gives the flowchart and the program in C language is to calculate the tension, pressure, etc. using the given values of variables for yarn and random packages. In this program the elasticity of yarn in extension EY and the modulus of compression of the cheese E was assumed to be constant at 5000 g and 200 g respectively. Wind angle of the random wound package was 16^{o} 4' and winding tension was 20 g. The dimensions used for the cheese are a core radius of 1 cm and a final radius is 5 cm. The diameter of the yarn is 0.05 cm. The radial angle of element (φ) was chosen 1 radian.

7.6.2 Forces through the faces of the added element

Fig. 7.7 shows the Qo and Zo of the element added. Forces in the axial and the circumferential direction are found to increase with the outer radius of the package due to the number of double traverses of yarn in a layer increases as the package builds up. The difference of gradient of the Qo and Zo depends on the wind angle of the yarn in the random package.

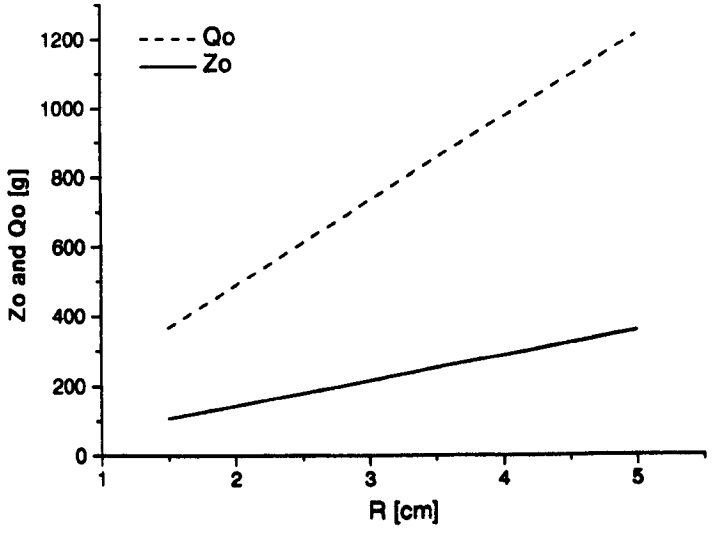

Fig 7.7 Forces in axial and circumferential direction at r=R

The value of Qo and Zo also depend on the winding tension T in the yarn. In this solution, winding tension applied to the yarn is 20 g. Pressure (Po) of element is equal to Qo due to element of radial angle chosen is 1 radian. For precision winding, Qo and Po increases and Zo reduces with the outer radius. This is due to the reduction in the wind angle with outer radius. And an increase gain reduces the number of yarn in element so that the forces reduce proportional to the gain.

7.6.3 Changes due to addition of a layer at outer radius

Fig 7.8 to Fig 7.12 show the effect on pressure (p), tension (t), forces in axial (z) and circumferential (q) direction and the radial distance (u) within a cheese with a value of 25 of the ratio EY/E when a layer of thickness (dR=0.1 cm) is added at outer radius (R=4.9 cm).

The value of p, the change in radial pressure, as shown by Fig 7.12 diminishes rapidly with r, but there is no significant change in p at r below 3 cm. The incremental compression u as shown by Fig 7.8 is similar with p and is dependant on p. The change in tension t (Fig 7.11) depends on the incremental compression (u), and the changes in circumferential component of force (q) and in axial component of force (z) shown in Fig 7.10 and Fig 7.9 depend on the changes in tension (t) and these are similar.

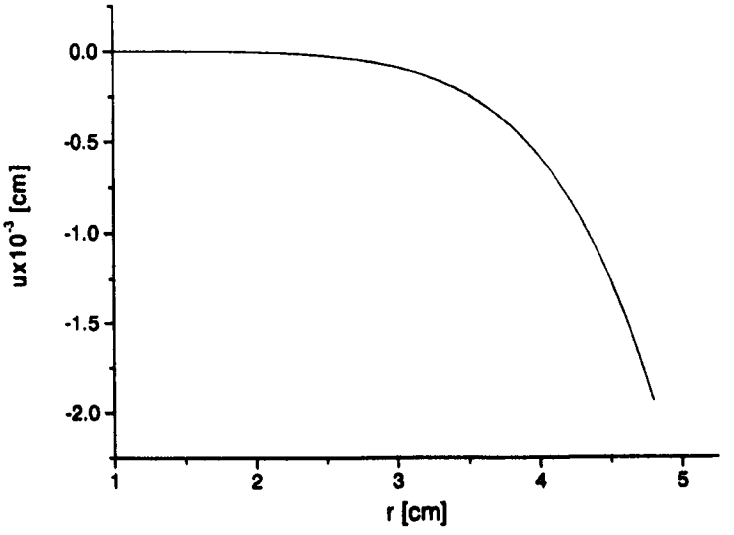

Fig 7.8 u - the incremental radial deformation in random wound package

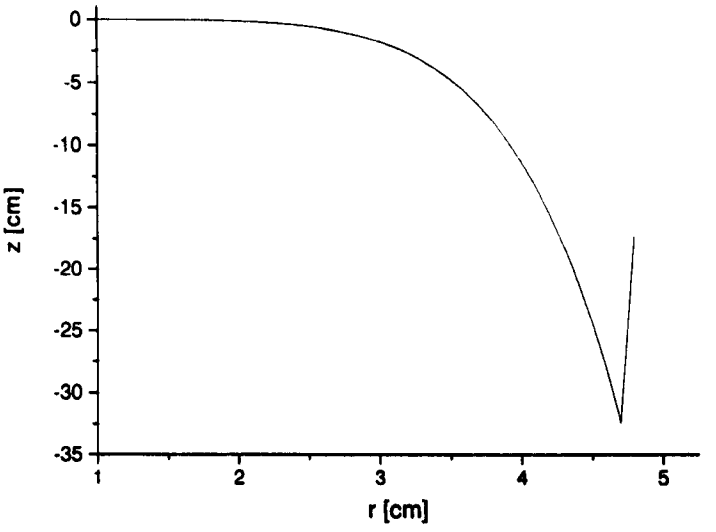

Fig 7.9 z - the change in axial component of the force in random wound package

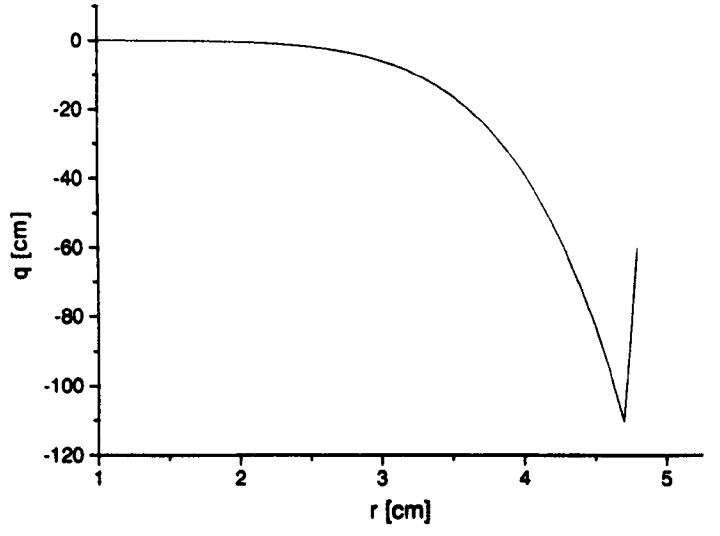

Fig 7.10 q - the change in circumferential component of the force in random wound package

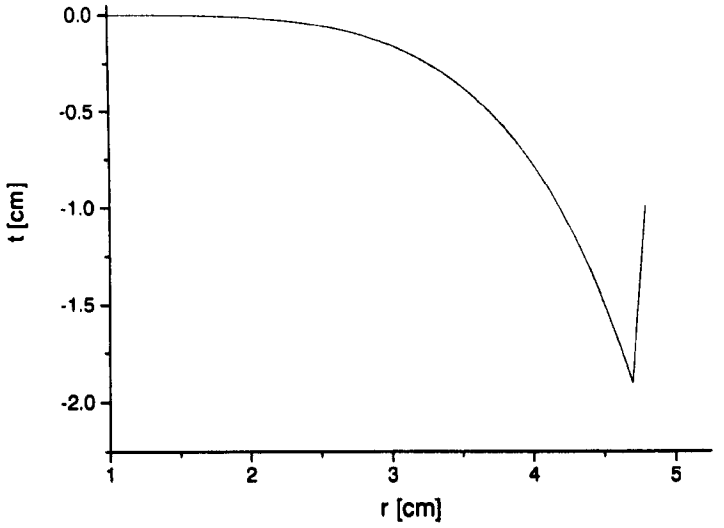

Fig 7.11 t – the change in yarn tension in random wound package

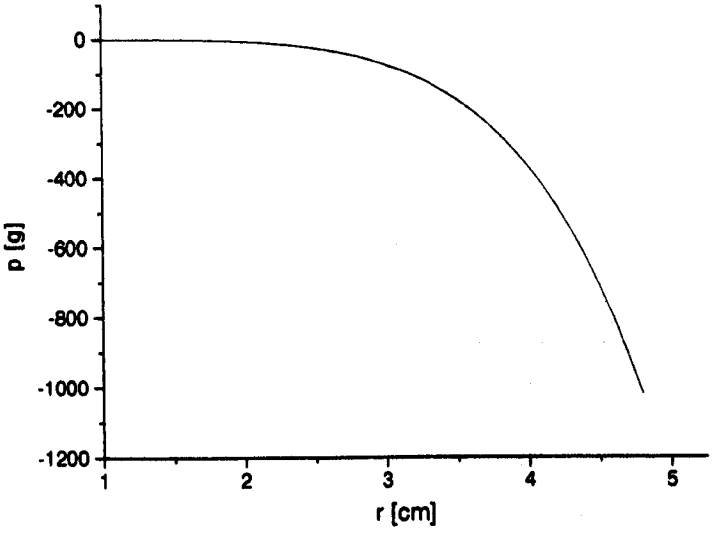

Fig 7.12 p – the change in radial pressure in random wound package

7.6.4 Results for a completed cheese

Fig 7.13 to Fig 7.17 show the distribution of compression, pressure, tension and forces in axial and circumferential direction within a completed cheese of radius of 5 cm.

The pressure at any given r increases rapidly for increase in R from r as shown by Fig 7.13. The maximum pressure occurs at the previous layer of added layer. The reason for increasing pressure is increasing the number of double traverse of yarn in an element.

The total radial displacement (U) at any radius depends on P, the radial pressure acting on the element. These graphs (Fig 7.14) show all values of r and R in a completed cheese of 5 cm. The curves of U against R for constant r are similar shape to those of P. The maximum value of U occurs at the previous layer of added layer.

The same effect can be observed at Fig 7.15, Fig 7.16 and Fig 7.17.

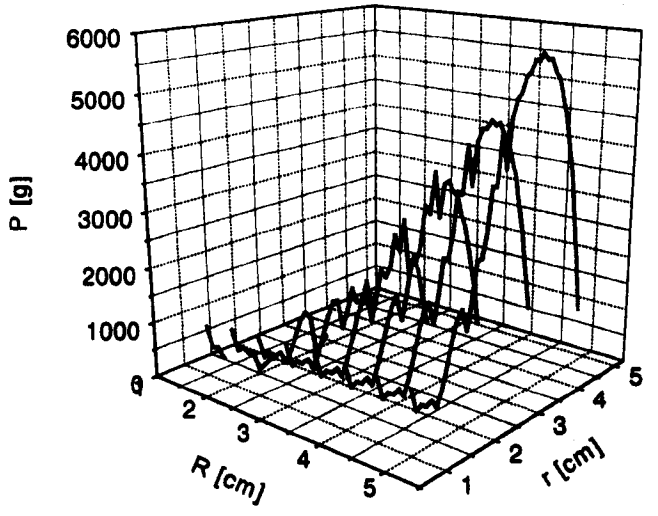

Fig 7.13 Pressure distribution in a completed random wound package

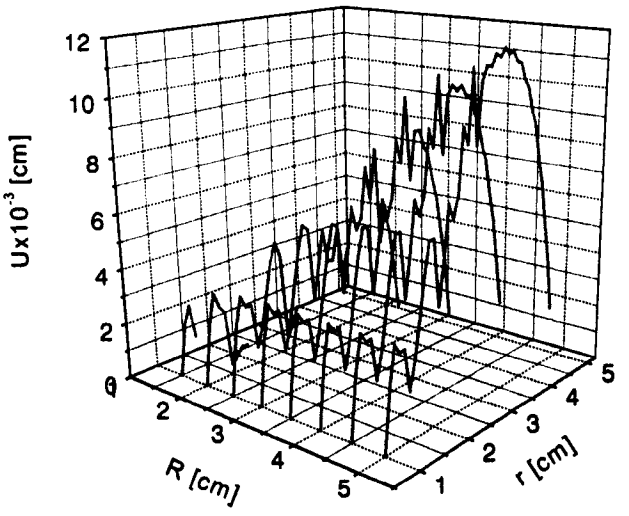

Fig 7.14 Total radial distance moved by the element in a random wound package

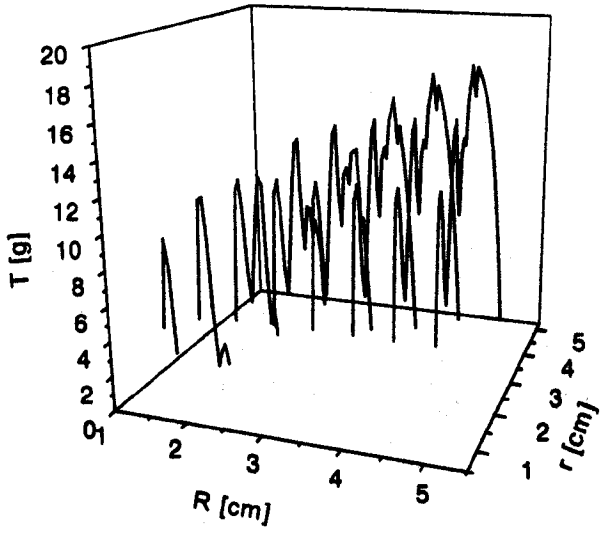

Fig 7.15 Yarn tension distribution in a completed random wound package

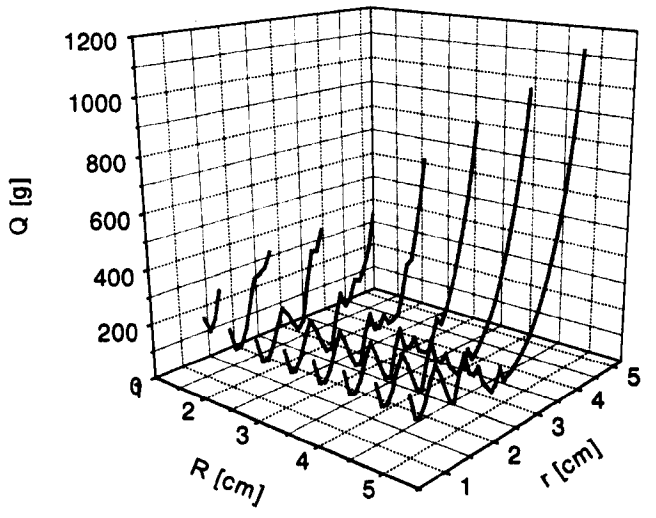

Fig 7.16 Circumferential component of the force distribution in a completed random wound package

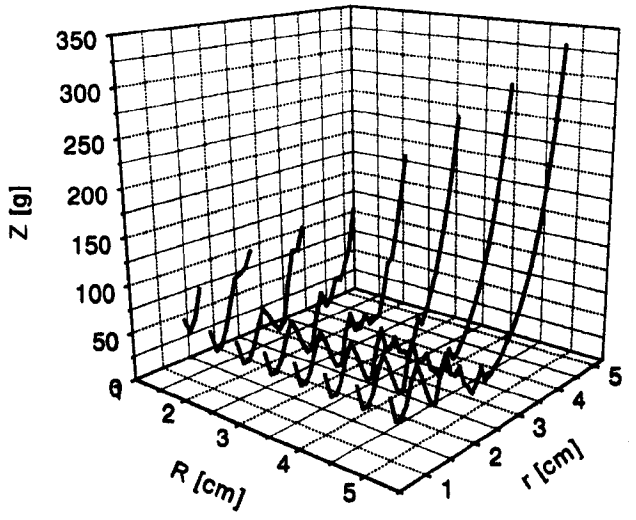

Fig 7.17 Axial component of the force distribution in random wound package

For comparison with the above results for random packages, the parameters for the same yarn as used above and similar package dimensions were used in a computer simulation program similar to that used by Jhalani for a precision wound package. The results given by Fig. 7.18 to Fig.7.28 show the corresponding graphs to those shown above.

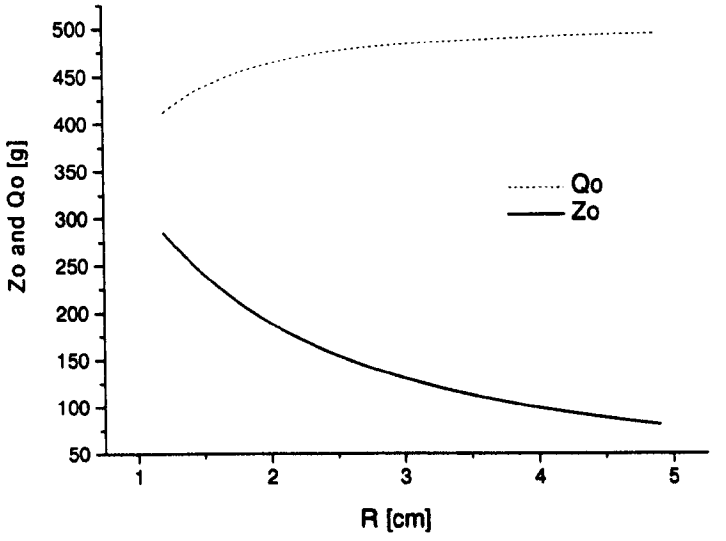

Fig 7.18 Forces in axial and circumferential direction at r=R in a precision wound package

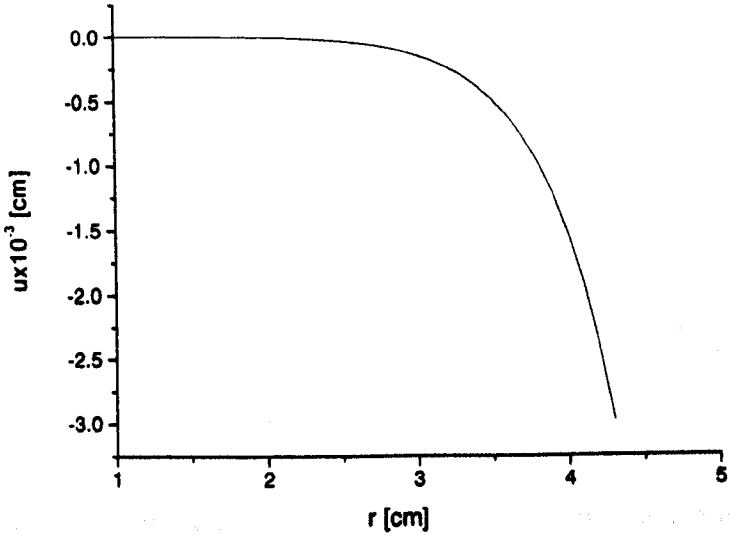

Fig 7.19 u- the incremental radial deformation in a precision wound package

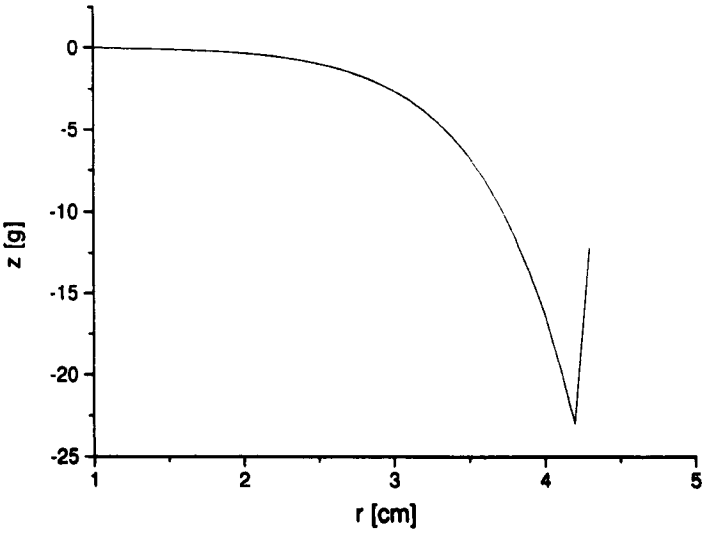

Fig 7.20 z the change in axial component of the force in a precision wound package

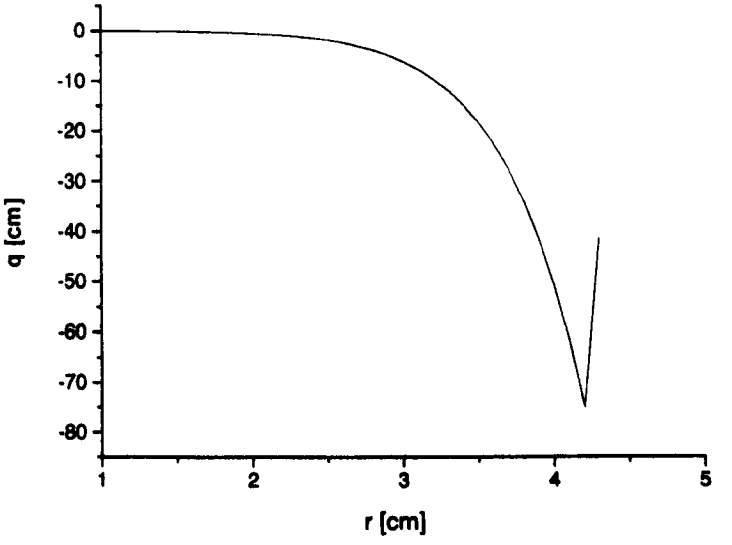

Fig 7.21 q the change in circumferential component of the force in a precision wound package.

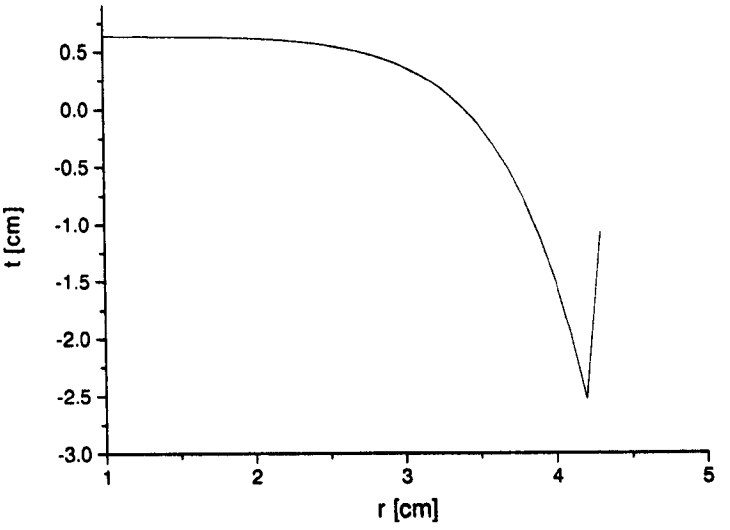

Fig 7.22 t – the change in yarn tension in a precision wound package

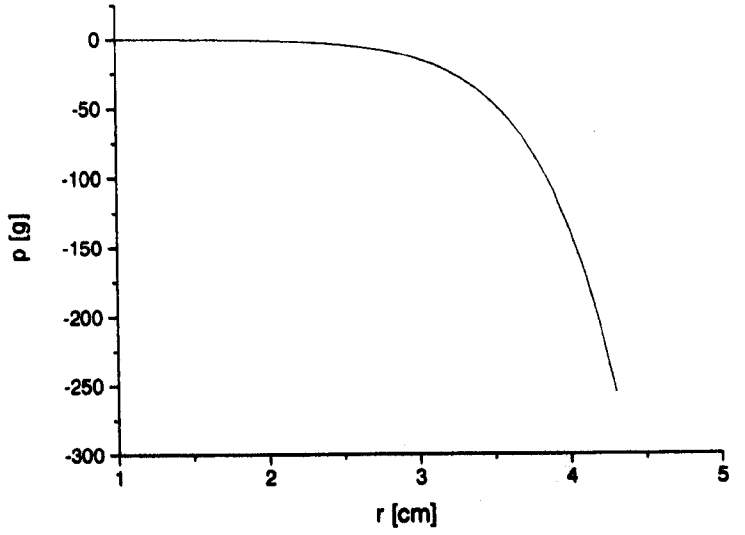

Fig 7.23 p – the change in radial pressure in a precision wound package

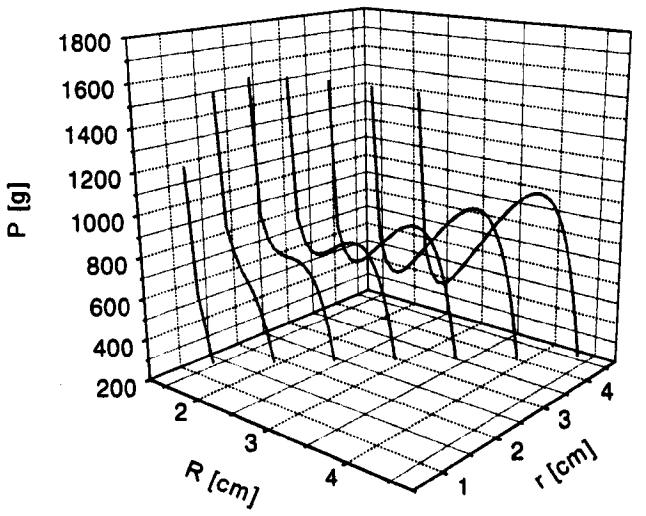

Fig 7.24 Pressure distribution in a completed precision package

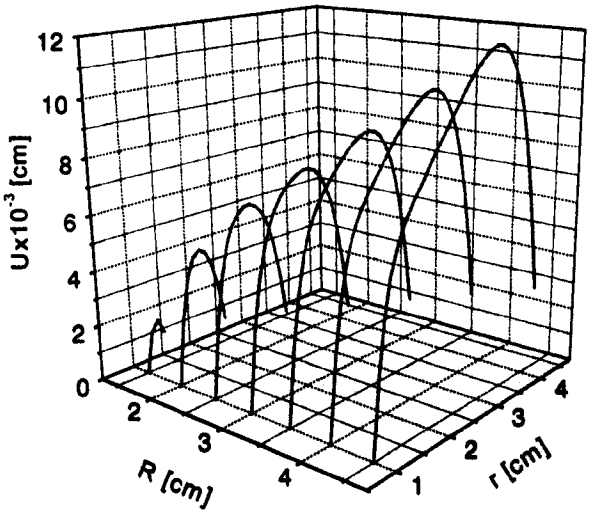

Fig 7.25 Total radial distance moved by the element in a completed precision package

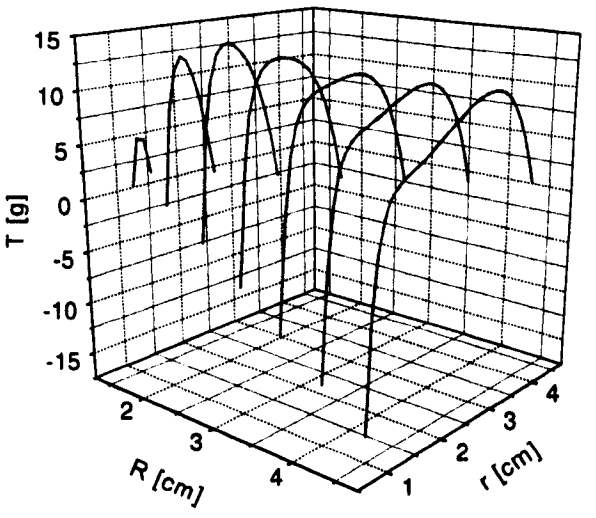

Fig 7.26 Yarn tension distribution in a completed precision package

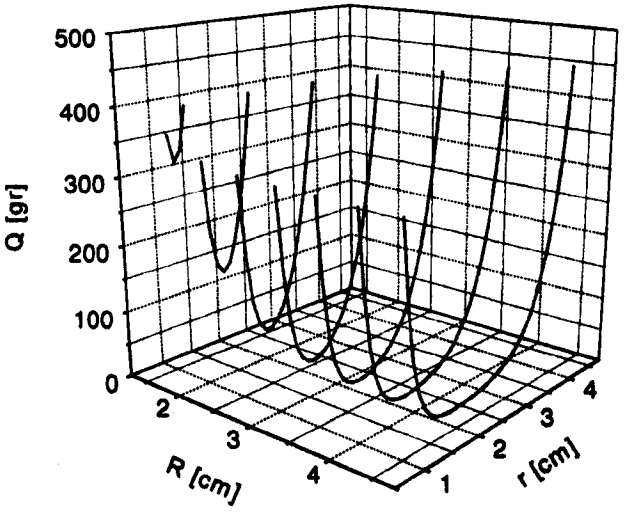

Fig 7.27 Circumferential component of the force distribution in a completed precision package.

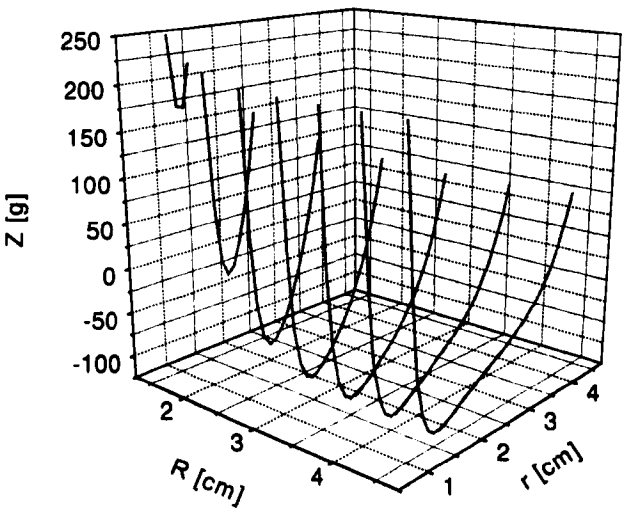

Fig 7.28 Axial component of the force distribution in a completed precision package

7.7 Discussion

The method used to simulate the random wound package was similar to that applied to the precision wound package by Jhalani. However, the results show considerable similarities in the behaviour of the parameters studied. The element chosen in this simulation of the behaviour of a random wound package was similar to that used for modelling a precision wound package. However the number of crossing points increases with radius of the element, unlike for the precision package. Due to the difficulty of calculating this, the experimental winder was used to experimentally provide suitable data to determine the number of double traverses at different values of package radius.

It was assumed that effective ribbon breaking was applied, and that this achieved an even distribution of yarn coils in the package.

The simulation is useful for studying the effect of changing certain variables. The modulus ratio particularly was shown to be a variable in Chapter 3. The present simulation assumed this to be a constant. However incorporating this as a variable was not attempted in this work due to the greater complexity of solution involved, and time limitations.

CHAPTER EIGHT

SUMMARY, CONCLUSION AND FUTURE WORK

8.1 Summary and Conclusion

Random winding undoubtedly finds wider application in the textile industry than precision winding. This is due to the acceptability of the random wound package for a wide range of uses, the greater simplicity of the winder involved, and the ease with which the random winder has been adapted for automatic winding of yarn packages. For these reasons it is the most economical process for package winding.

The tendency for ribbon formation is the major shortcoming of the random winding process, but there are a number of effective techniques that are used on commercial winders that reduce the problem to a large extent. The use of prewinders in many weaving and knitting operations has largely overcome yarn unwinding problems due to ribboning and have widened the acceptability of the random wound package.

As with other textile machines, yarn winders have benefited from advances in drive and control technologies. The widespread use of frequency controlled motor drives and microprocessor control have enabled simplification of the random winder. These advances will ensure the continued application of this type of winder in the textile industry. While newer developments such as the ribbon free random winder are available, the basic design incorporating the grooved drum is likely to be the basis of construction of the majority of random winders used by the industry.

The present work was basically aimed at achieving a method of active ribbon breaking, and evaluating its effectiveness in comparison with the passive ribbon breaking methods commonly incorporated in random winders. 'Active' in this sense implies the detection of the onset of ribboning on a random winder, and taking the ribbon breaking action repetitively till no further ribboning is detected. The use of a PC for the detection and control of ribboning was considered the best way forward and together with the necessary sensing devices, a mechatronic approach to the solution was intended.

The apparatus developed was based on a Schlafhorst Autoconer Model GKN, by incorporating shaft encoders on the drum shaft and the package spindle as described in Chapter 2. Additional sensors were provided for the measurement of the diameter of the package and the deformation of the package on the winding drum during winding. A powerful yet easily controllable motor drive was incorporated on the winder so as to be able to induce more effective intermittent slippage between the drum and the package, in the study of conventional ribbon breaking techniques. While the winder could be easily set for winding cones, the present work was confined to the winding of cheese packages.

The main objective of the above modifications was to achieve the detection of the onset of ribboning during winding. It was intended to achieve this by reading the package rotational position each time the grooved drum was at the start of a double traverse. Certain difficulties were experienced initially in obtaining reliable readings from the shaft encoders, but once these were solved, the method was found to be effective and easy to apply.

It was of special interest the study the rotation of the yarn package on the grooved drum. The grooved drum is solid and undeformable compared to the yarn package which is relatively soft. Under the controllable pressure maintained between the drum and the package during winding, some deformation of the package at the point of winding was inevitable. This is likely to cause some amount of slipping between the drum and the package over the small area of contact, and it was of interest to investigate the nature of such slip.

It was immediately evident, upon testing with a drum velocity meter constructed using the F/V converter IC LM2917, that no intermittent slip was experienced by the package, when the drum was driven at a constant speed. Naturally inertia will tend to prevent such speed fluctuations of a large package, but it was observed that no speed fluctuations occurred even with small packages. This method only indicated that that there were no random fluctuations of speed, and could not detect if any steady slip of a small magnitude was present.

8.1.1 ADT Diagram

It was found that by plotting the angular position of the yarn package at each beginning of a double traverse of the drum, with the anti-ribboning mechanism stopped, a diagram with identifiable features could be constructed on the VDU of the PC, that seemed to be sensitive to the winding conditions. This is described in Chapter 4. The diagram was named the ADT Diagram, and was in fact found to be a useful visual aid for the monitoring of the progress of the winding of a yarn package.

The diagram was used to study the rotation of a cheese when no yarn was added to it. The loss drag due to the absence of yarn tension during these studies was compensated by the addition of a light pulley and weighted cord arrangement. Under normal winding conditions such as package diameter, package speed, package pressure and frictional drag, the diagram gave a set of clearly seen straight lines, whose inclination basically depended on the ratio of diameters of the package and the drum. The introduction of axial package oscillation, while introducing axial slipping of the package on the drum, did not seem to affect the regularity of the ADT diagram to a significant extent.

The winding of a package normally provided an interesting ADT diagram. The dots forming the diagram now traced out regular peaks each time some form of ribboning was taking place. The great regularity of the diagram again indicated the absence of random slipping during winding, and clearly showed the nature of ribboning taking place. Major ribboning (at integer value of traverse ratio) and minor ribboning (at certain non integer values of traverse ratio) were clearly evident from the diagram.

8.1.2 Slippage

The study of the possibility of slippage of the package on the drum is of interest in this case of indirect driving where a hard drum drives a deformable cylinder. While the ADT diagram demonstrated the high constancy of the package rotational speed, it could not detect any small magnitude of constant slippage that could still be present. This possibility has been reported [Osawa 72, 76], and the experimental winder had the necessary capability to investigate such slippage.

The difficulty of measuring package diameter accurately, and the fact that the package deformed slightly on the drum posed a problem in calculating an 'expected' speed, for a given speed of drum rotation. However by counting the number of package rotations that take place for a given sufficiently high number of drum rotations, it was expected that any 'loss' of package revolutions can be measured, in response to the variation of certain winding parameters, such as package diameter, package speed and package pressure. The results of these experiments are reported in Chapter 3. The finite slippage that has been detected requires an explanation. It appears that the package is actually driven through its elastically deformed surface against the winding drum. It seems possible [Hannah 50, Parish 55, 58a, 58b] that this 'stretching' of the package surface achieves a slip free drive against the drum, and imparts a slightly reduced rotational speed to the package axis. Theoretical analysis of such slippage appears to be not too easy. Finite element analysis of the problem may provide an acceptable answer. However this still requires the measurement of certain elastic properties of the package surface.

8.1.3 Studies in Ribbon Breaking:

The ADT diagram also seemed to be suitable for the observation of ribbon breaking on the winder, and this was proved to be the case in the studies of ribbon breaking that were carried out. The standard method of interrupting the drum speed as provided on the winder was compared with that of directly interrupting the motor speed. The DC brushless motor drive could be easily controlled by the PC, to follow a chosen speed profile. It was found that the standard method of interrupting the drive to the grooved drum was of low efficiency compared to the method of interrupting the motor speed directly.

By applying interruption of motor speed at moments when ribbon occurrence was detected, active ribbon breaking was achieved as intended. Since the ribbon breaking action was continuously applied during the actual ribboning intervals, it was both physically observed as well as seen from the ADT diagram that more effective ribbon breaking was achieved by this method.

The study was extended to interruption of package speed by slightly lifting the package repeatedly during ribboning intervals. This is in fact a standard method incorporated on certain winders, but it is applied in a passive manner. By constructing a stepper motor based lifting arm, the experimental winder was provided with the capability of achieving the same action. The method provided the best ribbon breaking action attempted during this work. Results of these studies are given in Chapter 5.

It was necessary to carry out a determination of the effectiveness of the different ribbon breaking methods by a more objective method. Unwinding of yarn packages prepared by the different methods seemed to be the best. In the absence of a PPA for this purpose, a suitable apparatus was devised as described in Chapter 6. The results indicate the greater effectiveness of active ribbon breaking, on account of the lower unwinding tensions generated from packages prepared by this method.

8.1.4 Simulation

A yarn package is produced by the winding of a yarn under a suitable tension on to a suitable bobbin. The elastic nature of the yarn gives certain properties to the yarn package. The compression brought about by the outer layers of yarn will cause the inner layers to undergo elastic deformation and move inwards so as to assume a smaller radii than those that they were wound at. The resultant reduction in length of these layers will cause the tension of these layers to correspondingly drop.

The tension distribution within a yarn package is of interest as the behaviour of the yarn once it is unwound from the package during a subsequent process depends on its previous tension history. This is particularly important as a yarn cannot recover from its previous extension instantaneously, but does so over a period of time on account of viscoelasticity. Unfortunately there is no direct method of ascertaining the tension of yarn within a wound package. For this reason it is very useful to be able to calculate the stresses and deformations within a yarn package, in terms of the physical properties of a yarn.

Early on in this work, the report by Jhalani was studied, in which he had performed a computer simulation of the precision winding process so as to be able to calculate the

stresses and the layer movements etc. It was realised that the original work that had been carried out on a mainframe computer using ALGOL could be far more conveniently carried out now on a PC using the C language (Borland C++ 3.1), with the graphical representation of the results easily implemented using ORIGIN 4.10.

An attempt was made in this work to carry out a similar exercise in the computer simulation of a random wound package. The new simulation had to allow for the constant value of wind angle and also required the determination of the number of crossing points involved in a layer. The later information was obtained by winding trials which provided the number of double traverses wound in increasing the package diameter in 1 mm increments.

The results of the simulation of the cross wound package gives results comparable to those for a precision wound package as given in Chapter 7. The work carried out only involved the central section of the package, and assumed a constant modulus ratio, whereas the work reported in Chapter 3 showed that the modulus ratio in fact depends on inter-yarn pressure.

8.2 Future work

The concept of active ribbon breaking was found to be realistic and achievable. It also achieved better unwinding characteristics when compared with other methods of ribbon breaking.

Given that ribboning can be entirely eliminated today using controlled drives to the package spindle and the yarn guide, and the fact that such a winder will be mechanically simpler than a basic random winder capable of ribbon breaking leads to the question whether the conventional type of winder is of any importance any more.

In practice it seems that the random wound package produced using the standard grooved drum still enjoys wide acceptability. Ribbon free random winding should provide superior unwinding characteristics, but this process is evidently costlier and justifiable mostly is applications such as winding large producer packages of synthetic yarns.

Some observations based on this study as to future work are given below.

1. The experiments carried out on the lifting of the yarn package for ribbon breaking made use of a stepper motor driven lifting arm, whose height could track the rising position of the package spindle. This arrangement, while effective, was rather cumbersome. A controllable actuator of simpler construction is more desirable.

2. Study of the driving of the yarn package on the grooved drum

The very steady nature of package drive on the grooved drum and the measurable 'loss' of package revolutions under varying winding conditions require further study. It is practically impossible to detect any mechanical slippage that occurs in the contact zone between the package and the drum. A theoretical study to explain these observations will be of use in relation to package winding. It will require the understanding of the behaviour of the yarn package as an elastic body, and of the manner in which friction is involved in the driving of the package.

3. A more realistic computer simulation of the wound package is relevant. The availability of the increased speed and the power of the PC will facilitate this work. Greater understanding of the behaviour of the package formation process is essential in formulating a better simulation program. Such a program should also take into account the variable modulus ratio of the yarn, and ideally should incorporate such characteristics as viscoelasticity.

REFERENCES

[Beckett 67] Beckett, R. and Hurt, J., Numerical Calculations and Algorithms, McGraw-Hill, USA, 1967

[Beddoe 67] Beddoe, B. "Anisotropy of yarn wound on a flanged tube", *Journal of Strain Analysis*, 1967, vol:2 , No:3, page 207

[Catlow 62] Catlow, M.G., and Walls, G.W., A study of stress distribution in pirns, *Journal of Textile Industries*, 1962, 53, page 410-429

[Durur 96] Durur, G., A novel dizayn winding machines for random, MSc Thesis, Department of Textile Industries, Leeds University, 1996

[Distec Instr.] "Distec" Non-contact displacement measuring system, Graham & White Instruments Ltd., Hertfordshire, U.K.

[Electro-craft] DC Brushless Motor DM-20 and BRU-200 Servodrive, Electro-Craft Ltd., Fourth Avenue, Crewe, U.K.

[Hannah, 50] Hannah, M., The theory of high drafting, PhD Thesis, Department of Textile Industries, Leeds University, 1950

[Hebberling 69] Hebberling, F., "The maximum wind angle in winding of textile packages", *Textile Research Journal*, 1969 September, vol:39, No:9 page 799-808

[Jhalani 70] Jhalani, S.C., Stresses in yarn packages, PhD Thesis, Department of Textiles, Leeds University, 1970

[Kernighan 96] Kernighan, B. W. and Ritchie, D. M., The C Programming Language, Second Edition, New Delhi: Prentice-Hall of India Private Ltd., 1996

[Kyoto,89] Kyoto, K.O., "New method of package forming", *Melliand Textilberichte*, 1989, 70(9), p.643-646 (E 272-273)

[Law 80] Law, R.S., Deformation of yarn packages, MPhil, Department of Textile Industries, Leeds University, 1980

[Nakashima 68] Nakahisma, T. " Yarn tension in winding mechanism part:2 Stress in yarn beams", *Journal of the Textile Machinery Society of Japan*, 1968, vol:14, No:2, page 75

[National Semi.] LM2917 Frequency to Voltage Converter, National Semiconductor, Corporation, USA. Available: http://www.national.com/pf/LM/LM2917.html#Datasheet

[Nobauer 92] Nobauer, H. and Baumeler, M., "Measurement of unwinding resistance of yarn packages using the Package Performance Analyser", *Textil Praxis International*, 1992, November, pages 1034-1040

[Osawa 72] Osawa, G., and Koyama, T., " On the slippage between a yarn package and the grooved drum during winding", *Journal of the Textile Machinery Society of Japan,* 1972, Vol: 25, No:6, pages T.113-123

[Osawa 76] Osawa, G., and Koyama, T., " Effect of revolving resistance of package on slippage between yarn package and grooved drum during winding", *Journal of the Textile Machinery Society of Japan,* 1976, vol: 22, No: 2, pages: 34-37

[Oxtoby 87] Oxtoby, E., Spun Yarn Technology, Butterworth & Co. Ltd., 1987, page 183.

[Parish, 55] Parish, G. J., "Measurement of the pressure distribution between roller in contact", *British Journal of Applied Physics*, 1955, July, Vol:6, page 256.

[Parish, 58a] Parish, G. J., "Measurement of the pressure distribution between metal and rubber covered rollers", *British Journal of Applied Physics*, 1958, April, Vol: 9, page 158.

[Parish, 58b] Parish, G. J., "Apparent slip between metal and rubber-covered pressure rollers", *British Journal of Applied Physics*, 1958, November, Vol: 9, page 428.

[Rebsamen 88] Rebsamen, A., "Modern Package Building", *Textile Asia,* 1988, September, pages 130-136

[Rieter-Scragg] Rieter Scragg PPA3 Technical Data, Rieter-scragg Ltd, U.K.

[RS 332-098] RS stock numbers 332-098, Stepper motor drive board, RS Components Ltd., UK.

[RS 435-686] RS Data Sheet 97, stock numbers 435-686, Prototyping boards, RS Components Ltd., U.K.

[RS 435-692] RS stock numbers 435-692, Strain gauges amplifier P.C.B, RS Components Ltd., U.K.

[Schlafhorst 67] Schlafhorst Autoconer manual, W.Schlafhorst AG&Co., Monchengladbach, Germany.

[Schlafhorst] Company Catalogue, W.Schlafhorst AG&Co., Monchengladbach, Germany.

[SSM] Company Catalogue, SSM Scharer Schweiter Mettler AG, Zurich, Switzerland

[Sternheim 89] Sternheim, A, The Control of Beat-up Force Using a Microprocessor Controlled Hydraulic Actuator, PhD Thesis, Department of Textile Industries, Leeds University, 1989.

[TextInst 95] Textile Terms and Definition, Tenth Edition, Manchester: Textile Institute, 1995

[Ursiny 86] Ursiny, P. "New knowledge on tension built up within yarn package", *Textiltechnik*, 1986, vol:36, No:10, page 535

[Wegener 68] Wegener, E.H.W and Schubert G., "Die Ermittlung der Druckverteilung in Garnkörpern :How to determine the distribution of pressure in yarn bodies", *Textil-Praxis*, 1968, 23, page 226 ,In German

[Wegener 69] Wegener, E.H.W and Schubert G.,"Die verformung des Garnkörpers in Abhangigkeit von den spulbedingungen", *Textilindustrie*, 1969, vol: 71 No: 6 , page 389 and 456, In German

APPENDIX A

INSTRUMENTATION

A.1 Absolute Shaft Encoder

Model No: H25D-CW-8NB-7406R-EM20

Serial no: 16838

Company :Muirhead Vactric Component Ltd (BEI).

17 PIN

Pin	Colour		connected to:
A	Red	2^0	74LS244/1 pin 2 (MSB)
B	Blue	2^1	74LS244/1 pin 4
C	Green	2^2	74LS244/1 pin 6
D	Yellow	2^3	74LS244/1 pin 8
E	White	2^4	74LS244/1 pin 11
F	Black	2^5	74LS244/1 pin 13
G	Brown	2^6	74LS244/1 pin 16
H	Violet	2^7	74LS244/1 pin 17 (LSB)
J	Orange	Not connected	
K	Pink	+5V (Lamp Supply)	
L	Turquoise	Not connected	
M	Grey	Not Connected	
N	Red-Blue	Not Connected	
P	Red-Green	Ground	
R	Red-Yellow	0 V	
S	Red-White	+5V	
T	Red-Black	Case Ground	

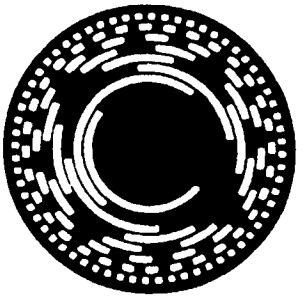

8 Bit Absolute Disc

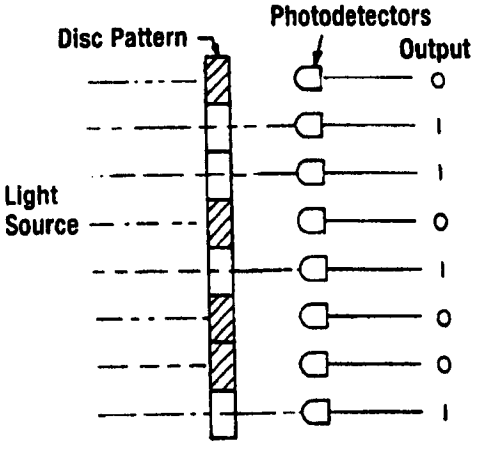

Fig A.1 Disk pattern of an absolute shaft encoder

A.2 Incremental Shaft Encoder

The incremental shaft encoder used is Leine&Linde which is PPR 512, VDC 12-30 volt , serial no: 11460257

The connection of wire of the shaft encoder follows :

A signal 1 green, B signal $\bar{1}$ white, C signal $\bar{2}$ Black, D signal 2 Yellow, E +E volt Red,

F 0 volt Blue, G signal 0 Brown, H signal $\bar{0}$ Violet

Pin	Colour		connected to:
A	Red	2^0	74LS244/1 pin 2 (MSB)
B	Blue	2^1	74LS244/1 pin 4
C	Green	2^2	74LS244/1 pin 6
D	Yellow	2^3	74LS244/1 pin 8
E	White	2^4	74LS244/1 pin 11
F	Black	2^5	74LS244/1 pin 13
G	Brown	2^6	74LS244/1 pin 16
H	Violet	2^7	74LS244/1 pin 17 (LSB)
J	Orange	Not connected	
K	Pink	+5V (Lamp Supply)	
L	Turquoise	Not connected	
M	Grey	Not Connected	
N	Red-Blue	Not Connected	
P	Red-Green	Ground	
R	Red-Yellow	0 V	
S	Red-White	+5V	
T	Red-Black	Case Ground	

A.3 Technical Specifications of Frequency Inverter

Motor Rating(kW)	0.37
Output Current(A)	2.2
Output Frequency	0-240Hz (programmable)
Input Supply Voltage	220-240V ±10% (1 ph)
Input Supply Frequency	50-60Hz ±5%
Protection Rating	IP20
Operating Temperature	45 ^{0}C max.
Current Limit	50-150%
Torque Boost	Up to 25% voltage
Acceleration / Deceleration	0.1 to 600 secs

A.4 Drum speed given by computer as decimal

DECIMAL	DRUM SPEED(RPM)
255	2133
215*	1801*
200	1677
150	1260
100	844
50	426

*The drum speed used when package was prepared for slippage and deformation experiment.

A.5 Stepper Motor

A.5.1 Technical specifications

Type	34
Step angle	1.8^0
Step angle tolerance	±3.25
Voltage	3 V d.c.
Current	1.7A
Resistance	1.8Ω
Inductance	5mH
Holding torque	1100mNm
Maximum working torque	650mNm
Detent torque nominal	100mNm
Rotor inertia	640 gcm^2
Maximum pull-in rate	800 steps/s
Ambient temperature	-40^0C to $+65^0C$
Weight	1350

A.5.2 Wiring detail of stepper motor and the control card

This circuit run the stepper motor by PC

The input comes from the interface card of PC and output goes to stepper motor card pin 19 for run/stop

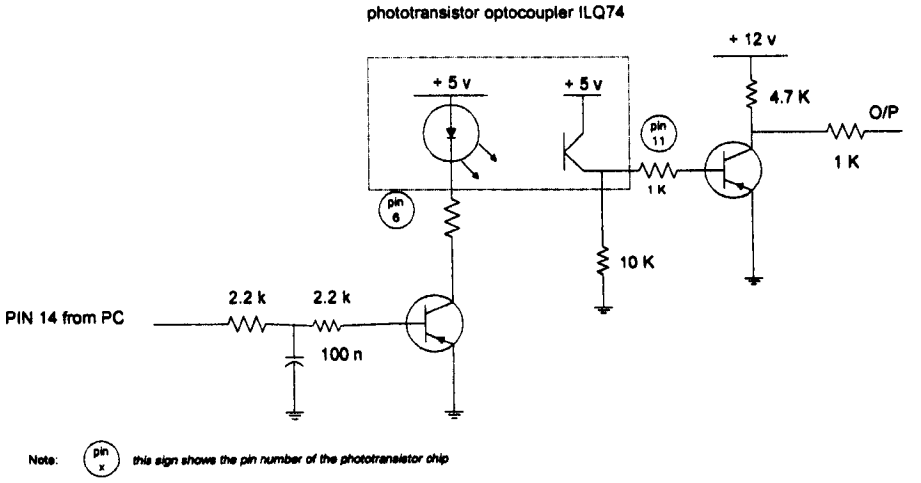

pin connection between computer card and stepper motor board

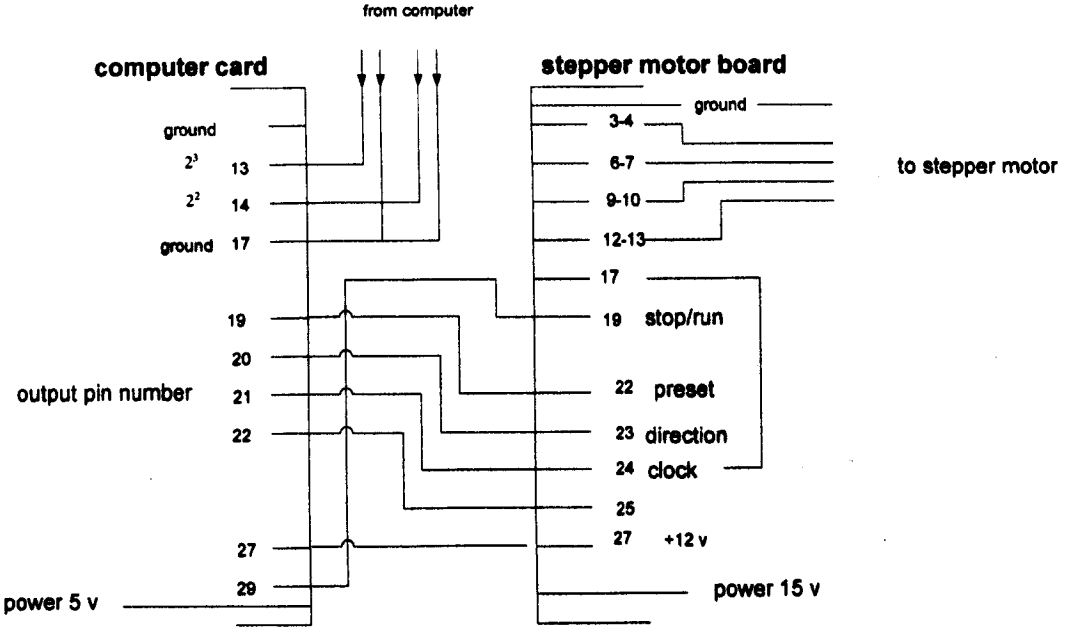

On-board oscillator assembly

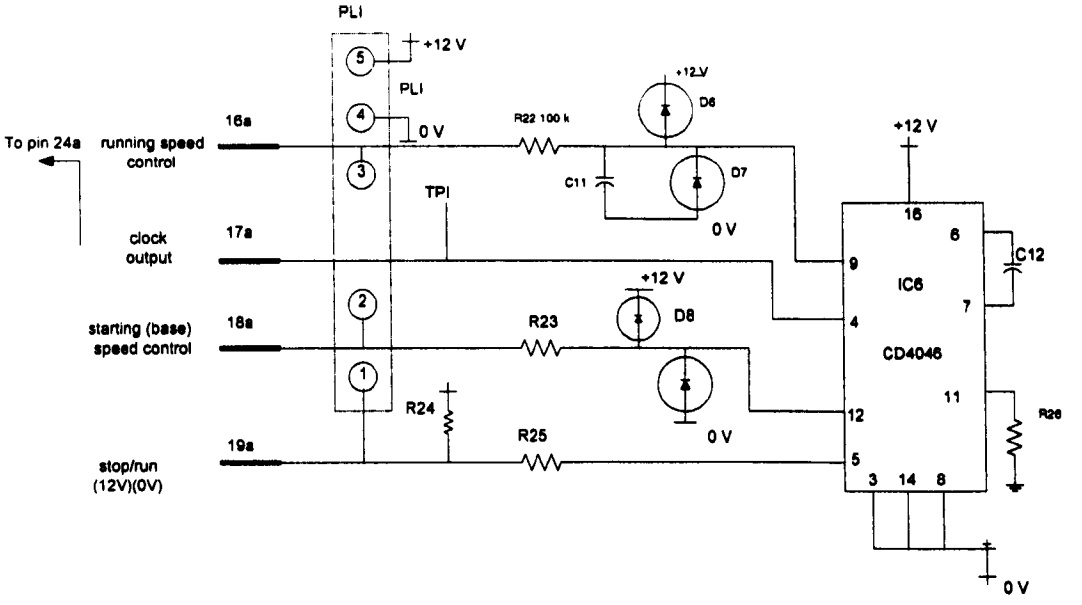

Underline resistor value soldered to the circuit

BOARD CONNECTIONS

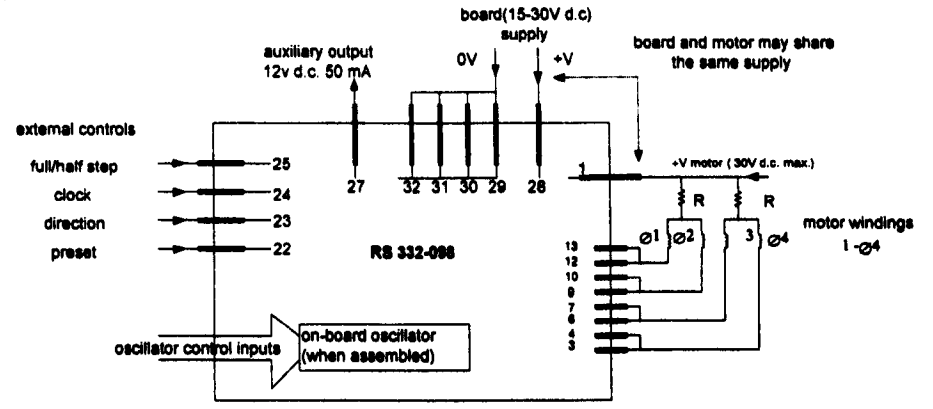

This circuit gives direction to the stepper motor by PC

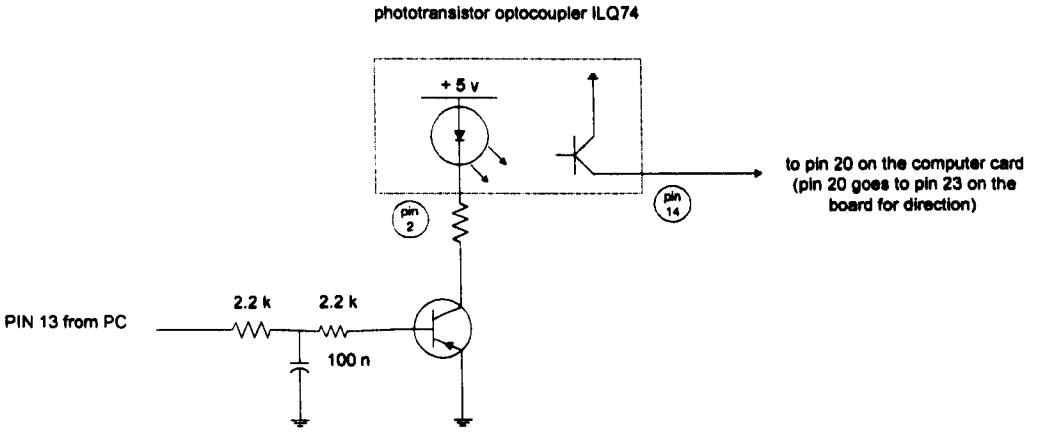

Note: (pin x) *this sign shows the pin number of the phototransistor chip*

Safety switches connection

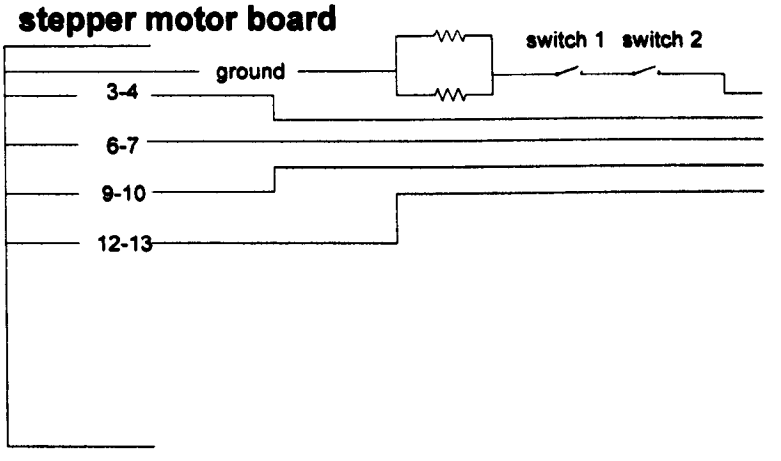

** when one of the swithches is pushed, the power of the motor is off*

APPENDIX B

B.1 All Results Of Experiment For Density

Pressure (kg)	Tension (g)	Radius (mm)	Diameter (mm)	Max (mm)	Min (mm)	Average (mm)	Weight (g)	Volume (cm3)	Density (gr/cm3)
2	30	81.39	162.78	134.5	119.6	127.05	1077	2284.81	0.47137
2	30	71.39	142.78	131.6	120.2	125.9	781	1659.84	0.47053
2	30	61.22	122.44	130	121.7	125.85	541	1125.98	0.48048
2	30	51.03	102.06	128.3	123.1	125.7	327	672.93	0.48593
2	30	40.98	81.96	127.2	123.9	125.55	148	307.40	0.48146
									0.47795
2	19	81.71	163.42	133.6	119.6	126.6	983	2297.47	0.42786
2	19	71.48	142.96	131.7	120.5	126.1	732	1667.57	0.43896
2	19	61.4	122.8	129.2	122	125.6	499	1132.44	0.44064
2	19	51.13	102.26	128.3	123.5	125.9	298	678.041	0.4395
2	19	40.89	81.78	127.2	124.6	125.9	130	305.34	0.42575
									0.43454
2	8	82.3	164.6	132.1	120.2	126.15	852	2327.65	0.36603
2	8	71.92	143.84	131.6	121	126.3	643	1695.25	0.3793
2	8	61.72	123.44	129.8	122.5	126.15	453	1153.01	0.39288
2	8	51.11	102.22	128.9	123.1	126	257	677.77	0.37918
2	8	41.05	82.1	127.3	124.5	125.9	120	310.53	0.38644
									0.38077
1.25	30	80.97	161.94	132.9	119.7	126.3	1018	2244.26	0.4536
1.25	30	71.01	142.02	132.3	120.2	126.25	754	1642.99	0.45892
1.25	30	60.72	121.44	129.9	120.3	125.1	505	1095.30	0.46106
1.25	30	50.58	101.16	128.1	124	126.05	306	656.697	0.46597
1.25	30	40.46	80.92	126.5	124.8	125.65	130	290.93	0.44684
									0.45728
1.25	19	80.24	160.48	132.6	119.8	126.2	890	2195.83	0.40531
1.25	19	70.32	140.64	131.1	121.1	126.1	661	1602.41	0.4125
1.25	19	59.8	119.6	129.4	122.6	126	450	1059.29	0.42481
1.25	19	50.19	100.38	128.1	124.3	126.2	265	641.90	0.41284
1.25	19	40.76	81.52	127.2	124.8	126	125	301.38	0.41475
									0.41405
1.25	8	80.88	161.76	132.4	120.5	126.45	790	2241.14	0.3525
1.25	8	71.6	143.2	131.4	121.8	126.6	583	1681.01	0.34682
1.25	8	61.12	122.24	129.2	123	126.1	405	1123.36	0.36053
1.25	8	51.04	102.08	127.8	123.8	125.8	247	673.87	0.36654
1.25	8	40.83	81.66	127.2	124.5	125.85	113	303.28	0.37259
									0.35979
0.7	30	80.95	161.9	133	119.1	126.05	1006	2238.54	0.4494
0.7	30	70.92	141.84	132.2	120.7	126.45	730	1640.52	0.44498
0.7	30	60.83	121.66	129.7	122.3	126	494	1108.47	0.44566
0.7	30	50.61	101.22	127.6	123.8	125.7	295	656.07	0.44965
0.7	30	40.44	80.88	126.1	124.6	125.35	125	289.60	0.43163
									0.44426
0.7	19	80.7	161.4	133.5	119.6	126.55	908	2231.35	0.40693
0.7	19	70.88	141.76	131	120.4	125.7	655	1628.55	0.4022
0.7	19	60.79	121.58	129.9	122.2	126.05	433	1106.98	0.39115
0.7	19	50.66	101.32	127.3	123.3	125.3	265	655.98	0.40398
0.7	19	40.46	80.92	126.5	124.6	125.55	115	290.7	0.3956
									0.39997
0.7	8	81.23	162.46	131.5	119.6	125.55	800	2247.57	0.35594
0.7	8	71.13	142.26	130.6	120.6	125.6	580	1641.26	0.35339
0.7	8	60.96	121.92	128.7	122.2	125.45	390	1109.87	0.35139
0.7	8	50.75	101.5	127.2	123.6	125.4	231	660.1	0.34995
0.7	8	40.69	81.38	126.4	124.5	125.45	103	297.82	0.34584
									0.3513

B.2 All Results Of Experiment For Slippage And Deformation

Pressure (kg)	Tension (g)	Radius from LVDT (mm)	Density (g/cm3)	Revolution (Drum rev. 2000)	Slippage (%)	Deformation (mm)	Revolution with drag (Drum rev 2000)	Slippage with drag effect (%)
2	30	39.9	0.45642	2229.3	0.32	1.17	2230	1.14
2	18	39.8	0.40335	2222.9	0.44	1.7	2224.2	1.64
2	9	39.8	0.36326	2194.5	1.35	2.95	2196.1	2.88
2	30	59.9	0.45998	1486	0.9	1.1	1486.5	1.07
2	18	60	0.42077	1484.3	1.02	1.05	1484.7	1.02
2	9	59.9	0.37005	1463.6	1.67	2.59	1464.4	2.54
2	30	79.7	0.452	1120.1	0.8	0.81	1120.4	0.78
2	18	79.6	0.40605	1118.9	1.27	1.04	1119.3	1.00
2	8	79.7	0.34327	1102.3	2.2	2.39	1102.9	2.33
1.25	30	39.8	0.43238	2234	0.34	1.21	2233	1.25
1.25	19	39.8	0.39544	2224.7	0.43	1.62	2224.3	1.64
1.25	8	39.9	0.35581	2205.2	0.75	2.24	2206.1	2.20
1.25	30	60.3	0.4547	1489.8	0.45	0.18	1490.3	0.15
1.25	19	59.7	0.42339	1500.3	0.57	0.48	1500.9	0.44
1.25	8	59.8	0.34513	1483	1.14	1.46	1483.6	1.42
1.25	30	79.8	0.44059	1120.4	0.41	0.66	1120.6	0.64
1.25	19	80	0.40289	1117.3	0.76	0.68	1117.5	0.67
1.25	8	80	0.34487	1109.8	1.11	1.35	1110.2	1.32
0.7	30	39.9	0.42018	2220	0.18	1.58	2214	1.85
0.7	19	39.9	0.38472	2216.1	0.18	1.75	2211.1	1.97
0.7	8	39.9	0.33254	2213.3	0.4	1.88	2212.2	1.93
0.7	30	60	0.43368	1495.6	0.28	0.29	1494.9	0.34
0.7	19	60.1	0.38472	1492.5	0.37	0.33	1492.3	0.35
0.7	8	60.1	0.34155	1487.4	0.55	0.67	1487.6	0.66
0.7	30	79.8	0.43672	1123.5	0.53	0.38	1123.6	0.37
0.7	19	80.1	0.4009	1119.4	0.53	0.37	1119.6	0.36
0.7	8	80.1	0.34611	1115.1	0.79	0.76	1115.4	0.73

APPENDIX C

SOFTWARE PROGRAM DESIGNED

C.1 Checking the diameter of the package during winding

```
// When thepackage reaches required diameter,
the program stop winding yarn to package
#include <stdio.h>
#include <conio.h>
#include <dos.h>
#include <math.h>
#include <stdlib.h>
#define SOC 0x300   /* start of conversion*/
#define SOCM   0x302
  /* start of conversion for motor speed*/
#define AD1    0x301
  /* Port address of first A/D for POT*/
#define AD2    0x306
  /* Port address of second A/D for LVD*/

#define A_lvdt  22.81
#define B1_lvdt  0.29
#define A_pot  25.4
#define B1_pot  0.28

#define radius 80

float x,y,p,lv,tp1,tl1,ttl1,ttp1;
float p1,l1,lvdt,pot,sonl1,sonp1;
void  main()
  {
    outportb(SOCM,255);
// adjust the speed of motor
    clrscr();
  do{
    do{
          y=0;
          ttp1=0;
          ttl1=0;
  while(y<20){
                    x=0;
                    tp1=0;
                    tl1=0;
    while(inportb(773)!=0);
  while(inportb(773)!=255){
                    outportb ( SOC, 0 ) ;
                    delay(1) ;
                    p=inportb ( AD1 ) ;
                    lv=inportb ( AD2 ) ;
                    tp1=tp1+p;
                    tl1=tl1+lv;
                    x++;
                }
                    l1=tl1/x;
                    p1= tp1/x;

              ttl1=ttl1+l1;
              ttp1=ttp1+p1;

              y++;
    }

 sonl1=ttl1/y;  // average reading in 20 cycles of
package
sonp1=ttp1/y;

lvdt=A_lvdt+(B1_lvdt*sonl1 )
pot=A_pot+(B1_pot*sonp1 )
   printf("lvdt-radi : %.2f\t ",lvdt);
   printf("pot-radi : %.2f\t",pot);
   printf("Deformation: %.3f\n",pot-lvdt);

   }while(lvdt < yaricap-1);
outportb(SOCM,215);
 }while(lvdt < yaricap);
 outportb(SOCM,0);
 getch();
 }
```

C. 2 – Drum speed checking

```
/*shows the number of reading between 0-255
at a revolution of drum */

#include<stdio.h>
#include<conio.h>
#define          SOC     0x302

FILE     *fptr ;
int a,m;
int data[256];
void starting_point();

void main()
{
          outportb(SOC,255);
          clrscr();
          starting_point();


    do{
          while( inportb(772) != 0 ){
             a=inportb(772);
             data[a]++;
             }
          a=inportb(772);
          data[a]++;
      }while(inportb(772) !=0 );

    do{
```

```
   while( inportb(772) == 0 ){
         a=inportb(772);
         data[a]++;
         }
         a=inportb(772);
         data[a]++;
    }while(inportb(772) ==0 );

for ( m=0 ; m < 256 ; m++ ){
     printf("%d  %d \t",m,data[m]);
      }
   fptr = fopen( "wdrum.txt" , "w") ;
    for ( m=0 ; m<256 ; m++ )
    fprintf(fptr, "%d  %d \n",m,data[m]);
   fclose ( fptr ) ;
   getch();
 }

   void starting_point()
         {
do{
         while( inportb(772) != 0 );
    }while(inportb(772) !=0 );
do{
    while( inportb(772) == 0 );
   }while(inportb(772) ==0 );
}
```

C.3 Counting the drum and package revolution

```
//This program for counting  revolution of package and drum at the same time.
#include <stdlib.h>
#include<stdio.h>
#include<conio.h>
#include<time.h>
#include<dos.h>
#include<math.h>

#define drum 90         // The drum diameter is 90 mm
#define SOC          0x300    /* start of conversion*/
#define SOCM     0x302   /* start of conversion for motor speed*/
#define AD1     0x301    /* Port address of first A/D*/
#define AD2     0x306    /* Port address of second A/D*/

#define A_lvdt  22.81
#define B1_lvdt  0.29
#define A_pot  25.4
#define B1_pot  0.28

int a,bd,bp,ld,lp;
float vary,count1,count2;
int m,read1=0,data[3],z;
float x,y,lv,tl1,ttl1;
float l1,lvdt,sonl1;
float p,tp1,ttp1;
float p1,pot,sonp1;
float tcount1=0,tcount2=0,tlvdt=0;

void diameter();

void main()
{
   outportb(SOCM,215); // adjust the speed of motor
   clrscr();
   printf("ready ! , hit any key ");
   getch();

   clrscr();
   printf(" NOW, CHECKING THE PACKAGE DIAMETER ON THE WINDING MACHINE, WAIT A SECOND ! ");
   diameter();
   clrscr();
   printf("DEFORMED  PACKAGE RADIUS IS NOW     %.2f\n",lvdt);
   printf("NON-DEFORMED PACKAGE RADIUS IS ALSO  %.2f\n",pot);
   printf("Deformation: %.3f\n\n",pot-lvdt);
   printf("Drum revolution is constant as 2000\n\n");

   while(m<5){

    count1=0;
    count2=0;
    read1=0;
    again1:
    for(z=0;z<4;z++){ data[z]=inportb(772);
                      }
    if ( data[0]!=data[1] && data[2]!=data[3] && data[0]!=data[2] ) goto again1;
    bd=data[0]; // bd= beginning reading of drum position

    bp=inportb(773); // bp= beginning reading of package position
    if (bd==0) bd=255;
          else bd=bd-1;  // to avoid reading as same as beginning reading
    if (bp==0) bp=255;  // so need to minus 1 from the first reading
          else bp=bp-1;

    while(count1 <2000){

                  do{
                        while( inportb(772) != bd ) {
```

```
a=inportb(773);

 if( a== bp && read1==0) {
                    count2++;
                    read1=1;
                 }
if ( a ==  bp+1 ) read1=0;
             }
 }while(inportb(772) != bd );

do{
    while( inportb(772) == bd ){
              a=inportb(773);
   if( a== bp && read1==0){
                count2++;
                read1=1;
               }
 if ( a == bp+1 ) read1=0;
              }
 }while(inportb(772) == bd );

    count1++;
 }

     again2:
     for(z=0;z<4;z++){ data[z]=inportb(772);
                       }
 if ( data[0]!=data[1] && data[2]!=data[3] &&
data[0]!=data[2]) goto again2;

     ld=data[0];
     lp=inportb(773);

 if (bp>lp) vary=(256-bp)+lp;
  // this is for decimal of package revolution
            else vary=lp-bp;

     count2=count2+(vary/255);
     printf("%d) ",m+1);
     printf(" PACKAGE : %.1f \n",count2);

     tcount1=tcount1+count1;
     tcount2=tcount2+count2;
     m++;
     delay(1000);
    }
printf("\n\n----------RESULTS ----------------
-------\n\n");
printf("Drum : %.1f  -  Average Package
revolution: %.1f \n",tcount1/m,tcount2/m);
printf("Radius of Package : %.2f\t",lvdt);
printf("slippage: %.2f
%\n",((((tcount1/m)*drum)-
(tcount2/m)*(lvdt)*2))*100)/((tcount1/m)*drum
);
    getch();

 }
```

```
void diameter()
{

        y=0;
        ttp1=0;
        ttl1=0;
        while(y<100){

        x=0;
        tp1=0;
        tl1=0;

        while(inportb(773)!=0);

         while(inportb(773)!=255){
                outportb ( SOC, 0 ) ;
                delay(1) ;

                p=inportb ( AD1 ) ;
                lv=inportb ( AD2 ) ;

                tp1=tp1+p;
                tl1=tl1+lv;
                x++;
          }
                l1=tl1/x;
                p1= tp1/x;

             ttl1=ttl1+l1;
             ttp1=ttp1+p1;
            y++;
   }
sonl1=ttl1/y;
// average reading in 10 cycles of package
sonp1=ttp1/y;

 pot=A_pot+(B1_pot*sonp1
  lvdt=A_lvdt+(B1_lvdt*sonl1 )
 }
```

C.4 for package deformation

```
#include <stdio.h>
#include <conio.h>
#include <dos.h>
#include <math.h>
#define SOC      0x300   /* start of
conversion*/
#define SOCM   0x302   /* start of conversion
for motor speed*/
#define AD1    0x301   /* Port address of first
A/D for POT*/
#define AD2    0x306   /* Port address of
second A/D for LVD*/

#define A_lvdt  22.81
#define B1_lvdt  0.29
```

```
#define A_pot  25.4
#define B1_pot  0.28

int loop;
float x,y,p,lv,tp1,tl1,ttl1,ttp1;
float p1,l1,lvdt,pot,sonl1,sonp1,tdeformation;
void  main()
  {
    outportb(SOCM,50); // adjust the speed of
motor
    clrscr();
     tdeformation=0;
     loop=0;
   while(loop<10){
         y=0;
         ttp1=0;
         ttl1=0;
         while(y<5){
         x=0;
         tp1=0;
         tl1=0;
         while(inportb(773)!=0);
          while(inportb(773)!=255){
                  outportb ( SOC, 0 ) ;
                  delay(1) ;
                  p=inportb ( AD1 ) ;
                  lv=inportb ( AD2 ) ;
                  tp1=tp1+p;
                  tl1=tl1+lv;
                  x++;
           }

                  l1=tl1/x;
                  p1= tp1/x;

              ttl1=ttl1+l1;
              ttp1=ttp1+p1;

             y++;
    }

 sonl1=ttl1/y;
 // average reading in 20 cycles of package
 sonp1=ttp1/y;
           lvdt=A_lvdt+(B1_lvdt*sonl1 );
           pot=A_pot+(B1_pot*sonp1 );

           printf("lvdt-radi : %.1f\t ",lvdt);
           printf("pot-radi : %.1f\t",pot);
           printf("Deformation: %.2f\n",pot-
lvdt);
  tdeformation=tdeformation+(pot-lvdt);
     loop++;
   }
 printf("\n\n Average deformation= %.2f\n
",tdeformation/10);
 getch();
 }
```

C.5 Eliminating a false reading at the absolute shaft encoder

C.5.1 The way of creating two loop

```
#include<stdio.h>
#include<conio.h>
#include <stdlib.h>
#include <dos.h>

#define SOCM    0x302   /* start of conversion
for motor speed  */

 int l=0;

void main()
{
outportb(SOCM,255);
// adjust the speed of motor

 while(l<500){
          do{
          while( inportb(772) != 0 );
           }while(inportb(772) !=0 );

          do{
          while( inportb(772) == 0 );
           }while(inportb(772) ==0 );

 printf (" %d , revolution\n");
                                }
 }
```

C.5.2 The way of comparing four reading

```
#include<stdio.h>
#include<conio.h>
#include <stdlib.h>
#include <dos.h>

  int read[3];
  int i,r;
  int top;

void main()
{
 while(l<500){
          again:
          for( r=0 ; r<3 ; r++){
          read[r]=inportb(772);
                              }
if ( read[0]==read[1] && read[2]==read[3] &&
read[0]==read[2] ) goto okey;
          else goto again;

okey:
if ( read[0] != 0 ) goto again;
```

```
do{
   while( inportb(772) == 0 );
   }while(inportb(772) ==0 );

  }
}
```

C.6 for ADT diagram

```
//This program for finding the beginnig of the
double traverse and
// read top shaft encoder, show it on the screen
and save it on the file.

#include<stdio.h>
#include<conio.h>
#include<graphics.h>
#include <stdlib.h>
#include <dos.h>
#include <math.h>

#define SOC      0x300   /* start of conversion
768=0x300*/
#define SOCM   0x302   /* start of conversion
for motor speed  */
#define AD1    0x301   /* Port address of first
A/D 769=0x301 */
#define AD2    0x306   /* Port address of
second A/D  774=0x306 */
#define A  22.81
#define B1  0.29

FILE    *fptr ;

 int gdriver = DETECT, gmode, errorcode;

 int top,k=0,y=0,l=0,i;
 int huge topfile[20000L];
 float huge w_ratio[20000L];
 float huge dia[20000L];
 float x,p,lv;  //for diameter
 float w,p1,l1,tp1,tl1; // for diameter
 float lvdt,lvdt_dia;
 float pot,pot_dia;

void grafik(),plot(),diameter();

void main()
{
        outportb(SOCM,255); // adjust the
speed of motor

        grafik();
        plot();

 while(y<20000){
        l=0;
        while(l<500){
diameter();
        do{
        while( inportb(772) != 0 );
          }while(inportb(772) !=0 );
        do{
        while( inportb(772) == 0 );
         }while(inportb(772) ==0 );
 if (k == 0 )  {
            top=inportb(773);
            topfile[y]=top;
            line(l,top*1.5,l,top*1.5);
            dia[y]=lvdt_dia;
            w_ratio[y]=w;
            y++;
            l++;
          }
             k++;
    if  ( k == 3 )  k=0;
                  }

        clearviewport();
        }

    getch();
    closegraph();

 //to write to the file
fptr = fopen( "ADTtum.txt" , "w") ;
for ( i=0 ; i<y ; i++ )fprintf ( fptr , "%d %d %.3f
%.2f \n" ,i, topfile[i],w_ratio[i],dia[i]) ;
        fclose ( fptr ) ;
  }

void diameter()
 {
    tl1=0;
        for(x=0 ; x<10 ;x++ ){
                outportb ( SOC, 0 ) ;
                delay(1) ;
                lv=inportb ( AD2 ) ;
                tl1=tl1+lv;
                }

                l1=tl1/10;
                lvdt=A+(B1*l1 );
        //w=(k*D/d); k:3 D:90 mm d=2*lvdt
                w=(270/(2*lvdt));
                lvdt_dia=(lvdt*2);

                gotoxy(1,1);
                printf("d=%.2f ",lvdt_dia);
                gotoxy(1,3);
                printf("w=%.3f",w);
                gotoxy(1,24);
                printf("No.DT:%d",y);
                // No. Dt - The number of
 double traverse

  }
```

```
void  grafik()
 {
  #define CLIP_ON 1   /* activates clipping in
  /* initialize graphics and local variables */
  initgraph(&gdriver, &gmode,
"c:\\borlandc\\bgi");

  /* read result of initialization */
  errorcode = graphresult();
  if (errorcode != grOk)  /* an error occurred */
  {
    printf("Graphics error: %s\n",
grapherrormsg(errorcode));
    printf("Press any key to halt:");
    getch();
    exit(1); /* terminate with an error code */
 }
}
void plot()
 {       setcolor(CYAN);
         rectangle(116,0,620,388);

         setcolor(YELLOW);
         outtextxy ( 110,386 , "-" ) ;
         outtextxy ( 110,290 , "-" ) ;
         outtextxy ( 110,194 , "-" ) ;
         outtextxy ( 110,98 , "-" ) ;
         outtextxy ( 110, 2 , "-" ) ;
         outtextxy ( 80, 386 , "360" ) ;
         outtextxy ( 80, 290 , "270" ) ;
         outtextxy ( 80, 194 , "180" ) ;
         outtextxy ( 80, 98 , "90" ) ;
         outtextxy ( 80, 2 , "0" ) ;

         outtextxy ( 118,400 , "|" ) ;
         outtextxy ( 218,400 , "|" ) ;
         outtextxy ( 318,400 , "|" ) ;
         outtextxy ( 418,400 , "|" ) ;
         outtextxy ( 518,400 , "|" ) ;
         outtextxy ( 618,400 , "|" ) ;
         //outtextxy ( x1+593, y2 , "|" ) ;
         outtextxy ( 118,415 , "0" ) ;
         outtextxy ( 218,415 , "100" ) ;
         outtextxy ( 318,415 , "200" ) ;
         outtextxy ( 418,415 , "300" ) ;
         outtextxy ( 518,415 , "400" ) ;
         outtextxy ( 600,415 , "500" ) ;
         //outtextxy ( x1+570, y2+15 , "600" ) ;

         setcolor(YELLOW);
         moveto(20,100);
         settextstyle(SANS_SERIF_FONT,VE
RT_DIR,1) ;
         outtext("The yarn position on the
package") ;
         moveto(250,450);
         settextstyle(SANS_SERIF_FONT,HORIZ_DIR
,1) ;
outtext(" Double traverse") ;

setviewport(118, 2, 618, 386, CLIP_ON);
 }
```

C.7 The basic program for disturbing the drum speed

```
#include <dos.h>
#include <conio.h>
#include <stdio.h>
# define  soc 0x302 // decimal 770

int x,y;
void main()
{
    clrscr();
    while (1){
            outportb(soc,255);
            delay(20000);

        for(x=0; x<221; x+=10){

    ourtportb(soc,255-x);
            delay(100);
                                          }
        ourtport(soc,35);
        delay(10000);

        for(x=0; x<221 ; x+=10);

    ourtport(soc,35+x);
            delay(500);
       }
```

C.8 All programme for disturbing the drum speed

```
#include<stdio.h>
#include<conio.h>
#include<graphics.h>
#include <stdlib.h>
#include <dos.h>
#include <math.h>

#define SOC 0x300   /* start of conversion
768=0x300*/
#define SOCM        0x302  /* start of
conversion for motor speed  */
#define AD1   0x301   /* Port address of
first A/D 769=0x301 */
#define AD2   0x306   /* Port address of
second A/D  774=0x306 */
#define A  22.81
#define B1  0.29
```

```
#define high_speed  255
#define low_speed   100

FILE          *fptr ;

 int gdriver = DETECT, gmode, errorcode;

 int
top,k=0,y=0,l=0,i,stepforlow_speed,stepfor
high_speed,vary[4],rib=0,v;
 int huge topfile[17000L];
 float huge w_ratio[17000L];
 float huge dia[17000L];
 float x,lv,w,l1,tl1,d;  //for diameter
 float p; // for follow the package arm
 float lvdt,lvdt_dia;

void
grafik(),plot(),diameter(),check_position_ar
m();
void ribboning(),lift(),back();

void main()
{
     outportb(SOCM,255);
// adjust the speed of motor

     grafik();
     plot();

 while(y<17000){
 //while(y<1000){
      l=0;
      while(l<500){
                diameter();


 //to find the beginning of Double Traverse
     do{
     while( inportb(772) == 0 );
       }while(inportb(772) ==0 );

    if (k == 0 )  {
 topfile[y]=inportb(773);

line(l,topfile[y]*1.5,l,topfile[y]*1.5);
                              dia[y]=lvdt_dia;
                              w_ratio[y]=w;
                              if ( rib==0 )
ribboning();

                              y++;
                              l++;
                    }
          k++;
          if  ( k == 3 )  k=0;

//duration as the package has high speed
if(rib==3) {
if ( (y-stepforhigh_speed) > 10 )
     rib=0;
       }

// duration of lower speed
if(rib==2) {
 if ( (y-stepforlow_speed) > 12 ){
     outportb(770,high_speed);
     stepforhigh_speed=y;
     rib=3;
       }
  }

// start low speed
if ( rib==1 ) { outportb(770,low_speed);
          stepforlow_speed=y;
          rib=2;
         }

do{
   while( inportb(772) != 0 );
  }while(inportb(772) !=0 );
 }

clearviewport();
}

 outportb(SOCM,0);
 getch();
  closegraph();
//to write to the file

fptr = fopen( "motor1.txt" , "w") ;
for ( i=0 ; i<y ; i++ )
fprintf ( fptr , "%d %d %.3f %.3f \n" ,i,
topfile[i],w_ratio[i],dia[i]) ;
//fprintf ( fptr , "%d %d \n" ,i, topfile[i]) ;
fclose ( fptr ) ;
}

void ribboning()
  {
if (topfile[y] < topfile[y-1] )
vary[0]=(256-topfile[y-1])+topfile[y];
     else   vary[0]=topfile[y]-topfile[y-1];

if (topfile[y] < topfile[y-2] )
vary[1]=(256-topfile[y-2])+topfile[y];
     else   vary[1]=topfile[y]-topfile[y-2];

 if (topfile[y] < topfile[y-3] )
vary[2]=(256-topfile[y-3])+topfile[y];
     else   vary[2]=topfile[y]-topfile[y-3];

if (topfile[y] < topfile[y-4] )
vary[3]=(256-topfile[y-4])+topfile[y];
     else   vary[3]=topfile[y]-topfile[y-4];
```

```
    for(v=0;v<4;v++){
    if (vary[v]<10 || vary[v] >245)  rib=1;
// rib=1 means that ribboning is occured
    }
 }



void diameter()
 {
    tl1=0;
    for(x=0 ; x<10 ;x++ ){
              outportb ( SOC, 0 ) ;
              delay(1) ;
              lv=inportb ( AD2 ) ;
              tl1=tl1+lv;

              }

              l1=tl1/10;
              lvdt=A+(B1*l1 );
    //w=(k*D/d); k:3 D:90 mm d=2*lvdt
              w=(270/(2*lvdt));
              lvdt_dia=(lvdt*2);
              gotoxy(1,1);
              printf("d=%.2f ",lvdt_dia);
              gotoxy(1,3);
              printf("w=%.3f",w);
              gotoxy(1,24);
              printf("No.DT:%d",y);
              // No. Dt - The number of
double traverse
}


void  grafik()
 {
  #define CLIP_ON 1   /* activates
clipping in
  /* initialize graphics and local variables
*/
  initgraph(&gdriver, &gmode,
"c:\\borlandc\\bgi");

  /* read result of initialization */
  errorcode = graphresult();
  if (errorcode != grOk)  /* an error
occurred */
  {
    printf("Graphics error: %s\n",
grapherrormsg(errorcode));
    printf("Press any key to halt:");
    getch();
    exit(1); /* terminate with an error code
*/
 }
}
void plot()
 {          setcolor(CYAN);
    rectangle(116,0,620,388);

    setcolor(YELLOW);
    outtextxy ( 110,386 , "-" ) ;
    outtextxy ( 110,290 , "-" ) ;
    outtextxy ( 110,194 , "-" ) ;
    outtextxy ( 110,98 , "-" ) ;
    outtextxy ( 110, 2 , "-" ) ;
    outtextxy ( 80, 386 , "360" ) ;
    outtextxy ( 80, 290 , "270" ) ;
    outtextxy ( 80, 194 , "180" ) ;
    outtextxy ( 80, 98 , "90" ) ;
    outtextxy ( 80, 2 , "0" ) ;

    outtextxy ( 118,400 , "|" ) ;
    outtextxy ( 218,400 , "|" ) ;
    outtextxy ( 318,400 , "|" ) ;
    outtextxy ( 418,400 , "|" ) ;
    outtextxy ( 518,400 , "|" ) ;
    outtextxy ( 618,400 , "|" ) ;
    //outtextxy ( x1+593, y2 , "|" ) ;
    outtextxy ( 118,415 , "0" ) ;
    outtextxy ( 218,415 , "100" ) ;
    outtextxy ( 318,415 , "200" ) ;
    outtextxy ( 418,415 , "300" ) ;
    outtextxy ( 518,415 , "400" ) ;
    outtextxy ( 600,415 , "500" ) ;
    //outtextxy ( x1+570, y2+15 , "600" ) ;

    setcolor(YELLOW);
    moveto(20,100);
    settextstyle(SANS_SERIF_FONT,VE
RT_DIR,1) ;
    outtext("The yarn position on the
package") ;
    moveto(250,450);
    settextstyle(SANS_SERIF_FONT,HO
RIZ_DIR,1) ;
    outtext(" Double traverse") ;

    setviewport(118, 2, 618, 386,
CLIP_ON);
 }
```

C.9 A Programme For Lifting The Package

```
#include<stdio.h>
#include<conio.h>
#include<graphics.h>
#include <stdlib.h>
#include <dos.h>
#include <math.h>

#define SOC 0x300    /* start of conversion
768=0x300*/
#define SOCM         0x302  /* start of
conversion for motor speed  */
```

```
#define AD1    0x301   /* Port address of
first A/D 769=0x301 */
#define AD2    0x306   /* Port address of
second A/D  774=0x306 */
#define A  22.81
#define B1  0.29

FILE          *fptr ;

 int gdriver = DETECT, gmode, errorcode;

int top,k=0,y=0,l=0,i,lift_step,
   vary[4],rib=0,tek,stop_step,
    stop_step1,v;
int huge topfile[17000L];
float huge w_ratio[17000L];
float huge dia[17000L];
float x,lv,w,l1,tl1,d;  //for diameter
float p; // for follow the package arm
float lvdt,lvdt_dia;

//  int topfile[1000];
//  float w_ratio[1000],dia[1000];

void
grafik(),plot(),diameter(),check_position_ar
m();
void ribboning(),lift(),back();

void main()
{
     outportb(SOCM,255); // adjust the
speed of motor

     grafik();
     plot();

 while(y<17000){
 //while(y<1000){
      l=0;
      while(l<500){
              diameter();
                 if ( rib ==0 )
check_position_arm();

//to find the beginning of Double Traverse
      do{
      while( inportb(772) == 0 );
        }while(inportb(772) ==0 );
    if (k == 0 )  {

topfile[y]=inportb(773);

line(l,topfile[y]*1.5,l,topfile[y]*1.5);
                          dia[y]=lvdt_dia;
                          w_ratio[y]=w;
                          if ( rib==0 )
ribboning();
                                y++;
                                l++;
                    }
          k++;
      if  ( k == 3 )  k=0;
/duration as the package lifted

if(rib==3) {  if ( (y-stop_step) > 8 )
     rib=4;
       }
// duration of lifting the package

if(rib==2) {   if ( (y-lift_step) > 3 ){
     outportb(771,4);
     stop_step=y;
     rib=3;
              }
  }

// start lifting
if ( rib==1 ) { outportb(771,0);
          lift_step=y;
          rib=2;
          //getch();
         }

//duration of package when it is back on the
drum
if(rib==6) {  if ( (y-stop_step1) > 5 )
     rib=0;
       }

// duration of moving back the package
until switch is off
     if ( rib==5 ){
     outportb ( SOC, 0 ) ;
     delay(1) ;
  if ( inportb ( AD1 ) !=0 ){

     outportb(771,12);
     stop_step1=y;
     rib=6;
               }
             }
 // start moving back the package
 if ( rib==4 ) { outportb(771,8);
               rib=5;
                 }

     do{
       while( inportb(772) != 0 );
      }while(inportb(772) !=0 );
     }

     clearviewport();
     }

     outportb(771,8);
```

```
        outportb ( SOC, 0 ) ;
        delay(1) ;
        p=inportb ( AD1 );
        while(p ==0 ){
        outportb ( SOC, 0 ) ;
                delay(1) ;
        p=inportb ( AD1 );
                }

        outportb(771,12);
        outportb(SOCM,0);
        getch();
        closegraph();

       //to write to the file

    fptr = fopen( "lift.txt" , "w") ;
    for ( i=0 ; i<y ; i++ )
fprintf ( fptr , "%d %d %.3f %.3f \n" ,i,
topfile[i],w_ratio[i],dia[i]) ;
//fprintf ( fptr , "%d %d \n" ,i, topfile[i]) ;
        fclose ( fptr ) ;
      }
void check_position_arm()
     {
        outportb ( SOC, 0 ) ;
        delay(1) ;
    if (inportb ( AD1 )!=0)  outportb(771,0);
        else  outportb(771,4);
     }

    void ribboning()
     {
       if (topfile[y] < topfile[y-1] )
    vary[0]=(256-topfile[y-1])+topfile[y];
        else  vary[0]=topfile[y]-topfile[y-1];

        if (topfile[y] < topfile[y-2] )
    vary[1]=(256-topfile[y-2])+topfile[y];
        else  vary[1]=topfile[y]-topfile[y-2];

        if (topfile[y] < topfile[y-3] )
    vary[2]=(256-topfile[y-3])+topfile[y];
        else  vary[2]=topfile[y]-topfile[y-3];

        if (topfile[y] < topfile[y-4] )
    vary[3]=(256-topfile[y-4])+topfile[y];
        else  vary[3]=topfile[y]-topfile[y-4];

        for(v=0;v<4;v++){
        if (vary[v]<10 || vary[v] >245)  rib=1;
    // rib=1 means that ribboning is occured
        }
     }
```

```
void diameter()
 {
    tl1=0;
    for(x=0 ; x<10 ;x++ ){
            outportb ( SOC, 0 ) ;
            delay(1) ;
            lv=inportb ( AD2 ) ;
            tl1=tl1+lv;

            }

            l1=tl1/10;
            lvdt=A+(B1*l1 );
    //w=(k*D/d); k:3 D:90 mm d=2*lvdt
            w=(270/(2*lvdt));
            lvdt_dia=(lvdt*2);
            gotoxy(1,1);
            printf("d=%.2f ",lvdt_dia);
            gotoxy(1,3);
            printf("w=%.3f",w);
            gotoxy(1,24);
            printf("No.DT:%d",y);
// No. Dt - The number of double traverse

  }


void  grafik()
 {
  #define CLIP_ON 1   /* activates
clipping in
  /* initialize graphics and local variables
*/
  initgraph(&gdriver, &gmode,
"c:\\borlandc\\bgi");

  /* read result of initialization */
  errorcode = graphresult();
  if (errorcode != grOk)  /* an error
occurred */
  {
    printf("Graphics error: %s\n",
grapherrormsg(errorcode));
    printf("Press any key to halt:");
    getch();
    exit(1); /* terminate with an error code
*/
 }
}
void plot()
 {          setcolor(CYAN);
    rectangle(116,0,620,388);

    setcolor(YELLOW);
    outtextxy ( 110,386 , "-" ) ;
    outtextxy ( 110,290 , "-" ) ;
    outtextxy ( 110,194 , "-" ) ;
    outtextxy ( 110,98 , "-" ) ;
    outtextxy ( 110, 2 , "-" ) ;
```

```
        outtextxy ( 80, 386 , "360" ) ;
        outtextxy ( 80, 290 , "270" ) ;
        outtextxy ( 80, 194 , "180" ) ;
        outtextxy ( 80, 98 , "90" ) ;
        outtextxy ( 80, 2 , "0" ) ;

        outtextxy ( 118,400 , "|" ) ;
        outtextxy ( 218,400 , "|" ) ;
        outtextxy ( 318,400 , "|" ) ;
        outtextxy ( 418,400 , "|" ) ;
        outtextxy ( 518,400 , "|" ) ;
        outtextxy ( 618,400 , "|" ) ;
        //outtextxy ( x1+593, y2 , "|" ) ;
        outtextxy ( 118,415 , "0" ) ;
        outtextxy ( 218,415 , "100" ) ;
        outtextxy ( 318,415 , "200" ) ;
        outtextxy ( 418,415 , "300" ) ;
        outtextxy ( 518,415 , "400" ) ;
        outtextxy ( 600,415 , "500" ) ;
        //outtextxy ( x1+570, y2+15 , "600" ) ;

        setcolor(YELLOW);
        moveto(20,100);
        settextstyle(SANS_SERIF_FONT,VE
    RT_DIR,1) ;
        outtext("The yarn position on the
    package") ;
        moveto(250,450);
        settextstyle(SANS_SERIF_FONT,HO
    RIZ_DIR,1) ;
        outtext(" Double traverse") ;

        setviewport(118, 2, 618, 386,
    CLIP_ON);
     }
```

C.10 For Package performance analyser

C.10.1 Read tension from tension probe

```
#include<stdio.h>
#include<conio.h>
#include<time.h>
#include<dos.h>

#define SOC     0x300           /*  start  of
conversion*/
#define SOCM    0x302   /* start of conversion
for motor speed*/
#define AD1     0x301   /* Port address of first
A/D*/
#define AD2     0x306     /* Port address of
second A/D*/

FILE    *package ;

int x,y,z;
int ppa; // first -row   second- col
float sec;
void main()
{
outportb(SOCM,200);
// adjust the speed of motor
clrscr();
printf(".....PRESS ANY KEY WHEN
READY.....");
getch();
outportb(SOCM,200); // adjust the speed of
motor
clrscr();
printf("  .....PROGRAM IN PROGRESS
.....");
package = fopen( "c:\\ppa.txt" , "w") ;
 //        for(y=0;y<75;y++){
          for(y=0;y<2;y++){
          for(x=0;x<20000;x++){
                    outportb ( SOC, 0 ) ;
                    delay(1) ;
                    ppa=inportb ( AD2 ) ;
          fprintf ( package , "%d \n" ,ppa) ;
                                        }
                                  }
printf(  "\n\n  .....PROGRAM IS ENDED
..... \n",sec);
          fclose ( package ) ;
          getch();
     }
```

C.10.2 Analyses PPA data

```
#include<stdio.h>
#include<stdlib.h>
#include<io.h>
#include<conio.h>
 int x,y,i,k;
 int data[256];
 int max=0,min=256;
 FILE    *fptr ;

 void main()
 {
clrscr() ;
if(  (fptr = fopen ("c:\\ppa.txt", "r" ))==NULL ){
               printf("Error opening file\n");
               exit(1);
               }
//        for(y=0;y<75;y++){
          for(y=0;y<2;y++){

          for(x=0;x<20000;x++){
           fscanf ( fptr , "%d" , &k ) ;
          data[k]++;
          if ( max<k ) max=k;
          if ( min>k ) min=k;
                    }

                                  }
```

```
for ( i = 0 ; i < 256 ; i++ )
          {
printf ( "%d - %u : " ,i,data[i] ) ;
          }
printf("\n   MAX=   %d            MIN=   %d
",max,min);

 getch();
if(   (fptr = fopen ("c:\\ppa_analyses.txt", "w"
))==NULL ){
printf("Error opening file\n");
     exit(1);
     }

for ( i=0 ; i<256 ; i++ )
fprintf ( fptr , "%d %u \n" ,i, data[i]) ;
  fclose ( fptr ) ;
  }
```

APPENDIX D

COMPUTER SIMULATION OF RANDOM WOUND PACKAGES

D.1 Computer program for solving the differential equation

A program is written in C language to solve the differential equation developed in Chapter 7 using constant values of E and EY. The symbols used in the program is given an equivalent notation under the section D.1.1.

D.1.1 Notation

T – To, the winding tension in the yarn

sr – the core radius at which the salculation starts

R – the outer radius

E - the modulus of compression of the cheese

EY - the elasticity of yarn in extension

S - the core radius

D - the diameter of yarn

RO - the outer radius of the cheese

dR - the radial thickness of the element

dr - the original radial thickness of the element

angle - the chosen element angle

cdu - $\partial u/\partial r$ at R. Its value is available from the boundary condition.

sdu – the guess or estimation of the value of $\partial u/\partial r$ at the core radius s.

du - $\partial u/\partial r$

d2u - $\partial^2 u/\partial^2 r$

au, asu – the values of u and U at the mid radius of a layer and obtain by averaging the values of these at the two end radii of the layer.

Su – U

c – a small number to specify the permissible difference between two successive values of u at a given r.

d – a small number to specify the permissible difference between the values of $\partial u/\partial r$ at r=R and cdu

Z - $(\partial Z/\partial r)dR=z$

PZ - An array for z

g – a small number used to vary the estimated value of $\partial u/\partial r$ at s.

C,C1,D1 – used in the formula to interpolate the value of sdu from the values of $\partial u/\partial r$ at r=R and r=s of the last two solution.

k – a counter to number the steps of r or layers with r.

p – a counter used in conjunction with 'h' or 'k' or both to call the value of a variable at any r.

ct – a counter to count the number of repetitions of calculation for one step or r.

h – a counter to count and number the steps of R.

l – a counter to count the number of times the calculation is repeated to solve the equation for the addition of a layer at R.

ZR – Zo

QR – Qo

pr – $(\partial p/\partial r)dR=p$

SAZ - $\int_r^R \frac{\partial Z}{\partial R} dR$

Sq - $\int_r^R \frac{\partial Q}{\partial R} dR$

St - $\int_r^R \frac{\partial T}{\partial R} dR$

Spr - $\int_r^R \frac{\partial P}{\partial R} dR$

D.1.2 The program structure

A subroutine on the program named trapezium is used to solve the equation from the core radius to the outer radius for one solution due to addition of a layer at R.the equation is integrated with assumed value of du (guessed or interpolated from the results of previous trial solution) at s. From the values of u, du, d2u at the core and the values at the next step of radius are interpolated by Euler's modified method. The values are then averaged repeatedly by the loop labelled 'correction' and the integration moves to the next step of r only when the difference between the two successive values of u at the same radius is small and less than limit set for it. The final values of u, du,

etc. are assigned to T arrays by k. This process of solving the random cheese layer by layer is controlled by the loop labelled ' layer' and allows the calculation to proceed up to r=R.

The loop 'diff press' ensures the correct solution of the equation due to the addition of a layer at R. The value of du at R is compared to cdu, the correct value of du ar r=R according to the boundary condition. If they differ more than permissible difference the program goes back to 'diff press' loop with a new value of du at s.

Final correct solution for variable are transferred from T arrays to P arrays and T arrays are free for next solution.

D 2 Flow chart of simulation program

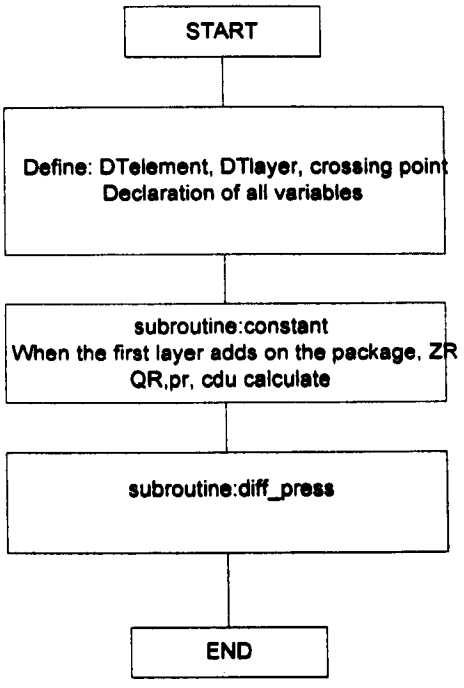

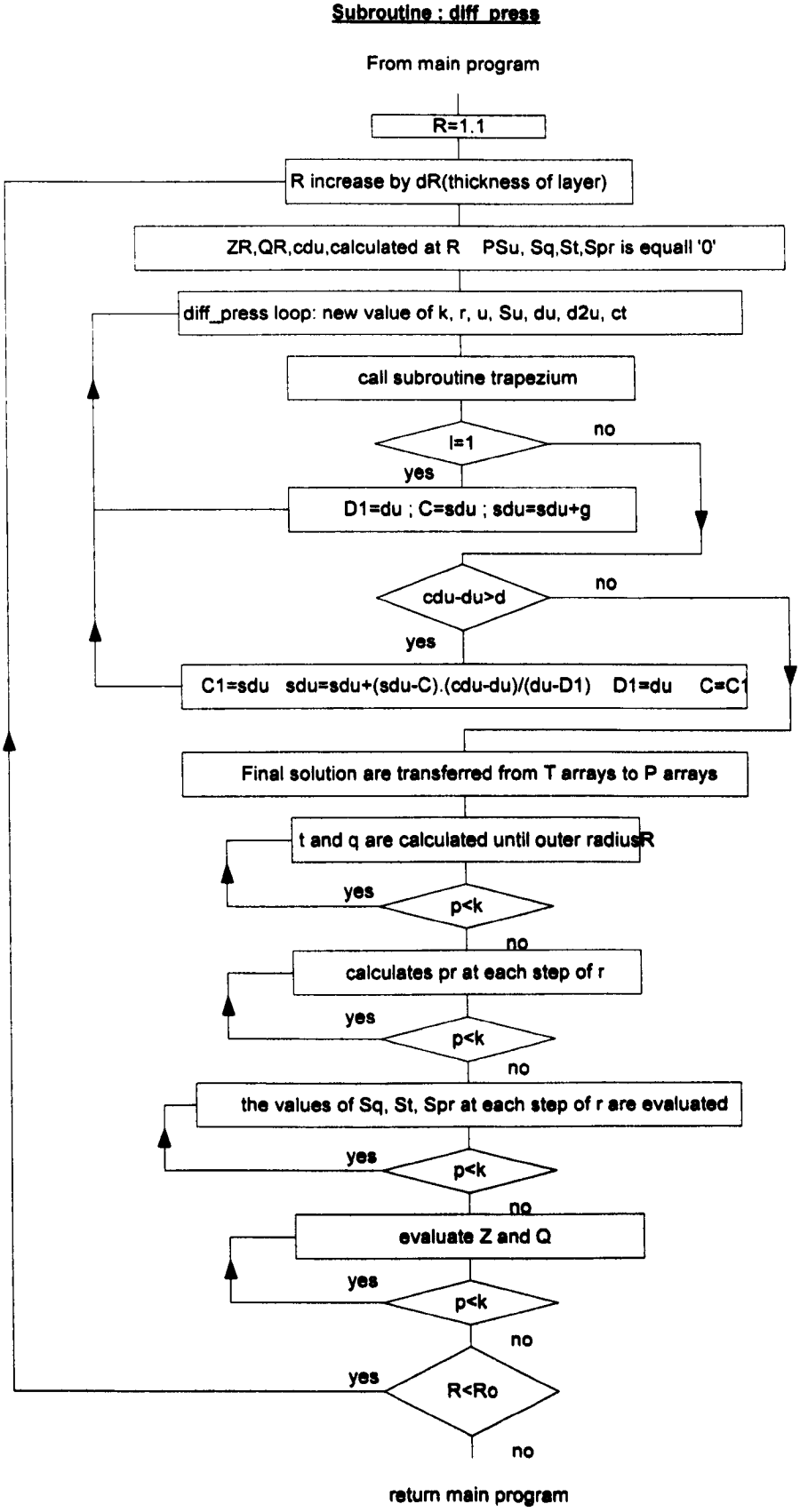
Subroutine : diff_press
From main program
R=1.1
R increase by dR(thickness of layer)
ZR,QR,cdu,calculated at R PSu, Sq,St,Spr is equall '0'
diff_press loop: new value of k, r, u, Su, du, d2u, ct
call subroutine trapezium
l=1
no
yes
D1=du ; C=sdu ; sdu=sdu+g
cdu-du>d
no
yes
C1=sdu sdu=sdu+(sdu-C).(cdu-du)/(du-D1) D1=du C=C1
Final solution are transferred from T arrays to P arrays
t and q are calculated until outer radiusR
yes
p<k
no
calculates pr at each step of r
yes
p<k
no
the values of Sq, St, Spr at each step of r are evaluated
yes
p<k
no
evaluate Z and Q
yes
p<k
no
yes
R<Ro
no
return main program

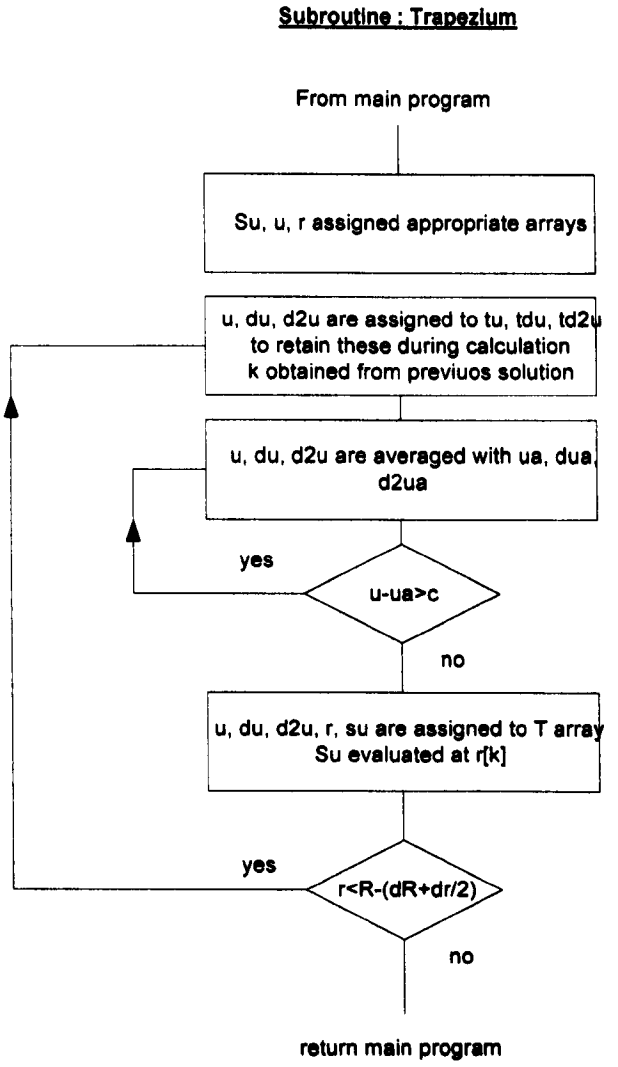

D 3 Computer program

```
// This program numerically calculates the deformation of an elemnet when
 // the the new layer added to the outer radius of random wound packages.

#include <conio.h>
#include <stdio.h>
#include <math.h>
#include <stdlib.h>

#define cosinus 0.959 //cos(16.4)=0.959
#define sinus  0.282 //sin(16.4)=0.282
#define DTelement  127*angle*R*dR
#define DTelement1  127*angle*r*dR
#define DTlayer  127*angle*R*D
#define DTlayer1  127*angle*r*D
#define crossing 2*pow((DTlayer),2)
#define crossing1 2*pow((DTlayer1),2)
```

```
#define diffDTlayer 127*angle*D

        char decision,option;
        int k,p,ct,h,l;
        int  step=15;
        double a,r,R,cdu,u,du,d2u,au,Su,asu,SZ,C,C1,D1,Z,variation1,pocdu,podu,variation;

        //All variables below constant to calculate the deformation of package
        float E=200, T=20, EY=5000, s=1, D=0.05;
        float RO=5, dR=0.1, sr=1, dr=0.1, angle=1;

        float d=0.002, c=0.001,g=0.0001, sdu=-0.013;

        double Tr[50],Pr[50],Tu[50],Pu[50],Tdu[50],Pdu[50],Td2u[50],
        Pd2u[50],TSu[50],PSu[50],Tct[50],Pct[50],ZR[50],QR[50],
        pr[50],q[50],t[50],SAZ[50],Sq[50],St[50],Spr[50],PZ[50];

        void  explanation(),constant(),constant_yaz(), diff_press(), trapezium(),optionsub();

main()
 {
        constant();
        diff_press();
        return(0);
  }

void constant()
 {
  clrscr();

        /* To calculate the constants values       */
        /* First layer added. R becomes s+dR */
        R=s+dR;
        ZR[1]=DTelement*T*sinus;
        QR[1]=DTelement*T*cosinus;
        pr[1]=-DTelement*T*cosinus*angle; //pressure = QR*angle(fi)
        Spr[1]=pr[1];
        cdu=-(DTelement*T*cosinus*angle)/(E*crossing);
 }

void constant_yaz()
 {
         clrscr();
        printf("First layer added. R becomes s+dR\n ");
        printf("ZR= %.2f\t QR = %.2f\t", ZR[1], QR[1]*angle);
        printf("pr = %.2f\n ",pr[1]*angle);
        printf("cdu = %.2f\t R=%.2f\n",cdu,R);
        //getch();
 }

void diff_press()
{
   clrscr();
   optionsub();
   h=1; SAZ[h]=0; Sq[h]=0; St[h]=0;
   for (R=R+dR; R < RO+0.2 ; R+=dR){

         h=h+1;
         ZR[h]=DTelement*T*sinus;
```

```
        QR[h]=DTelement*T*cosinus;
        cdu=-(DTelement*T*cosinus*angle)/(E*crossing);

         PSu[h]=0; SAZ[h]=0; Sq[h]=0; St[h]=0; Spr[h]=0;

        // differeating pressure
l=0;
do {
          k=1; r=sr; u=0; Su=0;    du=sdu; l=l+1; d2u=0; ct=0;

          trapezium();
        if (l==1){
                D1=du;C=sdu;sdu=sdu-g;decision='c'; /*c=continue*/
                 }
                if (cdu<0) pocdu=(-1)*cdu;
                if (du<0) podu=(-1)*du;

         variation=pocdu-podu;
         if ( variation<-0.01 || variation >0.01) {
                // Interpolation
                                C1=sdu;
                                sdu=sdu+double((sdu-C)*(cdu-du))/(du-D1);
                                D1=du; C=C1;   decision='c';
                                }
        else decision='s';/* s=stop*/

   }while(decision=='c');

  /*     transfer from T array to P array   */
    for(p=1;p<k;p++){
          PSu[p]=TSu[p];
          Pu[p]=Tu[p];
          Pr[p]=Tr[p];
          Pdu[p]=Tdu[p];
          Pd2u[p]=Td2u[p];
          Pct[p]=Tct[p];
                    }

// To calculate  z

          Pu[k+1]=0;  Pd2u[k+1]=0;PSu[k+1]=0;  r=sr-dr/2;  SZ=0;  k=0;
          do{
                    r=r+dr;k=k+1;
                    au=(Pu[k+1]+Pu[k])/2;
                    asu=(PSu[k+1]+PSu[k])/2;
                    Z=DTelement1*EY*(au/r)*sinus;
                    SZ=SZ+Z;
                    PZ[k]=Z;
            }while (r<(R-dr));

          /*To calculate t and q in each layer of package*/

           r=sr-dr/2;
           for(p=1; p < k ;p+=1){
                              r=r+dr;
                              au=(Pu[p+1]+Pu[p])/2;
                              t[p]=EY*au/r;
                              q[p]=E*crossing1*(dr/angle)*((Pd2u[p+1]+Pd2u[p])/2);
                             }
```

```
        if (option==1 & abs(R*10)==step){
        //if (option==1 ){
        printf("%.1f\t %.2f\t %.2f\t %.5f\t %.2f\t %.2f\n",R,ZR[h],QR[h]*angle, cdu,);
        step+=5;
                                }

        for(p=1; p < k ;p++){
                        pr[p]=E*crossing1*Pdu[p];
                         }

              if (option==2 & abs(R*10)==step){
              //if (option==2 ){

               for(p=1; p < k ;p++){

        printf("%.1f\t %.1f\t %.5f\t",R,Pr[p],Pu[p]*1000);
        printf("%.5f\t %.5f\t %.5f\t ",Pdu[p]*1000,Pd2u[p]*1000,PSu[p]*1000);
        printf("%.2f\t %.5f\t %.5f\t %.5f\t %.5f\n ",Pct[p],PZ[p],q[p]*angle,t[p],pr[p]*angle);
                        }
                        //getch();
                        printf("\n");step+=5;

                        }


       for(p=1;p<k;p++){

                SAZ[p]=SAZ[p]+PZ[p];
                Sq[p]=Sq[p]+q[p];
                St[p]=St[p]+t[p];
                Spr[p]=Spr[p]+pr[p];
                         }


        // to write the results depend on the selection on the screen

if (option==3 & abs(R*10)==step){
//if (option==3 ){
                printf("%.1f\t %.2f\t %.5f\t %.5f\t",R,Pr[p],SAZ[p],Sq[p]*angle);
                printf("%.5f\t %.5f\n",St[p],Spr[p]*angle);
                                                        }
                                printf("\n"); step+=5;
              }


              if (option==4 & abs(R*10)==step) {
              //if (option==4 ) {
                        for(p=1;p<k;p++){
        printf("%.1f\t %.2f\t",R,Pr[p]);
        printf("%.2f\t %.2f\t",(ZR[p]+SAZ[p]),(QR[p]+Sq[p])*angle);
                                        }
               printf("\n");step+=5;

               }
 }

}
```

```
void trapezium()
{
        double tu,tdu,td2u,ua,dua,d2ua;
        TSu[k]=Su;        Tu[k]=u;Tr[k]=r;  Tdu[k]=du; Td2u[k]=d2u; Tct[k]=ct;
         /* layer:*/
        do {
                        tu=u;  tdu=du;  td2u=d2u;
                        ct=1;   k=k+1;   r=r+dr;
                        u=tu+tdu*dr;
                        Su=PSu[k];
                        du=tdu+td2u*dr;
                        d2u=(DTelement1*(EY*(u/r))*cosinus*(angle/dr))/(E*crossing1);


                /*  corection:*/
                        do {
                                        ct=ct+2;
                                        dua=tdu+(td2u+d2u)*dr/2;
                                        ua=tu+(tdu+dua)*dr/2;
        d2ua=(DTelement1*(EY*(ua/r))*cosinus*(angle/dr))/(E*crossing1);


                                        du=tdu+(td2u+d2ua)*dr/2;
                                        u=tu+(tdu+du)*dr/2;
        d2u=(DTelement1*(EY*(u/r))*cosinus*(angle/dr))/(E*crossing1);

                                variation1=u-ua;
                        }while (variation1>c);
         TSu[k]=PSu[k]+u;
         Tu[k]=u;
         Tr[k]=r;
         Tdu[k]=du;
         Td2u[k]=d2u;
         Tct[k]=ct;

                }while (r < (R-(dR+dr/2)) );
}

        void optionsub()
        {
        option=4;
        if (option==1){  printf("R\t Zo\t Qo\t  cdu\n"); }

        if (option==2){
        printf("R\t r\t u\t du\t d2u\t U\t Pct\t PZ\t q\t t\t pr\n");
        printf("--\t --\t --\t --\t --\t --\t --\t --\t --\t --\n");
                }
        if (option==3){
        printf("R\t r\t SAZ\t Sq\t St\t Spr\n\n");
                }
        if (option==4){
        printf("R\t r\t (ZR+SAZ)\t (QR+Sq)*ang\n\n");
                }
                }
```

Appendix E 1

"The measurement of yarn thickness as applicable to cross wound packages"

P. Bandara, G. Durur

Proceedings of the 3rd International Conference on Novelties in Weaving Research and Technology, September, 23-24, 1999, Maribor, Slovenia, pages 74-82

THE MEASUREMENT OF YARN THICKNESS AS APPLICABLE TO CROSS WOUND YARN PACKAGES

Palitha Bandara, Güngör Durur
School of Textile Industries,
University of Leeds, Leeds LS2 9JT , U.K.

Abstract

In the winding of yarn packages, both the longitudinal elastic modulus and the transverse elastic modulus of the yarn concerned are important. While it is relatively easy to measure the longitudinal modulus, it is more difficult to measure the transverse modulus for yarn to yarn compression. The latter modulus is also dependent on the actual pressure at a yarn intersection.

A yarn thickness tester constructed using a linear eddy current proximity sensor was used to measure the thickness of layers of yarn so placed on the tester as to provide a number of intersecting points. The results of the measurements were used to obtain the relationship of load per intersecting point vs. deformation from which yarn transverse modulus can be determined over a range of loading values.

1. INTRODUCTION

When a cross wound yarn package is formed, a suitable level of tension is maintained in the yarn being wound. This tension causes pressure between adjacent layers of yarn, at points of intersection between them. As further layers are added on, the pressure exerted by one layer on the layer below would increase. The level of pressure at a given layer causes it to be compressed towards the centre, which leads to some loss of yarn tension. This inward layer movement and the radial pressure acting at that layer will be dependent on the elastic moduli of the yarn in its longitudinal and transverse directions.

While the stresses at a given point within a yarn package can be mathematically deduced using certain assumptions [1], modelling the package building process on a computer allows more practical considerations to be taken into account. Precision winding gives a yarn package with certain ideal geometrical properties and is therefore relatively easier to handle. The computer simulation of the winding of such a package has been carried out by many investigators [2].

Random winding is more widely used for producing yarn packages. The variable spacing between adjacent coils causes some greater difficulties in carrying out a computer simulation of the winding process, so as to calculate deformation and the stresses acting on a yarn layer.

A research project to study the random winding process, particularly to investigate methods of active ribbon breaking and their effectiveness is under way at the University of Leeds. A comprehensively instrumented random winder has been constructed for use in the project, and this has enabled the study of the winding process under a variety of conditions. Due to the

instrumentation provided, a number of geometrical and other parameters can be continuously measured during the building of a package. There is hence the additional opportunity to undertake a computer simulation of the winding process, so as to determine those parameters such as pressure and tension of yarns within the package, which cannot be directly measured.

As indicated above the yarn transverse modulus of the yarn is required to be determined, as it has a significant influence in determining how the yarns deform at yarn intersections within the package under the various levels of inter-yarn pressure.

It was decided to construct a simple electronic yarn thickness tester so that this property can be determined for a range of loads.

2. DESCRIPTION OF THE YARN THICKNESS TESTER

The thickness tester was constructed using an inductive proximity sensor [3], which was readily available. The sensor has an associated amplifier module giving a voltage output which varies directly as the distance between the face of the sensor and a steel target placed before it. The sensor used has a measuring range of 2 mm, and this was considered adequate for the purpose.

The tester (Fig. 1) has the proximity sensor mounted on the top surface of a die-cast metal box, chosen for convenience of use and its sufficient rigidity. To prevent the sensitivity of the probe from being reduced by the metal of the housing itself, the sensor was placed at the centre of a 25 mm diameter hole made at the centre of the top surface. This necessitated the adoption of a loading plate 'target', shaped as shown in the figure. The rectangular bearing surfaces on the plate give two equal areas of 10 cm^2 each. The actual area is not of consequence for yarn thickness measurement, but simply the yarn intersections in question should lie within these areas.

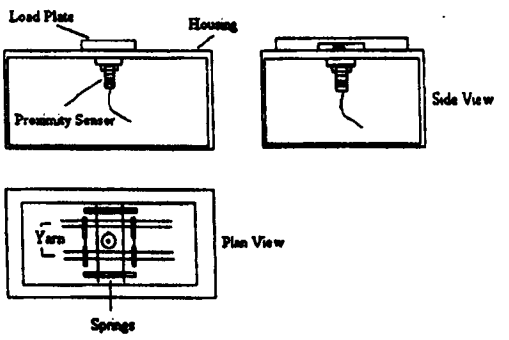

Figure 1 Configuration of the Tester

The output signal voltage is level shifted and amplified so as to give the calibration curve given by Fig. 2. The calibration was carried out using a number of steel shim strips of precise thickness placed under the target plate.

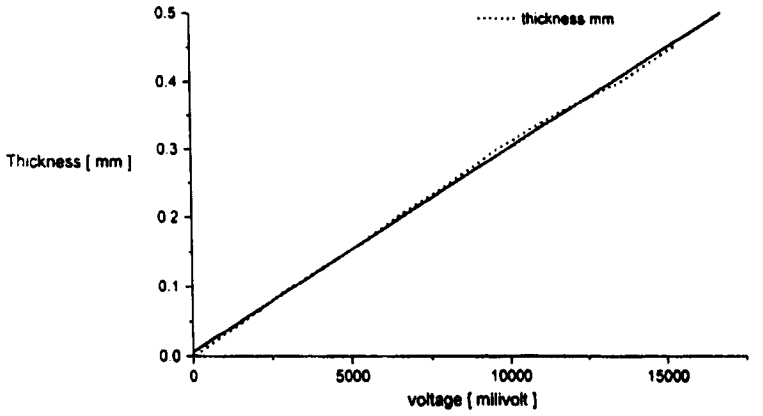

Fig 2 The calibration curve of tester

3. MEASUREMENT OF YARN THICKNESS

In this test, it was necessary to measure the compression of yarn under varying loads and with different numbers of intersecting yarn layers. To ensure a good accuracy in the measurement, it was important to place the yarns sufficiently close to each other with equal spacing between them. Actually the angle between the direction of yarn layers should be equal to that between intersecting yarns in the package which is about 60°. However, 90° was considered not an unrealistic value in the first instance.

The yarns in each layer were placed in the coils of four close coiled springs, placed as shown by Fig. 1 using suitable wire hooks. This ensured an equal and close spacing of yarns in each layer. When pressure is applied using the load plate, the outermost layers of yarn will have contact along their full length on the metal surfaces, whereas those that are held within the layers have yarn that bear on each other at intersections.

Tests were carried out with different numbers of yarn layers placed under the loading plate. It was ensured that there were equal numbers of yarn intersections on each side of the plate. Different numbers of yarn intersections were formed by laying the yarn under a low tension, of which the overall thickness was measured with a digital voltmeter. The measurement was repeated under different loads.

Table 1 gives the results of the testing carried out on a Tex R42/2 worsted yarn. The results were used to obtain the relationship between the thickness of yarn under different pressure levels.

Table 1 Thickness measurements

LOAD (g)	LOAD/POINT (g)	THICKNESS (mm)		
		2 LAYER (t_2)	3 LAYER (t_3)	6 LAYER (t_6)
Number of Intersections = 8				
130.5*	16.32	0.31	0.45	--
155.5	19.44	0.30	0.42	0.86
180.5	22.57	0.29	0.40	0.82
230.5	28.82	0.28	0.37	0.72
280.5	35.07	0.27	0.34	0.66
330.5	41.32	0.26	0.33	0.60
380.5	47.57	0.26	0.31	0.57
430.5	53.82	0.25	0.30	0.54
480.5	60.07	0.25	0.30	0.52
530.5	66.32	0.24	0.29	0.50
580.5	72.57	0.24	0.28	0.49
Number of Intersections = 18				
130.5	7.25	0.34	0.50	--
155.5	8.64	0.33	0.48	--
180.5	10.03	0.32	0.45	--
230.5	12.81	0.31	0.42	0.92
280.5	15.59	0.30	0.39	0.92
330.5	18.36	0.29	0.37	0.85
380.5	21.14	0.28	0.35	0.80
430.5	23.92	0.28	0.33	0.76
480.5	26.70	0.27	0.33	0.73
530.5	29.47	0.27	0.32	0.70
580.5	32.25	0.26	0.32	0.68
Number of Intersections = 32				
130.5	4.08	0.39	0.52	--
155.5	4.86	0.38	0.50	--
180.5	5.64	0.37	0.47	--
230.5	7.20	0.35	0.44	0.96
280.5	8.77	0.34	0.41	0.93
330.5	10.33	0.33	0.38	0.85
380.5	11.89	0.32	0.37	0.81
430.5	13.45	0.31	0.36	0.77
480.5	15.02	0.30	0.35	0.74
530.5	16.58	0.29	0.34	0.71
580.5	18.14	0.29	0.33	0.69

* Note : Weight of Load plate = 130.5 g.

4. RESULTS

On the tester, the outermost yarns of two or more layers placed on the tester contact with the flat metal surfaces on the one side, and make yarn to yarn contact on the other. All yarn in between bear on other yarns lying in a transverse direction. What is basically required is to determine is the thickness of a yarn, when compressed transversely between two similar yarns.

Let x = thickness of an intermediate yarn, and
y = thickness of an outer yarn,

These will be ideally constant for a given level of load

Thus the measured thickness of n layers

$$T = (n-2)x + 2y$$

If t is the measured thickness of n layers then (t-T) is a measure of the error in any one measurement. As the measurement is repeated for a number of values of n, it is possible to calculate $\bar{x}$ and $\bar{y}$, the best estimates of x and y, based on the method of least squares.

For this case it can be shown that, for a given load at each intersection,:

$$\bar{x} = \frac{N\sum_{i=1}^{N} t_i(n_i - 2) - \sum_{i=1}^{N} t_i \sum_{i=1}^{N} (n_i - 2)}{N\sum_{i=1}^{N} (n_i - 2)^2 - \sum_{i=1}^{N} (n_i - 2)\sum_{i=1}^{N} (n_i - 2)}$$

$$\bar{y} = \frac{\sum_{i=1}^{N} t_i}{2N} - \frac{\sum_{i=1}^{N} (n_i - 2)}{2N}\bar{x}$$

where N = Number of 'stacks' tested each with a different value of n

Once $\bar{x}$ is obtained, the transverse elastic modulus E may be defined as follows.

$$E = \frac{\Delta load}{\frac{\Delta \bar{x}}{\bar{x}}}$$

The results of the above calculations, for a range of load values, are given in Table 2 below.

load/point (g)	$\bar{x}$ (mm)	$\bar{y}$ (mm)	$\frac{\Delta\bar{x}}{\bar{x}}$	Δload (g)	E (g)
7.20	0.16	0.16	0.02	1.56	63.90
8.77	0.15	0.15	0.10	1.56	15.27
10.33	0.14	0.15	0.06	1.56	27.73
11.89	0.13	0.14	-0.21	0.92	-4.37
12.81	0.16	0.14	0.23	0.65	2.77
13.45	0.12	0.14	0.05	1.56	28.63
15.02	0.11	0.14	-0.41	0.57	-1.39
15.59	0.16	0.13	0.32	0.99	3.08
16.58	0.11	0.13	0.04	1.56	39.46
18.14	0.10	0.13	-0.40	0.22	-0.55
18.36	0.15	0.13	0.03	1.08	42.52
19.44	0.14	0.15	0.07	1.70	25.91
22.57	0.13	0.14	0.07	1.35	20.74
23.92	0.12	0.12	0.05	2.78	59.29
26.70	0.12	0.12	0.05	2.12	42.49
29.47	0.11	0.12	0.04	2.78	71.02
32.25	0.11	0.12	0.08	2.82	34.27
35.07	0.10	0.13	0.15	6.25	42.76
41.32	0.08	0.13	0.06	6.25	99.89
47.57	0.08	0.12	0.06	6.25	104.49
53.82	0.07	0.12	0.06	6.25	103.46
60.07	0.07	0.12	0.04	6.25	146.15
66.32	0.07	0.12	0.04	6.25	168.55

Table 2 Results of Analysis

$$\bar{x} = -0.00287 + 0.15383e^{\left(\frac{-(load/point-72)}{72.78}\right)}$$

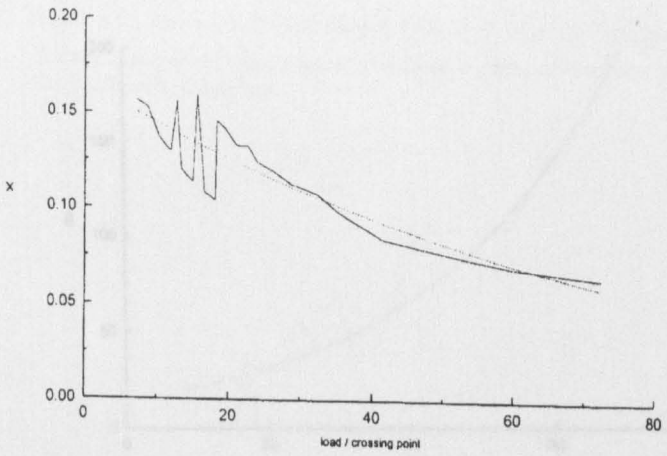

$$\bar{y} = 0.11966 + 0.0362 * e^{\left(\frac{-(load/point-72)}{1184}\right)}$$

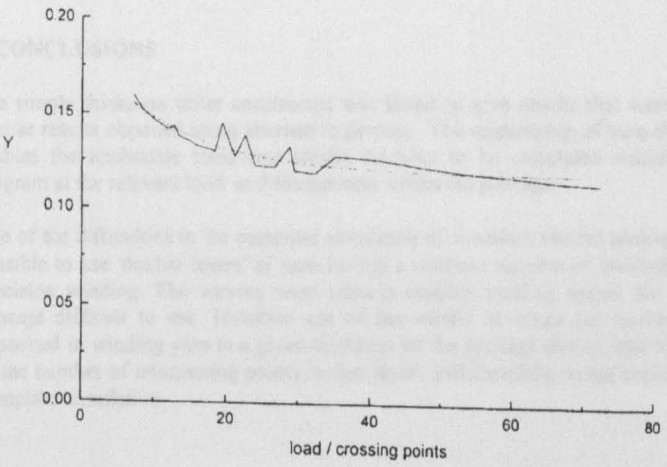

Figure 3 Variation of $\bar{x}$ and $\bar{y}$ with load

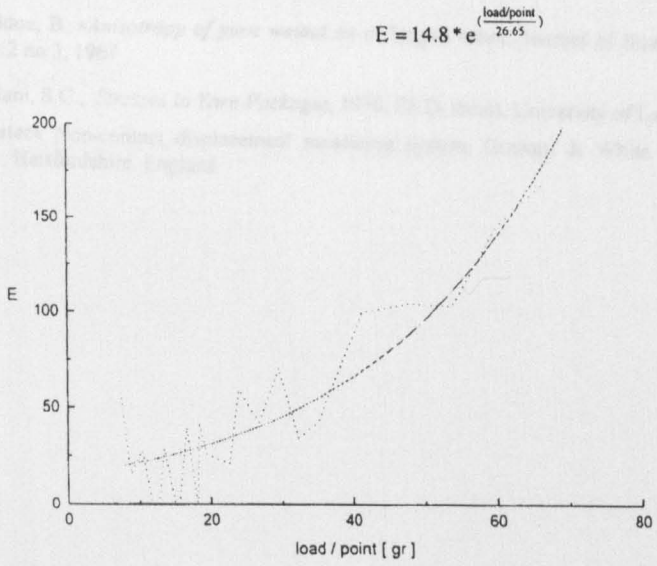

Figure 4 Variation of E with load

5. CONCLUSIONS

The simple thickness tester constructed was found to give results that were agreeable with similar results obtained using alternative devices. The relationship of yarn thickness vs. load enables the applicable transverse elastic modulus to be calculated within the simulation program at the relevant load at different radii within the package.

One of the difficulties in the computer simulation of a random wound package is that it is not possible to use 'double layers' of yarn having a constant number of intersecting points as in precision winding. The varying wind ratio in random winding makes the use of the layer concept difficult to use. However use of the winder to count the number of yarn turns deposited in winding yarn to a given thickness on the package should lead to a determination of the number of intersecting points in that 'layer', and thus help in the implementation of the computer simulation.

6. REFERENCES

[1] Beddoe, B. »*Anisotropy of yarn wound on a flanged tube*«, Journal of Strain Analysis, Vol:2 no:3, 1967

[2] Jhalani, S.C., *Stresses in Yarn Packages*, 1970, Ph.D. thesis, University of Leeds

[3] »Distec« Non-contact displacement measuring system, Graham & White Instruments Ltd., Hertfordshire, England

Dr. P.Bandara , School of Textile Industries, University of Leeds, Leeds LS2 9JT, U.K.
Phone: +44 113 2333786, Fax: +44 113 2333704, e-mail: m.p.u.bandara@leeds.ac.uk

Güngör Durur, Address as above, e-mail: texgd@leeds.ac.uk

Appendix E 2

"Improving the effectiveness of the ribbon breaking in random winding"

P. Bandara, G. Durur

Submitted to 'Mechatronics', Elsevier Sciences Ltd.,

Improving the effectiveness of ribbon breaking in random winding

P. Bandara *, G. Durur

School of Textile Industries, University of Leeds LS2 9JT

Abstract

Ribboning is a basic problem in random winding of yarn packages by the grooved drum method. Several methods of 'ribbon breaking' are used on commercial winders, but their effectiveness is rather limited. 'Active' ribbon breaking can be achieved, under programmed control, by initiating corrective action at times when ribboning actually occurs, thereby providing better unwinding characteristics to the wound package. Unwinding tests carried out on packages prepared by this method confirmed the greater effectiveness of active ribbon breaking.

Keywords: Random winding; Grooved drum; Ribboning; Ribbon breaking; Active ribbon breaking

1.Introduction:

Random winding is widely used for the preparation of yarn packages used in a variety of textile processes such as weaving and knitting. As shown by Fig. 1, on a random winder, the yarn package is rotated by frictional contact with a grooved drum, which also traverses the yarn so as to form a stable cross wound package. The groove has an endless helical formation, so that a complete double traverse of the yarn is provided over an integral number of rotations of the drum. Cylindrical ('cheese') as well as conical packages can be prepared on a random winder, although special provisions are required in winding packages with increased conicity. Due to the frictional drive to the package and the rubbing caused on the yarn by the groove, this type of winder is mainly used for winding spun yarn. However the simplicity of the winder and the fact that a very large proportion of yarns used are of the spun variety has resulted in its widespread use by the textile industry.

Ideally in a cross wound yarn package, the yarn turns should be equally spaced from one another. This promotes better dye penetration when the yarn is dyed in the package form. Also, when the package is subsequently used, yarn can be smoothly withdrawn by pulling it over one end of the package. The withdrawal tension should be small, and uniform from the full package to empty.

The random winder however has one major drawback in that during winding[1], the ratio of the diameter of the yarn package to that of the drum gradually diminishes and passes through several integer values. At these points successive yarn turns are deposited on one another causing a defect known as bunching or ribboning. Where the

* Corresponding author. Tel: +44-113-2333786
E-mail address: m.p.u.bandara@leeds.ac.uk

ratio differs from an integer by such values as 0.5 or 0.33, some minor ribboning can be observed, particularly as the package diameter becomes large.

In addition to causing some deformation of the package shape, ribboning also results in greater resistance to yarn withdrawal at these points. As such all random winders incorporate some means of minimising ribbon formation. All these methods effectively cause some intermittent slippage between the package and the drum, so that yarn turns are dispersed, which discourages ribbon formation. However the moments of applying this 'ribbon breaking' action are not synchronised with moments of ribbon formation and are therefore the ribbon breaking action is, on average, not optimum.

The problem of ribboning in random winding can be avoided in certain types of modern winders, where microprocessor control enables switching of traverse speeds so as to avoid those values of wind ratio that cause ribboning. However these machines cannot offer the convenience or the simplicity of the grooved drum, particularly for the construction of automatic winders suitable for higher winding speeds, and have not displaced the basic machine from popular use.

2. Purpose of the Work:

The work reported in this paper was aimed at realising a grooved drum random winder capable of initiating ribbon breaking action at the precise moments when ribboning takes place, so as to achieve a package with a more even yarn spacing and allow a more uniform unwinding tension[2].

3. Apparatus:

A commercially available random winder was modified as shown by Fig. 2 by the addition of shaft encoders on the grooved drum and the package shaft. Potentiometric sensors were also provided which enable the measurement of the package size as well as the deformation of package radius in contact with the drum.

3.1 Provisions for Ribbon Breaking:

The winder incorporates an intermediate roller in the drive to the package which can be set to disengage the motor for brief periods at a rate of 30 times a minute. This introduces some slippage between the drum and the package which reduces ribbon formation. It was realised that by replacing the standard drive motor by a DC brushless servo motor[3], a more effective speed interruption could be brought about. The method of lifting the yarn package for brief periods several times a minute is another effective ribbon breaking method, so it was decided to equip the experimental winder with such a facility as well. This was achieved by providing an arm, whose position could be controlled by a geared stepper motor. By lifting the arm to the required position, the package spindle could be lifted so that the package is made to leave contact with the drum surface, allowing it to lose some speed. This will briefly reduce the effective wind ratio below the particular value causing ribboning at that point. The period of lift can be controlled so that the package is not excessively slowed down. The procedure can be repeated swiftly, till the ribboning is over.

3.2 Instrumentation

Fig.1 is a schematic diagram of the random winder as modified for use in this work.

Several sensors were added to the winder so as to enable the above characteristics. The shaft encoder on the drum shaft was of the absolute type, and was set so that it gave a 0 reading whenever the yarn was at the left hand end of traverse. For control

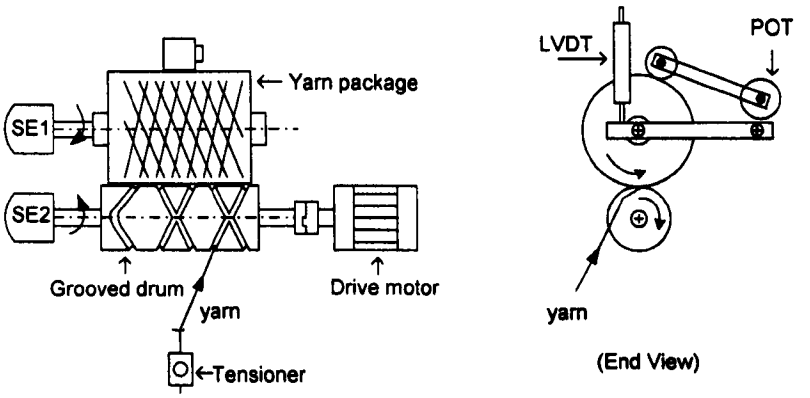

Fig. 1 Configuration of experimental winder

purposes this was considered the start position for a double traverse. An incremental shaft encoder was chosen for use on the package spindle, particularly as it did not need to be absolute, and the greater reliability of the readings provided by it. The pulses from this shaft encoder were fed to a divide by 8 counter to provide an 8-bit reading of shaft position.

As the project also concerned certain aspects of random winding other than ribboning, potentiometric sensors were provided to enable measuring the package diameter during winding, as well as the deformation of the package on the drum.

The DC brushless motor had its own electronic drive, but its speed had to be input as an analogue voltage. This was derived from a D/A converter.

The lifting arm for the package was provided with a microswitch to indicate engagement during a package lift, and disengagement during lowering. It was important to maintain the arm just below the package axis as the package diameter increased, and the switch facilitated control of the stepper motor to enable this action.

All the signals provided by the above sensors were interfaced to a PC (266 MHz processor) through an interface card placed in a PC slot.

In use the switching associated with the DC brushless motor and the PC power supply was found to contaminate the signals. The effect was quite noticeable on the readings provided by the drum shaft encoder. Careful application of standard screening methods achieved satisfactory immunity to electrical noise. Even so, the absolute shaft encoder caused an occasional 'rogue' reading. This was remedied by comparing 4 readings from the shaft encoder each time it was read, and discarding any unacceptable values till all 4 readings were the same. The fact that such spurious reading occurred quite rarely, as

well as the sufficiently high speed of the PC allowed this to be done without causing any limitation to measurements made.
In winding yarn, the tension maintained in the yarn acts as a resistive force to the rotation of the package. It appeared to be useful to introduce additional such resistance, and this was enabled by adding a light pulley to the package shaft, on which a weighted cord could be wrapped so as to impose an adjustable frictional drag.

4. Experimental Work

As the package is driven by frictional contact with the drum, as well as the fact that the package deforms to a small extent over the area of contact, there is kinematically the possibility of some slippage between the two surfaces. The instrumentation provided basically allows some investigation of this slip to be made. Slippage is of particular interest in random winding, as it has an obvious influence on ribboning.

The initial investigations therefore were directed towards measuring such slippage. The compressibility of the package made the precise determination of its diameter a difficult task. However, it was clear that by using a yarn package of constant diameter (i.e. one on which no further yarn is wound), any slippage can be detected by counting the number of revolutions of the package spindle made over a given number of drum revolutions. While this method will not enable an absolute measurement of slip, it can however measure any change of it as parameters such as rotational speed and pressure between the package and drum are changed. The lack of yarn tension can be compensated for by the pulley and cord arrangement indicated above.

5. Results:

The apparatus was first used to study the random winding process. It was quickly realised that by plotting the angular position of the package spindle at every start of a double traverse, an Angle of Double Traverse (ADT) diagram could be constructed on the VDU of the PC which was found to be very useful in following the progress of winding. It was seen that by rotating a yarn package of constant diameter (i.e. a package on which no additional yarn is wound) at the normal running speed, a very regular dot pattern is shown by the ADT (Fig.2). The inclination of the 'lines' depends on the particular wind ratio that corresponds to the package diameter. It was clear that despite the friction drive to the package, the package rotation was quite uniform, with no suggestion of random slipping. However as indicated by the measured diameter of the package and its deformation on the winding drum, a minute slippage of constant magnitude is likely to occur.

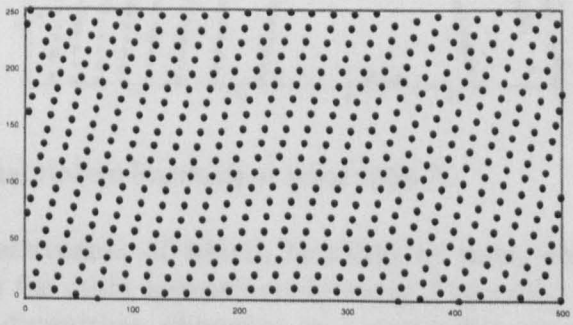

Figure 2 Rotation of constant diameter package with no drag (diameter :80 mm, wind ratio:3.4)

This may be mechanical slippage, or could be the result of the package surface at the point of drive being slightly stretched due to its elasticity[4]. Even with some mechanical drag introduced on package spindle, corresponding to the tension of yarn during winding, the figure remained unchanged.

When winding a package normally i.e. with its diameter gradually increasing, but with ribbon breaking measures disabled, the slope of the lines gradually changes, as shown by Fig. 3.

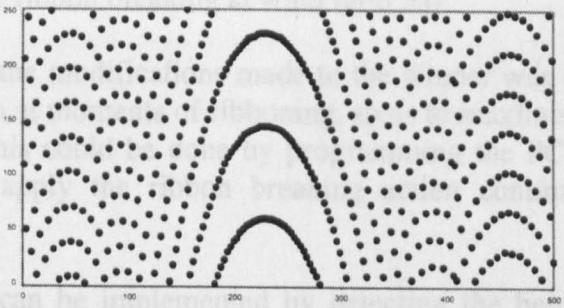

Figure 3 Winding of package at wind ratio 3.3

Depending on the actual value of wind ratio reached, the lines form a single peak or several of them. Where a single peak is seen, the wind ratio has an integer value at that point, where 3 peaks are seen the wind ratio is an integer plus 0.33 etc. When the ratio is an integer, the ribboning that occurs is most undesirable (major ribboning). Ribbon breaking is mostly needed at these intervals. Where the ratio is high, and not an integer, any ribboning (minor ribboning) that occurs quickly passes away. When the wind ratio descends to lower values such as 3 and 2, even minor ribboning persists longer.

It is really the major ribboning that cause significant difficulties with unwinding, and hence those that demand dispersal. The moments of major ribboning can be detected by software, and ribbon breaking can be effected 'actively' as compared with the passive ribbon breaking normally employed.

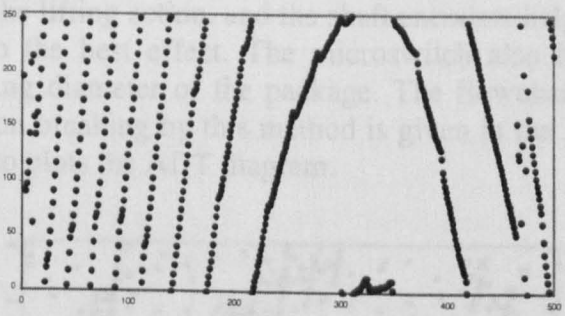

Fig 4. Effect of normal ribbon breaking at wind ratio 3.

Fig. 4 shows the effectiveness of ribbon breaking by using the standard method of disconnecting drive to the drum approximately every 2 seconds, provided on the basic winder. The method diminishes ribboning to a noticeable extent, but some remnant ribboning could be seen on the package.

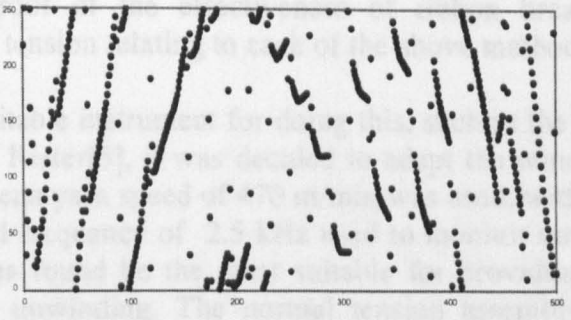

Fig 5. Effect of active ribbon breaking at wind ratio 3.0

The main purpose of the modifications made to the winder was to be able to apply the ribbon breaking action at moments of ribboning, so as to maximise the beneficial effect. As described above this could be done by programming the PC to detect the onset of ribboning, and then apply the ribbon breaking action continuously, till no more ribboning is detected.

Basically this action can be implemented by detecting the beginning of each double traverse, for example at the left hand end of the grooved drum, and checking the corresponding package angular position for coincidence within a small tolerance. This procedure can be extended to detect not only major ribboning as above, but also any minor ribboning as necessary. Each time such ribboning is detected, the programme will initiate the ribbon breaking procedure.

Fig 5 shows the effect of package slippage caused by introducing speed fluctuation of the drive motor itself, which is seen to be superior to the effect produced by the standard procedure provided on the winder.

It was realised however that the most effective method of ribbon breaking is to lift the package at brief intervals during ribboning. This achieved the best ribbon dispersal as shown by Fig. 6. The package lifting arm acted on the hub of the package arm, so as to minutely lift the package off the drum. This action slows the package down, thereby causing the wind ratio to drop below the value causing ribboning. The arm uses a microswitch to sense the lifting action, and the shaft encoders help to control the lift and the duration of lift to the best effect. The microswitch also helps to keep the arm following the increasing diameter of the package. The flowchart of actions that were programmed, for ribbon breaking by this method is given in the Appendix. The routine shown additionally also plots the ADT diagram.

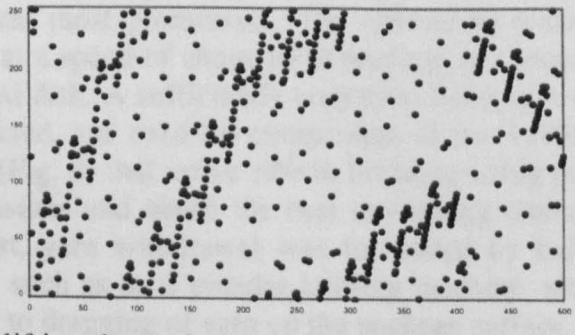

Fig 6. The results of lifting the package at wind ratio:2.

However the best proof of the effectiveness of ribbon breaking is obtained by comparing unwinding tension relating to each of the above method.

In the absence of a suitable instrument for doing this, such as the Package Performance Analyser (PPA) from Rieter[5], it was decided to adapt the winder for the purpose as shown by Fig. 7. A mean yarn speed of 470 m/min was used, with a single yarn tension probe having a natural frequency of 2.5 kHz used to monitor unwinding tension. The leaf spring shown was found be the most suitable for providing a minimum tension level for satisfactory unwinding. The normal tension assembly on the winder was adjusted to a minimum setting. There was bound to be an element of tension fluctuation arising from the fluctuation of yarn speed due to traversing (calculated to be no more than 4.2%), but the effect of this will be relatively small and constant from one test to another and hence unlikely to affect the comparison.

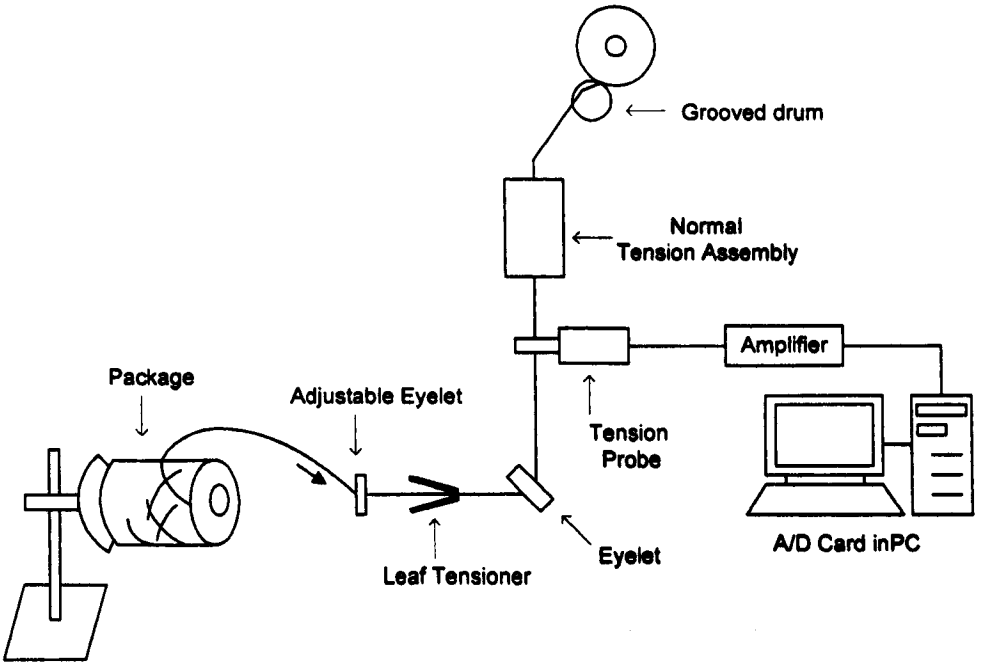

Fig. 7. Apparatus for measuring yarn unwinding tension

A number of packages were wound under the same winding conditions, some with no ribbon breaking, and others using each of the above 3 methods of ribbon breaking. The packages were wound to a diameter of 145 mm at a width of 125 mm, and were unwound under identical conditions as shown in the figure to a diameter of approximately 100 mm. This range of diameters encountered wind ratios of 2.0 and 2.5, at which ribboning was most prominent. The unwinding tension was recorded as a series of 8 bit values at a speed of about 1000 readings per second, generating about 1 M readings on the hard disk. A sufficiently smoothed histogram of tension values from each test was constructed, and used for comparison of the 3 ribbon breaking methods. The results, showed (Fig. 8) that active ribbon breaking using package lifting gave the lowest unwinding tensions and hence the best unwinding characteristics. At the yarn speed used in the test, yarn withdrawal was facilitated by ballooning, but at lower speeds of withdrawal such as on a circular knitting machine, ribboning is likely to be more problematic due to dragging of yarn on the package surface.

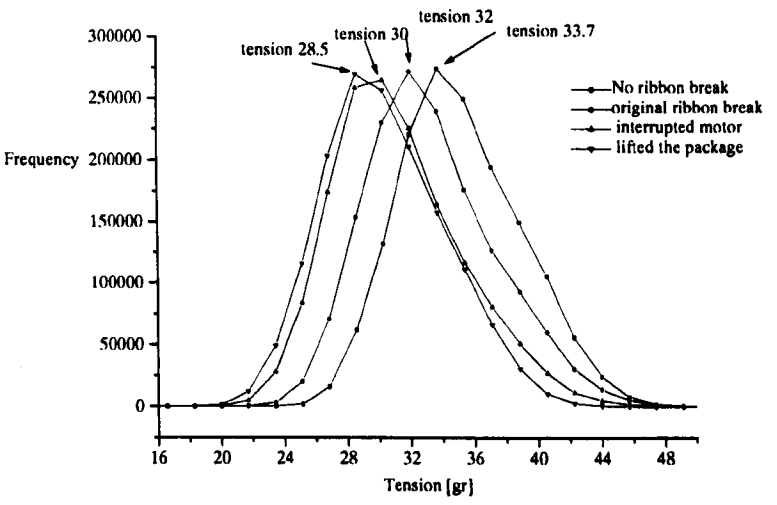

Fig. 8 The results of unwinding yarn tension

6. Conclusions

The ADT diagram is a useful means for studying the random winding process. It showed that no irregular slipping takes place in random winding under normal yarn winding tension settings, despite the indirect (surface) drive to the package employed. It was particularly useful in studying the effectiveness of the 3 ribbon breaking methods studied in this work.

As the standard ribbon breaking measures provided on random winders are applied at constant time intervals, it was felt that 'active' ribbon breaking as described above would prove to be more effective. This was in fact found to be the case by comparing the unwinding tension measured on yarn packages prepared by the different methods.

The standard random winder will continue to be used by the textile industry due to its simplicity and its suitability for use in automatic winders. As the use of microprocessor control has become relatively low in cost, methods such as the one reported here will prove to be useful in producing better random wound yarn packages.

The method of lifting the package minutely off the drum was found to be the most effective for ribbon breaking, when used 'actively' as described. However this method is more difficult to implement due to the increasing package diameter as winding progresses. In this work an arm attached to a geared stepper motor was used to implement the procedure, but a simpler mechatronic solution is desirable.

APPENDIX

Key to Symbols used in flowchart:

k : drum rotations within double traverse (0-2)
y : number of double traverses produced
l : no. of double traverses for diagram (0-500)
rib : variable to indicate stage of ribbon breaking
(0 = no action required)
(1-6 = stages of arm movement)
lift_step, stop_step: time duration of arm movements expressed in double traverses

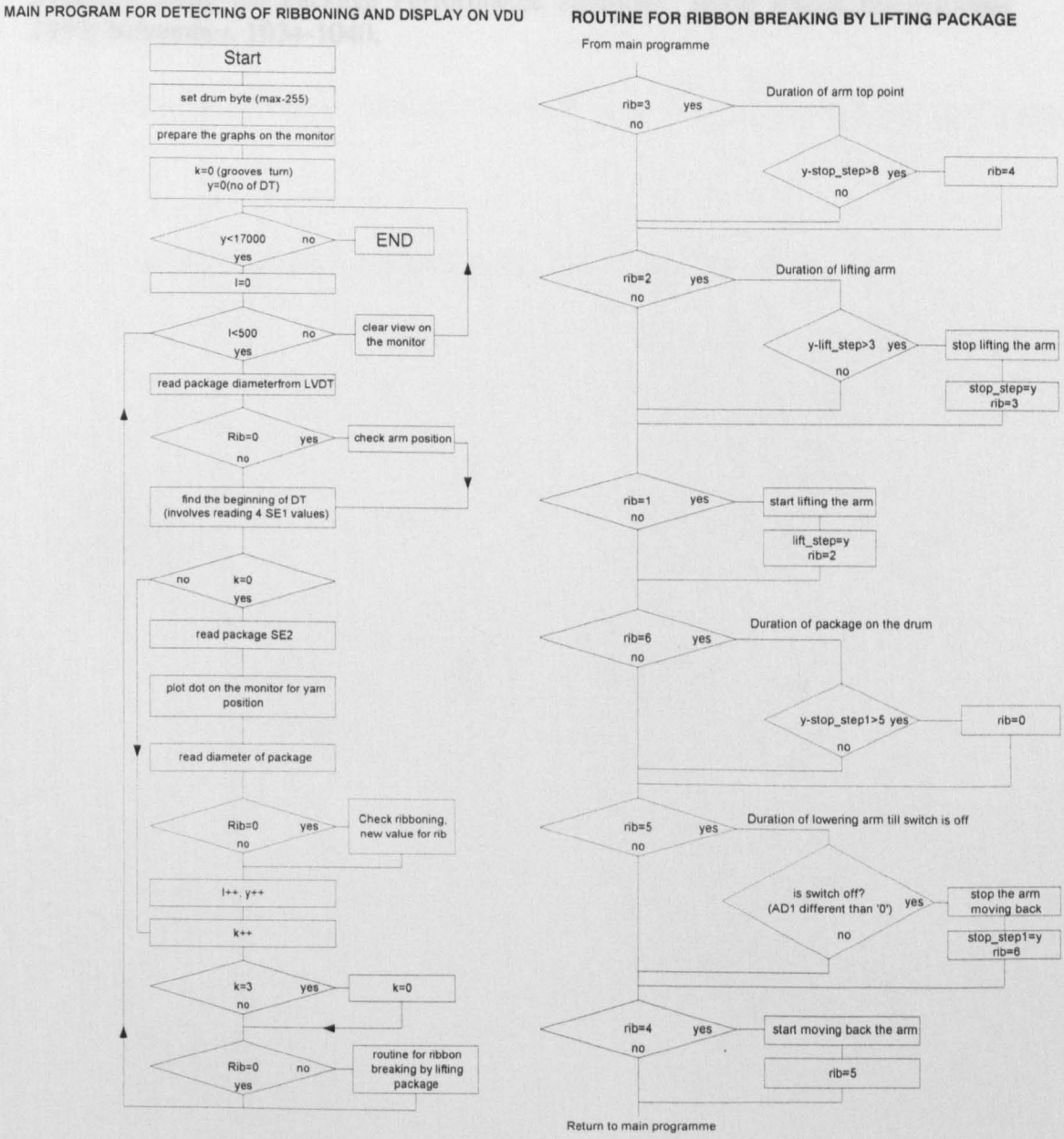

References

[1] Rebsamen, A. Modern Package Building. Textile Asia 1988; September, 130-136.

[2] Durur, G., PhD thesis(In preparation), University of Leeds, U.K., 2000

[3] DC Brushless Motor DM-20 and BRU-200 Servodrive, Electro-Craft Ltd., Fourth Avenue, Crewe, U.K.

[4] Osawa, G. and Koyama, T. On the Slippage between Yarn-Package and Grooved Drum During Winding. Journal of the Textile Machinery Society of Japan, 1972;25(6) T.113-123.

[5] Nobauer, H. and Baumeler, M. Measurement of unwinding resistance of yarn packages using the Package Performance Analyser. Textil Praxis International 1992; November, 1034-1040.

Appendix E 3

"The use of the Angle of Double Traverse diagram to study package formation in random winding and the effectiveness of different techniques of ribbon breaking"

P. Bandara, G. Durur

Paper ID: M2000-156

International Conference 'Mechatronics 2000', 6-8- September 2000, Atlanta, Georgia, USA

(Accepted for presentation and publication in proceedings)

ACTIVE RIBBON BREAKING IN RANDOM WINDING

G. Durur, P. Bandara

School of Textile Industries, University of Leeds, Leeds LS2 9JT, U.K.

Abstract: Ribboning is a basic problem in random winding of yarn packages by the grooved drum method. Several methods of 'ribbon breaking' are used on commercial winders, but their effectiveness is rather limited. 'Active' ribbon breaking can be achieved, under programmed control, by initiating corrective action at times when ribboning actually occurs, thereby providing better unwinding characteristics to the wound package. Unwinding tests carried out on packages prepared by this method confirmed the greater effectiveness of active ribbon breaking.

1. INTRODUCTION

Random winding is widely used for preparing yarn packages required in a variety of textile processes, particularly in weaving and knitting. Such a yarn package normally has the form of a cheese (cylinder) or a cone, and has a single yarn that is cross-wound so as to produce a stable and compact body. In use, the package is held stationary, and the yarn is withdrawn by pulling it over one end of the package. In a well prepared package, the yarn should unwind with a uniform unwinding tension.

On a random winder, shown schematically by Fig. 1, a cylindrical drum with an endless helical groove is used to traverse the yarn over the width of the package, and the package is rotated by contact with the surface of the drum.

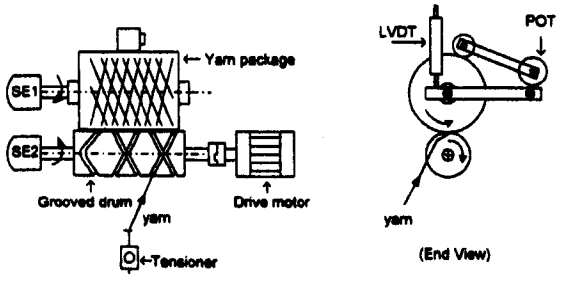

Fig. 1 Configuration of the Apparatus

As the drum is rotated at a constant speed, this ensures a constant yarn winding speed, up to several hundred meters/sec. As the package gradually builds up during winding, the wind ratio, which is the number of package rotations per double traverse of yarn, gradually decreases and passes through several integer values (Rebsamen, 1988). Each time the ratio reaches an integer, successive turns of yarn are laid on one another, and the effect persists till the ratio moves away from the integer value as the package diameter gradually increases. This bunching of yarn turns is known as ribboning, and is undesirable due to the distortion of package shape it causes, as well as the greater tension that needs to be applied to the yarn in over-end unwinding at these points.

There are several 'ribbon breaking' techniques used in random winding. Each of these causes some abrupt slippage of the package on the drum, once every few seconds during winding. This helps to disperse the yarn turns somewhat, and thereby minimise ribboning. However as the action is 'passive', in that the moments of its application are not coincident with those when ribboning actually occurs. The effectiveness of ribbon breaking is therefore not optimum.

Winders are available now which use speed controlled motors under microprocessor control, which prevent ribboning by switching traverse rates so as to avoid the integer values of wind ratio. However, the grooved drum random winder is still widely used by the industry due to its simplicity, and standard methods of ribbon avoidance are still applied on them.

2. OBJECTIVES

The research reported here was intended to devise a means of improving the effectiveness of ribbon breaking on a standard random winder by applying such action precisely at the times when ribboning actually occurred during winding. For this reason, it was necessary to provide the winder with the capability to detect the onset of ribboning whenever it occurred.

3. EXPERIMENTAL

The project (Durur, 2000) used a commercial winding head modified by adding a shaft encoder (8 bit) on the winding drum as well as on the package spindle. The basic winder incorporates a mechanical ribbon breaking mechanism, which briefly decouples the drum from the drive several times a minute. At each re-engagement of the drive some slippage is caused between the drum and the package as required. Two additional methods of ribbon breaking were introduced on the winder. One of these was implemented by replacing the standard drive motor by a DC brushless motor (Electro-Craft), which can be driven so as to produce sharp changes of drum speed. The other was to introduce a stepper motor controlled package lifting arm, which could be used to lift the package minutely off the drum and back at appropriate moments. Potentiometric sensors were added to measure the package diameter and the amount of package compression against the winding drum as winding progressed. All the above devices were interfaced to a PC for control and data acquisition purposes. These modifications resulted in a random winder that offered considerable scope for its mechatronic control.

The use of the shaft encoders proved somewhat difficult due to the pick up of electrical noise by electronic circuitry and measures were taken to minimise the problem. It was found that errors due to this problem could be eliminated by comparing four successive readings from the shaft encoders. This eliminated 'rogue' reading due to noise, as well as any erroneous readings that could occur as the shaft encoder stepped from one reading to the next. At a yarn winding speed of 450 m/min, each double traverse of the yarn took about 140 mS. The reading of the shaft encoders by the PC, even with error checking, was comparatively much faster at 1.7μS per reading and allowed the above procedure to be satisfactory. The PC was programmed using the C language.

The apparatus was first used to study the random winding process. It was quickly realised that by plotting the angular position of the package spindle at every start of a double traverse, an Angle of Double Traverse (ADT) diagram could be constructed on the VDU of the PC which was found to be very useful in following the progress of winding. It was seen that by rotating a yarn package of constant diameter (i.e. a package on which no additional yarn is wound) at the normal running speed, a very regular dot pattern is shown by the ADT (Fig.2). The inclination of the 'lines' depends on the particular wind ratio that corresponds to the package diameter. It was clear that despite the friction drive to the package, the package rotation was quite uniform, with no suggestion of random slipping. However as indicated by the measured diameter of the package and its deformation on the winding drum, a minute slippage of constant magnitude is likely to occur.

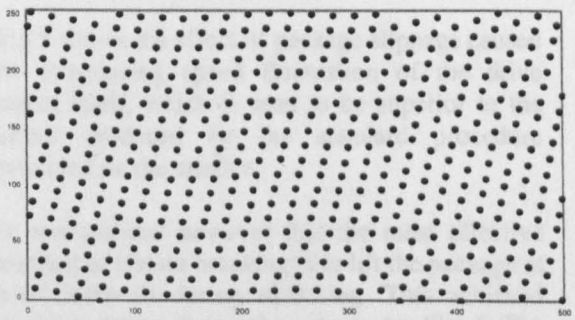

Fig. 2 Rotation of constant diameter package with no drag (diameter :80 mm, wind ratio:3.4)

This may be mechanical slippage, or could be the result of the package surface at the point of drive being slightly stretched due to its elasticity (Osawa and Koyama, 1972). Even with some mechanical drag introduced on the package spindle, corresponding to the tension of yarn during winding, the figure remained unchanged.

When winding a package normally i.e. with its diameter gradually increasing, but with ribbon breaking measures disabled, the slope of the lines gradually changes, as shown by Fig. 3.

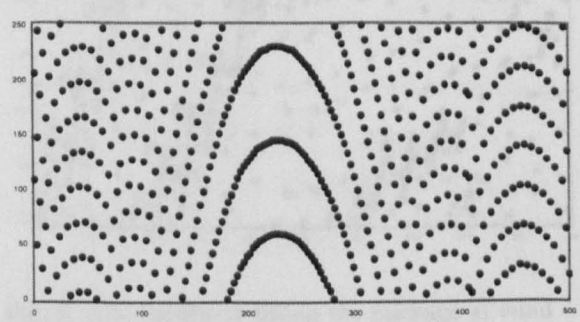

Fig. 3 Winding of package at wind ratio 3.3

Depending on the actual value of wind ratio reached, the lines form a single peak or several of them. Where a single peak is seen, the wind ratio has an integer value at that point, where 3 peaks are seen the wind ratio is an integer plus 0.33 etc. When the ratio is an integer, the ribboning that occurs is most undesirable (major ribboning). Ribbon breaking is mostly needed at these intervals. Where the ratio is high, and not an integer, any ribboning (minor ribboning) that occurs quickly passes away. When the wind ratio descends to lower values such as 3 and 2, even minor ribboning persists longer.

It is really the major ribboning that cause significant difficulties with unwinding, and hence those that demand dispersal. The moments of major ribboning can be detected by software, and ribbon breaking can be effected 'actively' as compared with the passive ribbon breaking normally employed.

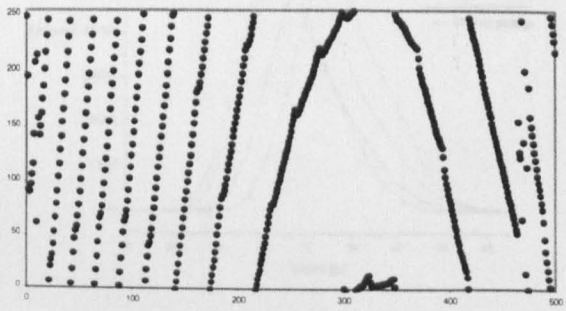

Fig. 4 Effect of normal ribbon breaking at wind ratio 3.

Fig. 4 shows the effectiveness of ribbon breaking by using the standard method of disconnecting drive to the drum approximately every 2 seconds, provided on the basic winder. The method diminishes ribboning to a noticeable extent, but some remnant ribboning could be seen on the package.

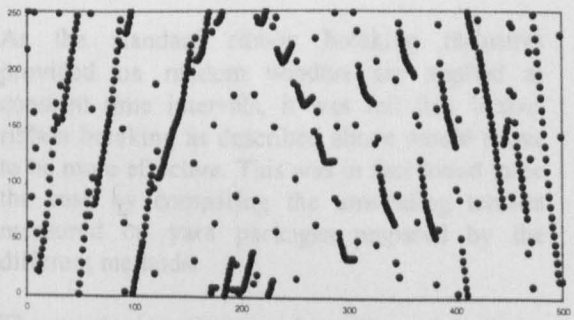

Fig. 5 Effect of active ribbon breaking at wind ratio 3

The main purpose of the modifications made to the winder was to be able to apply the ribbon breaking action at moments of ribboning, so as to maximise the beneficial effect. As described above this could be done by programming the PC to detect the onset of ribboning, and then apply the ribbon breaking action continuously, till no more ribboning is detected.

Basically this action can be implemented by detecting the beginning of each double traverse, for example at the left hand end of the grooved drum, and checking the corresponding package angular position for coincidence within a small tolerance. This procedure can be extended to detect not only major ribboning as above, but also any minor ribboning as necessary. Each time such ribboning is detected, the programme will initiate the ribbon breaking procedure.

Fig 5 shows the effect of package slippage caused by introducing speed fluctuation of the drive motor itself, which is seen to be superior to the effect produced by the standard procedure provided on the winder.

It was realised however that the most effective method of ribbon breaking is to lift the package at brief intervals during ribboning. This achieved the best ribbon dispersal as shown by Fig. 6. The package lifting arm acted on the hub of the package arm, so as to minutely lift the package off the drum. This action slows the package down, thereby causing the wind ratio to drop below the value causing ribboning. The arm uses a microswitch to sense the lifting action, and the shaft encoders help to control the lift and the duration of lift to the best effect. The microswitch also helps to keep the arm following the increasing diameter of the package. The flowchart of actions that were programmed, for ribbon breaking by this method is given in the Appendix. The routine shown additionally also plots the ADT diagram.

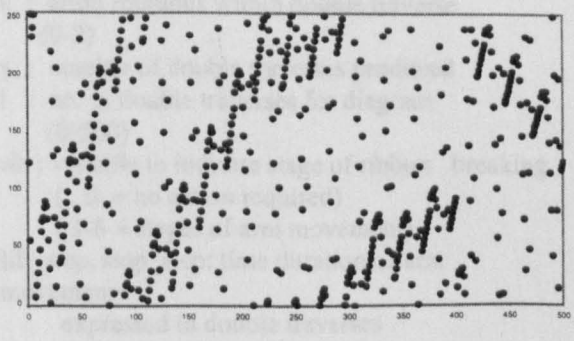

Fig. 6 The results of lifting the package at wind ratio:2.

However the best proof of the effectiveness of ribbon breaking is obtained by comparing unwinding tension relating to each method (Nobauer and Baumeler, 1992).

A number of packages were wound under the same winding conditions, but using each of the above 3 methods of ribbon breaking, and were evaluated as for evenness of unwinding tension. Tension was monitored during the unwinding of each package, by withdrawing yarn at 480 m/min. A tension probe having a natural frequency of 2.5 kHz was used and tension readings were recorded as 8 bit values, to provide some 1 M readings per package. The results of each test were used to construct a histogram of withdrawal tension. These are compared in Fig. 7. The results show that active ribbon breaking using package lifting gave the lowest unwinding tensions and hence the best unwinding characteristics.

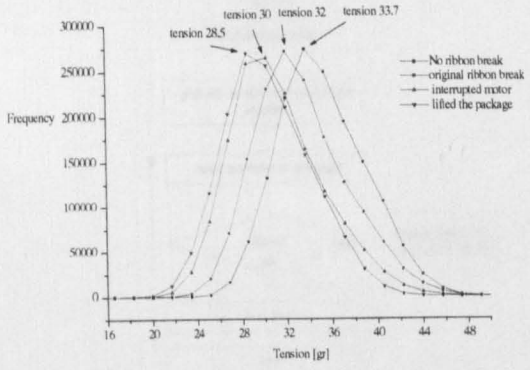

Fig. 7 The results of unwinding yarn tension

4. CONCLUSIONS

The ADT diagram is a useful means for studying the random winding process. It showed that no irregular slipping takes place in random winding under normal yarn winding tension settings, despite the indirect (surface) drive to the package employed. It was particularly useful in studying the effectiveness of the 3 ribbon breaking methods studied in this work.

As the standard ribbon breaking measures provided on random winders are applied at constant time intervals, it was felt that 'active' ribbon breaking as described above would prove to be more effective. This was in fact found to be the case by comparing the unwinding tension measured on yarn packages prepared by the different methods.

The standard random winder will continue to be used by the textile industry due to its simplicity and its suitability for use in automatic winders. As the use of microprocessor control has become relatively low in cost, methods such as the one reported here will prove to be useful in producing better random wound yarn packages.

The method of lifting the package minutely off the drum was found to be the most effective for ribbon breaking, when used 'actively' as described. However this method is more difficult to implement due to the increasing package diameter as winding progresses. In this work an arm attached to a geared stepper motor was used to implement the procedure, but a simpler mechatronic solution is desirable.

REFERENCES

Durur, G.,(2000), *PhD thesis* (In Preparation), University of Leeds, U.K.

Electro-Craft Ltd., DC Brushless Motor DM-20 and BRU-200 Servodrive, Fourth Avenue, Crewe, U.K.

Nobauer, H and Baumeler, M.,(1992), Measurement of unwinding resistance of yarn packages using the Package Performance Analyser, *Textil Praxis International*, **November**, pages 1034-1040

Osawa, G. and T. Koyama,(1972), On the Slippage between Yarn-Package and Grooved Drum During Winding, *Journal of the Textile Machinery Society of Japan*, **25, No:6**, T.113-123.

Rebsamen, A., (1988), Modern Package Building, *Textile Asia*, **September**, pages 130-136,

APPENDIX

Key to Symbols used in flowchart:

k : drum rotations within double traverse (0-2)
y : number of double traverses produced
l : no. of double traverses for diagram (0-500)
rib : variable to indicate stage of ribbon breaking
(0 = no action required)
(1-6 = stages of arm movement)
lift_step, stop_step: time duration of arm movements
expressed in double traverses

MAIN PROGRAM FOR DETECTING OF RIBBONING AND DISPLAY ON VDU

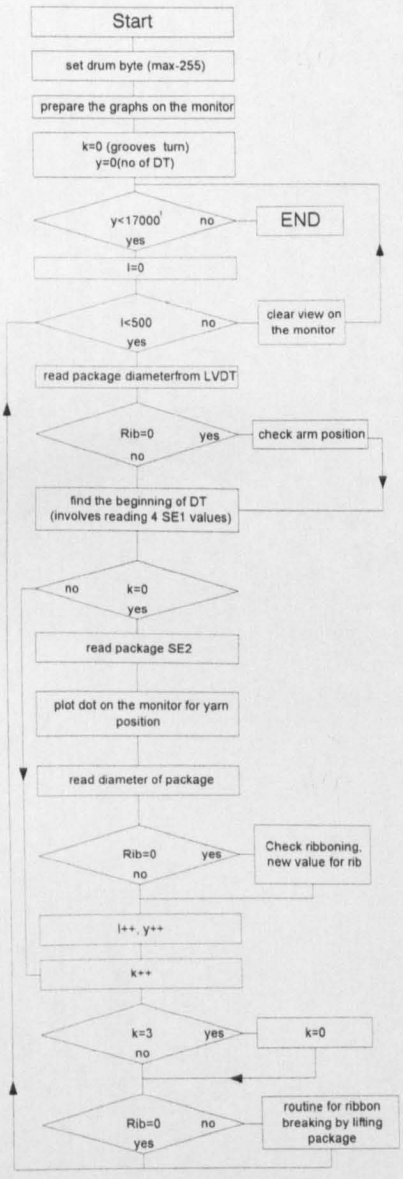

ROUTINE FOR RIBBON BREAKING BY LIFTING PACKAGE